University of Alberta

Cholesterol and Alzheimer's Disease-Related Pathology

by

Mahua Maulik

A thesis submitted to the Faculty of Graduate Studies and Research
in partial fulfillment of the requirements for the degree of

Doctor of Philosophy

Centre for Neuroscience

Spring 2013
Edmonton, Alberta

DEDICATION

To my family, for supporting me each step of the way

ABSTRACT

Alzheimer's disease (AD) is a complex neurodegenerative disorder believed to be triggered by the accumulation of β-amyloid (Aβ)-related peptides derived from the proteolytic processing of amyloid precursor protein (APP). Research over the last two decades has shown that alterations in the levels and/or subcellular distribution of cholesterol can influence Aβ metabolism and development of AD pathology, but the underlying mechanisms remain unclear. A number of recent studies have shown that AD exhibits some striking parallels with Niemann-Pick Type C (NPC) disease – an autosomal recessive disorder caused primarily by loss-of-function mutations in the *NPC1* gene. NPC disease, which is neuropathologically characterized by the intracellular accumulation of cholesterol, exhibits tau-positive neurofibrillary tangles and increased levels of Aβ-related peptides that are also the hallmarks of AD brains. To determine how alteration of the intracellular cholesterol level/distribution in the brain can influence the development of AD-related pathology, we have developed a new line of bigenic mice (ANPC) by crossing heterozygous Npc1-deficient mice with a well-established line of APP-transgenic mice (TgCRND8) overexpressing mutant human APP. The bigenic ANPC mice exhibited decreased life-span, accelerated cognitive and motor deficits and exacerbated glial as well as neuronal pathology including tau hyperphosphorylation/ cleavage, lysosomal dysfunction and neurodegeneration compared to littermates of other genotypes. Interestingly, reversal of cholesterol accumulation by 2-hydroxypropyl-β-cyclodextrin treatment was found to attenuate the observed behavioral and pathological abnormalities in ANPC mice, thus establishing the significance of cholesterol in the development of the pathology. Additionally, using ANPC mice and a complementary

stable cell line, we have demonstrated that intracellular cholesterol accretion can influence APP processing and the autophagic-lysosomal degradation pathway, causing progressive accumulation of Aβ-related peptides which can render the cells vulnerable to oxidative injury. In summary, our results suggest that alterations in cholesterol homeostasis can influence a wide spectrum of behavioral and neuropathological abnormalities observed in AD-related pathology.

ACKNOWLEDGEMENTS

It is a pleasure to thank the many people who have made this thesis possible. Especially,

I wish to extend my deepest gratitude to my PhD Supervisor, Dr. Satyabrata Kar, firstly for giving me the opportunity to work in such a wonderful and accomplished environment. His excellent supervision, understanding, encouragement and remarkable patience have helped me grow into a better scientist over the past few years. Thank you for being there for me at all times and giving me the freedom to work as I liked to fulfill my inquisitive mind.

I am especially grateful to the members of my graduate program committee, Dr. Elena Posse de Chaves and Dr. David Westaway, for the valuable discussions and thoughtful insights they have provided from the formative stages of this thesis, to the final draft.

I wish to thank Dr. Remi Quirion and Dr. Glen Baker, for their willingness to be the External Examiners for my thesis defense amidst their very busy schedule. I acknowledge all your constructive criticisms and suggestions for improving the manuscripts included in this thesis.

I wish to acknowledge all the past and present members of the Kar lab, with whom I had the privilege of working, for their incredible amount of help, support, and friendship. My special thanks to Anitha Kodam and Asha Amritraj, the two former members of my lab, for taking good care of me, both at work and outside, during my initial days in Edmonton. John Kim, Ronke Babatunde, Bibaswan Ghosal and Yanlin Wang - thank you for all the help with the animals without which I couldn't have completed the study within this time frame. Anna Verena Sasse, thank you for all your good work and especially all those days we spent together in preparing and running the gels for western blotting (not to mention your company on the trip to Washington, DC for Sfn 2011!).

On a special note, I would like to thank Dr. David Westaway, Director, Centre for Prions and Protein Folding diseases (CPPFD) and my committee member as well, for putting together such a wonderful Research Centre both in terms of facilities and people. I could not have asked for a better place to be trained as a young scientist and will always be proud of my academic roots. With this, I must also acknowledge all the members (past and present) of the Centre - thank you for the very friendly and helpful atmosphere. Special thanks to Agnes Lau, Beipei Shie, David Vergote, Jing Yang, Juan Duque Velasquez (Camillo), Kerry Ko, Laura Edwards-Ingrams, Lili Tang, Nathalie Daude, Robert Mercer, Sang Gyun Kang, and Timothy Revett for all the good times and laughter between everyday work. (Not to mention our brainstorming scientific discussions!)

I wish to thank Karrie Darichuk and Jasmine Snyder at CPPFD and Megan Airmet at the Centre for Neuroscience, for always being very helpful with different administrative and

non-administrative tasks during these years. Thank you for getting all the work done on time!

My special thanks are extended to the staffs at the two animal facilities, CPPFD and HSLAS at the University of Alberta for their excellent technical assistance. My work would not have been possible otherwise.

A special thanks to Dr. Xuejun Sun and Mrs. Geraldine Barron (Gerry) at the Cell Imaging facility, Cross Cancer Institute, University of Alberta. Thank you for all your time and assistance in carrying out the imaging studies.

I would also like to take this opportunity to thank our great collaborators, Dr. Jean E. Vance (University of Alberta, Edmonton, AB, Canada) and Dr. Gopal Thinakaran (The University of Chicago, Chicago, IL, USA), and Dr. Elena Posse de Chaves and Dr. David Westaway as well, for the valuable discussions and their generosity in providing the materials that were required to make this study possible. My grateful thanks are also extended to Dr. Simonetta Sipione (University of Alberta, Edmonton, AB, Canada), Dr. Peter Lobel (University of Medicine and Dentistry of New Jersey, NJ, USA) and Dr. Carolyn Scott (Kolling Institute of Medical Research, The University of Sydney, NSW, Australia) for their kind gifts of different antibodies that were used in this study.

On a personal note, I would like to acknowledge my family for their unconditional love and support throughout my life. I owe my deepest gratitude to my father for his endless support and constant source of encouragement, giving me the freedom to pursue my goals. I wish to honor the loving memories of my mother, who passed away during the period of this study. I remember her constant support and motivation even during the most difficult and challenging days. I warmly thank my dear sister, who has been the best of friends along this journey. Much appreciation is also given to my parents-in-law for their love and moral support. The most loving thanks belong to my dear husband, Mouli, for his love, encouragement, companionship, and co-operation during the years we have been together. Thanks for always putting a smile on my face even during the most frustrating times of long hours of work ending up with disappointing results.

Lastly, but most importantly, I gratefully acknowledge the Alberta Innovates Health Solutions for their generous funding support. I also thank all support from the Centre for Neuroscience and Faculty of Graduate Studies and Research, University of Alberta provided during this study. This study was financially supported by grants from Canadian Institutes of Health Research and University Hospital Foundation to Dr. Satyabrata Kar.

To each of the above, I extend my deepest appreciation. Thank you all!

Mahua Maulik
Edmonton, September 2012

TABLE OF CONTENTS

LIST OF TABLES

Chapter 1

Chapter 2

LIST OF FIGURES

Chapter 1

Chapter 2

Chapter 3

LIST OF ABBREVIATIONS

2-HPC	2-hydroxypropyl-β-cyclodextrin
ABC	ATP-binding cassette
ACAT	acyl-coenzyme-A cholesterol acetyltransferase
AD	Alzheimer's disease
ADAM	a disintegrin and metalloprotease
AICD	APP intracellular C-terminal domain
ANPC	APP transgenic and Npc1-null
APH-1	anterior pharynx defective 1
ApoE	apolipoprotein E
APP	amyloid precursor protein
Atg	autophagy-related protein
Aβ	β-amyloid
BACE1	β-site APP cleaving enzyme 1
Bax	Bcl-2-associated X ptotein
BBB	blood-brain barrier
BCA	bicinchoninic acid
Cdk5	cyclin dependent kinase 5
CNPase	2'3'-cyclic nucleotide 3'-phosphodiesterase
CNS	central nervous system
CTF	carboxy-terminal fragment
CTxB	cholera toxin subunit B
Cyto c	cytochrome c
Dhet	double heterozygous
ECE1/2	endothelin converting enzymes 1/2
ECL	enhanced chemiluminescence
EL	endosomal-lysosomal
ER	endoplasmic reticulum
ERK1/2	extracellular-signal regulated kinase 1/2

FAD	familial AD
GAPDH	glyceraldehyde-3-phosphate dehydrogenase
GFAP	glial fibrillary acidic protein
GSK-3β	glycogen synthase kinase-3β
HD	Huntington's disease
HDL	high-density lipoprotein
HMG-CoA	3-hydroxy-3-methylglutaryl-CoA
HMGCR	3-hydroxy-3-methylglutaryl-CoA reductase
HRP	horseradish peroxidase
Iba1	ionizing calcium-binding adaptor molecule 1
IDE	insulin-degrading enzyme
Igf2r	insulin-like growth factor 2 receptor
KPI	Kunitz-type serine protease inhibitor
LDLR	low-density lipoprotein receptor
LE/L	late-endosomes/lysosomes
LMP	lysosomal membrane permeabilization
LRP	low-density lipoprotein receptor related protein
LXR	liver X receptor
M6P	mannose-6-phosphate
mTOR	mammalian target of rapamycin
MI	memory index
NFTs	neurofibrillary tangles
NPC	Niemann-Pick type C
PD	Parkinson's disease
PEN-2	presenilin enhancer protein 2
PGPH	peptidyl-glutamyl peptide-hydrolyzing
PHF	paired helical filaments
PNS	peripheral nervous system
PS1/2	presenilin 1/2

PSD95	post synaptic density protein 95kD
ROS	reactive oxygen species
S1/2P	site-1/2 protease
sAPP	soluble APP
SCAP	SREBP cleavage-activating protein
SREBPs	sterol regulatory element binding proteins
SSD	sterol-sensing domain
TACE	tumor necrosis factor-α converting enzyme
Tg	transgenic
TGN	trans-Golgi network
VLDL	very low-density lipoprotein receptor
WT	wild-type

Chapter1: General Introduction and Literature Review

A portion of this chapter has been accepted for publication. Maulik M, Westaway D, Jhamandas J H and Kar S (2012) Molecular Neurobiology (09/2012; DOI:10.1007/s12035-012-8337-y).

1.1 Cholesterol and Brain

Cholesterol subserves a diverse array of functions in all mammalian tissues including the brain. However among all the tissues, the brain is the most cholesterol-rich organ in the body, containing approximately 25% of the total body cholesterol, despite representing only ~2% of the body mass (1, 2). Most of the brain cholesterol is unesterified [>99.5%, from (3)] which is present primarily (~70-80%) in the specialized membrane of myelin and to a lesser extent in the neurons and glial cells. Experimental work in both animals and humans has indicated that brain cholesterol is largely independent and unaffected by the serum levels, as the blood-brain barrier (BBB) is impermeable to circulating cholesterol. Functionally, cholesterol plays a critical role in neuronal development and maintenance of synaptic plasticity as well as functions such as formation of synapse, neurite outgrowth, synaptic vesicle transport and regulation of neurotransmitter release (4). As an essential component of the plasma membrane of all cells, it is involved in a tight control of ionic homeostasis, endocytosis and intracellular signaling mechanisms. In addition, cytoplasmic cholesterol serves as a precursor for the synthesis of steroid hormones, vitamin D and oxysterols (5, 6). With such functional pleiotropism, it is evident that cholesterol is a major regulator of neuronal activity and any imbalance in brain cholesterol levels will have severe consequences on brain function. It is thus absolutely essential that brain cholesterol levels are maintained under a tight regulation and harnessed in certain forms, locations and concentrations for normal functioning of the brain.

1.2 Brain cholesterol metabolism

In the peripheral tissues, cholesterol requirement is covered by *de novo* synthesis in the endoplasmic reticulum (ER) and by cellular uptake of dietary cholesterol in the form of lipoprotein complexes. However in the brain, under normal physiological conditions, the BBB prevents the entry of the lipoprotein complexes from the peripheral circulation. Thus, practically all (>95%) cholesterol present in the brain is synthesized *de novo* within this organ. Neuronal cholesterol is only synthesized in cell bodies and transported to axons for incorporation into their plasma membranes (7). In addition, unesterified cholesterol synthesized in the glia and complexed with the cholesterol trasporter

Apolipoprotein E (ApoE) is delivered to neurons by receptor-mediated endocytosis to supplement their endogenous need for the sterol. Based on the presence of many different lipoprotein receptors, and their involvement in neurite growth and repair of damaged neurons, there is a good agreement that sterol pools are constantly recycled within the brain between the different cell types mainly through the endosomal-lysosomal (EL) system. The turnover of brain cholesterol is relatively low compared to that within the periphery, with a half-life estimated to be 4-6 months in rodents (8) and 5 years in human (9). The excess cholesterol is exported from the brain in the form of 24S-hydroxycholesterol into the plasma. Therefore cholesterol homeostasis in the brain is maintained by the dynamic equilibrium of *de novo* synthesis, transport, storage and removal as described in greater details in the following paragraphs (see Fig. 1.1).

1.2.1 *De novo* synthesis of cholesterol in the brain

Essentially both neurons and glial cells can synthesize cholesterol *de novo*. Oligodendrocytes which govern the synthesis of myelin sheaths have the highest capacity to synthesize cholesterol, followed by astrocytes that synthesize at least 2-3 times more cholesterol than neurons (1, 10). Cholesterol is synthesized from acetate in a multi-enzyme cascade requiring more than 20 reactions mediated in five major stages (Fig. 1.2). The precursor acetyl CoA are first converted to 3-hydroxy-3-methylglutaryl-CoA (HMG-CoA) and then to mevalonate. Mevalonate is phosphorylated to isopentyl pyrophosphate and other active isoprenoids, which condense and combine to form squalene. Squalene is converted to lanosterol which is finally converted to cholesterol. Although various enzymes dictate the rate of each of these stages, the rate limiting step of cholesterol biosynthesis is the conversion of HMG-CoA to mevalonate catalyzed by the ER-bound 3-hydroxy-3-methylglutaryl-CoA reductase (HMGCR). The activity of this enzyme is controlled by the levels of cholesterol *via* two distinct mechanisms. First, a high cholesterol level exerts a feedback inhibition by activating HMGCR ubiquitination and subsequent proteasomal degradation. Secondly, HMGCR levels are also regulated by ER-bound transcription factors called sterol regulatory element binding proteins (SREBPs), which in turn are controlled by a sterol sensitive SREBP cleavage-activating protein (SCAP) (11). In the presence of sterols, full-length SREBP is restricted to the ER.

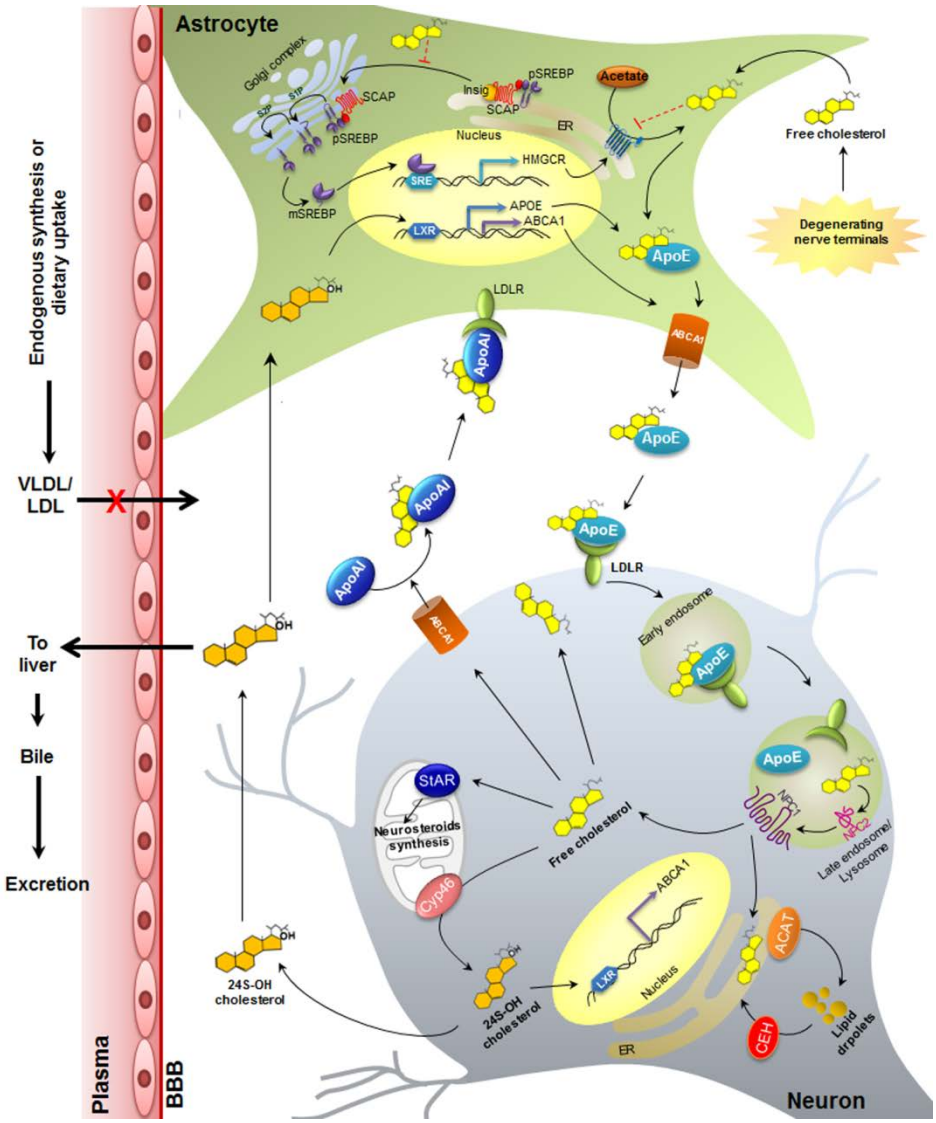

Figure 1.1. Brain cholesterol metabolism. In adult brain, the mature neurons mostly rely on the astrocytes for their cholesterol requirement. Apart from *de novo* synthesis, astrocytes can also internalize cholesterol derived from degenerating nerve terminals. The free cholesterol in the astrocytes provides negative feedback to HMGCR and the Insig-SREBP-SCAP complex to regulate endogenous synthesis of cholesterol. The excess free cholesterol is transported out of the cells by ABCA1, a membrane protein that facilitates the formation of ApoE-cholesterol-phospholipid complex in an ATP-dependent manner. Upon secretion from the astrocyte, the complex may bind to LDLR (or other members of the LDL receptor family) to be taken up by neurons. Following internalization and subsequent delivery to the late-endosomes/lysosomes, the lipoprotein complexes are hydrolysed to free cholesterol. This free cholesterol is then exported out of the late-endosomal/lysosomal compartment in an NPC1/2 dependent manner for its delivery to other cellular compartments such as the plasma membrane, ER and mitochondria where it can be actively used by the cell. Excess cholesterol can be stored as cholesterol esters in the form of lipid droplets in the cytosol, formed by ACAT, or packaged with ApoAI and phospholipids and secreted out of the cell by ABCA1. Cholesterol stored in the lipid droplets can be liberated by a cholesterol ester hydrolase (CEH) and used when required by the cell. Excess cholesterol can also be removed from neurons through its conversion into 24S-OH cholesterol mediated by cholesterol 24S-hydroxylase in the mitochondria. This sterol can now freely cross lipophilic membranes of the BBB, which usually prevents direct transport of cholesterol, for elimination. The 24S-OH cholesterol in neurons or when internalized by astrocytes can also induce LXR-regulated gene transcription.

Upon sterol depletion, SREBP interacts with SCAP and is transported from ER to the Golgi apparatus, where SREBP is proteolytically cleaved by two proteases, Site-1 protease (S1P) and Site-2 protease (S2P), and the released N-terminal domain acts as a transcription factor to subsequently enhance the levels of HMGCR (11, 12). Thus, ER appears to serve as a key site regulating cholesterol metabolism according to cellular demand.

1.2.2 Transport and storage of cholesterol in the brain

It is known that during development neurons synthesize most of the cholesterol required for growth and synaptogenesis, whereas mature neurons progressively lose such ability and become dependent on availability of exogenous cholesterol from astrocytes. The supply of cholesterol by astrocytes is also an energy saving process for neurons as more than 100 molecules of ATP are required to synthesize one molecule of cholesterol (1, 4, 13). Apart from its *de novo* synthesis, astrocytes can also internalize and recycle the cholesterol released from degenerating nerve terminals and deliver it back to neurons (14). The transport of cholesterol from astrocytes to neurons requires binding to one of the variants of ApoE, the most prevalent lipoprotein in the central nervous system (CNS) (15). First, cholesterol forms complexes with ApoE resembling the plasma high-density lipoprotein (HDL) particles, which are then secreted in a process involving ATP-binding cassette (ABC) membrane transport protein family members such as ABCA1 and ABCG1 (16, 17). The secreted ApoE-cholesterol complex is then internalized into neurons *via* a member of the low-density lipoprotein receptor (LDLR) family, mainly the LDLR itself and the low-density lipoprotein receptor related protein (LRP), but also to some extent *via* very low-density lipoprotein receptor (VLDL), ApoE receptor 2 and megalin (15, 18, 19). At present, the relative importance of various receptors in the internalization of cholesterol remains unknown which may contribute to the considerable redundancy in these systems. The receptor bound ApoE-cholesterol complexes following internalization are delivered to the late-endosomes/lysosomes (LE/L) where acid lipase hydrolyses the cholesterol esters within the lipoprotein complexes, resulting in the release of intracellular free cholesterol. This unesterified cholesterol subsequently exits the LE/L *via* Niemann Pick type C (NPC) 1 and 2 protein-dependent mechanism and is distributed

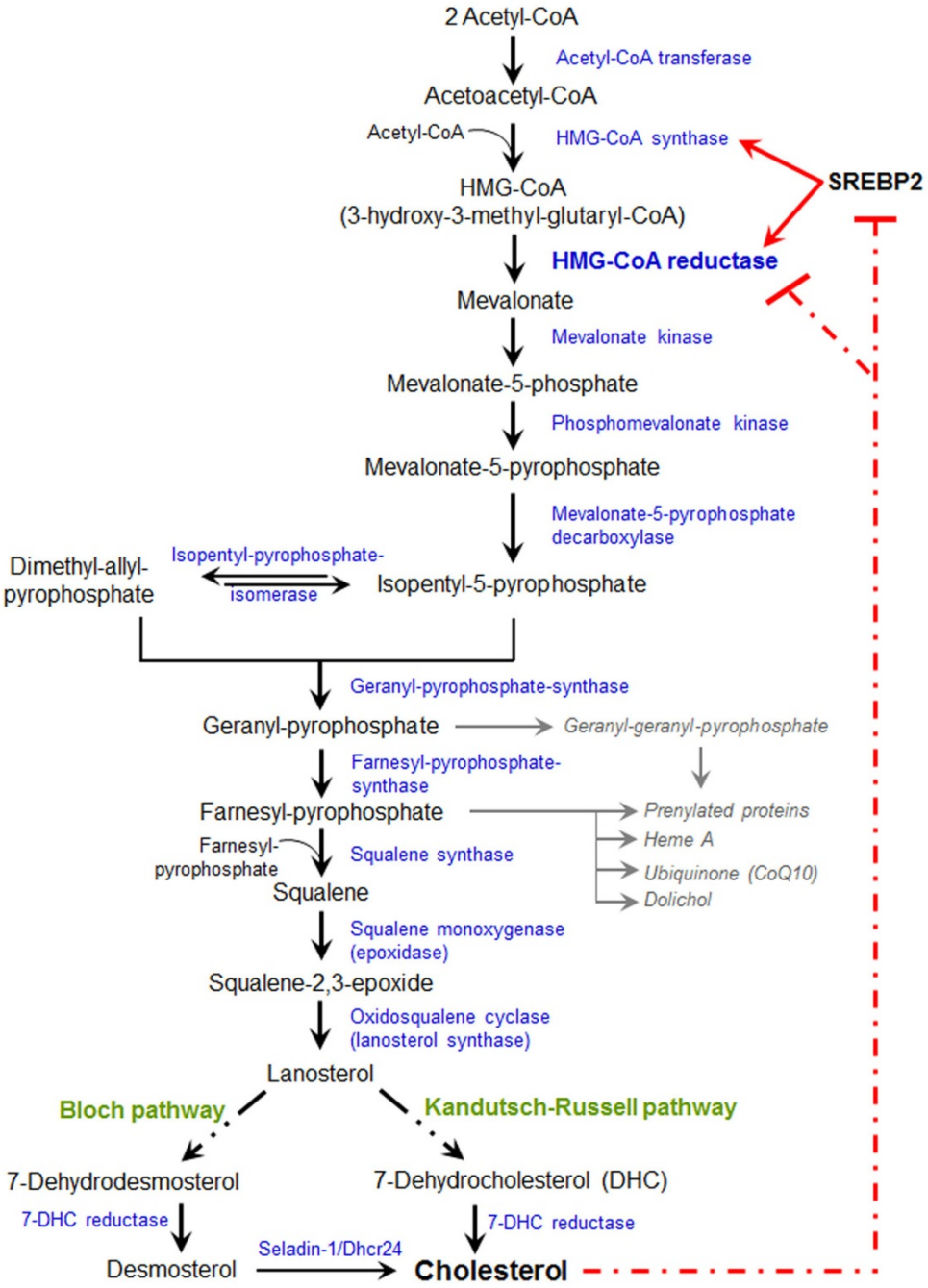

Figure 1.2. Schematic representation of the main steps involved in cholesterol biosynthesis from precursor Acetyl-CoA. All major enzymes in each metabolic reaction are shown in blue. The rate-limiting enzyme of the pathway is HMG-CoA-reductase which catalyzes the synthesis of mevalonate from HMG-CoA. The post-lanosterol steps of cholesterol biosynthesis have been divided into Bloch and Kandutsch–Russell pathways, which share the same enzymatic steps but differ by the stage at which the C24 double bond is reduced. The pathway is controlled at the HMG-CoA-reductase catalyzed rate-limiting step by feedback inhibition of cholesterol (broken red line) and positive regulation by SREBP2 (solid red arrows).

primarily to the plasma membrane as well as to the ER, which serves as a negative feedback sensor for the cholesterol homeostasis genes such as HMGCR and LDLR. Excess cholesterol, on the other hand, is esterified in the ER by the enzyme acyl-coenzyme-A cholesterol acetyltransferase (ACAT) and stored in cytoplasmic lipid droplets as a reserve pool (20-22). This intracellular pool of cholesterol serves as the source for synaptic and dendritic formation and remodeling (4).

1.2.3 Efflux of cholesterol from the brain

Since brain neurons and glial cells cannot degrade cholesterol, they rely on exporting cholesterol to the peripheral circulation for its disposal by the liver as bile. This helps to maintain a steady-state level of cholesterol in the brain. At present two different mechanisms exist for cholesterol elimination from the brain. The major mechanism by which cholesterol is excreted from the brain is by conversion to 24S-hydroxylcholesterol - an oxidised lipophilic metabolite that can freely cross the BBB (23). The conversion of free cholesterol to 24S-hydroxycholesterol is mediated by the cytochrome P450-containing enzyme cholesterol 24-hydroxylase, which is encoded by the *Cyp46a1* gene expressed rather selectively in the brain (24). High levels of this enzyme are found in certain neuronal cells such as pyramidal neurons of the hippocampus and cortex, Purkinje cells of the cerebellum, thalamic neurons and in hippocampal and cerebellar interneurons (25). Interestingly, some cholesterol 24-hydroxylase immunoreactivity has also been detected in glial cells from brains of Alzheimer's disease (AD) patients (23). It is estimated that about 40% of the total cholesterol turnover is mediated by cholesterol 24-hydroxylase (9, 25). Indeed, deletion of the *Cyp46a1* gene encoding cholesterol 24-hydroxylase leads to ~50% reduction in brain cholesterol excretion. This decrease, however, is compensated by the reduction in *de novo* synthesis thus suggesting a close relationship between synthesis and metabolism of cholesterol in the brain. The other mechanism of cholesterol elimination, called reverse cholesterol transport pathway, involves translocation of a fraction of brain cholesterol to the blood by membrane transport proteins such as ABCA1 (26, 27). The level of ABCA1 is partly regulated by cholesterol-derived ligand oxysterols (e.g., 24S-hydroxylcholesterol) of the liver X receptor (LXR), which has been shown to influence transcription of multiple genes

involved in cholesterol metabolism (28-32). It thus appears that both synthesis and elimination of cholesterol, especially in the adult brain, are not only tightly regulated but also compartmentalized. Astrocytes are responsible for majority of cholesterol synthesis but contribute relatively little to its elimination, whereas neurons with reduced synthetic ability can eliminate about two thirds of the cholesterol from the brain (27).

1.3 Cholesterol in neurodegenerative diseases

Michael S. Brown and Joseph L. Goldstein in their Nobel lecture for Physiology or Medicine in 1985 described cholesterol as a "Janus faced" molecule, having both positive and negative consequences. While their elegant comments at that time referred to cholesterol in the peripheral circulation, we now know that those comments apply to brain cholesterol as well. Thus, while cholesterol plays many important roles in the brain and is required for its optimal functioning, altered regulation of this sterol can lead to various pathological abnormalities. The metabolism of cholesterol in the brain and its implications for neurologic diseases have been extensively reviewed in recent years (27, 33, 34). Accumulating evidence suggests that aberrant brain cholesterol metabolism contributes to the pronounced and progressive neurodegeneration that occurs in AD, Huntington's disease and Parkinson's disease (PD). Moreover, cholesterol is an indispensable component of myelin membranes that insulates and protects nerves, and its availability in oligodendrocytes subserves as a rate-limiting factor for brain maturation. Thus a disturbance in brain cholesterol homeostasis is most likely to affect the growth, maintenance or repair of the myelin sheath, ultimately disrupting fast nerve signaling that has been implicated in a large number of neurodegenerative demyelinating diseases, the most common one being Multiple Sclerosis. Apart from these well-known diseases, prominent neurologic manifestations also occur in many hereditary diseases such as Niemann-Pick type C (NPC) disease, Smith-Lemli-Opitz syndrome, Tangier disease, neuronal ceroid lipofuscinosis, lathosterolosis, desmosterolosis and cerebrotendinous xanthomatosis which have been attributed to accumulation and/or aberrant metabolism of cholesterol. Table 1.1 presents a summary of some of these neurodegenerative disorders that are associated with altered cholesterol metabolism. In this thesis, our primary objective is to understand the role of cholesterol in the development of AD pathology,

Table 1.1: Neurodegenerative disorders associated with an altered sterol metabolism/levels

Disease	Mutated Gene (s)	[1]Inheritance	Sterol disturbances	Neurological phenotype
Alzheimer's disease	Polygenic: *APP*, *PS1* or *PS2*	AuD and sporadic	Cholesterol homeostasis	Senile dementia with impairements in short-term memory and executive cortical functions
Huntington's disease	*HTT*	AuD	Cholesterol biosynthesis	Progressive motor, psychiatric and cognitive dysfunctions
Parkinson's disease	Polygenic: *PARK2*, *PARK*, *PINK1*, *SNCA*or *LRRK2*	AuD (*SNCA*, *LRRK2*), AR (*PARK2*, *PARK*, *PINK1*) and sporadic	Cholesterol homeostasis	Neuropsychiatric disorder including speech, cognition, mood, behaviour, psychotic, balance and movement disturbances
Niemann-Pick type C	*NPC1* and *NPC2*	AR	Cholesterol transport and homeostasis; accumulation of unesterified cholesterol in LE/L	Cerebellar ataxia, vertical supranuclear gaze palsy, dysarthria, dysphagia, dystonia, dementia, seziures and psychiatric disturbances
Smith-Lemli-Opitz syndrome	*DHCR7*	AR	Cholesterol biosynthesis; elevated 7-dehydrocholesterol levels	Mental retardation, microcephaly, developemental delay, autism, learning and behavioural problems
Tangier disease	*ABCA1*	AR	HDL deficiency; dimished ability to transport cholesterol out of cells	Small fibre-type neuropathy and syringomyelia
Cerebrotendinous xanthomatosis	*CYP27A1*	AR	Loss of mitochondrial sterol 27-β-hydroxylase function; abnormal accumulation of 7-α cholesterol and cholesterol	Dementia, seizures, hallucinations, depression and difficulty with coordinating movements and speech

Table contd……..

Table 1.1 continued .....

Disease	Mutated Gene (s)	[1]Inheritance	Sterol disturbances	Neurological phenotype
Lathosterolosis	*SC5DL*	AR	Cholesterol biosynthesis	Psychomotor retardation, microcephaly
Desmosterolosis	*DHCR24*	AR	Cholesterol biosynthesis; elevated desmosterol levels	Psychomotor retardation, microcephaly, spasticity with severe convulsions
Neuronal ceroid lipofuscinosis	Polygenic: *PPT1*, *TPP1*, *CLN3*, *CLN5*, *CLN6*, *DNAJC5*, *MFSD8*, *CLN8*, or *CTSD*	AR (*PPT1*, *TPP1*, *CLN3*, *CLN5*, *CLN6*, *MFSD8*, *CLN8*, and *CTSD*) and AuD (*DNAJC5*)	Cholesterol homeostasis; enhanced cholesterol synthesis and accumulation of cholesteryl esters	Progressive intellectual and motor deterioration, seizures and visual impairement

[1]AuD: Autosomal Dominant; AR: Autosomal Recessive

which exhibits some intriguing parallels with the NPC disease. Hence, a review of the current literature focusing on the involvement of aberrant brain cholesterol metabolism in AD and NPC pathologies is provided in the following two sections.

1.4.1 Alzheimer's disease (AD) etiology

AD, the most common cause of dementia affecting the elderly, is a progressive neurodegenerative disorder. It is characterized by a global deterioration of intellectual function that includes memory impairment, loss of language function and visuospatial deficits. Motor abnormalities are uncommon until the late phases of the disease and basic activities of daily living are gradually impaired as the pathology enters advanced phases. Psychosis and agitation also develop during middle or later phases of the disease. The average course of AD is approximately a decade, but the rate of progression is variable (35-37). Epidemiological data have shown that AD afflicts about 8-10% of the population over 65 years of age and its prevalence doubles every 5 years thereafter (38, 39). This fact, together with a steady increase in life expectancy, particularly in industrialized nations, makes AD one of the most serious health problems of this century (40).

It has long been accepted that both genetic and environmental factors can contribute to the development of the disease. In the majority of cases, AD appears to occur as sporadic disease after the age of 65 years, but in a small proportion (~6-8%) of cases the disease is inherited as an autosomal dominant trait and appears as an early-onset form prior to 65 years of age. To date, mutations within three genes – the amyloid precursor protein (*APP*) gene on chromosome 21, the presenilin 1 (*PSEN1*) gene on chromosome 14 and the presenilin 2 (*PSEN2*) gene on chromosome 1 – have been identified as the cause of early-onset familial AD (FAD) (41-44). While these findings are of importance in elucidating the biological pathogenesis of AD, it is vital to recognize that mutations in these three genes may only account for 30-50% of all autosomal dominant early-onset cases. The inheritance of late-onset AD is more complex than that of the early-onset form. However, association studies have identified candidate genes that significantly increase the risk for late-onset disease. The ε4 allele of the *ApoE* gene, on chromosome 19, is one such risk factor. Possessing a single copy of the allele may

increase the chance of developing AD two- to five-fold, whereas having two ε4 alleles raises this probability to more than five-fold (13, 20, 41-43, 45, 46). Additional genome-wide association studies have shown that variants in some novel susceptibility genes such as clusterin [*ApoJ* on chromosome 8; (47, 48)], phosphatidylinositol-binding clathrin assembly protein [*PICALM* on chromosome 11; (47, 48)], complement receptor 1 [*CR1* on chromosome 1; (48)], bridging integrator 1 [*BIN1*, located on chromosome 2; (49)] and sortilin-related receptor 1 [*SORL1* on chromosome 11; (50)] may be associated in enhancing the risk of AD, but these need to be validated in future studies (51, 52). Other major factors that may play an important role in the pathogenesis of AD include aging, whereas prior head trauma and oxidative stress are also believed to enhance the risk of AD (53, 54).

1.4.2 Neuropathological features of AD

Neuropathological features associated with both familial and sporadic AD include intracellular neurofibrillary tangles (NFTs), extracellular parenchymal amyloid deposits and loss of neurons and synaptic integrity in specific brain areas (55). Structurally, NFTs consist of paired helical filaments (PHF) and occasional single straight filaments, that mainly contain a hyper/abnormal phosphorylated form of microtubule associated protein, tau. Under normal condition, tau binds and stabilizes microtubule by reversible phosphorylation and dephosphorylation process mediated *via* protein kinases and phosphatases, respectively. Phosphorylated tau, if not dephosphorylated, is unable to bind microtubules, undergoes polymerization into straight filaments and then is cross-linked by glycosylation to form PHF-tau (56-58). Evidence suggests that NFTs are generally found in large numbers, particularly in cortex, hippocampus, amygdala and certain subcortical nuclei in the AD brain. The formation of PHF-tau reduces the ability of tau to stabilize microtubules, leading to disruption of neuronal transport and eventual death of the affected neurons (56-60). The extent of neurofibrillary pathology, particularly the number of cortical NFTs, correlates positively with the severity of dementia observed in patients, but it should be emphasized that NFTs are found in a variety of other neurodegenerative disorders without any evidence of neuritic plaques such as frontotemporal dementia and parkinsonism linked to chromosome 17 (FTDP-17),

progressive supranuclear palsy, Pick's disease and corticobasal degeneration (57, 58, 61-64).

Neuritic plaques are multicellular lesions containing a compact deposit of amyloid peptides in a milieu of reactive astrocytes, activated microglia and dystrophic neurites. The major amyloid peptides that are found in the plaques are β-amyloid$_{1-42}$ (Aβ_{1-42}) and Aβ_{1-40}, peptides that are generated by proteolytic cleavage of APP. These plaques are most prominent in areas affected by neurodegeneration such as entorhinal cortex, hippocampus and association cortices (64-66). The number of plaques does not correlate with the severity of dementia, *albeit* a clinical correlation between elevated levels of Aβ peptide in the brain and cognitive decline has been reported (67). Several lines of evidence suggest that accumulation of Aβ peptides in the brain may, over time, initiate and/or contribute to AD pathogenesis. These include the association of some AD cases to inherited *APP* mutations (41, 43, 64), the elevation of Aβ peptides and appearance of amyloid plaques in advance of other pathology in AD brains (68, 69), the increased production of Aβ_{1-42} *in vivo* and *in vitro*, by pathogenic mutations in *PSEN1* and *PSEN2* (43, 64) and the *in vitro* neurotoxic potential of fibrillar Aβ peptides (64, 70, 71). Over-production and/or reduced clearance of Aβ peptides are likely key to amyloid aggregation, which in turn contributes to the development of NFTs and subsequent neuronal degeneration (65, 72, 73).

Selective synapse loss along with neuronal dysfunction and death are part of the elemental lesions associated with AD pathology. Regions that are severely affected in AD brains include the hippocampus, entorhinal cortex, amygdala, neocortex, some subcortical areas such as basal forebrain cholinergic neurons, serotonergic neurons of the dorsal raphe and noradrenergic neurons of the locus coeruleus (74-76). Biochemical investigations of autopsy tissues indicate that various neurotransmitters/modulators, including acetylcholine, serotonin, glutamate, noradrenaline and somatostatin, are differentially altered in AD brains (64, 77). One of the most consistent observations is a profound reduction in the activity of the acetylcholine synthesizing enzyme choline acetyltransferase in the neocortex that correlates positively with the severity of dementia

(76, 78). Interestingly, other cholinergic neurons which are located in the brainstem or in the striatum are found to be relatively spared or affected during late stages of the disease (76, 77, 79). At present, neither the cause of selective degeneration of neurons nor the mechanisms associated with the development of pathological features in AD brains have been clearly established. However, an increasing amount of evidence derived from genetic, epidemiological and biochemical studies over the past decade has suggested a critical role for cholesterol in AD pathogenesis. It is believed that increased cholesterol levels can enhance the risk of developing AD by influencing multiple pathways, but the mechanisms by which cholesterol can regulate these events need to be addressed in order to better understand its role in AD pathology.

1.4.3 Link between AD pathology and cholesterol

The major risk factor for late-onset AD, as mentioned earlier, is the presence of ε4 allele of ApoE gene located on chromosome 19. This gene which codes for a 229 amino acid protein involved in cholesterol transport exists in three different isoforms i.e., ε2, ε3 and ε4. Individuals carrying one or two copies of the ε4 allele have three and eight times higher risk of developing AD respectively, compared to individuals with the ε3 (the most common) or ε2 forms (80, 81). Inheritance of ApoE ε4 allele also lowers the age of onset of dementia by as many as 7-9 years per allele in a gene-dose-dependent manner (80, 82). The ε4 variant differs from ε2 and ε3 by having arginine residues instead of cysteine at positions 158 and 112, respectively. The amino acid substitutions have a critical role in determining the three-dimensional structure of ApoE leading to changes to its protein binding properties. Therefore the proposed mechanism by which ApoE appears to impact AD is through its effect on Aβ binding. ApoE has been shown to accelerate the formation of Aβ fibrils (83), with the ApoE ε4 isoform being most efficient in promoting fibrillogenesis *in vitro* (84). This is further supported by *in vivo* studies showing that mice expressing ApoE ε4 and APP have accelerated Aβ deposition compared with mice expressing the other ApoE isoforms or no ApoE (85, 86). Additionally, blocking Aβ and ApoE interaction using a synthetic peptide not only reduces Aβ fibril formation *in vitro* but also reduces Aβ plaque load in a mouse model of AD (87). ApoE is also involved in promotion of Aβ clearance from the brain. Consistent observations have shown that

ApoE causes the proteolytic break-down of the Aβ peptide in an isoform-specific fashion, and in particular, the ε4 isoform being not very effective, resulting in increased vulnerability to AD in individuals with the ε4 genotype (88-92).

Other genes related to cholesterol metabolism have also been linked to AD, *albeit* none as unequivocally as ApoE. These include genes encoding ApoJ (involved in the transport of cholesterol) (47, 48, 60), LRP (a major receptor for ApoE in the brain) (93), the enzyme cholesterol 24-hydroxylase (responsible for the catabolism of cholesterol to 24S-hydroxycholesterol) (93-97), ABCA1 (involved in the efflux of cholesterol from the brain) (36, 98, 99) and the enzyme ACAT1 (responsible for the esterification of cholesterol) (41). Clearly, the identification of an escalating number of probable associations between AD and other genes linked to cholesterol metabolism in the recent years shows the potential importance of cholesterol metabolism in the etiology of AD. However, many of these associations have not been replicated by other studies (41), and therefore the strength of these associations remain to be established.

Several epidemiological studies have shown that high cholesterol levels in mid-life correlate strongly with amyloid deposition and the risk of developing AD in later life (100-103). Levels of plasma LDL at post-mortem have also been found to be higher in AD patients than in control populations (104). Conversely, patients taking cholesterol lowering drugs such as statins have been reported to have a lower incidence of AD than the general population, *albeit* more recent prospective studies have produced conflicting results (103, 105-108). There is evidence that cholesterol levels may influence AD neuropathology, as neurons bearing NFTs contain higher levels of free cholesterol than tangle free neurons (101, 109). More recently, using comparative lipidomic analysis of brain tissues from AD and commonly used AD mouse models revealed significant changes in many lipids in the affected (i.e., prefrontal cortex and entorhinal cortex) *vs.* unaffected (cerebellum) regions of the brain, thus reinforcing the potential link between lipid anomalies and AD pathogenesis (110).

A number of biochemical studies have provided a strong link between cholesterol level and generation/deposition of Aβ peptides. Animals recapitulating AD pathology when fed with high cholesterol diets showed increased levels/accumulation of Aβ peptides, whereas treatment with cholesterol lowering drugs resulted in lower Aβ levels and/or deposition. The influence of cholesterol on Aβ production/levels have been replicated in cultured cells by removal of existing cholesterol or addition of exogenous cholesterol (27, 100, 103). Whether the generation of Aβ peptides simply reflects responsiveness to cholesterol levels, metabolism and/or distribution within subcellular compartments remains unclear. Since the peripheral and central cholesterol pools are not readily interchangeable (1, 10), it is critical to determine the molecular mechanisms by which altered regulation of cholesterol in the periphery can influence Aβ production/deposition in the brain. In this part of the introductory chapter, an overview of the recent findings on how levels of cholesterol and its distribution can influence Aβ production, clearance, aggregation and toxicity, and their potential implications in AD pathology is presented.

1.4.4 The Amyloid Precursor Protein (APP) and Animal models of AD

APP, localized on chromosome 21 at 21q21.2 was the first gene to be identified in association with inherited susceptibility to AD (111-114). It is a member of a larger gene family that includes the amyloid precursor-like proteins (*APLP1* and *APLP2*) in mammals (115, 116). APP, together with APLP1 and APLP2, are highly conserved in evolution and have substantial homology in their structure (except for the Aβ region) and also share similar functions (117, 118). The *APP* gene encodes 8 alternatively spliced transcripts of which 3 are most common: APP695, APP751 and APP770. The APP695, the most abundant form in the brain, is expressed predominantly in neurons. The longer APP751 and APP770 isoforms that harbor an additional domain homologous to the Kunitz-type serine protease inhibitor (KPI) motif are present mostly in glial cells and other non-neuronal tissues (64, 119, 120). Structurally, APP is a type I integral membrane protein with a large N-terminal extracellular/luminal domain, a short membrane-spanning domain and a small cytoplasmic C-terminal tail. The Aβ region is partially embedded within the transmembrane domain and includes 28 amino acids of the ectodomain and 12

to 14 amino acids of the adjacent membrane-spanning domain. In neurons, APP is cotranslationally translocated into the ER via its signal peptide and then posttranslationally modified ("matured" via *N*- and *O*-glycosylation, sulfation and phosphorylation) through the secretory pathway (64). Its acquisition of *N*- and *O*-linked sugars occurs rapidly after biosynthesis, and the mature APP is then transported in membrane vesicles along the axon by fast axonal transport to synaptic terminals (121-123). Both during and after the trafficking through the secretory pathway, APP itself can mediate certain functions within the cells and also can simultaneously undergo proteolytic processing to release secreted derivatives into vesicle lumens and/or the extracellular space (see below).

The precise physiological role of full-length APP is enigmatic but a plethora of functions have been attributed to this molecule including cell survival/death, regulator of neuronal processes (such as neurite outgrowth, dendritic arborization, synaptogenesis, synaptic plasticity and neuronal excitability), calcium and metal homeostasis, cell adhesion and as a cell surface receptor (124-126). Additionally, APP isoforms containing the KPI domain can act as potent inhibitors of serine proteases. Despite the multitude of functions, deletion of the *App* gene did not significantly affect the phenotype or life expectancy of mice (127). *App* knockout mice display only minor weight loss, reduced forelimb grip strength, decreased locomotor activity and reactive gliosis in the cortex later in adult life. One study reported that synaptic markers are also reduced in *App* knockout mice which correlate rather well with deficits in learning and memory as well as synaptic plasticity (128). Interestingly, *App*/*Aplp2* and *Aplp1/Aplp2*, but not *App*/*Aplp1* double knockout mice, show early postnatal lethality, indicating that members of the *APP* gene family exhibit partial overlapping functions (129). This is further supported by the fact that triple knockouts involving *App, Aplp1,* and *Aplp2* genes lead to death shortly after birth (130). Abnormal developments in the CNS and peripheral nervous system (PNS) have been repeatedly observed in both *App/Aplp2* double and *App/Aplp1/Aplp2* triple knockout animals (131-134). In the PNS, *App/Aplp2* double knockout mice exhibit a mismatch between presynaptic and postsynaptic markers at the neuromuscular junctions along with excessive nerve terminal sprouting and defective neurotransmitter release

(133, 134). *App/Aplp1/Aplp2* triple knockouts, on the other hand, show scattered cortical migration abnormalities (130). Taken together, these knockout studies clearly suggest an essential role for the APP family of proteins in the development of the nervous system relating to the synapse structure and function as well as in neuronal migration.

The importance of APP in AD pathogenesis relates predominantly to its role as a precursor to the potentially cytotoxic Aβ fragment, which has been shown to have a central role in the amyloid hypothesis (135). The pathogenic APP mutations reported thus far in early-onset FAD (see http://molgen-www.uia.ac. be/ADMutations) all occur within or near the Aβ region and act by either altering APP processing, leading to increased Aβ production, or altering the propensity of Aβ to aggregate into β-sheet amyloid fibrils. To validate the *in vivo* role of Aβ in AD pathogenesis, several lines of transgenic (Tg) mice have been developed with a variety of promoters and APP FAD mutations on different genetic backgrounds of the mouse strain. Some of the most commonly used APP-Tg models are described in Table 1.2. The early efforts to create Tg mouse models of AD emphasized on the APP FAD mutations as these were the first genetic link to be identified in AD (136-139). These early APP-Tg mice exhibit high levels of mutant human APP and Aβ, and progressively reproduce many of the pathological hallmarks of AD including extracellular Aβ deposition, gliosis, dystrophic neurites containing hyperphosphorylated tau and loss of synaptic density with regional specificity resembling that seen in human AD (Table 1.2). Most of these models have also been shown to develop cognitive deficits in a variety of behavioural paradigms including the Morris water maze test (Table 1.2) (136, 138, 140, 141). Moreover, the morphology of the extracellular Aβ deposits in aged APP-Tg mice parallels the amyloid pathology in human AD brains, with plaques spanning a continuum from diffuse to dense core of Aβ deposits surrounded by dystrophic neurities and reactive gliosis. Crossing of the mutant APP-Tg mice with mice over-expressing mutant PS1 transgene demonstrated dramatic acceleration of $A\beta_{1-42}$ production and extracellular Aβ deposition, suggesting a critical role for $A\beta_{1-42}$ in driving AD pathology (142, 143). However, none of these APP and/or APP/PS1-Tg mouse models recapitulate the complete spectrum of AD neuropathology in the absence of neuronal loss and/or development of NFT lesions that characterize AD

pathology (144-146). To understand the functional inter-relationships between Aβ and tau proteins in AD pathogenesis, APP-Tg models were crossed with well-established tau-Tg models, which are known to develop florid neurofibrillary pathology in the absence of any extracellular Aβ deposition (147-149). The APP-tau double transgenic mice were found to develop enhanced NFT pathology when compared to single tau-Tg littermates. These studies were further extended by Oddo and colleagues who developed a triple transgenic mouse model (3xTg-AD) harbouring mutant APP, PS1 and tau transgenes which showed accelerated development of tau pathology compared to the single tau-Tg littermates (150). This model also demonstrated that the NFT pathology developed several months after the extracellular Aβ deposition, supporting the hypothesis that Aβ accumulation can accelerate, if not initiate, the development of NFT lesions – a notion consistent with the proposed amyloid hypothesis for AD pathogenesis.

Despite the failure of the earlier Tg models to recapitulate the widespread loss of neurons seen in human AD brains, some of the recently developed APP-Tg mice exhibit robust loss of neurons in brain areas affected in AD pathology. For example, the recently developed APP^{SL}PS1KI line (151, 152) and 5XFAD (153) mice show significant loss of hippocampal CA1/2 neurons and the pyramidal neurons of cortex, respectively. In both these models, neuron loss precedes intraneuronal Aβ accumulation, suggesting potential involvement of intraneuronal Aβ in AD pathology (154-156). A more recent regulatable transgenic model (rTg3696AB) of AD, which generates both human Aβ and tau in the brain, displays a striking degree of neuronal loss in the hippocampus and cortex, as observed in AD pathology (157). Why most of the APP-Tg models do not exhibit significant loss of neurons in spite of a robust Aβ pathology remains unclear, but may relate to the different combinations of FAD mutants, expression levels of mutant proteins, promoters used in each line and/or up-regulation of survival mechanisms to protect neurons against Aβ-induced toxicity. Regardless of the phenotypes, these models provide evidence for the role of Aβ peptides in AD neuropathology and also are found to be invaluable, to some extent, in the development of future therapeutics.

Table 1.2: Summary of the widely used APP-Tg mouse models of AD

Transgenic line	Mouse strain	Transgenic Construct	Gene Mutation	Promoter	Transgene Expression level	Age of Onset of Aβ deposits	Neuropathology	Refs.
PD-APP	C57BL6 x DBA2 x Swiss Webster	Human APP770 minigene expressing APP 695, 751 and 770 isoforms	APP: V717F	Human *PDGF-β*	10x	6 months	High Aβ42 levels, age-dependent Aβ deposits (mostly diffuse plaques), dystrophic neurites, gliosis, synaptic loss, impaired spatial memory but no neuronal loss or NFTs	(137, 140, 145)
Tg2576	C57BL6 x SJL	Human APP695 cDNA	APP: KM670/671NL	Hamster *PrP*	5.5x	9 months	Impaired learning and memory deficits accompanying increased Aβ40 (5-fold) and Aβ42 (14-fold) levels, diffuse and dense cored Aβ plaques, dystrophic neurites, tau hyperphosphorylation, gliosis, vascular amyloidosis without any neuron loss or NFTs	(138)
APP23	C57BL6 x DBA/2	Human APP751 cDNA	APP: KM670/671NL	Murine *Thy1*	7x	6 months	High Aβ42 levels, limited hippocampal CA1 neuronal loss correlated with Aβ plaques, age-dependent cognitive decline prior to amyloid deposition, cerebral vascular amyloidosis, hyperphorylated tau in distorted neurites surrounding the congophilic plaques but no NFTs	(139, 144)

Table contd……..

Table 1.2 continued …...

Transgenic line	Mouse strain	Transgenic Construct	Gene Mutation	Promoter	Transgene Expression level	Age of Onset of Aβ deposits	Neuropathology	Refs.
TgCRND8	C3H/He x C57BL6	Human APP695 cDNA	APP: KM670/671NL, V717F	Hamster *PrP*	5x	3 months	Early-onset Aβ plaques and neuritic pathology, high Aβ42 levels associated with early cognitive deficits, gliosis and tau hyperphosphorylation but no neuronal loss or NFTs	(136)
PSAPP	C57BL6-SJL x Swiss webster/B6 D2F1	HuAPP695 cDNA; PS1 cDNA	APP: KM670/671NL; PS1: M146L	APP: Hamster *Prp;* PS1: rat *PDGF-β*	APP: 5.5x; PS1:2-3x	6 months	Incresed Aβ42(43) levels, accelerated Aβ plaques, gliosis, reduced performance in a Y-maze reflecting hippocampal dysfunction	(143)
3xTg-AD	129 x C57BL6	Human APP695 and 4R0N[$]-Tau cDNA in PS1 knockin background	APP: KM670/671NL; Tau: P301L; PS1: M146V	APP & Tau: Murine *Thy1.2*	APP & Tau: 2-4x in hemizygous and 4-8x in homozygous	6 months	Age-dependent Aβ plaques, followed by the developement of NFTs (12 months), synaptic dysfunction including LTP deficits appearing before plaque and tangle pathology	(150)
5xFAD	C57BL6 x SJL	Human APP695and PS1 cDNA	APP: KM670/671NL, I716V, V717I; PS1: M146L, L286V	Murine *Thy1*	APP: <5.5x; PS1: not mentioned	2 month	Increased Aβ42 level, intraneuronal Aβ accumulation preceeding amyloid deposition, gliosis, synaptic and neuronal loss, spatial learning deficits, no NFTs	(153)
rTg3696AB	FVB/N x 129S6	Human APP695 and 4R0N-Tau cDNA	APP: KM670/671NL, V717I; Tau: P301L	*CAMKII*	APP & Tau: 3x	4 months	Age-dependent Aβ plaques, followed by NFTs, gliosis and neuron loss	(157)

[$]4R0N : four repeat tau without amino terminal inserts

1.4.5 Cholesterol and APP metabolism

The first evidence that cholesterol may impact Aβ production in the brain was provided in 1994, when Sparks et al. (158) demonstrated that dietary cholesterol increases amyloid production in rabbits. Since then a great deal of work has been carried out to investigate the influence of cholesterol on APP processing and/or Aβ generation. Cholesterol, being an integral part of the membrane, can influence multiple functions including endocytosis and translocation of substrates to proteins embedded in the membrane. The distribution of cholesterol within membrane, however, is not uniform and its content increases as the membranes move from the ER through the Golgi apparatus to the plasma membrane (159). There is also evidence of marked asymmetry in the dispersion of cholesterol between the two leaflets of the bilayer, with ~85% of the total membrane cholesterol residing in the cytofacial leaflet and ~15% in the exofacial leaflet. The importance of asymmetric distribution across the extracellular and cytoplasmic faces of the lipid bilayer is not fully understood, but its modification can influence membrane fluidity as well as normal functioning of the cell (160, 161). Interestingly, the lateral dispersion of cholesterol in any given part of the membrane is also not uniform as some patches, termed lipid-rafts, are more highly enriched with cholesterol than the neighboring non-raft regions. Lipid-rafts are detergent-resistant dynamic assemblies of membrane proteins and lipids that float freely within the membrane bilayer and have been implicated in intracellular trafficking of proteins, transmembrane signaling, lipid and protein sorting and regulated proteolysis (162-164). Within these raft domains, cholesterol enables orderly packing of the sphingolipids and gangliosides along with certain types of proteins that tend to intercalate with the raft structure. Removal of cholesterol therefore results in dissociation, deregulation and/or inactivation of most raft proteins. Although lipid-rafts are highly abundant at plasma membrane, they are assembled first in the Golgi and are evident in the anterograde vesicles trafficking from the Golgi to the plasma membrane. These rafts are constantly endocytosed from the plasma membrane *via* endocytic pathway and then either recycled back to plasma membrane or returned to Golgi apparatus. Considering that APP and its processing enzymes are associated with lipid-raft domains (165, 166), it is likely that components of membrane cholesterol can modulate Aβ production, aggregation and clearance. Additionally, there is evidence that intracellular

cholesterol distribution within subcellular compartments can affect trafficking of APP and/or its processing enzymes, leading to altered levels of Aβ production. This has been demonstrated using both *in vitro* cell culture and mouse models having altered subcellular cholesterol distribution caused by genetic or pharmacologic manipulation of proteins involved in cholesterol metabolism like NPC1 and ACAT1. Although precise mechanisms remain to be established, we have herein provided, following a brief overview of APP proteolytic processing, the current understanding on how membrane and subcellular cholesterol levels/distribution can influence Aβ generation by regulating alternative APP processing pathways.

1.4.5a APP processing and Aβ generation

Aβ peptides, the principal component of neuritic plaques in AD brains, are a group of hydrophobic peptides containing 39-43 amino acid residues derived by sequential proteolytic processing of APP (111, 124, 135, 167, 168). Mature APP is proteolytically processed by either the non-amyloidogenic α-secretase or amyloidogenic β-secretase pathways (Fig. 1.3). The α-secretase activity cleaves the Aβ domain within Lys^{16} and Leu^{17} residues, thus precluding the formation of full-length Aβ peptide. This pathway yields a soluble N-terminal APPα (sAPPα) and a membrane tethered 10kD C-terminal fragment (α-CTF or C83) that can be further processed by γ-secretase to release an extracellular 3kD P3 peptide (i.e., $Aβ_{17-40}$ or $Aβ_{17-42}$) and the cytoplasmic APP intracellular C-terminal domain (AICD) fragment (Fig. 1.3A). The α-secretase cleavage occurs mostly at the cell surface, although it can be mediated to some extent during the secretory intracellular trafficking of APP (126, 135, 169, 170). The identity of α-secretase is somewhat complicated as several enzymes including three members of a disintegrin and metalloprotease (ADAM) family, namely ADAM9, ADAM10 and ADAM17, have been shown to cleave APP within Aβ domain (171, 172). However, the majority of studies suggest that ADAM10 can act as a major α-secretase in the brain (173, 174).

The amyloidogenic β-secretase pathway, which results in the formation of intact Aβ peptide, is mediated by the sequential actions of β-secretase and γ-secretase enzymes (Fig. 1.3A). The β-secretase cleavage generates a truncated soluble APPβ (sAPPβ) and a

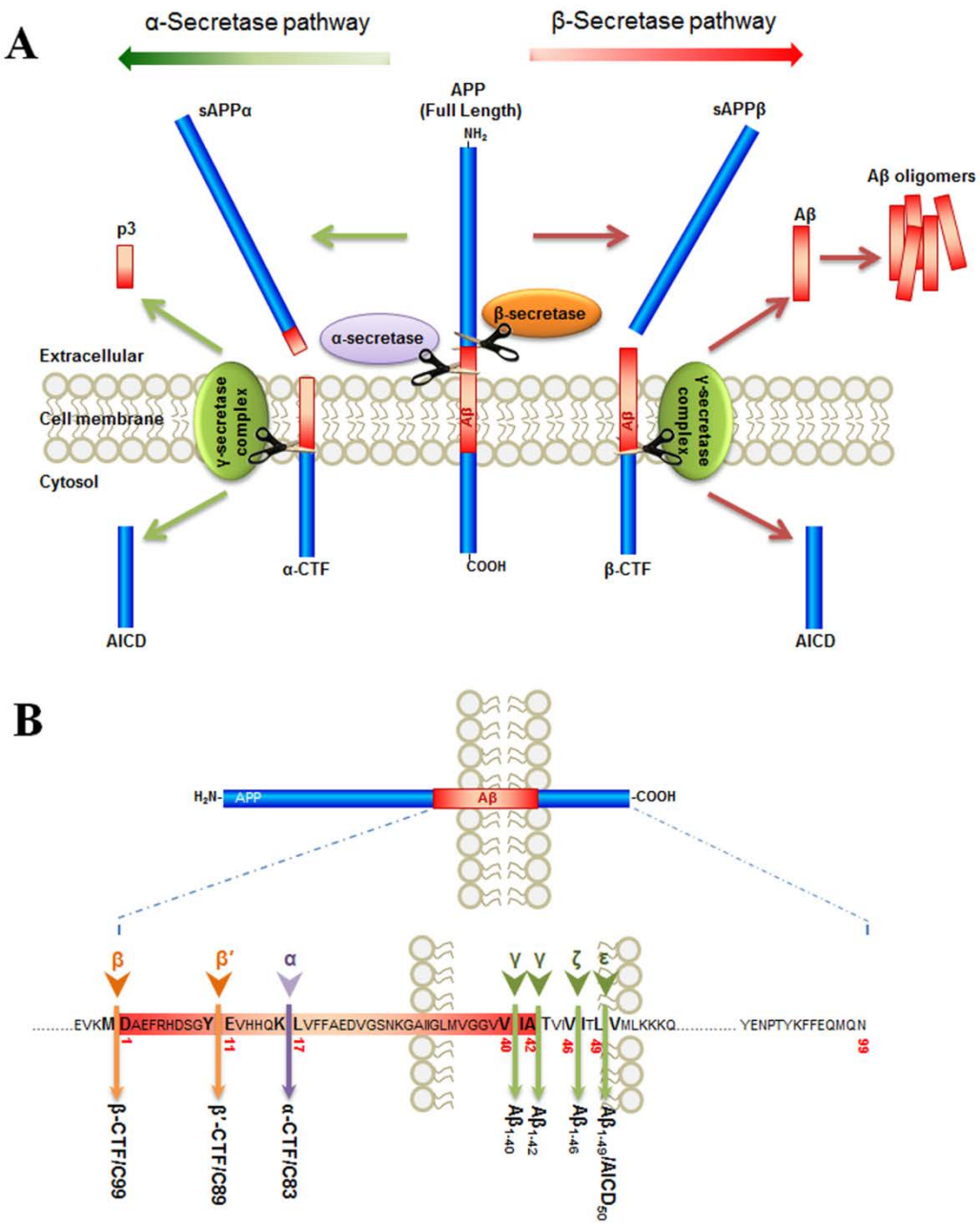

Figure 1.3. (A) Alternate processing of APP. The α-secretase pathway (left) involves sequential cleavages by α- and γ-secretases resulting in the generation of a soluble N-terminal APP fragment (sAPPα) and C-terminal fragments (p3 and AICD). The amyloidogenic β-secretase APP processing pathway (right) involves initial cleavage by β-secretase followed by γ-secretase resulting in the generation of a soluble N-terminal sAPPβ fragment, full-length Aβ peptide and AICD. Aβ peptides oligomerize and provide the initial trigger to AD pathogenesis. **(B)** APP processing enzymes and their cleavage sites. The amino acid sequence of Aβ and the APP carboxy-terminal region are shown in single letter amino acid codes. The left orange arrows indicate the β- and β'-cleavage sites of BACE1. The middle purple arrow indicates the α-secretase cleavage site, which precludes the formation of full-length Aβ. The right green arrows indicate the multiple cleavage sites for γ-secretase, which are located within the transmembrane region. The major products of the cleavages are mentioned at the bottom of the respective arrows.

membrane bound Aβ-containing C-terminal fragment (β-CTF or C99). Further proteolysis of the β-CTF by γ-secretase yields the full-length Aβ peptides and the AICD (64, 65, 175-179). The γ-secretase can cleave at multiple sites within the transmembrane domain of APP, generating Aβ peptides of various lengths (see Fig. 1.3B) (180, 181). Cell culture studies have suggested that the majority of Aβ is generated in the endosomal recycling pathway, while a minority of the peptides is produced in the secretory pathway within the ER and Golgi apparatus (Fig. 1.4) (168, 182-186). Under normal conditions ~90% of secreted Aβ peptides are $A\beta_{1-40}$, a soluble form of the peptide that can slowly convert to an insoluble β-sheet configuration. In contrast, ~10% of secreted Aβ peptides are $A\beta_{1-42/43}$, species that are highly fibrillogenic and are more toxic to neurons than $A\beta_{1-40}$ (64, 65). β-secretase is an aspartyl protease called β-site APP cleaving enzyme 1 (BACE1) that localizes predominantly in the late-Golgi/trans-Golgi network (TGN) and endosomes, consistent with amyloidogenic processing of APP during secretory and endocytic/recycling pathways (168, 179, 184, 187). The γ-secretase, on the other hand, comprises the aspartyl protease PS1/2 and three cofactors [i.e., nicastrin, presenilin enhancer protein 2 (PEN-2) and anterior pharynx defective 1 (APH-1)] that are required for substrate recognition, complex assembly and targeting the complex to its site of action (188-193). The assembly of γ-secretase complex starts with the stabilization of nascent PS1 by nascent nicastrin and APH-1 followed by PEN-2 to complete the assembly process (194). Gene knockout, knockdown and mutational studies have established that PS1 is the catalytic subunit of γ-secretase (178, 192, 195). There is also evidence that PS1, apart from being a part of the enzyme complex, may be involved in the acidification of lysosomes and regulation of neurotransmitter release from the brain (196, 197). Some studies suggested that α- and β-secretases may compete for APP substrate and thus increased activity of one pathway may result in decreased processing by the other. In normal cells the non-amyloidogenic pathway usually dominates over the amyloidogenic pathway, but the relative activities of these alternative pathways can be regulated by a variety of factors, including the stimulation of receptors for neurotransmitters and growth factors (198, 199). The influence of cholesterol on amyloid formation is of particular interest in view of the evidence that intracellular trafficking and localization of APP and

components of its processing enzymes are regulated by levels/distribution of cholesterol within the cells (Fig. 1.4).

1.4.5b Cholesterol and Aβ production under *in vitro* paradigms

A large number of experiments performed using primary neurons or peripheral cell lines show that increase in cellular cholesterol levels can enhance Aβ production and reduce α-secretase cleavage of APP (200, 201). Conversely, reducing cholesterol levels by stripping off the membrane cholesterol with methyl-β-cyclodextrin or by treating with HMGCR inhibitors can enhance α-secretase cleavage and inhibit Aβ production (201-205) (see Table 1.3). One possible explanation for the alteration of APP processing through the modification of cellular/membrane cholesterol levels is that the localization of APP and its secretases are differentially affected by lipid composition, thereby altering the cleavage of APP. Accumulated evidence clearly indicates that α-secretase ADAM10 mostly resides in the low-cholesterol non-raft domains (204), whereas a subset of β-secretase BACE1 and four components of γ-secretase are associated with lipid-raft domains of the membrane (206-209). APP, on the other hand, is believed to exist in two separate pools within the cell membrane, one associated with lipid-rafts and other in the phospholipid-rich domain (210). These observations raised the possibility that the amyloidogenic processing of APP occurs in cholesterol-rich lipid-rafts, while the non-amyloidogenic processing occurs mainly in the phospholipid-rich regions of the membrane outside the rafts, and that altering cellular cholesterol levels regulates the processing of APP through these two pathways. Under physiological conditions only very minor amounts of APP appear to be present in detergent-resistant rafts (165, 211), thereby making α-secretase pathway the predominant pathway. However, increasing membrane cholesterol levels may elevate the percentage of rafts in the membranes and consequently enhance the activity/contact between APP and their processing enzymes BACE1 and γ-secretase, leading to increased production of Aβ peptides. This notion is supported by three distinct lines of elegant experiments: i) targeting BACE1 exclusively to the lipid-rafts by adding glycosylphosphatidylinositol (GPI)-anchor strongly upregulates its activity (212), ii) antibodies cross linking APP and BACE1 showed that these two proteins copatched with raft markers and dramatically increase the production

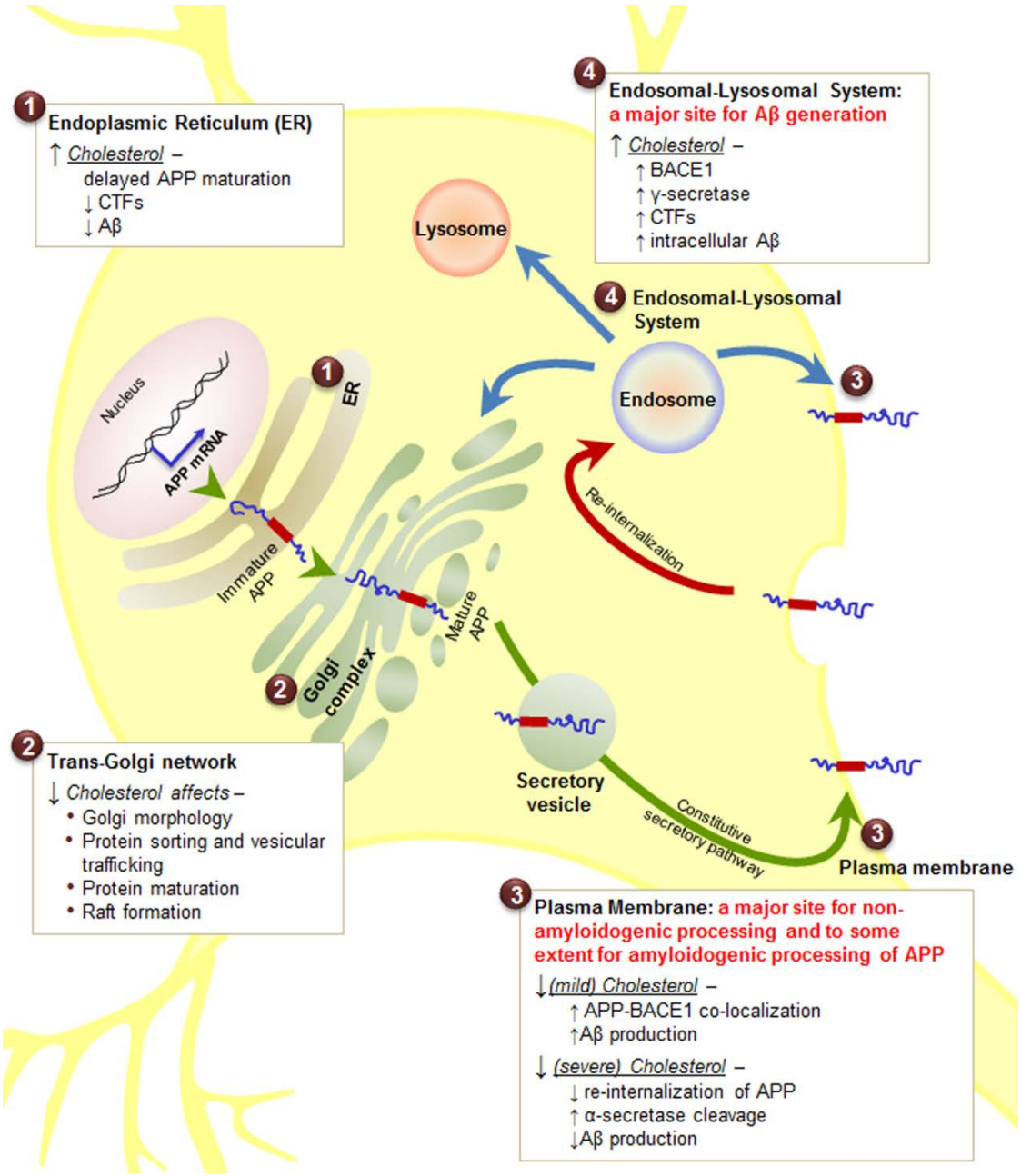

Figure 1.4. Influence of altered cholesterol levels in different cellular compartments on APP processing. Newly synthesized APP molecules are trafficked in the constitutive secretory pathway (green arrow) following full maturation of the holoprotein in the endoplasmic reticulum (ER) and trans-Golgi network. Aβ can be generated during this transit within the ER and/or Golgi network and secreted as part of the constitutive secretory pathway. Alternatively, full-length APP can travel to the plasma membrane, where it is predominantly cleaved by α-secretase, precluding the generation of intact Aβ peptides. A subset of APP is reinternalized (red arrow) into the endocytic compartments from where some APP is subsequently trafficked (blue arrows) back to the cell surface or to the lysosomes. Amyloidogenic processing occurs during passage through the endocytic organelles, where APP encounters β- and γ-secretases. Transport of APP from the endosomes to the Golgi mediated by retromers can also occur prior to its cleavage. Cholesterol level/distribution in different cellular compartments including the ER, Golgi network, plasma membrane and endosomal-lysosomal system can influence the outcome of Aβ production.

of Aβ peptides in a cholesterol-dependent manner (210) and iii) inhibition or absence of γ-secretase activity can lead to increased accumulation of APP-CTFs in the lipid-raft microdomains (208).

A decrease in cholesterol levels which may disrupt the integrity of lipid-raft domains, on the other hand, can increase the activity of α-secretase, leading to non-amyloidogenic processing of APP. This mechanism may partly involve accumulation of APP at the cell surface and altered membrane fluidity (204). In contrast, selective removal of membrane cholesterol by methyl β-cyclodextrin was found to decrease soluble APPα levels in human embryonic kidney cells transfected with human APP751, indicating that cholesterol reduction may under certain conditions restrict the interaction between APP and α-secretase (200). Additionally, it has been demonstrated that a mild reduction in membrane cholesterol (<25%) in cultured hippocampal neurons can paradoxically increase Aβ production by promoting β-secretase cleavage of APP, whereas a significant depletion in membrane cholesterol (>35%) can lead to a marked decrease in Aβ production. It is suggested that moderate reduction in cholesterol level triggers displacement of BACE1 from raft domains and promotes its proximity to APP in non-raft domains, leading to increased amyloidogenic processing of APP (202). Thus, it is likely that the extent of cholesterol depletion may have a critical role in determining the outcome of Aβ production. The cholesterol lowering drugs statins also appear to have two opposing actions on Aβ metabolism. While reduced cholesterol levels as a consequence of statin treatment of cells favored the α-secretase pathway and decreased Aβ secretion, the cholesterol-independent effects of statins, decreasing isoprenoid levels, resulted in the accumulation of APP, amyloidogenic fragments and intracellular Aβ (201, 203, 204, 213). Another critical issue that confounds proper interpretation of statin studies on Aβ production is the pleiotropic effects of cholesterol depletion on Golgi morphology and vesicular trafficking, which are consequences of changes in both membrane fluidity and curvature (214-216). Whether the responsiveness of APP processing to cholesterol metabolism reflects a role for cholesterol alone or the presence of other factor(s) in the lipid environment common to many membrane bound proteins remains to be determined.

In addition to the effect of cholesterol on membrane lipid ordering, defective transport and/or excess accumulation of cholesterol in the subcellular compartments have also been shown to regulate proteolytic processing of APP. This is supported by the evidence that a dose-dependent reduction in secreted Aβ species occurs in cultured neurons and neuroblastoma cells exposed to a cholesterol transport-inhibiting agent, U18666A (217, 218). It has been suggested that inhibition of cholesterol transport from the endocytic compartment to the ER may affect re-internalization of surface APP, leading to decreased production of Aβ-related peptides. On the other hand, retention of cholesterol in the EL compartment induced accumulation of γ-secretase along with β-CTF and Aβ-related peptides in the vesicular organelles involved in cholesterol sorting (218, 219). Another intriguing observation was that cholesterol esters derived from free cholesterol by the action of the enzyme ACAT have also been shown to modulate Aβ production. Inhibiting ACAT function in cells by genetic or pharmacological means can suppress Aβ generation, whereas increasing the levels of cholesterol esters can have the opposite effects (21). These data, however, indicate that reduction of ACAT activity decreases both α- and β-CTF products simultaneously, thus suggesting an indirect modulation of APP processing. Indeed, recently it has been demonstrated that ACAT inhibition causes delayed maturation of full-length APP in the early secretory pathway, thus limiting its availability for processing by secretases (220). It appears that the ratio between free and total cholesterol regulated by the enzyme ACAT may have a critical role in influencing generation/secretion of Aβ peptides. There is evidence that increased cholesterol efflux mediated by ABCA1 decreases Aβ production by reducing BACE1 and γ-secretase cleavage of APP (221, 222). Sphingolipids, another major constituent of membrane raft domains, are also involved in the regulation of APP processing. Lowering sphingolipid levels either by inhibiting serine palmitoyltransferase, which is involved in an early step of sphingolipid biosynthesis or by mutating one of the serine palmitoyltransferase enzyme subunits, elevates α-secretase cleavage (223).

Table 1.3: Effects of modulating cholesterol levels on APP processing under i*n vitro* conditions

Cholesterol modulation	Cell type used	Experimental condition	Effects on APP processing	References
↑ Cholesterol	HEK 293 cells stably transfected with APP_{751}	Exogenous cholesterol solubilized in methyl-β-cyclodextrin or ethanol	↑ mature and immature APP; ↓ sAPPα and total soluble APP production	(200)
↑ Cholesterol	HEK cells transfected with APP_{695}	Exogenous cholesterol solubilized in methyl-β-cyclodextrin added	↑ intracellular β-secretase cleavage products; ↑secreted $Aβ_{40}$ and $Aβ_{42}$	(201)
↓ Cholesterol	Rat hippocampal neurons	Cholesterol depleted by 70% using methyl-β-cyclodextrin or lovastatin	↓β-CTF and Aβ production; no change in total sAPP	(205)
↓ Cholesterol	HEK cells transfected with APP_{695}	Cholesterol depleted using lovastatin	↓ intracellular β-secretase cleavage products; ↓secreted $Aβ_{40}$	(201)
↓ Cholesterol	Rat hippocampal and mixed cortical neurons expressing SFV-human APP	Cholesterol depleted using simvastatin or lovastatin	↓ β-CTF and secretory and intracellular Aβ production	(203)
↓ Cholesterol	HEK 293 and SHSY5Y cells	Cholesterol depleted using methyl-β-cyclodextrin or lovastatin	↑ sAPPα production; ↓ Aβ production	(204)
↓ Cholesterol (~30%)	Rat hippocampal neurons and CHO cells constitutively expressing human APP	Moderate cholesterol reduction by mevilonin and methyl-β-cyclodextrin	↑ β-CTF and Aβ production	(202)
↓ Cholesterol	HEK293cells stably transfected with Swedish mutant human APP_{695}; SH-SY5Y cells; Primary cortical neurons and astrocytes from Tg2576 mice	Cells treated with lovastatin or simvastatin in presence or absence of mevalonate	↑ sAPPα and C83 production; ↓ Aβ secretion	(213)

A number of recent studies have indicated that cholesterol can interact directly with β-CTF and possibly APP to form a complex, which may favor amyloidogenic pathway by promoting localization of APP/β-CTF to cholesterol rich membrane domains and organelles where γ-secretase and β-secretase reside (224). Earlier studies have shown that under the conditions of high cholesterol, cholesterol can bind APP and Aβ directly at the α-secretase cleavage site, which leads to the inhibition of the α-secretase activity and increased production of Aβ peptides (225). It has been suggested that a central hydrophobic cluster located on residues 17-21 (LVFFA) of Aβ peptide, which is critical in peptide aggregation, may participate in cholesterol binding. These results, taken together, suggest that cholesterol binding can also directly influence generation as well as aggregation of Aβ peptide (226, 227).

1.4.5c Cholesterol and Aβ production under *in vivo* paradigms

In keeping with data from *in vitro* experiments, numerous *in vivo* studies have provided cogent examples for the involvement of cholesterol in APP processing (see Tables 1.4, 1.5). However, the results are somewhat equivocal and the underlying mechanisms have not been as well studied. The first experimental evidence of interplay between cholesterol and APP processing revealed that a high-cholesterol diet for as short as 4 weeks can increase Aβ immunoreactivity in rabbit hippocampal neurons (158). This result has been extended to guinea pigs (203), African green monkeys (228) and transgenic mice overexpressing mutant APP – all showing a strong correlation between plasma cholesterol and Aβ levels. Experiments with one line of APP transgenic mice showed that a high cholesterol diet can increase Aβ levels and plaques burden, while treating these mice with a cholesterol lowering drug can decrease serum cholesterol levels along with Aβ production and deposition in the brain (229, 230). Several additional studies in related transgenic mouse models have also supported the notion that elevated peripheral cholesterol levels can increase brain Aβ production and deposition (231-239). However, other studies have reported that increased plasma cholesterol may be associated with unchanged (240) or even reduced Aβ levels (241, 242), while lowering plasma cholesterol may either decrease (243), not affect (240) or even elevate (244) brain Aβ levels. Thus the impact of altering plasma cholesterol *in vivo* on brain Aβ remains

Table 1.4: Effects of increasing peripheral cholesterol levels on APP metabolism *in vivo*

Animal Model	Modulation of peripheral cholesterol	Effect on Brain Cholesterol levels	Effects on APP processing	References
Adult female rabbits	Fed on 2% cholesterol diet for 4, 6 or 8 weeks	Not determined	↑ intraneuronal Aβ immunoreactivity and extracellular Aβ deposits	(158)
APPswe mice of 210-408 days of age	Fed on high-cholesterol diet (5%) for 8 weeks	Increasing trend in total brain cholesterol although not significant	↓ $A\beta_{40}$ and $A\beta_{42}$ levels; ↓ sAPPα and sAPPβ production	(242)
PSAPP (Tg2576 x PS1M146V) mice at 5 wks	Fed on 5% high-fat/high-cholesterol diet for 7 weeks	↑ total CNS cholesterol	↑ Aβ levels and deposits; ↑ β-CTF production; ↓ sAPPα production	(229)
Female APP-Tg (Tg2576) mice at 2 months of age	Fed on high-fat/high-cholesterol diet for 7-9 months	Not determined	↑ Aβ deposition	(238)
Male APPswe mice	Fed on high fat/high cholesterol Western-type diet until 1 year	↑ cerebral cholesterol levels	↑ Aβ levels	(235)
Male African green monkeys	Fed on high saturated fat diet for 5 years	Not determined	↑ Aβ deposition	(228)
APP-Tg (B6Tg2576) mice at 7-9 months of age	Fed on high- fat/high-cholesterol diet for 4 months	Not determined	↑ Aβ deposits	(236)
Female APP-Tg (Tg2576) mice at 12 months of age	Fed on high-fat/high-cholesterol diet for 6 weeks	↑ total brain cholesterol	↓ $A\beta_{40}$ levels; ↓ sAPPα production; ↑ AICD	(241)
Adult female rabbits	Fed on 1% cholesterol diet for 7 months	No alteration in free cholesterol levels but ↑ cholesterol content of CA1 neurons	↑ β-CTF production; ↑ $A\beta_{42}$ levels and deposition	(231)

Table contd……

Table 1.4 continued …..

Animal Model	Modulation of peripheral cholesterol	Effect on Brain Cholesterol levels	Effects on APP processing	References
New Zealand white male rabbits (1.5–2 years old)	Fed with 2% (w:w) cholesterol for 12 weeks	Not determined	↑ hippocampal and cortical $A\beta_{40/42}$ levels ; ↑ aggregated Aβ only in cortex	(234)
PDGFB-APPwt mice (4-months old)	Fed on high fat/cholesterol diet for 2 months	Not determined	↑ cortical levels of $A\beta_{40}$ with no significant change in $A\beta_{42}$; ↑ CTF level	(239)
Adult male Wister rats	Fed on 2% cholesterol diet for 15 days	No alteration	Aβ levels remained unaffected	(240)
APP/PS1 mice (6-months old)	Fed on high cholesterol diet for 12months	No alteration	↑ plaque burden	(232, 233)
TgCRND8 mice (4-wks old)	Fed on high fat diet from 4 wks until 18 wks of age	Not determined	↑ brain levels of solubilizable Aβ; no effect on plaque burden	(237)

Table 1.5: Effects of decreasing peripheral cholesterol levels on APP metabolism *in vivo*

Animal Model	Modulation of peripheral cholesterol	Effect on Brain Cholesterol levels	Effects on APP processing	References
Adult male guineapigs	Treated with high dose of simvastatin (0.5%) for 3 weeks	No alteration in total brain cholesterol levels; ↓ lathosterol : cholesterol, ↓ *de novo* brain cholesterol synthesis	↓ $A\beta_{40}$ and $A\beta_{42}$ levels	(203)
8 week old male and female PSAPP (Tg2576 x PS1M146V) mice	Treated with a daily dose (250 mg/kg) of cholesterol lowering drug BM15.766 for 5 weeks	↓ Brain cholesterol levels	↓ Aβ load and levels and β-CTF production; ↑ sAPPα production	(230)
8 week old male and female PSAPP (Tg2576 x PS1M146V) mice	Treated with Lipitor at 30 mg/kg b.wt.[1]/day, p.o.[1], for 8 wks.	No alteration of CNS cholesterol levels	↓ $A\beta_{40}$ and $A\beta_{42}$ levels and accumulation	(243)
12 month-old male and female APP-Tg (Tg2576) mice	Treated with 0.2% (100 mg/kg per day) lovastatin for 3 weeks	Not determined	↑ $A\beta_{40/42}$ levels and deposition, sAPPβ and CTFβ in female mice; no change in male mice	(244)
Adult male Wister rats	Simvastatin (10-20 mg/kg b.wt.) or atorvastatin (10-20 mg/kg b.wt.) for 15 days	↓ Brain lathosterol and cholesterol synthesis rate	Aβ levels remained unaffected	(240)

[1]b.wt.: body weight; p.o.: peroral (oral administration)

controversial and the reasons for the apparent discrepancy may reside in either the genetic background of the mice used, the transgenes present in mouse models, variability in age, gender of the animals and/or treatment conditions. More importantly, given the fact that cholesterol in the brain is synthesized *de novo* and little or none of the peripheral cholesterol can cross an intact BBB, the extent to which dietary/peripheral modulation of cholesterol can influence cerebral cholesterol homeostasis remains ambiguous. Unfortunately, many of these studies have reported effects of a high-cholesterol diet on levels of Aβ and other molecules in the brain without actually assessing whether brain cholesterol levels are changed by the same treatment (Tables 1.4, 1.5). Thus, it is unclear as to whether the alteration of cerebral APP processing was a direct consequence of alteration in brain cholesterol or some indirect mechanisms triggered by modulation of peripheral cholesterol.

Apart from regulating serum cholesterol levels either by diet or pharmacological treatments, a number of studies have used genetic models of cholesterol loading or depletion to evaluate the potential role of brain cholesterol metabolism in APP processing (see Table 1.6). Some of the initial studies with APP transgenic mice where ApoE expression was knocked down showed a dramatic decrease in fibrillar Aβ levels and deposits (245-248). Modulation of expression of LDLR, the major ApoE receptor in the brain, however, generated inconsistent results, with LDLR downregulation leading to both unaltered or increased Aβ deposition and LDLR overexpression triggering decreased Aβ deposition (249-251). Surprisingly, however, lowering the peripheral cholesterol by deficiency of ApoAI, the primary plasma-lipoprotein in mice, which also resulted in reductions in brain cholesterol without any effect on brain ApoE levels, showed no difference in Aβ pathology (252). The reason for these inconsistent results from studies modulating cholesterol transport/uptake in the brain is not entirely clear but may be due to influences of ApoE on Aβ aggregation and clearance. Mice deficient in the cholesterol synthesizing enzyme seladin-1 showed lowered brain cholesterol levels and increased production of Aβ peptides through the amyloidogenic pathway, whereas opposite effects were found in seladin-1 overexpressing mice (253). Studies from AD patients also revealed that seladin-1 is down regulated in brain areas exhibiting high levels of amyloid

deposition (254, 255). Additionally, while hippocampal samples from normal human brains showed only a small pool of endogenous APP is colocalized with BACE1 in a detergent-soluble membrane fraction, samples from AD brains with a moderate reduction in membrane cholesterol levels demonstrated much higher levels of APP and BACE1 colocalization. These results suggest that a mild reduction in membrane cholesterol levels may enhance the colocalization of APP and BACE1 in the detergent-soluble membrane fraction which can lead to increased production of Aβ peptides (202, 256). Interestingly, a 50% reduction of cholesterol synthesis in the brain caused by genetic deletion of the cholesterol 24-hydroxylase gene did not significantly affect APP expression and amyloid plaque deposition in the cortex and hippocampus of mutant APP-Tg mice. It is suggested that decreased cholesterol synthesis was balanced by an equivalent reduction in cholesterol turnover with no apparent change in the steady-state brain cholesterol levels (257). There is also evidence that deficiency in the cholesterol transporter ABCA1 can increase Aβ deposition in mutant APP transgenic mice with a significant reduction in total brain ApoE (28, 258, 259), whereas overexpression of the transporter can have the reverse effects (260). In a complementary approach, ACAT gene ablation in 3xTg-AD not only reduces amyloid plaques and $A\beta_{1-42}$ levels but also ameliorates cognitive deficits (261). This is consistent with the results obtained with the *in vivo* inhibition of ACAT activity by the drug CP-113818 in mutant APP transgenic mice (262). However, given the evidence of an extremely high ratio between free and esterified cholesterol in the adult human brain, it is somewhat difficult to understand how ACAT could be capable of modulating APP processing under *in vivo* conditions (10). Additionally, down-regulation of ABCA2 has been recently demonstrated to reduce Aβ production by altering maturation and subcellular localization of nicastrin (263).

Accumulation of free cholesterol within brain neurons caused by mutation of the *NPC1* gene have shown to increase the intracellular levels of Aβ peptides (219, 264) along with redistribution of PS1 from ER to rab5-positive early endosomal compartments (265, 266). This is consistent with the observed increase in intraneuronal Aβ in human NPC brains (219). Using Npc1-deficient mice, we have also found that the levels and expression of APP and BACE1 are elevated in the more severely affected cerebellar

Table 1.6: Effects of genetic modulation of different cholesterol metabolism genes on APP and Aβ metabolism

Approach	Model studied	Effect on brain cholesterol metabolism	Effect on APP metabolism	References
Modulating cholesterol synthesis	Seladin1$^{+/-}$ mice	↓ cholesterol levels and disorganized cholesterol-rich detergent-resistant membrane domains	↑$A\beta_{40}$ and $A\beta_{42}$ levels	(253)
Modulating intracellular cholesterol trafficking/ distribution	Acat1$^{-/-}$ x 3xTg-AD	↑ 24S-OH cholesterol; ↓HMGCR; ↓sterol synthesis	↓ human APPsw, sAPPα, β-CTF and Aβ; ↓Aβ deposition	(261)
	Npc1$^{-/-}$ mice	Intracellular cholesterol accumulation	↑ $A\beta_{40}$ and $A\beta_{42}$; ↑APP-CTFs	(266, 267)
	Npc1$^{+/-}$ x APP/PS1	Not determined	↑ $A\beta_{42}$ levels; ↑Aβ deposition	(268)
	Abca2$^{-/-}$ mice	Not determined	↓ Aβ generation by altered γ-secretase processing	(263)
Modulating cholesterol removal/ efflux	Cyp46a1$^{-/-}$ x APPsw	↓ cholesterol turnover compensated by ↓ *de novo* cholesterol synthesis	↓ insoluble $A\beta_{40}$ and $A\beta_{42}$ but no alteration in plaque deposition	(257)
	Abca1$^{-/-}$ x APP23	↓ lipidated-ApoE levels	↑Aβ deposition and cerebral amyloid angiopathy; no change in APP, sAPP or CTF levels	(258)
	Abca1$^{-/-}$ x APP-Tg-SwDI/B; Abca1$^{-/-}$ x APP/PS1	↓ lipidated-ApoE levels	↑Aβ deposition only in APP-Tg-SwDI/B; no alteration in APP and Aβ levels	(28)
	Abca1$^{-/-}$ x PDAPP	↓ lipidated-ApoE levels	↑Aβ levels and deposition; no change in APP or CTF	(259)
	Abca1/PDAPP -Tg mice	↑ lipidated-ApoE levels	↓ Aβ levels and deposition; absence of thioflavine S-positive amyloid plaques	(260)

Table contd…

Table 1.6 continued…..

Approach	Model studied	Effect on brain cholesterol metabolism	Effect on APP metabolism	References
Modulating cholesterol transport and uptake	$ApoE^{-/-}$ x Tg2576; $ApoE^{-/-}$ x PDAPP	Not determined	↓ Aβ deposition; absence of thioflavine S-positive amyloid deposits; altered anatomical distribution of Aβ deposits; no alteration in total Aβ and $Aβ_{42}$ levels	(245-248)
	$ApoAI^{-/-}$ x PDAPP	↓ brain cholesterol; unaltered ApoE levels	No effect on $Aβ_{40/42}$ levels or plaque load	(252)
	$LDLR^{-/-}$ x PDAPP	No effect on brain cholesterol levels; ↑ ApoE levels	No effect on Aβ levels or deposition	(250)
	$LDLR^{-/-}$ x Tg2576	↑ ApoE levels	↑Aβ deposition	(249)
	LDLR x APP/PS1 Tg mice	↓ ApoE levels	↓ Aβ deposition and ↑ Aβ clearance	(251)

region prior to changes in the relatively less affected hippocampus, whereas γ-secretase components are enhanced in both brain regions at the same time. Interestingly, a subset of reactive astrocytes, which under normal conditions do not express APP or its processing enzymes, are found to display high levels of APP as well as β- and γ-secretase components in the Npc1-deficient mouse brains. Additionally, the levels of α- and β-CTFs were apparently increased in the cerebellum of Npc1-deficient mice (267), thus raising the possibility that enhanced levels and processing of APP may be associated with the development of pathology and/or degenerative events observed in brains. This is partly supported by a recent study which showed that partial depletion of cholesterol trafficking Npc1 protein in mice overexpressing mutant APP as well as PS1 can enhance Aβ levels and deposition (268). However, intracellular accumulation of cholesterol has not yet been established in this animal model of AD; thus it remains unclear whether the observed alterations were due to disturbances in cholesterol trafficking or the consequence of other effects. Collectively, these results suggest that cholesterol sequestration in neuronal cells can play a causal role in Aβ production, which can subsequently influence AD-related pathology.

1.4.5d Cholesterol in Aβ aggregation and neurotoxicity

In addition to its influence on APP processing, a number of studies using cultured cells and animal models have investigated the link between cellular cholesterol levels, Aβ aggregation and cell viability. Under normal physiological conditions, Aβ peptides are present mostly as a soluble monomeric isoforms without necessarily causing any dysfunction and/or death of neurons (269-271). In fact, some recent studies have suggested a neuroprotective role for monomeric $A\beta_{1-42}$ in the brain (272). However, certain pathological conditions/stimuli can trigger a complex conformational re-arrangement and self-assembly of Aβ peptides to form a heterogeneous mixture of higher molecular-weight oligomers, protofibrils and fibrils. The conversion of monomeric Aβ peptides to aggregated isoforms is necessary for the expression of its toxic effects and there is emerging evidence that soluble Aβ oligomers, but not the fibrils deposited in the neuritic plaques, are the proximate neurotoxin in AD pathology (273-279). This is substantiated by a number of studies demonstrating that levels of soluble Aβ oligomers in

the brain correlate much better than fibrils or plaques with the onset, progression and severity of AD pathology (67, 277, 278, 280-282). Although the mechanisms associated with abnormal aggregation of Aβ peptides under pathological conditions have not yet been determined, a growing body of evidence suggests that cholesterol-rich lipid-rafts may play a much more sinister role in catalyzing the conversion of the aggregation-prone Aβ peptide to its neurotoxic, oligomeric state. In fact, Aβ oligomers isolated from AD patients are found to be associated with the lipid-raft microdomains in a cholesterol-dependent manner and depletion of cholesterol was found to reduce aggregation of Aβ peptides (283). However, it is currently unclear whether a direct interaction between Aβ and cholesterol, an overall depletion in lipid-raft domains or the subsequent changes in their composition/properties can lead to reduced peptide aggregation.

It has been reported that cholesterol can facilitate Aβ aggregation through the structural modification of other lipid-raft components including gangliosides, which are glycosphingolipids with one or more sialic acid moieties attached to the sugar chain (284). Some studies have shown that ganglioside GM1 found predominantly in the CNS can bind and promote aggregation of Aβ peptides in lipid-raft microdomains (285, 286). Interaction between ganglioside sialic acid and Aβ induces a conformational re-arrangement of the peptide chain from an α-helix-rich to a β-sheet-rich structure (285, 287), leading to the generation of a GM1/Aβ complex, which acts as an endogenous seed to promote amyloid oligomerization and subsequent fibril formation (288-290). Amyloid fibrils formed in the presence of gangliosides have been shown to be the primary mediators of oxidative attack on plasma membranes (291). A recent study using reconstituted membranes revealed that cholesterol can either facilitate or inhibit the interaction of Aβ peptides with lipid-rafts through fine-tuning of the ganglioside conformation (292). This reinforces the notion that Aβ binding and aggregation within the neuronal lipid-raft domains is most likely mediated by multiple players rather than any single membrane component.

Since Aβ toxicity is associated with the aggregation state of the peptide, many studies have investigated the relationship between cholesterol and the toxic effects of Aβ

peptides. Some studies have shown that decreasing cholesterol levels can be protective and increasing cholesterol levels can render the cells vulnerable to Aβ-induced toxicity. This is supported by the evidence that i) decreasing cholesterol levels in plasma membrane can reduce toxicity whereas an increase in cholesterol level can induce higher toxicity in cultured PC12 cells (293) as well as in mixed cultures containing hippocampal neurons and astrocytes (294), ii) potentiation of Aβ toxicity mediated by increased cholesterol levels in human neuroblastoma cells is found to be associated with a sustained elevation of reactive oxygen species production (295), iii) depletion of cholesterol and membrane-associated sialic acid residue or inhibition of cholesterol and ganglioside synthesis can protect cultured PC12 cells from Aβ toxicity (296), iv) increasing membrane cholesterol levels in mature hippocampal neurons render them more vulnerable to Aβ-induced toxicity than immature neurons (297), v) mitochondrial cholesterol accumulation in cultured neurons as well as in brain of mice with SREBP overexpression or deletion of the *NPC1* gene can enhance the toxic effects of Aβ peptides (298) and vi) rats fed with a high-cholesterol diet exhibit a greater increase in neuronal vulnerability to Aβ toxicity than the rats fed with high fat or standard diet (299).

A number of studies, in contrast to the aforementioned results, have reported contradictory effects i.e., increasing cholesterol levels can protect the cells against Aβ toxicity, whereas decreasing cholesterol levels can enhance toxic potency of the peptide. This is substantiated by data which showed that i) high membrane cholesterol resulting from seladin-1 overexpression or treatment with polyethylene glycol-cholesterol significantly protects cells against Aβ toxicity, whereas low membrane cholesterol in cells treated with the seladin-1 inhibitor 5,22E-cholestadien-3-ol or with methyl-β-cyclodextrin results in cell vulnerability to Aβ peptide (300), ii) cultured PC12 cells and neurons with high membrane cholesterol levels are resistant but those with low cholesterol levels are vulnerable to Aβ toxicity (301-304). Evidence from rat primary cortical cultured neurons further indicates that increased cholesterol levels can protect neurons from toxicity induced by soluble oligomeric Aβ peptide but not from that of fibrillar Aβ peptide (302). These results, taken together, suggest that interactions between cholesterol and Aβ peptide are rather complex and subtle changes in the levels and/or

distribution of cholesterol in various cell compartments may have contrasting effects on Aβ toxicity, possibly due to its influence on the state of aggregation, production or degradation of the peptide. Additionally, it is likely that a fluctuation in cholesterol levels may alter the physical properties of lipid-rafts, thereby modulating Aβ binding as well as cell viability.

1.4.5e Cholesterol and Aβ internalization

Several lines of experimental evidence suggest the existence of distinct pools of extracellular and intracellular Aβ peptides in the brain. The precise origin of intracellular Aβ is not clear but appears to derive from endogenous synthesis as well as uptake from the extracellular source. The extracellular Aβ peptide, depending on the cells, can either lead to a cascade of events including toxicity or can be degraded *via* endosomal-lysosomal pathways (305-312). The molecular events mediating internalization of Aβ peptide rely not only on the cell types but also on the conformation state of the peptide. There is evidence that glial cells internalize Aβ peptide *via* phagocytosis, pinocytosis as well as endocytosis. Neurons, on the other hand, are considered to mediate Aβ internalization mostly *via* clathrin-dependent endocytosis, but many other endocytic processes independent of clathrin may also mediate cellular uptake of Aβ peptide (309, 313). It has been reported that Aβ endocytosis precedes its aggregation at the membrane and internalization of oligomeric Aβ isoform occurs more efficiently than fibrillar peptide (311, 313-316). Given the evidence that Aβ peptide can bind lipid components of the membrane, more recent studies have suggested a role for lipid-rafts in Aβ internalization *albeit* a raft-independent mechanism seems to occur under certain conditions (309, 313).

Studies involving cervical sympathetic cultured neurons clearly depicted that internalized Aβ oligomers co-localized with cholera toxin subunit B (CTxB), a lipid-raft marker that specifically binds ganglioside GM1, suggesting that internalization occurs at lipid-raft possibly *via* GM1 binding. Additionally, simultaneous reduction of both cellular cholesterol and sphingolipid levels were found to decrease Aβ uptake into sympathetic neurons. This event occurs selectively in neuronal axons (and not in cell bodies) and is independent of clathrin but requires dynamin which is responsible for the cleavage of the

invaginated vesicles from the plasma membrane (317). A more recent study using mouse neuroblastoma cells also showed co-localization of internalized Aβ with CTxB and pharmacological inhibition of lipid-raft-dependent endocytosis decreased uptake of soluble Aβ peptide (318). Collectively, these results suggest a critical role for cholesterol in the internalization of Aβ-related peptides in specific cell types/conditions, but it is yet to be determined whether the lipid component or the associated receptor proteins present in the membrane are involved in the internalization of the peptide. This is because Aβ peptide, in addition to lipids, is known to bind/interact with a number of membrane receptors including LRP1, nicotinic acetylcholine receptors, glutamatergic N-methyl-D-aspartate receptors and receptors for advanced glycation end products which may act as endocytosis carriers of the Aβ-receptor protein complex (309, 313). Thus it would be of interest to determine from future studies not only the contributions of lipid-raft *vs* non-raft pathways in Aβ endocytosis but also the role of the putative receptors, if any, regulating the internalization of the peptide in neurons that are vulnerable in AD brains.

1.4.5f Cholesterol and Aβ degradation

A number of recent studies have indicated that cholesterol may have a critical role in the clearance of Aβ-related peptides by regulating the level and/or activity of their degrading enzymes. Multiple proteases within the brain, including insulin-degrading enzyme (IDE), neprilysin, endothelin converting enzymes (ECE1 and ECE2) and plasmin, have been shown to degrade Aβ peptide [reviewed in (319, 320)]. IDE is a zinc metalloendopeptidase expressed predominantly in neurons but also evident in glial cells (321, 322). After synthesis IDE is transported *via* the secretory pathway to either become associated with the cell surface membrane or to be secreted outside of the cell. Both of these scenarios predict significant extracellular degrading activity for Aβ applied into the cell medium. Thus, it is possible that an alteration in cholesterol levels/distribution can compromise the transport and release of this protease into the extracellular space and hence its Aβ-degradaing activity. Alternatively, given the evidence that a subset of IDE is localized in a lipid-raft microdomain (323), a change in membrane cholesterol level can directly influence Aβ-degrading activity of the enzyme. Neprilysin is a type II membrane protein that has been shown to degrade intracellular, cell surface and extracellular Aβ

(324). Interestingly, a subset of neprilysin, especially the mature form, has been found to be associated with rafts (325), but some studies targeting neprilysin to rafts failed to efficiently degrade Aβ in this fraction (326). In contrast, plasmin is a raft-resident serine protease generated from the inactive precursor plasminogen by tissue-type or urokinase-type plasminogen activator (256). The levels of plasmin are lower in AD brains than in age-matched controls, possibly due to lower membrane cholesterol content and raft disorganization (256). This is supported by the observation that the mice deficient in cholesterol-synthesizing enzyme seladin-1 exhibit disorganized lipid-rafts with impaired plasmin activation, whereas opposite effects were seen in seladin-1-overexpressing mice (253, 327). There is also evidence that ApoE can trigger the proteolytic break-down of the Aβ peptide in an isoform-specific fashion (91). More recently, it has been shown that ApoE promotes intracellular Aβ clearance by reducing cellular cholesterol levels which triggers the trafficking of Aβ to lysosomes for degradation (328). The multiplicity of Aβ-degrading enzymes within the brain, together with the existence of other possible ways to influence the production and clearance of Aβ peptides, could probably limit the phenotypic impact of the deficiency of any single Aβ-degrading enzymes on Aβ levels in the brain.

1.4.6 Cholesterol homeostasis as a potential target for reducing Aβ

Although the complexity of the link between cholesterol and AD is only beginning to be appreciated, a myriad of studies over the last 15 years have nonetheless provided tantalizing indications that reduction of Aβ levels by altering cholesterol levels/distribution may be of therapeutic relevance. In fact, the first reported clinical studies based on retrospective epidemiological data showed a strong inverse relationship between AD and treatment with the cholesterol lowering drugs statins – competitive inhibitors of the cholesterol synthesizing enzyme HMGCR used widely in the treatment of hypercholesterolemia in humans (329, 330). This work was rapidly replicated by other investigators (108, 331, 332) and confirmed in some clinical studies showing that statins reduce the levels of 24S-hydroxycholesterol (an indicator of cerebral cholesterol metabolism) as well as Aβ peptides (333, 334). This is further supported by a number of *in vitro* studies demonstrating that statins can reduce Aβ production (203, 230, 335),

formation of Aβ oligomers (336) as well as toxicity induced by Aβ peptide (337-339). These results are substantiated with some *in vivo* studies which reported a statin-induced attenuation of Aβ plaque formation in transgenic mice overexpressing Aβ peptide *albeit* gender may have a role in regulating the effects of statins (230, 244, 340). Notwithstanding these data, evidence from prospective clinical studies is somewhat inconsistent, with some studies showing reduced incidence of AD with statin use (105-108, 332), while others report no benefits (341-344). The discrepancy in the clinical results may relate to the time point of statin exposure, early adult life *vs* late life, dose and duration of statin use or certain limitations of prospective trials such as the shorter periods of statin use, lack of dementia classification, not controlling for other vascular factors and lack of monitoring of statin compliance (345).

The evidence that all types of statins tested seem to have a similar impact on risk of AD and brain cholesterol despite the fact that more lipophilic drugs such as lovastatin and simvastatin can cross the BBB much more easily than the more hydrophilic pravastatin and atorvastatin raise the possibility that the effects of this class of drugs may be indirect, perhaps through a peripheral action. It is possible that statin-induced reductions in peripheral cholesterol may affect brain cholesterol *via* the degradation product 27-hydroxycholesterol which can cross the BBB and is actively taken up by the brain (346). There is also evidence that statins may have cholesterol-independent pleiotropic properties such as inhibition of isoprenoid production (213), clearance of Aβ-related peptides (347), immunological effects on microglia (348, 349), antioxidant (350), anti-apoptotic (351, 352) as well as anti-inflammatory (353) effects which may account for some of the mechanisms of action of these drugs in AD patients. Alternatively, it is likely that statins may reduce the levels of ApoE and cholesterol in the brain, leading to subsequent decreases in Aβ levels and deposition. This is supported by findings that brain cholesterol levels do not respond to lovastatin in ApoE knockout mice (354). Thus, more animal and clinical studies are required not only to clarify the current contradictions but also to define the direct and indirect beneficial effects of statins, if any, in the treatment of AD patients.

A plethora of other cholesterol-modifying strategies that have been shown to attenuate Aβ production/deposition include alterations in the level and/or activity of seladin1, ACAT, ABCA1 and Cyp46, all of which are known to function at different steps of cholesterol homeostasis (Fig. 1.1). Preventing the down-regulation of the cholesterol synthesizing enzyme seladin1 appears to be a sound therapeutic strategy on account of its ability to attenuate apoptosis and the loosening of membrane compartmentalization and thus amyloid accumulation/impaired signaling (27). Some recent therapeutic approaches include small molecule inhibitors of ACAT such as CP113,818 and CI-1011, which do not affect the cellular cholesterol levels, but re-distribute cholesterol from inert cytosolic lipid droplets to free membrane cholesterol. These inhibitors were found to reduce both soluble and insoluble Aβ levels, decrease amyloid burden and improve spatial learning in mutant APP transgenic mice (262, 355, 356), thus making them promising preclinical candidates for the treatment of AD. Modulation of brain cholesterol efflux by regulating the ABCA1 expression appears to be another potential therapeutic approach. While deletion of ABCA1 increased amyloid deposition in the absence of any changes in total or cleaved APP products, overexpression of the transporter over six fold virtually eliminated the formation of mature amyloid plaques without altering APP processing in mutant APP transgenic mice (28, 258-260). These findings indicate that excess ABCA1 possibly mitigates *in vivo* amyloid deposition by promoting ApoE-mediated Aβ clearance (321). Furthermore, ABCA1 is partially regulated by LXRs and it has been shown that the LXR agonist TO-901317 can reduce Aβ generation and improve cognitive functions in animal models of AD (221, 357-359), whereas mice lacking LXR exhibit exacerbated AD-related pathology (360). Understanding which of the LXR target genes confer the beneficial effects for AD may provide an underlying basis for the development of effective LXR agonists as therapeutic agent for AD. In addition to LXR agonists, activation of the *Cyp46* gene, which encodes the enzyme responsible for most of the cholesterol removal from the brain, represents another potential target for modulating brain cholesterol levels. Histone deacetylase inhibitors (e.g., valproate and vorinostat) are the only class of compounds known to enhance mRNA expression of the enzyme (361), although it is likely that such reagents would induce global changes in the transcriptome. Treatment of

AD mouse models with valporate reduced Aβ production, neuritic plaque formation and behavioral deficits (362), thus suggesting a potential role for the enzyme in AD pathogenesis. Thus, taken together, these studies indicate that cholesterol homeostasis offers multiple untapped targets that can be modulated to develop potential therapeutic strategies for the treatment of AD.

1.5.1 Niemann-Pick type C (NPC) disease etiology and neuropathology

NPC disease is a fatal, neurodegenerative, lysosomal lipid-storage disorder with an autosomal recessive mode of inheritance. It is a relatively rare disease with a prevalence of about 1 in 120,000-150,000 live births (363). The majority of cases result from mutations in the *NPC1* gene (95%) while the remainder (5%) is caused by mutations in the *NPC2* gene. Loss of function mutations in either of these genes results in an indistinguishable biochemical and clinical phenotype. The clinical presentation of NPC is extremely heterogeneous, with age of onset ranging from the perinatal period to adult age, occasionally as late as the seventh decade of life (363). Typically, clinical manifestations become evident in early childhood and death usually occurs during the teenage years. NPC is classically a neurovisceral condition where visceral involvement and neurologic manifestations arise at different times and follow completely independent courses (363). The typical neurologic phenotype includes cerebellar ataxia, vertical supranuclear gaze palsy, dysarthria, dysphagia, and a progressive dementia. Cataplexy, seizures and dystonia are other quite common features and psychiatric disturbances are frequent especially in late-onset patients. The progression of the disease in the periphery is characterized by enlargement of the liver and spleen and sometimes lung, which results from the infiltration of lipid-laden macrophages termed foam cells (364). At the biochemical level, NPC disease is characterized by an accumulation of unesterified cholesterol and other lipids, including sphingomyelin, sphingosine and gangliosides (GM2 and GM3) within the LE/L of various tissues including the CNS. In the neurons, these lipid disturbances are accompanied by considerable neuroaxonal dystrophy with the formation of axonal spheroids and meganeurites, ectopic dendritogenesis as well as NFTs. The tangles are usually present in the the hippocampus, medial temporal lobes, cingulate gyrus and entorhinal region without any evidence of amyloid deposition.

However, NPC patients with two copies of ApoE ε4 alleles display conspicuous neurofibrillary pathology along with detectable deposition of Aβ-related peptides (365). These changes are accompanied by activation of astrocytes and microglia, progressive demyelination of the white matter and cerebral atrophy. Severe degeneration of neurons is also evident in the cerebellar Purkinje layer, whereas other areas that are affected to some extent include the brain stem, pons, thalamus and cortex (7, 364). At present very little is known about the basis of this selective neuronal vulnerability but some recent studies have begun to unravel the molecular mechanisms associated with NPC pathogenesis.

1.5.2 Functions of NPC1 and NPC2 proteins

Despite identification of the two human *NPC* genes (*NPC1* located on chromosome18q11-q12 and *NPC2* on 14q24.3) more than a decade ago, the molecular functions of the NPC proteins are just recently being unraveled. It has long been known that both of these proteins are ubiquitously expressed and function in exporting LDL-derived unesterified cholesterol from the LE/L. The fact that deficiency of either protein results in virtually identical cellular and clinical phenotypes indicates that these proteins act sequentially in the same pathway in regulating intracellular cholesterol transport.

Human NPC1 is a 1278 amino acid integral polytopic protein that is primarily localized to the LE/L, but also cycles through the trans-Golgi network (366, 367). This protein contains 13 putative transmembrane regions that are separated by luminal glycosylated loops (368, 369). Five of the transmembrane domains contain a putative sterol-sensing domain (SSD) that exhibits sequence homology to those identified in other proteins involved in sterol metabolism, such as HMGCR and SCAP (368). The role of the SSD in NPC1 is not yet clear. Although mutations in this region of the protein prevented the binding of a photoactivatable analog of cholesterol to NPC1, direct binding of cholesterol to this domain has yet not been demonstrated (370). Other domains of the NPC1 protein include a C-terminal di-leucine lysosomal targeting motif, a cysteine-rich loop located C-terminal to the SSD (a mutation hot-spot), and an N-terminal luminal leucine zipper motif suggesting that NPC1 might interact with other, as yet unidentified,

proteins (369, 371-375). Recently, Kwon et al. reported the crystal structure of the N-terminal domain of NPC1 and revealed that this domain binds to cholesterol so that the 3β-OH group of the cholesterol molecule is buried within the binding pocket and the iso-octyl side-chain is exposed on the surface (376). Moreover, binding and dissociation of cholesterol to NPC1 appear to be accelerated by the presence of NPC2 (377).

NPC2 (previously called HE1), on the other hand, is a 151-amino acid, soluble lysosomal glycoprotein protein that uses mannose-6-phosphate (M6P) reorganization marker for targeting to the EL system (378). NPC2 binds cholesterol and a subset of other sterols at submicromolar affinity with a 1:1 stochiometry (379-381). NPC2 has been previously shown to transfer cholesterol *in vitro* between model membranes which were found to be accelerated by the presence of an acidic environment such as that encountered in the LE/L lumen (379). High-resolution crystal structure (381, 382) and mutational studies (383) have identified a hydrophobic cholesterol-binding pocket in NPC2. Interestingly, NPC2 appears to bind cholesterol in an orientation opposite to that of NPC1 with the iso-octyl chain buried in the cholesterol binding pocket of NPC2 and the 3β-OH group exposed to the LE/L lumen. Recently, NPC2 has been shown to transfer cholesterol from membranes to N-terminal domain of NPC1 (376).

Based on these findings, a “hydrophobic hand-off” model has been recently proposed for the concerted action of the two NPC proteins in transferring unesterified cholesterol out of the LE/L (Fig. 1.5) (376). According to this model, unesterified cholesterol derived from hydrolysis of endocytosed LDL-cholesterol is initially bound by NPC2 which subsequently transfers the cholesterol to the N-terminal domain of NPC1 (376). Although this model predicts that NPC1 and NPC2 proteins physically interact, no such interaction has yet been demonstrated (384). This model further predicts that NPC1 inserts the iso-octyl sidechain of cholesterol into the lysosomal outer membrane from where it can be transported across the cytosolic compartment of the cell to the ER and plasma membrane (376).

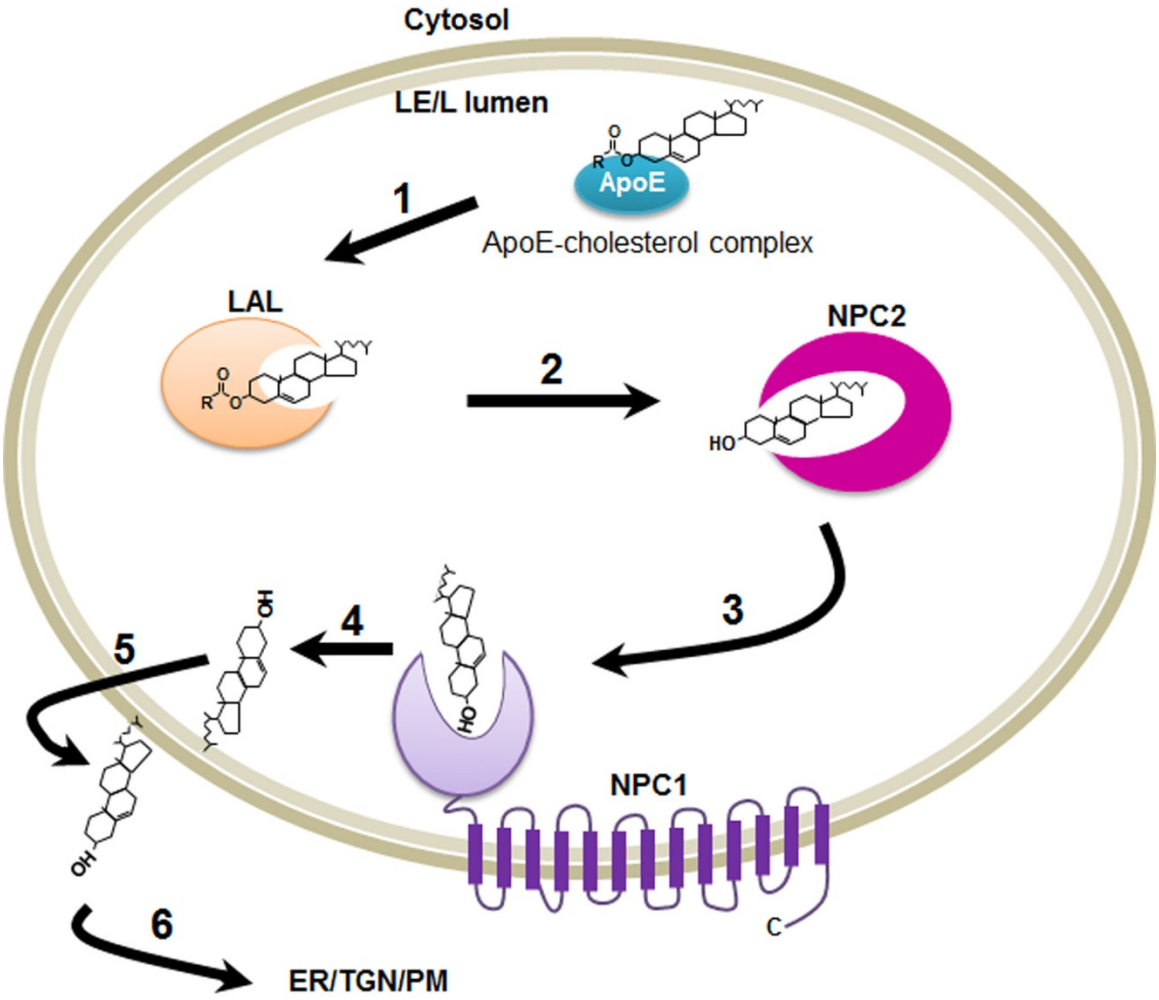

Figure 1.5: Suggested mechanisms for concerted action of NPC1 and NPC2 proteins in mediating cholesterol efflux from late-endosomes/lysosomes (LE/L). (1) Cholesterol esters in the endocytosed lipoprotein complex are hydrolyzed by lysosomal acid lipase (LAL) to unesterified cholesterol. (2) NPC2 (LE/L luminal protein) binds unesterified cholesterol with the iso-octyl chain in the binding pocket. (3) NPC2 transfers cholesterol to the N-terminal domain of NPC1 (LE/L limiting membrane protein), which binds cholesterol with its hydroxyl group buried in the binding pocket. (4) NPC1 delivers the unesterified cholesterol to the luminal leaflet of the LE/L limiting membrane, (5) from where it can spontaneously flip to the cytosolic side and (6) then be carried to various destinations such as endoplasmic reticulum (ER), trans-Golgi network (TGN) and plasma membrane (PM) within the cell by an yet unknown mechanism.

1.5.3 Animal models of NPC disease

Animal models of NPC disease include two well-characterized murine NPC1 models, namely BALB/c-*npc1*^{nih} and C57BL/KsJ-*npc1*^{spm}, each of which arose due to spontaneous null-mutation in the *Npc1* gene (364, 385-387). An Npc2 hypomorphic

mouse model also exists, which expresses 0-4% residual Npc2 protein in various tissues and exhibits a phenotype identical to that in Npc1-null mice (388). In addition, a feline model with a mutation in *NPC1* that recapitulates the human NPC disease (389-391) along with fruit fly (392) and yeast (393, 394) models have been used to study NPC disease. However, the most widely used and best-characterized model of NPC disease is the BALB/c-*npc1*^{nih} mouse (Npc1-null) that completely lacks the Npc1 protein (385). Mice that are homozygous for the mutation in *Npc1* are asymptomatic at birth, but recapitulate many aspects of the human disease, including accumulation of unesterified cholesterol in the LE/L system, activation of microglia and astrocytes as well as loss of the myelin sheath throughout the CNS. Progressive loss of neurons is also evident in the cerebellum, prefrontal cortex, thalamus and brainstem. However, unlike the human disease, intracellular NFTs have not been detected in the Npc1-null mouse model, although site-specific hyperphosphorylation of tau protein has been reported. The cellular changes in Npc1-null mice are accompanied by behavioral impairments paralleling the neurological and systemic symptoms of the human disorder, including abnormal gait and rotarod performance, cognitive deficits, weight loss and early death occurring between 12 and 15 weeks (364, 395).

1.5.4 Cellular abnormalities in NPC-deficient cells

The most classical interpretation of NPC disease is a defect in trafficking of LDL-derived cholesterol resulting in an overall cellular dysfunction. Although the endocytic uptake of LDL and the subsequent hydrolysis of LDL-derived cholesteryl esters to unesterified cholesterol in LE/L are normal in NPC1-deficient cells, the transport of unesterified cholesterol from LE/L to the ER, Golgi and plasma membrane is impaired (396-398). Thus, despite having abnormally higher amount cholesterol in LE/L, the cell senses a lack of cholesterol in the ER and up-regulates cholesterol synthesis, production of LDL receptors and markedly reduces cholesterol esterification by ACAT (397, 399-401). In contrast to the LDL-derived cholesterol, intracellular transport of endogenously synthesized cholesterol to the plasma membrane is not disrupted (398, 402), nor is the trafficking of HDL-derived cholesterol affected by NPC1-deficiency (403). The endogenously synthesized cholesterol can, however, also become trapped in the LE/L

following re-endocytosis from the plasma membrane, *albeit* much more slowly than LDL-derived cholesterol (398, 402). Furthermore, cholesterol that is taken up through bulk-phase endocytosis also gets trapped within the LE/L compartment of NPC1-deficient cells (404). Thus, it appears that an initial sequestration of cholesterol taken up *via* the endocytic pathway might subsequently induce further accumulation of cholesterol and a variety of other lipids, including sphingomyelin, sphingosine, bis(monoacylglycero)phosphate, and complex glycosphingolipids (particularly the gangliosides GM2 and GM3) within the LE/L of NPC1-deficient cells (405, 406). However, there are some data which point towards the accumulation of these "other lipids" as the primary defect in NPC1-deficient cells although their precise role in mediating the cellular dysfunction underlying NPC disease still needs further investigation (406).

While it is well established that defects in either NPC1 or NPC2 protein may cause a "traffic jam" of lipids in LE/L, there is also evidence that general vesicular trafficking pathways that are regulated by the Rab family of GTPases are severally affected in these cells (407-410). Under normal conditions, M6P receptors usually carry newly synthesized lysosomal enzymes from the TGN to endosomes, and then return to TGN for another round of transport. Transport of the M6P receptors from late endosomes to the TGN is coordinated by Rab9 - a member of the Rab family (>60 members) of GTPases, which are involved in intracellular vesicular transport (408-410). Altered levels of cholesterol have been shown to influence distribution/trafficking of cation-independent M6P receptors (Igf2r) within cells (411-413). Earlier studies using cultured cells have demonstrated that cholesterol accumulation induced by treatment with U18666A or siRNA-mediated NPC1 depletion can cause redistribution of the Igf2r to endosomes and impair its retrograde transport from late endosomes to the trans-Golgi network (411, 414). In a recent study it has been shown that cholesterol enrichment not only disrupts trafficking of the Igf2r receptor but also causes accumulation of Rab9 in late-endosomes, thus suggesting that targeting of a variety of proteins is likely to be impaired in NPC-deficient cells (408). Interestingly, overexpression of Rab9 or increasing the amount of Rab9 by protein transduction was found to attenuate cholesterol accumulation in NPC1-

deficient cells (415-417). Similar results were obtained when some other members of the Rab family of proteins such as Rab4, Rab7 and Rab8 (but not Rab11) were overexpressed in NPC1-deficient cells, thus suggesting that increased expression of these proteins may partially bypass a deficiency of NPC1 (415, 416, 418). This is supported in part by an *in vivo* study which showed that overexpression of Rab9 can increase the life-span of Npc1-null mice by 22% along with delaying the onset of disease symptoms (419). Some recent studies have indicated that fusion and fission events between late endosomes and lysosomes that are essential for egress of lysosomal cargo are severely impaired in NPC1- and NPC2-deficient cells (420). It appears that NPC1 and NPC2 work independently of one another in different aspects of this process. While NPC2 plays a role in membrane fission events required for reformation of new lysosomes and release of lysosomal cargo-containing membrane vesicles, NPC1 is involved in retrograde fusion of lysosomes with late-endosomes that is important for egress of certain membrane-impermeable lysosomal cargo out of the cell (420). Impairment of these events might cause a build-up of toxic metabolites in the LE/L by inhibiting the release of molecules from NPC1-deficient cells (367, 420, 421). Thus, lipid accumulation within the LE/L can severely disrupt the trafficking of a variety of molecules *via* the endocytic pathway in NPC-deficient cells.

Accompanying the impaired vesicular trafficking, the levels of the lysosomal enzymes were found to be up-regulated in NPC1-deficient cells (422) and also in Npc1-null mice (423, 424). Furthermore, a previous study from our lab has demonstrated that the up-regulation in the cytosolic levels/activity of the lysosomal enzymes cathepsin B and D was significantly higher in the affected cerebellum (which shows extensive neuronal death) than the unaffected hippocampus (which does not exhibit neurodegeneration), thereby indicating the possible involvement of lysosomal leakage in determining the neuronal vulnerability observed in NPC pathology (423).

Accumulated evidence suggests that LE/L cholesterol sequestration in NPC1-deficient cells also affects mitochondrial cholesterol distribution (425). Mitochondria are crucial for providing cells with energy in the form of ATP, and also play a role in

signaling, steroidogenesis, cellular growth, differentiation and death. Thus, mitochondrial dysfunction has been implicated in a variety of neurodegenerative disorders including AD, PD and NPC pathologies (426). In contrast to the ER and plasma membrane, the cholesterol content of mitochondrial membranes appears to be increased in Npc1-null brains (425, 427). This is most likely due to the increased amounts of unesterified cholesterol that are available for export out of the LE/L to different cell compartments in the absence of the NPC proteins. Indeed, RNA silencing of the LE/L membrane protein MLN64, which has been implicated in the mobilization of lysosomal cholesterol into mitochondria (428), decreased the mitochondrial cholesterol content, suggesting that in NPC1-deficient cells a greater export of cholesterol from LE/L occurs *via* this pathway (427). Since cholesterol regulates membrane fluidity, an increase in mitochondrial membrane cholesterol adversely affects its function and stability, triggering mitochondria-mediated apoptotic cell death. Concomittantly, the mitochondrial membrane potential, the activity of ATP synthase, the levels of ATP and mitochondrial antioxidant glutathione are all decreased in NPC1-deficient neurons (425) making these cells more vulnerable to toxicity induced by $A\beta_{42}$, tumor necrosis factor-α and Fas (298, 429). Npc1-null brains have also been reported to have disrupted neurosteroidogenesis that can affect neuronal growth and differentiation and modulate neurotransmitter functions, raising the possibility that neurosteroid treatment may be useful in ameliorating progression of the disease pathogenesis (430).

1.5.5 Reversal of cholesterol accumulation as treatment for NPC

Although several therapeutic strategies have been attempted (405, 431), none of them have yet been approved for effective treatment of NPC disease. Cholesterol reducing approaches including those of statins, low-cholesterol diet and ezetimibe, while reducing peripheral cholesterol burden, failed to ameliorate NPC disease neuropathology and clinical outcomes (432, 433). This is probably because the peripheral and the brain cholesterol are largely maintained as two distinct pools and most lipid-lowering drugs do not successfully permeate the BBB to mediate their effects. However, some exciting new findings indicate that oral or intrathecal delivery of cholesterol-mobilizing cyclodextrins might provide the basis for an effective treatment for NPC disease.

Cyclodextrins are a family of cyclic oligosaccharides that bind cholesterol in their hydrophobic core and are frequently used experimentally to deplete cholesterol from the plasma membrane of cells (434) as well as to solubilize various pharmaceuticals (435). A number of recent studies have shown that a single subcutaneous injection of 2-hydroxypropyl-β-cyclodextrin (2-HPC) into 7-day-old Npc1-null mice reduced cholesterol accumulation in LE/L, significantly delayed neurodegeneration and prolonged their life-span (436). In addition, 2-HPC markedly improved liver function (436) and excretion of sequestered cholesterol into bile from the Npc1-null mice (437). Surprisingly, the lungs of Npc1-null mice were resistant to the beneficial effects of 2-HPC (437). Administration of 2-HPC to older (49-day-old) Npc1-null mice was found to be less effective, possibly due to closure of the BBB and/or the progressive nature of the disease. While the hepatic and neurological functions of these animals were improved, their life-span was not extended, suggesting that administration of 2-HPC early in life provides the most benefit. Repeated injections of 2-HPC over several weeks were found to be more effective in reducing pathology and prolonging life-span of Npc1-null (438, 439). Additionally, 2-HPC was found to be equally beneficial to both Npc1-null and Npc2-hypomorphic mice (438).

The mechanism underlying the beneficial effect of 2-HPC has not yet been completely elucidated. The current model suggests that 2-HPC enters the endocytic pathway of NPC-deficient cells through bulk-phase endocytosis and releases cholesterol and other lipids from the LE/L to the metabolically active pool in the ER (440). This notion is supported by three distinct lines of evidence: (i) 2-HPC treatment significantly reduced the levels of the mRNAs encoding SREBP2 and its target genes (HMGCR and LDLR), decreased cholesterol synthesis and increased cholesteryl ester levels in NPC1-deficient mouse brains and livers, (ii) the mRNAs encoding LXR target genes (ABCA1 and ABCG1) were increased by 2-HPC administration, indicating greater cholesterol efflux from the cell (436, 441) and (iii) ACAT-mediated cholesterol esterification in NPC1-deficient cultured human fibroblasts were increased following 2-HPC treatment, suggesting mobilization of the sequestered cholesterol from the LE/L to the ER (442).

Thus, 2-HPC appears to bypass the essential requirement for NPC2–NPC1 interaction by some unknown mechanism and release the sequestered cholesterol from the LE/L in NPC-deficient cells.

These observations suggest that reversing the cholesterol accumulation by 2-HPC might be useful for treating NPC pathology. Cyclodextrins are relatively non-toxic and have long been approved for human use as a vehicle for drug delivery (435, 443). An "Orphan Drug Designation" to treat eight-year old identical twins with NPC disease upon request of their parents with the support of Children's Hospital Oakland has also been sought recently for 2-HPC from the US Food and Drug Administration (see http://www.nnpdf.ca/Cyclodextrin.html). However, translation of most of these studies to human patients is not straightforward as the exact nature of 2-HPC's mode of action remains unclear. Although subcutaneous injection of 2-HPC markedly improves the neurodegeneration and prolongs life-span of Npc1-null mice, the amount of 2-HPC that enters the brain from the peripheral circulation has not been clearly established (444). Another major obstacle, considering the delay in diagnosis of NPC patients, is the early treatment strategy (usually long before the onset of overt neurodegenerative symptoms) that seems to have the most beneficial effects (445). Nonetheless, the recent demonstration that 2-HPC administration can reverse the NPC pathology and extend the life span of Npc-deficient mice clearly raises the possibility of a novel therapeutic intervention of individuals with NPC disease.

1.6 Cholesterol, amyloid and neurodegeneration: is there a link?

A number of recent studies have shown that NPC and AD, despite being distinct diseases, exhibit some striking similarities including altered cholesterol levels/metabolism, endosomal/lysosomal abnormalities, presence of NFTs, mitochondrial dysfunction and glia-mediated neuroinflammation. The NFTs observed in most juvenile/adult NPC patients are structurally and immunologically indistinguishable from the tangles in AD brains (446-450). Moreover, the neurofibrillary pathology is reported to be more pronounced in the brains of NPC patients, who are homozygous for ApoE ε4 alleles, the most consistent genetic risk factor that has been associated with AD (365). Interestingly,

these NPC patients also exhibit Aβ deposits in selected brain regions in the form of diffuse plaques. Some recent studies from NPC patients as well as animal models have shown that levels of Aβ-related peptides are increased in the vulnerable brain regions (219) and/or cerebrospinal fluid (451), thus raising the possibility of a functional role of Aβ-related peptides in NPC pathogenesis.

Although cholesterol is not sequestered in AD as observed in NPC pathology, there is evidence that high cholesterol levels increase the risk of AD and that the levels of NPC1 mRNA/protein are altered in the vulnerable regions of AD brains (100, 102-104, 452-454). In addition, neurons bearing NFTs have been shown to exhibit higher levels of unesterified cholesterol in AD brains than do the neighboring tangle-free neurons (109). More recently, comparative lipidomic analysis of brain tissues from AD patients and commonly used mutant APP-Tg mouse models has revealed significant changes in many lipids including cholesterol in the affected (i.e., prefrontal cortex and entorhinal cortex) *vs* unaffected (cerebellum) regions, thus reinforcing the potential link between lipid anomalies and AD pathogenesis (101, 110). Additionally, as mentioned above, many lines of experimental evidence suggest that alteration in cholesterol homeostasis can influence APP metabolism including Aβ production, aggregation, clearance and toxicity, which may be of relevance in the development and/or progression of AD pathogenesis. These results, taken together, not only suggest of a functional inter-relationship between cholesterol, APP metabolism and neurodegeneration, but also raise the possibility that a better understanding of the exact nature of this relationship may be of relevance for the development of more effective strategies in preventing/attenuating AD pathology.

1.7 Thesis objectives

A number of earlier studies, as summarized above, have indicated that enhanced cholesterol levels can have deleterious effects on the development of AD pathology by altering APP processing that favors increased production of Aβ-related peptides (203, 205, 229, 230). In contrast to the amyloidogenic processing of APP, some studies have found that increased plasma cholesterol may be associated with unchanged (250) or reduced (241, 242) brain Aβ levels, while lowering plasma cholesterol can have opposite

effects (202, 244, 252). These paradoxical results were obtained either under *in vitro* conditions or using *in vivo* models where cholesterol levels were modulated by dietary intake. Since cholesterol in the brain is synthesized *de novo* and plasma-lipoproteins are unable to cross the BBB, it is important to determine how alterations in cholesterol levels and its subcellular distribution within neurons can influence production and/or degradation of Aβ-related peptides. Under normal conditions, mature neurons mostly rely on cholesterol secreted from astrocytes as lipoprotein complexes to maintain their function. The lipoprotein complexes taken up by neurons are first delivered to the EL system where they are hydrolysed to release free cholesterol and subsequently exported *via* a NPC1-NPC2 protein-dependent mechanism and distributed to the other cellular compartments including ER and plasma membrane. Given the evidence that the EL system acts as a major site for Aβ production and exhibits marked changes in "at risk" neurons in both AD and NPC brains, it is of critical relevance to establish how alteration in the cholesterol levels within the EL system can influence production and clearance of Aβ peptides. Additionally, convergence of factors that promote parallels between NPC and AD indicate that tau-positive NFTs, which may have a role in the loss of neurons, possibly lie downstream of abnormal cholesterol and APP metabolism in both diseases. However, very little is currently known about the functional interaction between altered cholesterol and APP metabolism and their significance in the development of tau pathology and neurodegeneration. We hypothesize that, "*altered neuronal levels/distribution of cholesterol can play an important role in modulating APP metabolism and is causally linked to abnormal tau phosphorylation/cleavage, which in turn can have a deleterious impact on the overall neuronal function, leading to cell death*". To address this hypothesis, we have established the following three objectives:

1. To study the influence of intracellular cholesterol accumulation on the development of AD-related pathology by genetic manipulation of the intracellular cholesterol transport in a mouse model overexpressing human APP. To do so, we have developed a novel bigenic mouse line (ANPC) by crossing mutant human APP-Tg (TgCRND8) mice (136) with mice deficient in Npc1 protein (385). Using the ANPC mice and the littermates of other genotypes we have first evaluated how intracellular cholesterol

accumulation in the presence of human APP expression can influence the expression profiles of some selected genes involved in APP and cholesterol metabolism, intracellular trafficking and cell death mechanisms in the cerebellum *vs.* the hippocampus. This study will help us to understand the selective changes in the expression profile of molecules that may be involved in the development and/or progression of the pathology. (Chapter 2)

2. To determine the age-related behavioural and neuropathological abnormalities with a special focus on tau phosphorylation/cleavage and neurodegeneration in the cholesterol accumulating APP-Tg mice (ANPC) compared to its littermates. To further establish the significance of cholesterol in the disease pathogenesis, we treated the ANPC mice with 2-HPC to reverse the intracellular accumulation of cholesterol and then evaluated the effects on the pathological changes. This study was designed to understand how intracellular accumulation of cholesterol can influence the pathological features other than Aβ levels/deposition in AD brains. (Chapter 3)

3. To determine the influence of intracellular cholesterol accumulation on APP metabolism and its significance in the development of the pathological changes. We have addressed this objective by using our ANPC bigenic mice which provide a suitable platform to evaluate how accumulation of cholesterol within the EL system can regulate APP levels and processing under *in vivo* conditions. In parallel, we have generated a stable cell line by knocking down Npc1 expression in mouse neuroblastoma (N2a) cells overexpressing mutant human APP to define the molecular mechanisms by which cholesterol accumulation can influence APP metabolism at the cellular level. This study is designed to understand the underlying mechanisms by which intracellular cholesterol accumulation can influence APP metabolism in *in vitro* and *in vivo* models of APP overexpression. (Chapter 4)

More details on the objectives of each of these studies and their results are presented in a series of three manuscripts, following which a general discussion of the results is presented in the last chapter.

1.8 References

1. Dietschy, J.M. and Turley, S.D. (2004) Thematic review series: Brain lipids. Cholesterol metabolism in the central nervous system during early development and in the mature animal. *J Lipid Res,* 45, 1375-1397.

2. Maron, D.J., Fazio, S. and Linton, M.F. (2000) Current perspectives on statins. *Circulation,* 101, 207-213.

3. Martins, I.J., Berger, T., Sharman, M.J., Verdile, G., Fuller, S.J. and Martins, R.N. (2009) Cholesterol metabolism and transport in the pathogenesis of Alzheimer's disease. *J Neurochem,* 111, 1275-1308.

4. Pfrieger, F.W. (2003) Cholesterol homeostasis and function in neurons of the central nervous system. *Cell Mol Life Sci,* 60, 1158-1171.

5. Ikonen, E. (2006) Mechanisms for cellular cholesterol transport: defects and human disease. *Physiol Rev,* 86, 1237-1261.

6. Miller, W.L. (1987) Structure of genes encoding steroidogenic enzymes. *J Steroid Biochem,* 27, 759-766.

7. Vance, J.E., Hayashi, H. and Karten, B. (2005) Cholesterol homeostasis in neurons and glial cells. *Semin Cell Dev Biol,* 16, 193-212.

8. Serougne-Gautheron, C. and Chevallier, F. (1973) Time course of biosynthetic cholesterol in the adult rat brain. *Biochim Biophys Acta,* 316, 244-250.

9. Bjorkhem, I., Lutjohann, D., Diczfalusy, U., Stahle, L., Ahlborg, G. and Wahren, J. (1998) Cholesterol homeostasis in human brain: turnover of 24S-hydroxycholesterol and evidence for a cerebral origin of most of this oxysterol in the circulation. *J Lipid Res,* 39, 1594-1600.

10. Bjorkhem, I. and Meaney, S. (2004) Brain cholesterol: long secret life behind a barrier. *Arterioscler Thromb Vasc Biol,* 24, 806-815.

11. Goldstein, J.L., DeBose-Boyd, R.A. and Brown, M.S. (2006) Protein sensors for membrane sterols. *Cell,* 124, 35-46.

12. Anderson, R.G. (2003) Joe Goldstein and Mike Brown: from cholesterol homeostasis to new paradigms in membrane biology. *Trends Cell Biol,* 13, 534-539.

13. Poirier, J., Baccichet, A., Dea, D. and Gauthier, S. (1993) Cholesterol synthesis and lipoprotein reuptake during synaptic remodelling in hippocampus in adult rats. *Neuroscience,* 55, 81-90.

14. Jurevics, H. and Morell, P. (1995) Cholesterol for synthesis of myelin is made locally, not imported into brain. *J Neurochem,* 64, 895-901.

15. Beffert, U., Danik, M., Krzywkowski, P., Ramassamy, C., Berrada, F. and Poirier, J. (1998) The neurobiology of apolipoproteins and their receptors in the CNS and Alzheimer's disease. *Brain Res Brain Res Rev,* 27, 119-142.

16. Karten, B., Campenot, R.B., Vance, D.E. and Vance, J.E. (2006) Expression of ABCG1, but not ABCA1, correlates with cholesterol release by cerebellar astroglia. *J Biol Chem,* 281, 4049-4057.

17. Wahrle, S.E., Jiang, H., Parsadanian, M., Legleiter, J., Han, X., Fryer, J.D., Kowalewski, T. and Holtzman, D.M. (2004) ABCA1 is required for normal central nervous system ApoE levels and for lipidation of astrocyte-secreted apoE. *J Biol Chem,* 279, 40987-40993.

18. Bu, G. (2009) Apolipoprotein E and its receptors in Alzheimer's disease: pathways, pathogenesis and therapy. *Nat Rev Neurosci,* 10, 333-344.

19. Herz, J. (2009) Apolipoprotein E receptors in the nervous system. *Curr Opin Lipidol,* 20, 190-196.

20. Poirier, J. (2003) Apolipoprotein E and cholesterol metabolism in the pathogenesis and treatment of Alzheimer's disease. *Trends Mol Med,* 9, 94-101.

21. Puglielli, L., Konopka, G., Pack-Chung, E., Ingano, L.A., Berezovska, O., Hyman, B.T., Chang, T.Y., Tanzi, R.E. and Kovacs, D.M. (2001) Acyl-coenzyme A: cholesterol acyltransferase modulates the generation of the amyloid beta-peptide. *Nat Cell Biol,* 3, 905-912.

22. Rudel, L.L., Lee, R.G. and Cockman, T.L. (2001) Acyl coenzyme A: cholesterol acyltransferase types 1 and 2: structure and function in atherosclerosis. *Curr Opin Lipidol,* 12, 121-127.

23. Bogdanovic, N., Bretillon, L., Lund, E.G., Diczfalusy, U., Lannfelt, L., Winblad, B., Russell, D.W. and Bjorkhem, I. (2001) On the turnover of brain cholesterol in patients with Alzheimer's disease. Abnormal induction of the cholesterol-catabolic enzyme CYP46 in glial cells. *Neurosci Lett,* 314, 45-48.

24. Lund, E.G., Guileyardo, J.M. and Russell, D.W. (1999) cDNA cloning of cholesterol 24-hydroxylase, a mediator of cholesterol homeostasis in the brain. *Proc Natl Acad Sci U S A,* 96, 7238-7243.

25. Lund, E.G., Xie, C., Kotti, T., Turley, S.D., Dietschy, J.M. and Russell, D.W. (2003) Knockout of the cholesterol 24-hydroxylase gene in mice reveals a brain-specific mechanism of cholesterol turnover. *J Biol Chem,* 278, 22980-22988.

26. Kim, W.S., Rahmanto, A.S., Kamili, A., Rye, K.A., Guillemin, G.J., Gelissen, I.C., Jessup, W., Hill, A.F. and Garner, B. (2007) Role of ABCG1 and ABCA1 in regulation of neuronal cholesterol efflux to apolipoprotein E discs and suppression of amyloid-beta peptide generation. *J Biol Chem,* 282, 2851-2861.

27. Martin, M., Dotti, C.G. and Ledesma, M.D. (2010) Brain cholesterol in normal and pathological aging. *Biochim Biophys Acta,* 1801, 934-944.

28. Hirsch-Reinshagen, V., Maia, L.F., Burgess, B.L., Blain, J.F., Naus, K.E., McIsaac, S.A., Parkinson, P.F., Chan, J.Y., Tansley, G.H., Hayden, M.R. *et al.* (2005) The absence of ABCA1 decreases soluble ApoE levels but does not diminish amyloid deposition in two murine models of Alzheimer disease. *J Biol Chem,* 280, 43243-43256.

29. Lehmann, J.M., Kliewer, S.A., Moore, L.B., Smith-Oliver, T.A., Oliver, B.B., Su, J.L., Sundseth, S.S., Winegar, D.A., Blanchard, D.E., Spencer, T.A. *et al.* (1997) Activation of the nuclear receptor LXR by oxysterols defines a new hormone response pathway. *J Biol Chem,* 272, 3137-3140.

30. Wang, N., Lan, D., Chen, W., Matsuura, F. and Tall, A.R. (2004) ATP-binding cassette transporters G1 and G4 mediate cellular cholesterol efflux to high-density lipoproteins. *Proc Natl Acad Sci U S A,* 101, 9774-9779.

31. Wang, N., Silver, D.L., Thiele, C. and Tall, A.R. (2001) ATP-binding cassette transporter A1 (ABCA1) functions as a cholesterol efflux regulatory protein. *J Biol Chem,* 276, 23742-23747.

32. Wang, Y., Rogers, P.M., Stayrook, K.R., Su, C., Varga, G., Shen, Q., Nagpal, S. and Burris, T.P. (2008) The selective Alzheimer's disease indicator-1 gene (Seladin-1/DHCR24) is a liver X receptor target gene. *Mol Pharmacol,* 74, 1716-1721.

33. Bjorkhem, I., Leoni, V. and Meaney, S. (2010) Genetic connections between neurological disorders and cholesterol metabolism. *J Lipid Res,* 51, 2489-2503.

34. Liu, J.P., Tang, Y., Zhou, S., Toh, B.H., McLean, C. and Li, H. (2010) Cholesterol involvement in the pathogenesis of neurodegenerative diseases. *Mol Cell Neurosci,* 43, 33-42.

35. Katzman, R., Kawas, C. (1994) The epidemiology of dementia and Alzheimer disease. In Terry, R.D., Katzman, R., Bick, K.L. (ed.), *Alzheimer Disease*. New York: Raven Press, pp. 105 - 122.

36. Katzov, H., Chalmers, K., Palmgren, J., Andreasen, N., Johansson, B., Cairns, N.J., Gatz, M., Wilcock, G.K., Love, S., Pedersen, N.L. *et al.* (2004) Genetic variants of ABCA1 modify Alzheimer disease risk and quantitative traits related to beta-amyloid metabolism. *Hum Mutat,* 23, 358-367.

37. Whitehouse, P.J. (1997) Genesis of Alzheimer's disease. *Neurology,* 48, S2-7.

38. Bertram, L. and Tanzi, R.E. (2005) The genetic epidemiology of neurodegenerative disease. *J Clin Invest,* 115, 1449-1457.

39. Cummings, J.L. (2004) Alzheimer's disease. *N Engl J Med,* 351, 56-67.

40. National Institute of Aging (2012) 2010 Alzheimer's Disease Progress Report: A Deeper Understanding. National Institues of Health.

41. Bertram, L., McQueen, M.B., Mullin, K., Blacker, D. and Tanzi, R.E. (2007) Systematic meta-analyses of Alzheimer disease genetic association studies: the AlzGene database. *Nat Genet,* 39, 17-23.

42. Holmes, C. (2002) Genotype and phenotype in Alzheimer's disease. *Br J Psychiatry,* 180, 131-134.

43. St George-Hyslop, P.H. and Petit, A. (2005) Molecular biology and genetics of Alzheimer's disease. *C R Biol,* 328, 119-130.

44. Tanzi, R.E. and Bertram, L. (2005) Twenty years of the Alzheimer's disease amyloid hypothesis: a genetic perspective. *Cell,* 120, 545-555.

45. Coon, K.D., Myers, A.J., Craig, D.W., Webster, J.A., Pearson, J.V., Lince, D.H., Zismann, V.L., Beach, T.G., Leung, D., Bryden, L. *et al.* (2007) A high-density whole-genome association study reveals that APOE is the major susceptibility gene for sporadic late-onset Alzheimer's disease. *J Clin Psychiatry,* 68, 613-618.

46. Strittmatter, W.J., Saunders, A.M., Schmechel, D., Pericak-Vance, M., Enghild, J., Salvesen, G.S. and Roses, A.D. (1993) Apolipoprotein E: high-avidity binding to beta-amyloid and increased frequency of type 4 allele in late-onset familial Alzheimer disease. *Proc Natl Acad Sci U S A,* 90, 1977-1981.

47. Harold, D., Abraham, R., Hollingworth, P., Sims, R., Gerrish, A., Hamshere, M.L., Pahwa, J.S., Moskvina, V., Dowzell, K., Williams, A. *et al.* (2009) Genome-wide association study identifies variants at CLU and PICALM associated with Alzheimer's disease. *Nat Genet,* 41, 1088-1093.

48. Lambert, J.C., Heath, S., Even, G., Campion, D., Sleegers, K., Hiltunen, M., Combarros, O., Zelenika, D., Bullido, M.J., Tavernier, B. *et al.* (2009) Genome-wide association study identifies variants at CLU and CR1 associated with Alzheimer's disease. *Nat Genet,* 41, 1094-1099.

49. Seshadri, S., Fitzpatrick, A.L., Ikram, M.A., DeStefano, A.L., Gudnason, V., Boada, M., Bis, J.C., Smith, A.V., Carassquillo, M.M., Lambert, J.C. *et al.* (2010) Genome-wide analysis of genetic loci associated with Alzheimer disease. *JAMA,* 303, 1832-1840.

50. Rogaeva, E., Meng, Y., Lee, J.H., Gu, Y., Kawarai, T., Zou, F., Katayama, T., Baldwin, C.T., Cheng, R., Hasegawa, H. *et al.* (2007) The neuronal sortilin-related receptor SORL1 is genetically associated with Alzheimer disease. *Nat Genet,* 39, 168-177.

51. Hollingworth, P., Harold, D., Jones, L., Owen, M.J. and Williams, J. (2011) Alzheimer's disease genetics: current knowledge and future challenges. *Int J Geriatr Psychiatry,* 26, 793-802.

52. Lambert, J.C. and Amouyel, P. (2011) Genetics of Alzheimer's disease: new evidences for an old hypothesis? *Curr Opin Genet Dev*, 21, 295-301.

53. Chen, J.H., Lin, K.P. and Chen, Y.C. (2009) Risk factors for dementia. *J Formos Med Assoc*, 108, 754-764.

54. Muller-Spahn, F. and Hock, C. (1999) Risk factors and differential diagnosis of Alzheimer's disease. *Eur Arch Psychiatry Clin Neurosci*, 249 Suppl 3, 37-42.

55. Querfurth, H.W. and LaFerla, F.M. (2010) Alzheimer's disease. *N Engl J Med*, 362, 329-344.

56. Brion, J.P., Anderton, B.H., Authelet, M., Dayanandan, R., Leroy, K., Lovestone, S., Octave, J.N., Pradier, L., Touchet, N. and Tremp, G. (2001) Neurofibrillary tangles and tau phosphorylation. *Biochem Soc Symp*, 81-88.

57. Iqbal, K., Alonso, A.C., Gong, C.X., Khatoon, S., Pei, J.J., Wang, J.Z. and Grundke-Iqbal, I. (1998) Mechanisms of neurofibrillary degeneration and the formation of neurofibrillary tangles. *J Neural Transm Suppl*, 53, 169-180.

58. Lee, V.M. (1996) Regulation of tau phosphorylation in Alzheimer's disease. *Ann N Y Acad Sci*, 777, 107-113.

59. Billingsley, M.L. and Kincaid, R.L. (1997) Regulated phosphorylation and dephosphorylation of tau protein: effects on microtubule interaction, intracellular trafficking and neurodegeneration. *Biochem J*, 323 (Pt 3), 577-591.

60. Johnson, G.V. and Jenkins, S.M. (1999) Tau protein in normal and Alzheimer's disease brain. *J Alzheimers Dis*, 1, 307-328.

61. Bierer, L.M., Hof, P.R., Purohit, D.P., Carlin, L., Schmeidler, J., Davis, K.L. and Perl, D.P. (1995) Neocortical neurofibrillary tangles correlate with dementia severity in Alzheimer's disease. *Arch Neurol*, 52, 81-88.

62. Lopez, O.L. and DeKosky, S.T. (2003) [Neuropathology of Alzheimer's disease and mild cognitive impairment]. *Rev Neurol*, 37, 155-163.

63. Nelson, P.T., Braak, H. and Markesbery, W.R. (2009) Neuropathology and cognitive impairment in Alzheimer disease: a complex but coherent relationship. *J Neuropathol Exp Neurol*, 68, 1-14.

64. Selkoe, D.J. (2001) Alzheimer's disease: genes, proteins, and therapy. *Physiol Rev*, 81, 741-766.

65. Clippingdale, A.B., Wade, J.D. and Barrow, C.J. (2001) The amyloid-beta peptide and its role in Alzheimer's disease. *J Pept Sci*, 7, 227-249.

66. Dickson, D.W. (1997) The pathogenesis of senile plaques. *J Neuropathol Exp Neurol*, 56, 321-339.

67. Naslund, J., Haroutunian, V., Mohs, R., Davis, K.L., Davies, P., Greengard, P. and Buxbaum, J.D. (2000) Correlation between elevated levels of amyloid beta-peptide in the brain and cognitive decline. *JAMA,* 283, 1571-1577.

68. Giaccone, G., Tagliavini, F., Linoli, G., Bouras, C., Frigerio, L., Frangione, B. and Bugiani, O. (1989) Down patients: extracellular preamyloid deposits precede neuritic degeneration and senile plaques. *Neurosci Lett,* 97, 232-238.

69. Tanzi, R.E. (1996) Neuropathology in the Down's syndrome brain. *Nat Med,* 2, 31-32.

70. Pike, C.J., Burdick, D., Walencewicz, A.J., Glabe, C.G. and Cotman, C.W. (1993) Neurodegeneration induced by beta-amyloid peptides in vitro: the role of peptide assembly state. *J Neurosci,* 13, 1676-1687.

71. Yankner, B.A. (1996) Mechanisms of neuronal degeneration in Alzheimer's disease. *Neuron,* 16, 921-932.

72. Hardy, J. and Selkoe, D.J. (2002) The amyloid hypothesis of Alzheimer's disease: progress and problems on the road to therapeutics. *Science,* 297, 353-356.

73. Mawuenyega, K.G., Sigurdson, W., Ovod, V., Munsell, L., Kasten, T., Morris, J.C., Yarasheski, K.E. and Bateman, R.J. (2010) Decreased clearance of CNS beta-amyloid in Alzheimer's disease. *Science,* 330, 1774.

74. DeKosky, S.T., Scheff, S.W. and Styren, S.D. (1996) Structural correlates of cognition in dementia: quantification and assessment of synapse change. *Neurodegeneration,* 5, 417-421.

75. Kar, S., Slowikowski, S.P., Westaway, D. and Mount, H.T. (2004) Interactions between beta-amyloid and central cholinergic neurons: implications for Alzheimer's disease. *J Psychiatry Neurosci,* 29, 427-441.

76. Ladner, C.J. and Lee, J.M. (1998) Pharmacological drug treatment of Alzheimer disease: the cholinergic hypothesis revisited. *J Neuropathol Exp Neurol,* 57, 719-731.

77. Francis, P.T., Palmer, A.M., Snape, M. and Wilcock, G.K. (1999) The cholinergic hypothesis of Alzheimer's disease: a review of progress. *J Neurol Neurosurg Psychiatry,* 66, 137-147.

78. Davies, P. and Maloney, A.J. (1976) Selective loss of central cholinergic neurons in Alzheimer's disease. *Lancet,* 2, 1403.

79. Muir, J.L. (1997) Acetylcholine, aging, and Alzheimer's disease. *Pharmacol Biochem Behav,* 56, 687-696.

80. Corder, E.H., Saunders, A.M., Strittmatter, W.J., Schmechel, D.E., Gaskell, P.C., Small, G.W., Roses, A.D., Haines, J.L. and Pericak-Vance, M.A. (1993) Gene dose

of apolipoprotein E type 4 allele and the risk of Alzheimer's disease in late onset families. *Science,* 261, 921-923.

81. Slooter, A.J., Cruts, M., Kalmijn, S., Hofman, A., Breteler, M.M., Van Broeckhoven, C. and van Duijn, C.M. (1998) Risk estimates of dementia by apolipoprotein E genotypes from a population-based incidence study: the Rotterdam Study. *Arch Neurol,* 55, 964-968.

82. Jarvik, G.P., Wijsman, E.M., Kukull, W.A., Schellenberg, G.D., Yu, C. and Larson, E.B. (1995) Interactions of apolipoprotein E genotype, total cholesterol level, age, and sex in prediction of Alzheimer's disease: a case-control study. *Neurology,* 45, 1092-1096.

83. Tomiyama, T., Corder, E.H. and Mori, H. (1999) Molecular pathogenesis of apolipoprotein E-mediated amyloidosis in late-onset Alzheimer's disease. *Cell Mol Life Sci,* 56, 268-279.

84. Wisniewski, T., Castano, E.M., Golabek, A., Vogel, T. and Frangione, B. (1994) Acceleration of Alzheimer's fibril formation by apolipoprotein E in vitro. *Am J Pathol,* 145, 1030-1035.

85. Carter, D.B., Dunn, E., McKinley, D.D., Stratman, N.C., Boyle, T.P., Kuiper, S.L., Oostveen, J.A., Weaver, R.J., Boller, J.A. and Gurney, M.E. (2001) Human apolipoprotein E4 accelerates beta-amyloid deposition in APPsw transgenic mouse brain. *Ann Neurol,* 50, 468-475.

86. Holtzman, D.M., Bales, K.R., Tenkova, T., Fagan, A.M., Parsadanian, M., Sartorius, L.J., Mackey, B., Olney, J., McKeel, D., Wozniak, D. *et al.* (2000) Apolipoprotein E isoform-dependent amyloid deposition and neuritic degeneration in a mouse model of Alzheimer's disease. *Proc Natl Acad Sci U S A,* 97, 2892-2897.

87. Sadowski, M., Pankiewicz, J., Scholtzova, H., Ripellino, J.A., Li, Y., Schmidt, S.D., Mathews, P.M., Fryer, J.D., Holtzman, D.M., Sigurdsson, E.M. *et al.* (2004) A synthetic peptide blocking the apolipoprotein E/beta-amyloid binding mitigates beta-amyloid toxicity and fibril formation in vitro and reduces beta-amyloid plaques in transgenic mice. *Am J Pathol,* 165, 937-948.

88. Bell, R.D., Sagare, A.P., Friedman, A.E., Bedi, G.S., Holtzman, D.M., Deane, R. and Zlokovic, B.V. (2007) Transport pathways for clearance of human Alzheimer's amyloid beta-peptide and apolipoproteins E and J in the mouse central nervous system. *J Cereb Blood Flow Metab,* 27, 909-918.

89. Deane, R., Sagare, A., Hamm, K., Parisi, M., Lane, S., Finn, M.B., Holtzman, D.M. and Zlokovic, B.V. (2008) apoE isoform-specific disruption of amyloid beta peptide clearance from mouse brain. *J Clin Invest,* 118, 4002-4013.

90. DeMattos, R.B., Cirrito, J.R., Parsadanian, M., May, P.C., O'Dell, M.A., Taylor, J.W., Harmony, J.A., Aronow, B.J., Bales, K.R., Paul, S.M. *et al.* (2004) ApoE and

clusterin cooperatively suppress Abeta levels and deposition: evidence that ApoE regulates extracellular Abeta metabolism in vivo. *Neuron,* 41, 193-202.

91. Jiang, Q., Lee, C.Y., Mandrekar, S., Wilkinson, B., Cramer, P., Zelcer, N., Mann, K., Lamb, B., Willson, T.M., Collins, J.L. *et al.* (2008) ApoE promotes the proteolytic degradation of Abeta. *Neuron,* 58, 681-693.

92. Koistinaho, M., Lin, S., Wu, X., Esterman, M., Koger, D., Hanson, J., Higgs, R., Liu, F., Malkani, S., Bales, K.R. *et al.* (2004) Apolipoprotein E promotes astrocyte colocalization and degradation of deposited amyloid-beta peptides. *Nat Med,* 10, 719-726.

93. Kolsch, H., Lutjohann, D., Ludwig, M., Schulte, A., Ptok, U., Jessen, F., von Bergmann, K., Rao, M.L., Maier, W. and Heun, R. (2002) Polymorphism in the cholesterol 24S-hydroxylase gene is associated with Alzheimer's disease. *Mol Psychiatry,* 7, 899-902.

94. Borroni, B., Archetti, S., Agosti, C., Akkawi, N., Brambilla, C., Caimi, L., Caltagirone, C., Di Luca, M. and Padovani, A. (2004) Intronic CYP46 polymorphism along with ApoE genotype in sporadic Alzheimer Disease: from risk factors to disease modulators. *Neurobiol Aging,* 25, 747-751.

95. Combarros, O., Infante, J., Llorca, J. and Berciano, J. (2004) Genetic association of CYP46 and risk for Alzheimer's disease. *Dement Geriatr Cogn Disord,* 18, 257-260.

96. Johansson, A., Katzov, H., Zetterberg, H., Feuk, L., Johansson, B., Bogdanovic, N., Andreasen, N., Lenhard, B., Brookes, A.J., Pedersen, N.L. *et al.* (2004) Variants of CYP46A1 may interact with age and APOE to influence CSF Abeta42 levels in Alzheimer's disease. *Hum Genet,* 114, 581-587.

97. Papassotiropoulos, A., Streffer, J.R., Tsolaki, M., Schmid, S., Thal, D., Nicosia, F., Iakovidou, V., Maddalena, A., Lutjohann, D., Ghebremedhin, E. *et al.* (2003) Increased brain beta-amyloid load, phosphorylated tau, and risk of Alzheimer disease associated with an intronic CYP46 polymorphism. *Arch Neurol,* 60, 29-35.

98. Shibata, N., Kawarai, T., Lee, J.H., Lee, H.S., Shibata, E., Sato, C., Liang, Y., Duara, R., Mayeux, R.P., St George-Hyslop, P.H. *et al.* (2006) Association studies of cholesterol metabolism genes (CH25H, ABCA1 and CH24H) in Alzheimer's disease. *Neurosci Lett,* 391, 142-146.

99. Wollmer, M.A., Streffer, J.R., Lutjohann, D., Tsolaki, M., Iakovidou, V., Hegi, T., Pasch, T., Jung, H.H., Bergmann, K., Nitsch, R.M. *et al.* (2003) ABCA1 modulates CSF cholesterol levels and influences the age at onset of Alzheimer's disease. *Neurobiol Aging,* 24, 421-426.

100. Di Paolo, G. and Kim, T.W. (2011) Linking lipids to Alzheimer's disease: cholesterol and beyond. *Nat Rev Neurosci,* 12, 284-296.

101. Matsuzaki, T., Sasaki, K., Hata, J., Hirakawa, Y., Fujimi, K., Ninomiya, T., Suzuki, S.O., Kanba, S., Kiyohara, Y. and Iwaki, T. (2011) Association of Alzheimer disease pathology with abnormal lipid metabolism: the Hisayama Study. *Neurology,* 77, 1068-1075.

102. Pappolla, M.A., Bryant-Thomas, T.K., Herbert, D., Pacheco, J., Fabra Garcia, M., Manjon, M., Girones, X., Henry, T.L., Matsubara, E., Zambon, D. *et al.* (2003) Mild hypercholesterolemia is an early risk factor for the development of Alzheimer amyloid pathology. *Neurology,* 61, 199-205.

103. Reiss, A.B. and Voloshyna, I. (2012) Regulation of cerebral cholesterol metabolism in Alzheimer disease. *J Investig Med,* 60, 576-582.

104. Kuo, Y.M., Emmerling, M.R., Bisgaier, C.L., Essenburg, A.D., Lampert, H.C., Drumm, D. and Roher, A.E. (1998) Elevated low-density lipoprotein in Alzheimer's disease correlates with brain abeta 1-42 levels. *Biochem Biophys Res Commun,* 252, 711-715.

105. Haag, M.D., Hofman, A., Koudstaal, P.J., Stricker, B.H. and Breteler, M.M. (2009) Statins are associated with a reduced risk of Alzheimer disease regardless of lipophilicity. The Rotterdam Study. *J Neurol Neurosurg Psychiatry,* 80, 13-17.

106. Sparks, D.L., Kryscio, R.J., Sabbagh, M.N., Connor, D.J., Sparks, L.M. and Liebsack, C. (2008) Reduced risk of incident AD with elective statin use in a clinical trial cohort. *Curr Alzheimer Res,* 5, 416-421.

107. Wolozin, B., Wang, S.W., Li, N.C., Lee, A., Lee, T.A. and Kazis, L.E. (2007) Simvastatin is associated with a reduced incidence of dementia and Parkinson's disease. *BMC Med,* 5, 20.

108. Zamrini, E., McGwin, G. and Roseman, J.M. (2004) Association between statin use and Alzheimer's disease. *Neuroepidemiology,* 23, 94-98.

109. Distl, R., Meske, V. and Ohm, T.G. (2001) Tangle-bearing neurons contain more free cholesterol than adjacent tangle-free neurons. *Acta Neuropathol,* 101, 547-554.

110. Chan, R.B., Oliveira, T.G., Cortes, E.P., Honig, L.S., Duff, K.E., Small, S.A., Wenk, M.R., Shui, G. and Di Paolo, G. (2012) Comparative lipidomic analysis of mouse and human brain with Alzheimer disease. *J Biol Chem,* 287, 2678-2688.

111. Kang, J., Lemaire, H.G., Unterbeck, A., Salbaum, J.M., Masters, C.L., Grzeschik, K.H., Multhaup, G., Beyreuther, K. and Muller-Hill, B. (1987) The precursor of Alzheimer's disease amyloid A4 protein resembles a cell-surface receptor. *Nature,* 325, 733-736.

112. St George-Hyslop, P.H., Tanzi, R.E., Polinsky, R.J., Haines, J.L., Nee, L., Watkins, P.C., Myers, R.H., Feldman, R.G., Pollen, D., Drachman, D. *et al.* (1987) The genetic defect causing familial Alzheimer's disease maps on chromosome 21. *Science,* 235, 885-890.

113. Tanzi, R.E., Gusella, J.F., Watkins, P.C., Bruns, G.A., St George-Hyslop, P., Van Keuren, M.L., Patterson, D., Pagan, S., Kurnit, D.M. and Neve, R.L. (1987) Amyloid beta protein gene: cDNA, mRNA distribution, and genetic linkage near the Alzheimer locus. *Science,* 235, 880-884.

114. Goate, A., Chartier-Harlin, M.C., Mullan, M., Brown, J., Crawford, F., Fidani, L., Giuffra, L., Haynes, A., Irving, N., James, L. *et al.* (1991) Segregation of a missense mutation in the amyloid precursor protein gene with familial Alzheimer's disease. *Nature,* 349, 704-706.

115. Slunt, H.H., Thinakaran, G., Von Koch, C., Lo, A.C., Tanzi, R.E. and Sisodia, S.S. (1994) Expression of a ubiquitous, cross-reactive homologue of the mouse beta-amyloid precursor protein (APP). *J Biol Chem,* 269, 2637-2644.

116. Wasco, W., Bupp, K., Magendantz, M., Gusella, J.F., Tanzi, R.E. and Solomon, F. (1992) Identification of a mouse brain cDNA that encodes a protein related to the Alzheimer disease-associated amyloid beta protein precursor. *Proc Natl Acad Sci U S A,* 89, 10758-10762.

117. Bayer, T.A., Cappai, R., Masters, C.L., Beyreuther, K. and Multhaup, G. (1999) It all sticks together--the APP-related family of proteins and Alzheimer's disease. *Mol Psychiatry,* 4, 524-528.

118. Coulson, E.J., Paliga, K., Beyreuther, K. and Masters, C.L. (2000) What the evolution of the amyloid protein precursor supergene family tells us about its function. *Neurochem Int,* 36, 175-184.

119. Kitaguchi, N., Takahashi, Y., Tokushima, Y., Shiojiri, S. and Ito, H. (1988) Novel precursor of Alzheimer's disease amyloid protein shows protease inhibitory activity. *Nature,* 331, 530-532.

120. Ponte, P., Gonzalez-DeWhitt, P., Schilling, J., Miller, J., Hsu, D., Greenberg, B., Davis, K., Wallace, W., Lieberburg, I. and Fuller, F. (1988) A new A4 amyloid mRNA contains a domain homologous to serine proteinase inhibitors. *Nature,* 331, 525-527.

121. Koo, E.H., Sisodia, S.S., Archer, D.R., Martin, L.J., Weidemann, A., Beyreuther, K., Fischer, P., Masters, C.L. and Price, D.L. (1990) Precursor of amyloid protein in Alzheimer disease undergoes fast anterograde axonal transport. *Proc Natl Acad Sci U S A,* 87, 1561-1565.

122. Suzuki, T., Araki, Y., Yamamoto, T. and Nakaya, T. (2006) Trafficking of Alzheimer's disease-related membrane proteins and its participation in disease pathogenesis. *J Biochem,* 139, 949-955.

123. Haass, C., Kaether, C., Thinakaran, G. and Sisodia, S. (2012) Trafficking and Proteolytic Processing of APP. *Cold Spring Harb Perspect Med,* 2, a006270.

124. O'Brien, R.J. and Wong, P.C. (2011) Amyloid precursor protein processing and Alzheimer's disease. *Annu Rev Neurosci,* 34, 185-204.

125. Reinhard, C., Hebert, S.S. and De Strooper, B. (2005) The amyloid-beta precursor protein: integrating structure with biological function. *EMBO J,* 24, 3996-4006.

126. Thinakaran, G. and Koo, E.H. (2008) Amyloid precursor protein trafficking, processing, and function. *J Biol Chem,* 283, 29615-29619.

127. Zheng, H., Jiang, M., Trumbauer, M.E., Sirinathsinghji, D.J., Hopkins, R., Smith, D.W., Heavens, R.P., Dawson, G.R., Boyce, S., Conner, M.W. *et al.* (1995) beta-Amyloid precursor protein-deficient mice show reactive gliosis and decreased locomotor activity. *Cell,* 81, 525-531.

128. Dawson, G.R., Seabrook, G.R., Zheng, H., Smith, D.W., Graham, S., O'Dowd, G., Bowery, B.J., Boyce, S., Trumbauer, M.E., Chen, H.Y. *et al.* (1999) Age-related cognitive deficits, impaired long-term potentiation and reduction in synaptic marker density in mice lacking the beta-amyloid precursor protein. *Neuroscience,* 90, 1-13.

129. Anliker, B. and Muller, U. (2006) The functions of mammalian amyloid precursor protein and related amyloid precursor-like proteins. *Neurodegener Dis,* 3, 239-246.

130. Herms, J., Anliker, B., Heber, S., Ring, S., Fuhrmann, M., Kretzschmar, H., Sisodia, S. and Muller, U. (2004) Cortical dysplasia resembling human type 2 lissencephaly in mice lacking all three APP family members. *EMBO J,* 23, 4106-4115.

131. Wang, B., Yang, L., Wang, Z. and Zheng, H. (2007) Amyolid precursor protein mediates presynaptic localization and activity of the high-affinity choline transporter. *Proc Natl Acad Sci U S A,* 104, 14140-14145.

132. Wang, Z., Wang, B., Yang, L., Guo, Q., Aithmitti, N., Songyang, Z. and Zheng, H. (2009) Presynaptic and postsynaptic interaction of the amyloid precursor protein promotes peripheral and central synaptogenesis. *J Neurosci,* 29, 10788-10801.

133. Wang, P., Yang, G., Mosier, D.R., Chang, P., Zaidi, T., Gong, Y.D., Zhao, N.M., Dominguez, B., Lee, K.F., Gan, W.B. *et al.* (2005) Defective neuromuscular synapses in mice lacking amyloid precursor protein (APP) and APP-Like protein 2. *J Neurosci,* 25, 1219-1225.

134. Yang, G., Gong, Y.D., Gong, K., Jiang, W.L., Kwon, E., Wang, P., Zheng, H., Zhang, X.F., Gan, W.B. and Zhao, N.M. (2005) Reduced synaptic vesicle density and active zone size in mice lacking amyloid precursor protein (APP) and APP-like protein 2. *Neurosci Lett,* 384, 66-71.

135. Selkoe, D.J. (2008) Biochemistry and molecular biology of amyloid beta-protein and the mechanism of Alzheimer’s disease. In *Handb Clin Neurol* Vol. 89, pp. 245-260.

136. Chishti, M.A., Yang, D.S., Janus, C., Phinney, A.L., Horne, P., Pearson, J., Strome, R., Zuker, N., Loukides, J., French, J. *et al.* (2001) Early-onset amyloid deposition and cognitive deficits in transgenic mice expressing a double mutant form of amyloid precursor protein 695. *J Biol Chem*, 276, 21562-21570.

137. Games, D., Adams, D., Alessandrini, R., Barbour, R., Berthelette, P., Blackwell, C., Carr, T., Clemens, J., Donaldson, T., Gillespie, F. *et al.* (1995) Alzheimer-type neuropathology in transgenic mice overexpressing V717F beta-amyloid precursor protein. *Nature,* 373, 523-527.

138. Hsiao, K., Chapman, P., Nilsen, S., Eckman, C., Harigaya, Y., Younkin, S., Yang, F. and Cole, G. (1996) Correlative memory deficits, Abeta elevation, and amyloid plaques in transgenic mice. *Science,* 274, 99-102.

139. Sturchler-Pierrat, C., Abramowski, D., Duke, M., Wiederhold, K.H., Mistl, C., Rothacher, S., Ledermann, B., Burki, K., Frey, P., Paganetti, P.A. *et al.* (1997) Two amyloid precursor protein transgenic mouse models with Alzheimer disease-like pathology. *Proc Natl Acad Sci U S A,* 94, 13287-13292.

140. Chen, G., Chen, K.S., Knox, J., Inglis, J., Bernard, A., Martin, S.J., Justice, A., McConlogue, L., Games, D., Freedman, S.B. *et al.* (2000) A learning deficit related to age and beta-amyloid plaques in a mouse model of Alzheimer's disease. *Nature,* 408, 975-979.

141. Eriksen, J.L. and Janus, C.G. (2007) Plaques, tangles, and memory loss in mouse models of neurodegeneration. *Behav Genet,* 37, 79-100.

142. Borchelt, D.R., Ratovitski, T., van Lare, J., Lee, M.K., Gonzales, V., Jenkins, N.A., Copeland, N.G., Price, D.L. and Sisodia, S.S. (1997) Accelerated amyloid deposition in the brains of transgenic mice coexpressing mutant presenilin 1 and amyloid precursor proteins. *Neuron,* 19, 939-945.

143. Holcomb, L., Gordon, M.N., McGowan, E., Yu, X., Benkovic, S., Jantzen, P., Wright, K., Saad, I., Mueller, R., Morgan, D. *et al.* (1998) Accelerated Alzheimer-type phenotype in transgenic mice carrying both mutant amyloid precursor protein and presenilin 1 transgenes. *Nat Med,* 4, 97-100.

144. Calhoun, M.E., Wiederhold, K.H., Abramowski, D., Phinney, A.L., Probst, A., Sturchler-Pierrat, C., Staufenbiel, M., Sommer, B. and Jucker, M. (1998) Neuron loss in APP transgenic mice. *Nature,* 395, 755-756.

145. Irizarry, M.C., Soriano, F., McNamara, M., Page, K.J., Schenk, D., Games, D. and Hyman, B.T. (1997) Abeta deposition is associated with neuropil changes, but not with overt neuronal loss in the human amyloid precursor protein V717F (PDAPP) transgenic mouse. *J Neurosci,* 17, 7053-7059.

146. McGowan, E., Eriksen, J. and Hutton, M. (2006) A decade of modeling Alzheimer's disease in transgenic mice. *Trends Genet,* 22, 281-289.

147. Lewis, J., Dickson, D.W., Lin, W.L., Chisholm, L., Corral, A., Jones, G., Yen, S.H., Sahara, N., Skipper, L., Yager, D. *et al.* (2001) Enhanced neurofibrillary degeneration in transgenic mice expressing mutant tau and APP. *Science,* 293, 1487-1491.

148. Perez, M., Ribe, E., Rubio, A., Lim, F., Moran, M.A., Ramos, P.G., Ferrer, I., Isla, M.T. and Avila, J. (2005) Characterization of a double (amyloid precursor protein-tau) transgenic: tau phosphorylation and aggregation. *Neuroscience,* 130, 339-347.

149. Ribe, E.M., Perez, M., Puig, B., Gich, I., Lim, F., Cuadrado, M., Sesma, T., Catena, S., Sanchez, B., Nieto, M. *et al.* (2005) Accelerated amyloid deposition, neurofibrillary degeneration and neuronal loss in double mutant APP/tau transgenic mice. *Neurobiol Dis,* 20, 814-822.

150. Oddo, S., Caccamo, A., Shepherd, J.D., Murphy, M.P., Golde, T.E., Kayed, R., Metherate, R., Mattson, M.P., Akbari, Y. and LaFerla, F.M. (2003) Triple-transgenic model of Alzheimer's disease with plaques and tangles: intracellular Abeta and synaptic dysfunction. *Neuron,* 39, 409-421.

151. Casas, C., Sergeant, N., Itier, J.M., Blanchard, V., Wirths, O., van der Kolk, N., Vingtdeux, V., van de Steeg, E., Ret, G., Canton, T. *et al.* (2004) Massive CA1/2 neuronal loss with intraneuronal and N-terminal truncated Abeta42 accumulation in a novel Alzheimer transgenic model. *Am J Pathol,* 165, 1289-1300.

152. Schmitz, C., Rutten, B.P., Pielen, A., Schafer, S., Wirths, O., Tremp, G., Czech, C., Blanchard, V., Multhaup, G., Rezaie, P. *et al.* (2004) Hippocampal neuron loss exceeds amyloid plaque load in a transgenic mouse model of Alzheimer's disease. *Am J Pathol,* 164, 1495-1502.

153. Oakley, H., Cole, S.L., Logan, S., Maus, E., Shao, P., Craft, J., Guillozet-Bongaarts, A., Ohno, M., Disterhoft, J., Van Eldik, L. *et al.* (2006) Intraneuronal beta-amyloid aggregates, neurodegeneration, and neuron loss in transgenic mice with five familial Alzheimer's disease mutations: potential factors in amyloid plaque formation. *J Neurosci,* 26, 10129-10140.

154. Echeverria, V. and Cuello, A.C. (2002) Intracellular A-beta amyloid, a sign for worse things to come? *Mol Neurobiol,* 26, 299-316.

155. Gouras, G.K., Almeida, C.G. and Takahashi, R.H. (2005) Intraneuronal Abeta accumulation and origin of plaques in Alzheimer's disease. *Neurobiol Aging,* 26, 1235-1244.

156. Tseng, B.P., Kitazawa, M. and LaFerla, F.M. (2004) Amyloid beta-peptide: the inside story. *Curr Alzheimer Res,* 1, 231-239.

157. Paulson, J.B., Ramsden, M., Forster, C., Sherman, M.A., McGowan, E. and Ashe, K.H. (2008) Amyloid plaque and neurofibrillary tangle pathology in a regulatable mouse model of Alzheimer's disease. *Am J Pathol,* 173, 762-772.

158. Sparks, D.L., Scheff, S.W., Hunsaker, J.C., 3rd, Liu, H., Landers, T. and Gross, D.R. (1994) Induction of Alzheimer-like beta-amyloid immunoreactivity in the brains of rabbits with dietary cholesterol. *Exp Neurol,* 126, 88-94.

159. Schroeder, F., Gallegos, A.M., Atshaves, B.P., Storey, S.M., McIntosh, A.L., Petrescu, A.D., Huang, H., Starodub, O., Chao, H., Yang, H. *et al.* (2001) Recent advances in membrane microdomains: rafts, caveolae, and intracellular cholesterol trafficking. *Exp Biol Med (Maywood),* 226, 873-890.

160. Hayashi, H., Igbavboa, U., Hamanaka, H., Kobayashi, M., Fujita, S.C., Wood, W.G. and Yanagisawa, K. (2002) Cholesterol is increased in the exofacial leaflet of synaptic plasma membranes of human apolipoprotein E4 knock-in mice. *Neuroreport,* 13, 383-386.

161. Wood, W.G., Schroeder, F., Avdulov, N.A., Chochina, S.V. and Igbavboa, U. (1999) Recent advances in brain cholesterol dynamics: transport, domains, and Alzheimer's disease. *Lipids,* 34, 225-234.

162. Jacobson, K., Mouritsen, O.G. and Anderson, R.G. (2007) Lipid rafts: at a crossroad between cell biology and physics. *Nat Cell Biol,* 9, 7-14.

163. Lingwood, D. and Simons, K. (2010) Lipid rafts as a membrane-organizing principle. *Science,* 327, 46-50.

164. Simons, K. and Ehehalt, R. (2002) Cholesterol, lipid rafts, and disease. *J Clin Invest,* 110, 597-603.

165. Bouillot, C., Prochiantz, A., Rougon, G. and Allinquant, B. (1996) Axonal amyloid precursor protein expressed by neurons in vitro is present in a membrane fraction with caveolae-like properties. *J Biol Chem,* 271, 7640-7644.

166. Lee, S.J., Liyanage, U., Bickel, P.E., Xia, W., Lansbury, P.T., Jr. and Kosik, K.S. (1998) A detergent-insoluble membrane compartment contains A beta in vivo. *Nat Med,* 4, 730-734.

167. Price, D.L. and Sisodia, S.S. (1998) Mutant genes in familial Alzheimer's disease and transgenic models. *Annu Rev Neurosci,* 21, 479-505.

168. Small, S.A. and Gandy, S. (2006) Sorting through the cell biology of Alzheimer's disease: intracellular pathways to pathogenesis. *Neuron,* 52, 15-31.

169. Lichtenthaler, S.F. (2012) Alpha-secretase cleavage of the amyloid precursor protein: proteolysis regulated by signaling pathways and protein trafficking. *Curr Alzheimer Res,* 9, 165-177.

170. Sisodia, S.S. (1992) Beta-amyloid precursor protein cleavage by a membrane-bound protease. *Proc Natl Acad Sci U S A,* 89, 6075-6079.

171. Allinson, T.M., Parkin, E.T., Turner, A.J. and Hooper, N.M. (2003) ADAMs family members as amyloid precursor protein alpha-secretases. *J Neurosci Res,* 74, 342-352.

172. Kojro, E. and Fahrenholz, F. (2005) The non-amyloidogenic pathway: structure and function of alpha-secretases. *Subcell Biochem,* 38, 105-127.

173. Kuhn, P.H., Wang, H., Dislich, B., Colombo, A., Zeitschel, U., Ellwart, J.W., Kremmer, E., Rossner, S. and Lichtenthaler, S.F. (2010) ADAM10 is the physiologically relevant, constitutive alpha-secretase of the amyloid precursor protein in primary neurons. *EMBO J,* 29, 3020-3032.

174. Postina, R., Schroeder, A., Dewachter, I., Bohl, J., Schmitt, U., Kojro, E., Prinzen, C., Endres, K., Hiemke, C., Blessing, M. *et al.* (2004) A disintegrin-metalloproteinase prevents amyloid plaque formation and hippocampal defects in an Alzheimer disease mouse model. *J Clin Invest,* 113, 1456-1464.

175. Esch, F.S., Keim, P.S., Beattie, E.C., Blacher, R.W., Culwell, A.R., Oltersdorf, T., McClure, D. and Ward, P.J. (1990) Cleavage of amyloid beta peptide during constitutive processing of its precursor. *Science,* 248, 1122-1124.

176. Grziwa, B., Grimm, M.O., Masters, C.L., Beyreuther, K., Hartmann, T. and Lichtenthaler, S.F. (2003) The transmembrane domain of the amyloid precursor protein in microsomal membranes is on both sides shorter than predicted. *J Biol Chem,* 278, 6803-6808.

177. Qi-Takahara, Y., Morishima-Kawashima, M., Tanimura, Y., Dolios, G., Hirotani, N., Horikoshi, Y., Kametani, F., Maeda, M., Saido, T.C., Wang, R. *et al.* (2005) Longer forms of amyloid beta protein: implications for the mechanism of intramembrane cleavage by gamma-secretase. *J Neurosci,* 25, 436-445.

178. Selkoe, D.J. and Wolfe, M.S. (2007) Presenilin: running with scissors in the membrane. *Cell,* 131, 215-221.

179. Vassar, R., Bennett, B.D., Babu-Khan, S., Kahn, S., Mendiaz, E.A., Denis, P., Teplow, D.B., Ross, S., Amarante, P., Loeloff, R. *et al.* (1999) Beta-secretase cleavage of Alzheimer's amyloid precursor protein by the transmembrane aspartic protease BACE. *Science,* 286, 735-741.

180. Chavez-Gutierrez, L., Bammens, L., Benilova, I., Vandersteen, A., Benurwar, M., Borgers, M., Lismont, S., Zhou, L., Van Cleynenbreugel, S., Esselmann, H. *et al.* (2012) The mechanism of gamma-Secretase dysfunction in familial Alzheimer disease. *EMBO J,* 31, 2261-2274.

181. Takami, M., Nagashima, Y., Sano, Y., Ishihara, S., Morishima-Kawashima, M., Funamoto, S. and Ihara, Y. (2009) gamma-Secretase: successive tripeptide and tetrapeptide release from the transmembrane domain of beta-carboxyl terminal fragment. *J Neurosci,* 29, 13042-13052.

182. Cook, D.G., Forman, M.S., Sung, J.C., Leight, S., Kolson, D.L., Iwatsubo, T., Lee, V.M. and Doms, R.W. (1997) Alzheimer's A beta(1-42) is generated in the endoplasmic reticulum/intermediate compartment of NT2N cells. *Nat Med,* 3, 1021-1023.

183. Greenfield, J.P., Tsai, J., Gouras, G.K., Hai, B., Thinakaran, G., Checler, F., Sisodia, S.S., Greengard, P. and Xu, H. (1999) Endoplasmic reticulum and trans-Golgi network generate distinct populations of Alzheimer beta-amyloid peptides. *Proc Natl Acad Sci U S A,* 96, 742-747.

184. Koo, E.H. and Squazzo, S.L. (1994) Evidence that production and release of amyloid beta-protein involves the endocytic pathway. *J Biol Chem,* 269, 17386-17389.

185. LaFerla, F.M., Green, K.N. and Oddo, S. (2007) Intracellular amyloid-beta in Alzheimer's disease. *Nat Rev Neurosci,* 8, 499-509.

186. Takahashi, R.H., Milner, T.A., Li, F., Nam, E.E., Edgar, M.A., Yamaguchi, H., Beal, M.F., Xu, H., Greengard, P. and Gouras, G.K. (2002) Intraneuronal Alzheimer abeta42 accumulates in multivesicular bodies and is associated with synaptic pathology. *Am J Pathol,* 161, 1869-1879.

187. Cole, S.L. and Vassar, R. (2007) The Alzheimer's disease beta-secretase enzyme, BACE1. *Mol Neurodegener,* 2, 22.

188. Francis, R., McGrath, G., Zhang, J., Ruddy, D.A., Sym, M., Apfeld, J., Nicoll, M., Maxwell, M., Hai, B., Ellis, M.C. *et al.* (2002) aph-1 and pen-2 are required for Notch pathway signaling, gamma-secretase cleavage of betaAPP, and presenilin protein accumulation. *Dev Cell,* 3, 85-97.

189. Levitan, D., Lee, J., Song, L., Manning, R., Wong, G., Parker, E. and Zhang, L. (2001) PS1 N- and C-terminal fragments form a complex that functions in APP processing and Notch signaling. *Proc Natl Acad Sci U S A,* 98, 12186-12190.

190. Serneels, L., Van Biervliet, J., Craessaerts, K., Dejaegere, T., Horre, K., Van Houtvin, T., Esselmann, H., Paul, S., Schafer, M.K., Berezovska, O. *et al.* (2009) gamma-Secretase heterogeneity in the Aph1 subunit: relevance for Alzheimer's disease. *Science,* 324, 639-642.

191. Steiner, H., Fluhrer, R. and Haass, C. (2008) Intramembrane proteolysis by gamma-secretase. *J Biol Chem,* 283, 29627-29631.

192. Wolfe, M.S., Xia, W., Ostaszewski, B.L., Diehl, T.S., Kimberly, W.T. and Selkoe, D.J. (1999) Two transmembrane aspartates in presenilin-1 required for presenilin endoproteolysis and gamma-secretase activity. *Nature,* 398, 513-517.

193. Yu, G., Nishimura, M., Arawaka, S., Levitan, D., Zhang, L., Tandon, A., Song, Y.Q., Rogaeva, E., Chen, F., Kawarai, T. *et al.* (2000) Nicastrin modulates

presenilin-mediated notch/glp-1 signal transduction and betaAPP processing. *Nature,* 407, 48-54.

194. Iwatsubo, T. (2004) Assembly and activation of the gamma-secretase complex: roles of presenilin cofactors. *Mol Psychiatry,* 9, 8-10.

195. De Strooper, B., Annaert, W., Cupers, P., Saftig, P., Craessaerts, K., Mumm, J.S., Schroeter, E.H., Schrijvers, V., Wolfe, M.S., Ray, W.J. *et al.* (1999) A presenilin-1-dependent gamma-secretase-like protease mediates release of Notch intracellular domain. *Nature,* 398, 518-522.

196. Lee, J.H., Yu, W.H., Kumar, A., Lee, S., Mohan, P.S., Peterhoff, C.M., Wolfe, D.M., Martinez-Vicente, M., Massey, A.C., Sovak, G. *et al.* (2010) Lysosomal proteolysis and autophagy require presenilin 1 and are disrupted by Alzheimer-related PS1 mutations. *Cell,* 141, 1146-1158.

197. Zhang, C., Wu, B., Beglopoulos, V., Wines-Samuelson, M., Zhang, D., Dragatsis, I., Sudhof, T.C. and Shen, J. (2009) Presenilins are essential for regulating neurotransmitter release. *Nature,* 460, 632-636.

198. Mills, J. and Reiner, P.B. (1999) Regulation of amyloid precursor protein cleavage. *J Neurochem,* 72, 443-460.

199. Roberson, M.R. and Harrell, L.E. (1997) Cholinergic activity and amyloid precursor protein metabolism. *Brain Res Brain Res Rev,* 25, 50-69.

200. Bodovitz, S. and Klein, W.L. (1996) Cholesterol modulates alpha-secretase cleavage of amyloid precursor protein. *J Biol Chem,* 271, 4436-4440.

201. Frears, E.R., Stephens, D.J., Walters, C.E., Davies, H. and Austen, B.M. (1999) The role of cholesterol in the biosynthesis of beta-amyloid. *Neuroreport,* 10, 1699-1705.

202. Abad-Rodriguez, J., Ledesma, M.D., Craessaerts, K., Perga, S., Medina, M., Delacourte, A., Dingwall, C., De Strooper, B. and Dotti, C.G. (2004) Neuronal membrane cholesterol loss enhances amyloid peptide generation. *J Cell Biol,* 167, 953-960.

203. Fassbender, K., Simons, M., Bergmann, C., Stroick, M., Lutjohann, D., Keller, P., Runz, H., Kuhl, S., Bertsch, T., von Bergmann, K. *et al.* (2001) Simvastatin strongly reduces levels of Alzheimer's disease beta -amyloid peptides Abeta 42 and Abeta 40 in vitro and in vivo. *Proc Natl Acad Sci U S A,* 98, 5856-5861.

204. Kojro, E., Gimpl, G., Lammich, S., Marz, W. and Fahrenholz, F. (2001) Low cholesterol stimulates the nonamyloidogenic pathway by its effect on the alpha -secretase ADAM 10. *Proc Natl Acad Sci U S A,* 98, 5815-5820.

205. Simons, M., Keller, P., De Strooper, B., Beyreuther, K., Dotti, C.G. and Simons, K. (1998) Cholesterol depletion inhibits the generation of beta-amyloid in hippocampal neurons. *Proc Natl Acad Sci U S A,* 95, 6460-6464.

206. Kalvodova, L., Kahya, N., Schwille, P., Ehehalt, R., Verkade, P., Drechsel, D. and Simons, K. (2005) Lipids as modulators of proteolytic activity of BACE: involvement of cholesterol, glycosphingolipids, and anionic phospholipids in vitro. *J Biol Chem*, 280, 36815-36823.

207. Osenkowski, P., Ye, W., Wang, R., Wolfe, M.S. and Selkoe, D.J. (2008) Direct and potent regulation of gamma-secretase by its lipid microenvironment. *J Biol Chem*, 283, 22529-22540.

208. Vetrivel, K.S., Cheng, H., Lin, W., Sakurai, T., Li, T., Nukina, N., Wong, P.C., Xu, H. and Thinakaran, G. (2004) Association of gamma-secretase with lipid rafts in post-Golgi and endosome membranes. *J Biol Chem*, 279, 44945-44954.

209. Wahrle, S., Das, P., Nyborg, A.C., McLendon, C., Shoji, M., Kawarabayashi, T., Younkin, L.H., Younkin, S.G. and Golde, T.E. (2002) Cholesterol-dependent gamma-secretase activity in buoyant cholesterol-rich membrane microdomains. *Neurobiol Dis*, 9, 11-23.

210. Ehehalt, R., Keller, P., Haass, C., Thiele, C. and Simons, K. (2003) Amyloidogenic processing of the Alzheimer beta-amyloid precursor protein depends on lipid rafts. *J Cell Biol*, 160, 113-123.

211. Parkin, E.T., Turner, A.J. and Hooper, N.M. (1999) Amyloid precursor protein, although partially detergent-insoluble in mouse cerebral cortex, behaves as an atypical lipid raft protein. *Biochem J*, 344 Pt 1, 23-30.

212. Cordy, J.M., Hussain, I., Dingwall, C., Hooper, N.M. and Turner, A.J. (2003) Exclusively targeting beta-secretase to lipid rafts by GPI-anchor addition up-regulates beta-site processing of the amyloid precursor protein. *Proc Natl Acad Sci U S A*, 100, 11735-11740.

213. Cole, S.L., Grudzien, A., Manhart, I.O., Kelly, B.L., Oakley, H. and Vassar, R. (2005) Statins cause intracellular accumulation of amyloid precursor protein, beta-secretase-cleaved fragments, and amyloid beta-peptide via an isoprenoid-dependent mechanism. *J Biol Chem*, 280, 18755-18770.

214. Hansen, G.H., Niels-Christiansen, L.L., Thorsen, E., Immerdal, L. and Danielsen, E.M. (2000) Cholesterol depletion of enterocytes. Effect on the Golgi complex and apical membrane trafficking. *J Biol Chem*, 275, 5136-5142.

215. Hao, M., Mukherjee, S., Sun, Y. and Maxfield, F.R. (2004) Effects of cholesterol depletion and increased lipid unsaturation on the properties of endocytic membranes. *J Biol Chem*, 279, 14171-14178.

216. Vetrivel, K.S. and Thinakaran, G. (2010) Membrane rafts in Alzheimer's disease beta-amyloid production. *Biochim Biophys Acta*, 1801, 860-867.

217. Davis, W., Jr. (2008) The cholesterol transport inhibitor U18666a regulates amyloid precursor protein metabolism and trafficking in N2aAPP "Swedish" cells. *Curr Alzheimer Res,* 5, 448-456.

218. Runz, H., Rietdorf, J., Tomic, I., de Bernard, M., Beyreuther, K., Pepperkok, R. and Hartmann, T. (2002) Inhibition of intracellular cholesterol transport alters presenilin localization and amyloid precursor protein processing in neuronal cells. *J Neurosci,* 22, 1679-1689.

219. Jin, L.W., Shie, F.S., Maezawa, I., Vincent, I. and Bird, T. (2004) Intracellular accumulation of amyloidogenic fragments of amyloid-beta precursor protein in neurons with Niemann-Pick type C defects is associated with endosomal abnormalities. *Am J Pathol,* 164, 975-985.

220. Huttunen, H.J., Puglielli, L., Ellis, B.C., MacKenzie Ingano, L.A. and Kovacs, D.M. (2009) Novel N-terminal cleavage of APP precludes Abeta generation in ACAT-defective AC29 cells. *J Mol Neurosci,* 37, 6-15.

221. Koldamova, R.P., Lefterov, I.M., Staufenbiel, M., Wolfe, D., Huang, S., Glorioso, J.C., Walter, M., Roth, M.G. and Lazo, J.S. (2005) The liver X receptor ligand T0901317 decreases amyloid beta production in vitro and in a mouse model of Alzheimer's disease. *J Biol Chem,* 280, 4079-4088.

222. Sun, Y., Yao, J., Kim, T.W. and Tall, A.R. (2003) Expression of liver X receptor target genes decreases cellular amyloid beta peptide secretion. *J Biol Chem,* 278, 27688-27694.

223. Sawamura, N., Ko, M., Yu, W., Zou, K., Hanada, K., Suzuki, T., Gong, J.S., Yanagisawa, K. and Michikawa, M. (2004) Modulation of amyloid precursor protein cleavage by cellular sphingolipids. *J Biol Chem,* 279, 11984-11991.

224. Beel, A.J., Sakakura, M., Barrett, P.J. and Sanders, C.R. (2010) Direct binding of cholesterol to the amyloid precursor protein: An important interaction in lipid-Alzheimer's disease relationships? *Biochim Biophys Acta,* 1801, 975-982.

225. Yao, Z.X. and Papadopoulos, V. (2002) Function of beta-amyloid in cholesterol transport: a lead to neurotoxicity. *FASEB J,* 16, 1677-1679.

226. Esler, W.P., Stimson, E.R., Ghilardi, J.R., Lu, Y.A., Felix, A.M., Vinters, H.V., Mantyh, P.W., Lee, J.P. and Maggio, J.E. (1996) Point substitution in the central hydrophobic cluster of a human beta-amyloid congener disrupts peptide folding and abolishes plaque competence. *Biochemistry,* 35, 13914-13921.

227. Massi, F. and Straub, J.E. (2001) Probing the origins of increased activity of the E22Q "Dutch" mutant Alzheimer's beta-amyloid peptide. *Biophys J,* 81, 697-709.

228. Schmechel, D., Sullivan, P., Mace, B., Sawyer, J. and Rudel, L. (2002) High saturated fat diets are associated with abeta deposition in primates. *Neurobiol Aging,* 23, S323.

229. Refolo, L.M., Malester, B., LaFrancois, J., Bryant-Thomas, T., Wang, R., Tint, G.S., Sambamurti, K., Duff, K. and Pappolla, M.A. (2000) Hypercholesterolemia accelerates the Alzheimer's amyloid pathology in a transgenic mouse model. *Neurobiol Dis,* 7, 321-331.

230. Refolo, L.M., Pappolla, M.A., LaFrancois, J., Malester, B., Schmidt, S.D., Thomas-Bryant, T., Tint, G.S., Wang, R., Mercken, M., Petanceska, S.S. *et al.* (2001) A cholesterol-lowering drug reduces beta-amyloid pathology in a transgenic mouse model of Alzheimer's disease. *Neurobiol Dis,* 8, 890-899.

231. Ghribi, O., Larsen, B., Schrag, M. and Herman, M.M. (2006) High cholesterol content in neurons increases BACE, beta-amyloid, and phosphorylated tau levels in rabbit hippocampus. *Exp Neurol,* 200, 460-467.

232. Hooijmans, C.R., Rutters, F., Dederen, P.J., Gambarota, G., Veltien, A., van Groen, T., Broersen, L.M., Lutjohann, D., Heerschap, A., Tanila, H. *et al.* (2007) Changes in cerebral blood volume and amyloid pathology in aged Alzheimer APP/PS1 mice on a docosahexaenoic acid (DHA) diet or cholesterol enriched Typical Western Diet (TWD). *Neurobiol Dis,* 28, 16-29.

233. Hooijmans, C.R., Van der Zee, C.E., Dederen, P.J., Brouwer, K.M., Reijmer, Y.D., van Groen, T., Broersen, L.M., Lutjohann, D., Heerschap, A. and Kiliaan, A.J. (2009) DHA and cholesterol containing diets influence Alzheimer-like pathology, cognition and cerebral vasculature in APPswe/PS1dE9 mice. *Neurobiol Dis,* 33, 482-498.

234. Jaya Prasanthi, R.P., Schommer, E., Thomasson, S., Thompson, A., Feist, G. and Ghribi, O. (2008) Regulation of beta-amyloid levels in the brain of cholesterol-fed rabbit, a model system for sporadic Alzheimer's disease. *Mech Ageing Dev,* 129, 649-655.

235. Levin-Allerhand, J.A., Lominska, C.E. and Smith, J.D. (2002) Increased amyloid-levels in APPSWE transgenic mice treated chronically with a physiological high-fat high-cholesterol diet. *J Nutr Health Aging,* 6, 315-319.

236. Li, L., Cao, D., Garber, D.W., Kim, H. and Fukuchi, K. (2003) Association of aortic atherosclerosis with cerebral beta-amyloidosis and learning deficits in a mouse model of Alzheimer's disease. *Am J Pathol,* 163, 2155-2164.

237. Pedrini, S., Thomas, C., Brautigam, H., Schmeidler, J., Ho, L., Fraser, P., Westaway, D., Hyslop, P.S., Martins, R.N., Buxbaum, J.D. *et al.* (2009) Dietary composition modulates brain mass and solubilizable Abeta levels in a mouse model of aggressive Alzheimer's amyloid pathology. *Mol Neurodegener,* 4, 40.

238. Shie, F.S., Jin, L.W., Cook, D.G., Leverenz, J.B. and LeBoeuf, R.C. (2002) Diet-induced hypercholesterolemia enhances brain A beta accumulation in transgenic mice. *Neuroreport,* 13, 455-459.

239. Thirumangalakudi, L., Prakasam, A., Zhang, R., Bimonte-Nelson, H., Sambamurti, K., Kindy, M.S. and Bhat, N.R. (2008) High cholesterol-induced neuroinflammation and amyloid precursor protein processing correlate with loss of working memory in mice. *J Neurochem,* 106, 475-485.

240. Cibickova, L., Hyspler, R., Micuda, S., Cibicek, N., Zivna, H., Jun, D., Ticha, A., Brcakova, E. and Palicka, V. (2009) The influence of simvastatin, atorvastatin and high-cholesterol diet on acetylcholinesterase activity, amyloid beta and cholesterol synthesis in rat brain. *Steroids,* 74, 13-19.

241. George, A.J., Holsinger, R.M., McLean, C.A., Laughton, K.M., Beyreuther, K., Evin, G., Masters, C.L. and Li, Q.X. (2004) APP intracellular domain is increased and soluble Abeta is reduced with diet-induced hypercholesterolemia in a transgenic mouse model of Alzheimer disease. *Neurobiol Dis,* 16, 124-132.

242. Howland, D.S., Trusko, S.P., Savage, M.J., Reaume, A.G., Lang, D.M., Hirsch, J.D., Maeda, N., Siman, R., Greenberg, B.D., Scott, R.W. *et al.* (1998) Modulation of secreted beta-amyloid precursor protein and amyloid beta-peptide in brain by cholesterol. *J Biol Chem,* 273, 16576-16582.

243. Petanceska, S.S., DeRosa, S., Olm, V., Diaz, N., Sharma, A., Thomas-Bryant, T., Duff, K., Pappolla, M. and Refolo, L.M. (2002) Statin therapy for Alzheimer's disease: will it work? *J Mol Neurosci,* 19, 155-161.

244. Park, I.H., Hwang, E.M., Hong, H.S., Boo, J.H., Oh, S.S., Lee, J., Jung, M.W., Bang, O.Y., Kim, S.U. and Mook-Jung, I. (2003) Lovastatin enhances Abeta production and senile plaque deposition in female Tg2576 mice. *Neurobiol Aging,* 24, 637-643.

245. Bales, K.R., Verina, T., Cummins, D.J., Du, Y., Dodel, R.C., Saura, J., Fishman, C.E., DeLong, C.A., Piccardo, P., Petegnief, V. *et al.* (1999) Apolipoprotein E is essential for amyloid deposition in the APP(V717F) transgenic mouse model of Alzheimer's disease. *Proc Natl Acad Sci U S A,* 96, 15233-15238.

246. Bales, K.R., Verina, T., Dodel, R.C., Du, Y., Altstiel, L., Bender, M., Hyslop, P., Johnstone, E.M., Little, S.P., Cummins, D.J. *et al.* (1997) Lack of apolipoprotein E dramatically reduces amyloid beta-peptide deposition. *Nat Genet,* 17, 263-264.

247. Holtzman, D.M., Fagan, A.M., Mackey, B., Tenkova, T., Sartorius, L., Paul, S.M., Bales, K., Ashe, K.H., Irizarry, M.C. and Hyman, B.T. (2000) Apolipoprotein E facilitates neuritic and cerebrovascular plaque formation in an Alzheimer's disease model. *Ann Neurol,* 47, 739-747.

248. Irizarry, M.C., Cheung, B.S., Rebeck, G.W., Paul, S.M., Bales, K.R. and Hyman, B.T. (2000) Apolipoprotein E affects the amount, form, and anatomical distribution of amyloid beta-peptide deposition in homozygous APP(V717F) transgenic mice. *Acta Neuropathol,* 100, 451-458.

249. Cao, D., Fukuchi, K., Wan, H., Kim, H. and Li, L. (2006) Lack of LDL receptor aggravates learning deficits and amyloid deposits in Alzheimer transgenic mice. *Neurobiol Aging,* 27, 1632-1643.

250. Fryer, J.D., Demattos, R.B., McCormick, L.M., O'Dell, M.A., Spinner, M.L., Bales, K.R., Paul, S.M., Sullivan, P.M., Parsadanian, M., Bu, G. *et al.* (2005) The low density lipoprotein receptor regulates the level of central nervous system human and murine apolipoprotein E but does not modify amyloid plaque pathology in PDAPP mice. *J Biol Chem,* 280, 25754-25759.

251. Kim, J., Castellano, J.M., Jiang, H., Basak, J.M., Parsadanian, M., Pham, V., Mason, S.M., Paul, S.M. and Holtzman, D.M. (2009) Overexpression of low-density lipoprotein receptor in the brain markedly inhibits amyloid deposition and increases extracellular A beta clearance. *Neuron,* 64, 632-644.

252. Fagan, A.M., Christopher, E., Taylor, J.W., Parsadanian, M., Spinner, M., Watson, M., Fryer, J.D., Wahrle, S., Bales, K.R., Paul, S.M. *et al.* (2004) ApoAI deficiency results in marked reductions in plasma cholesterol but no alterations in amyloid-beta pathology in a mouse model of Alzheimer's disease-like cerebral amyloidosis. *Am J Pathol,* 165, 1413-1422.

253. Crameri, A., Biondi, E., Kuehnle, K., Lutjohann, D., Thelen, K.M., Perga, S., Dotti, C.G., Nitsch, R.M., Ledesma, M.D. and Mohajeri, M.H. (2006) The role of seladin-1/DHCR24 in cholesterol biosynthesis, APP processing and Abeta generation in vivo. *EMBO J,* 25, 432-443.

254. Greeve, I., Hermans-Borgmeyer, I., Brellinger, C., Kasper, D., Gomez-Isla, T., Behl, C., Levkau, B. and Nitsch, R.M. (2000) The human DIMINUTO/DWARF1 homolog seladin-1 confers resistance to Alzheimer's disease-associated neurodegeneration and oxidative stress. *J Neurosci,* 20, 7345-7352.

255. Iivonen, S., Hiltunen, M., Alafuzoff, I., Mannermaa, A., Kerokoski, P., Puolivali, J., Salminen, A., Helisalmi, S. and Soininen, H. (2002) Seladin-1 transcription is linked to neuronal degeneration in Alzheimer's disease. *Neuroscience,* 113, 301-310.

256. Ledesma, M.D., Abad-Rodriguez, J., Galvan, C., Biondi, E., Navarro, P., Delacourte, A., Dingwall, C. and Dotti, C.G. (2003) Raft disorganization leads to reduced plasmin activity in Alzheimer's disease brains. *EMBO Rep,* 4, 1190-1196.

257. Halford, R.W. and Russell, D.W. (2009) Reduction of cholesterol synthesis in the mouse brain does not affect amyloid formation in Alzheimer's disease, but does extend lifespan. *Proc Natl Acad Sci U S A,* 106, 3502-3506.

258. Koldamova, R., Staufenbiel, M. and Lefterov, I. (2005) Lack of ABCA1 considerably decreases brain ApoE level and increases amyloid deposition in APP23 mice. *J Biol Chem,* 280, 43224-43235.

259. Wahrle, S.E., Jiang, H., Parsadanian, M., Hartman, R.E., Bales, K.R., Paul, S.M. and Holtzman, D.M. (2005) Deletion of Abca1 increases Abeta deposition in the PDAPP transgenic mouse model of Alzheimer disease. *J Biol Chem,* 280, 43236-43242.

260. Wahrle, S.E., Jiang, H., Parsadanian, M., Kim, J., Li, A., Knoten, A., Jain, S., Hirsch-Reinshagen, V., Wellington, C.L., Bales, K.R. *et al.* (2008) Overexpression of ABCA1 reduces amyloid deposition in the PDAPP mouse model of Alzheimer disease. *J Clin Invest,* 118, 671-682.

261. Bryleva, E.Y., Rogers, M.A., Chang, C.C., Buen, F., Harris, B.T., Rousselet, E., Seidah, N.G., Oddo, S., LaFerla, F.M., Spencer, T.A. *et al.* (2010) ACAT1 gene ablation increases 24(S)-hydroxycholesterol content in the brain and ameliorates amyloid pathology in mice with AD. *Proc Natl Acad Sci U S A,* 107, 3081-3086.

262. Hutter-Paier, B., Huttunen, H.J., Puglielli, L., Eckman, C.B., Kim, D.Y., Hofmeister, A., Moir, R.D., Domnitz, S.B., Frosch, M.P., Windisch, M. *et al.* (2004) The ACAT inhibitor CP-113,818 markedly reduces amyloid pathology in a mouse model of Alzheimer's disease. *Neuron,* 44, 227-238.

263. Michaki, V., Guix, F.X., Vennekens, K., Munck, S., Dingwall, C., Davis, J.B., Townsend, D.M., Tew, K.D., Feiguin, F., De Strooper, B. *et al.* (2012) Down-regulation of the ATP-binding cassette transporter 2 (Abca2) reduces amyloid-beta production by altering Nicastrin maturation and intracellular localization. *J Biol Chem,* 287, 1100-1111.

264. Yamazaki, T., Chang, T.Y., Haass, C. and Ihara, Y. (2001) Accumulation and aggregation of amyloid beta-protein in late endosomes of Niemann-pick type C cells. *J Biol Chem,* 276, 4454-4460.

265. Annaert, W.G., Levesque, L., Craessaerts, K., Dierinck, I., Snellings, G., Westaway, D., George-Hyslop, P.S., Cordell, B., Fraser, P. and De Strooper, B. (1999) Presenilin 1 controls gamma-secretase processing of amyloid precursor protein in pre-golgi compartments of hippocampal neurons. *J Cell Biol,* 147, 277-294.

266. Burns, M., Gaynor, K., Olm, V., Mercken, M., LaFrancois, J., Wang, L., Mathews, P.M., Noble, W., Matsuoka, Y. and Duff, K. (2003) Presenilin redistribution associated with aberrant cholesterol transport enhances beta-amyloid production in vivo. *J Neurosci,* 23, 5645-5649.

267. Kodam, A., Maulik, M., Peake, K., Amritraj, A., Vetrivel, K.S., Thinakaran, G., Vance, J.E. and Kar, S. (2010) Altered levels and distribution of amyloid precursor protein and its processing enzymes in Niemann-Pick type C1-deficient mouse brains. *Glia,* 58, 1267-1281.

268. Borbon, I.A. and Erickson, R.P. (2010) Interactions of Npc1 and amyloid accumulation/deposition in the APP/PS1 mouse model of Alzheimer's. *J Appl Genet*.

269. Haass, C., Schlossmacher, M.G., Hung, A.Y., Vigo-Pelfrey, C., Mellon, A., Ostaszewski, B.L., Lieberburg, I., Koo, E.H., Schenk, D., Teplow, D.B. *et al.* (1992) Amyloid beta-peptide is produced by cultured cells during normal metabolism. *Nature,* 359, 322-325.

270. Shoji, M. (2002) Cerebrospinal fluid Abeta40 and Abeta42: natural course and clinical usefulness. *Front Biosci,* 7, d997-1006.

271. Vigo-Pelfrey, C., Lee, D., Keim, P., Lieberburg, I. and Schenk, D.B. (1993) Characterization of beta-amyloid peptide from human cerebrospinal fluid. *J Neurochem,* 61, 1965-1968.

272. Giuffrida, M.L., Caraci, F., Pignataro, B., Cataldo, S., De Bona, P., Bruno, V., Molinaro, G., Pappalardo, G., Messina, A., Palmigiano, A. *et al.* (2009) Beta-amyloid monomers are neuroprotective. *J Neurosci,* 29, 10582-10587.

273. Cleary, J.P., Walsh, D.M., Hofmeister, J.J., Shankar, G.M., Kuskowski, M.A., Selkoe, D.J. and Ashe, K.H. (2005) Natural oligomers of the amyloid-beta protein specifically disrupt cognitive function. *Nat Neurosci,* 8, 79-84.

274. Dahlgren, K.N., Manelli, A.M., Stine, W.B., Jr., Baker, L.K., Krafft, G.A. and LaDu, M.J. (2002) Oligomeric and fibrillar species of amyloid-beta peptides differentially affect neuronal viability. *J Biol Chem,* 277, 32046-32053.

275. Haass, C. and Selkoe, D.J. (2007) Soluble protein oligomers in neurodegeneration: lessons from the Alzheimer's amyloid beta-peptide. *Nat Rev Mol Cell Biol,* 8, 101-112.

276. Kayed, R., Head, E., Thompson, J.L., McIntire, T.M., Milton, S.C., Cotman, C.W. and Glabe, C.G. (2003) Common structure of soluble amyloid oligomers implies common mechanism of pathogenesis. *Science,* 300, 486-489.

277. Lesne, S., Kotilinek, L. and Ashe, K.H. (2008) Plaque-bearing mice with reduced levels of oligomeric amyloid-beta assemblies have intact memory function. *Neuroscience,* 151, 745-749.

278. Roychaudhuri, R., Yang, M., Hoshi, M.M. and Teplow, D.B. (2009) Amyloid beta-protein assembly and Alzheimer disease. *J Biol Chem,* 284, 4749-4753.

279. Shankar, G.M. and Walsh, D.M. (2009) Alzheimer's disease: synaptic dysfunction and Abeta. *Mol Neurodegener,* 4, 48.

280. Lue, L.F., Kuo, Y.M., Roher, A.E., Brachova, L., Shen, Y., Sue, L., Beach, T., Kurth, J.H., Rydel, R.E. and Rogers, J. (1999) Soluble amyloid beta peptide concentration as a predictor of synaptic change in Alzheimer's disease. *Am J Pathol,* 155, 853-862.

281. McLean, C.A., Cherny, R.A., Fraser, F.W., Fuller, S.J., Smith, M.J., Beyreuther, K., Bush, A.I. and Masters, C.L. (1999) Soluble pool of Abeta amyloid as a

determinant of severity of neurodegeneration in Alzheimer's disease. *Ann Neurol,* 46, 860-866.

282. Tomic, J.L., Pensalfini, A., Head, E. and Glabe, C.G. (2009) Soluble fibrillar oligomer levels are elevated in Alzheimer's disease brain and correlate with cognitive dysfunction. *Neurobiol Dis,* 35, 352-358.

283. Schneider, A., Schulz-Schaeffer, W., Hartmann, T., Schulz, J.B. and Simons, M. (2006) Cholesterol depletion reduces aggregation of amyloid-beta peptide in hippocampal neurons. *Neurobiol Dis,* 23, 573-577.

284. Rushworth, J.V. and Hooper, N.M. (2010) Lipid rafts: Linking Alzheimer's amyloid-beta production, aggregation, and toxicity at neuronal membranes. *Int J Alzheimers Dis,* 2011, 603052.

285. Kakio, A., Nishimoto, S., Yanagisawa, K., Kozutsumi, Y. and Matsuzaki, K. (2002) Interactions of amyloid beta-protein with various gangliosides in raft-like membranes: importance of GM1 ganglioside-bound form as an endogenous seed for Alzheimer amyloid. *Biochemistry,* 41, 7385-7390.

286. Matsuzaki, K., Kato, K. and Yanagisawa, K. (2010) Abeta polymerization through interaction with membrane gangliosides. *Biochim Biophys Acta,* 1801, 868-877.

287. McLaurin, J., Franklin, T., Fraser, P.E. and Chakrabartty, A. (1998) Structural transitions associated with the interaction of Alzheimer beta-amyloid peptides with gangliosides. *J Biol Chem,* 273, 4506-4515.

288. Choo-Smith, L.P., Garzon-Rodriguez, W., Glabe, C.G. and Surewicz, W.K. (1997) Acceleration of amyloid fibril formation by specific binding of Abeta-(1-40) peptide to ganglioside-containing membrane vesicles. *J Biol Chem,* 272, 22987-22990.

289. Kim, S.I., Yi, J.S. and Ko, Y.G. (2006) Amyloid beta oligomerization is induced by brain lipid rafts. *J Cell Biochem,* 99, 878-889.

290. Okada, T., Ikeda, K., Wakabayashi, M., Ogawa, M. and Matsuzaki, K. (2008) Formation of toxic Abeta(1-40) fibrils on GM1 ganglioside-containing membranes mimicking lipid rafts: polymorphisms in Abeta(1-40) fibrils. *J Mol Biol,* 382, 1066-1074.

291. Zampagni, M., Evangelisti, E., Cascella, R., Liguri, G., Becatti, M., Pensalfini, A., Uberti, D., Cenini, G., Memo, M., Bagnoli, S. *et al.* (2010) Lipid rafts are primary mediators of amyloid oxidative attack on plasma membrane. *J Mol Med,* 88, 597-608.

292. Yahi, N., Aulas, A. and Fantini, J. (2010) How cholesterol constrains glycolipid conformation for optimal recognition of Alzheimer's beta amyloid peptide (Abeta1-40). *PLoS One,* 5, e9079.

293. Lin, M.S., Chen, L.Y., Wang, S.S., Chang, Y. and Chen, W.Y. (2008) Examining the levels of ganglioside and cholesterol in cell membrane on attenuation the cytotoxicity of beta-amyloid peptide. *Colloids Surf B Biointerfaces,* 65, 172-177.

294. Abramov, A.Y., Ionov, M., Pavlov, E. and Duchen, M.R. (2011) Membrane cholesterol content plays a key role in the neurotoxicity of beta-amyloid: implications for Alzheimer's disease. *Aging Cell,* 10, 595-603.

295. Ferrera, P., Mercado-Gomez, O., Silva-Aguilar, M., Valverde, M. and Arias, C. (2008) Cholesterol potentiates beta-amyloid-induced toxicity in human neuroblastoma cells: involvement of oxidative stress. *Neurochem Res,* 33, 1509-1517.

296. Wang, S.S., Rymer, D.L. and Good, T.A. (2001) Reduction in cholesterol and sialic acid content protects cells from the toxic effects of beta-amyloid peptides. *J Biol Chem,* 276, 42027-42034.

297. Nicholson, A.M. and Ferreira, A. (2009) Increased membrane cholesterol might render mature hippocampal neurons more susceptible to beta-amyloid-induced calpain activation and tau toxicity. *J Neurosci,* 29, 4640-4651.

298. Fernandez, A., Llacuna, L., Fernandez-Checa, J.C. and Colell, A. (2009) Mitochondrial cholesterol loading exacerbates amyloid beta peptide-induced inflammation and neurotoxicity. *J Neurosci,* 29, 6394-6405.

299. Gonzalo-Ruiz, A., Perez, J.L., Sanz, J.M., Geula, C. and Arevalo, J. (2006) Effects of lipids and aging on the neurotoxicity and neuronal loss caused by intracerebral injections of the amyloid-beta peptide in the rat. *Exp Neurol,* 197, 41-55.

300. Cecchi, C., Rosati, F., Pensalfini, A., Formigli, L., Nosi, D., Liguri, G., Dichiara, F., Morello, M., Danza, G., Pieraccini, G. *et al.* (2008) Seladin-1/DHCR24 protects neuroblastoma cells against Abeta toxicity by increasing membrane cholesterol content. *J Cell Mol Med,* 12, 1990-2002.

301. Arispe, N. and Doh, M. (2002) Plasma membrane cholesterol controls the cytotoxicity of Alzheimer's disease AbetaP (1-40) and (1-42) peptides. *FASEB J,* 16, 1526-1536.

302. Sponne, I., Fifre, A., Koziel, V., Oster, T., Olivier, J.L. and Pillot, T. (2004) Membrane cholesterol interferes with neuronal apoptosis induced by soluble oligomers but not fibrils of amyloid-beta peptide. *FASEB J,* 18, 836-838.

303. Yip, C.M., Elton, E.A., Darabie, A.A., Morrison, M.R. and McLaurin, J. (2001) Cholesterol, a modulator of membrane-associated Abeta-fibrillogenesis and neurotoxicity. *J Mol Biol,* 311, 723-734.

304. Zhou, Y. and Richardson, J.S. (1996) Cholesterol protects PC12 cells from beta-amyloid induced calcium disordering and cytotoxicity. *Neuroreport,* 7, 2487-2490.

305. Allaman, I., Gavillet, M., Belanger, M., Laroche, T., Viertl, D., Lashuel, H.A. and Magistretti, P.J. (2010) Amyloid-beta aggregates cause alterations of astrocytic metabolic phenotype: impact on neuronal viability. *J Neurosci,* 30, 3326-3338.

306. Chung, H., Brazil, M.I., Soe, T.T. and Maxfield, F.R. (1999) Uptake, degradation, and release of fibrillar and soluble forms of Alzheimer's amyloid beta-peptide by microglial cells. *J Biol Chem,* 274, 32301-32308.

307. D'Andrea, M.R., Nagele, R.G., Wang, H.Y., Peterson, P.A. and Lee, D.H. (2001) Evidence that neurones accumulating amyloid can undergo lysis to form amyloid plaques in Alzheimer's disease. *Histopathology,* 38, 120-134.

308. Ditaranto, K., Tekirian, T.L. and Yang, A.J. (2001) Lysosomal membrane damage in soluble Abeta-mediated cell death in Alzheimer's disease. *Neurobiol Dis,* 8, 19-31.

309. Mohamed, A. and Posse de Chaves, E. (2011) Abeta internalization by neurons and glia. *Int J Alzheimers Dis,* 2011, 127984.

310. Pihlaja, R., Koistinaho, J., Malm, T., Sikkila, H., Vainio, S. and Koistinaho, M. (2008) Transplanted astrocytes internalize deposited beta-amyloid peptides in a transgenic mouse model of Alzheimer's disease. *Glia,* 56, 154-163.

311. Song, M.S., Baker, G.B., Todd, K.G. and Kar, S. (2011) Inhibition of beta-amyloid1-42 internalization attenuates neuronal death by stabilizing the endosomal-lysosomal system in rat cortical cultured neurons. *Neuroscience,* 178, 181-188.

312. Wyss-Coray, T., Lin, C., Yan, F., Yu, G.Q., Rohde, M., McConlogue, L., Masliah, E. and Mucke, L. (2001) TGF-beta1 promotes microglial amyloid-beta clearance and reduces plaque burden in transgenic mice. *Nat Med,* 7, 612-618.

313. Lai, A.Y. and McLaurin, J. (2011) Mechanisms of amyloid-β peptide uptake by neurons: the role of lipid rafts and lipid raft-associated proteins. *Int J Alzheimers Dis,* 2011, 548380.

314. Chafekar, S.M., Baas, F. and Scheper, W. (2008) Oligomer-specific Abeta toxicity in cell models is mediated by selective uptake. *Biochim Biophys Acta,* 1782, 523-531.

315. Mandrekar, S., Jiang, Q., Lee, C.Y., Koenigsknecht-Talboo, J., Holtzman, D.M. and Landreth, G.E. (2009) Microglia mediate the clearance of soluble Abeta through fluid phase macropinocytosis. *J Neurosci,* 29, 4252-4262.

316. Yu, C., Nwabuisi-Heath, E., Laxton, K. and Ladu, M.J. (2010) Endocytic pathways mediating oligomeric Abeta42 neurotoxicity. *Mol Neurodegener,* 5, 19.

317. Saavedra, L., Mohamed, A., Ma, V., Kar, S. and de Chaves, E.P. (2007) Internalization of beta-amyloid peptide by primary neurons in the absence of apolipoprotein E. *J Biol Chem,* 282, 35722-35732.

318. Singh, T.D., Park, S.Y., Bae, J.S., Yun, Y., Bae, Y.C., Park, R.W. and Kim, I.S. (2010) MEGF10 functions as a receptor for the uptake of amyloid-beta. *FEBS Lett,* 584, 3936-3942.

319. Eckman, E.A. and Eckman, C.B. (2005) Abeta-degrading enzymes: modulators of Alzheimer's disease pathogenesis and targets for therapeutic intervention. *Biochem Soc Trans,* 33, 1101-1105.

320. Miners, J.S., Baig, S., Palmer, J., Palmer, L.E., Kehoe, P.G. and Love, S. (2008) Abeta-degrading enzymes in Alzheimer's disease. *Brain Pathol,* 18, 240-252.

321. Fan, J., Donkin, J. and Wellington, C. (2009) Greasing the wheels of Abeta clearance in Alzheimer's disease: the role of lipids and apolipoprotein E. *Biofactors,* 35, 239-248.

322. Vekrellis, K., Ye, Z., Qiu, W.Q., Walsh, D., Hartley, D., Chesneau, V., Rosner, M.R. and Selkoe, D.J. (2000) Neurons regulate extracellular levels of amyloid beta-protein via proteolysis by insulin-degrading enzyme. *J Neurosci,* 20, 1657-1665.

323. Bulloj, A., Leal, M.C., Surace, E.I., Zhang, X., Xu, H., Ledesma, M.D., Castano, E.M. and Morelli, L. (2008) Detergent resistant membrane-associated IDE in brain tissue and cultured cells: Relevance to Abeta and insulin degradation. *Mol Neurodegener,* 3, 22.

324. Kanemitsu, H., Tomiyama, T. and Mori, H. (2003) Human neprilysin is capable of degrading amyloid beta peptide not only in the monomeric form but also the pathological oligomeric form. *Neurosci Lett,* 350, 113-116.

325. Sato, K., Tanabe, C., Yonemura, Y., Watahiki, H., Zhao, Y., Yagishita, S., Ebina, M., Suo, S., Futai, E., Murata, M. *et al.* (2012) Localization of mature neprilysin in lipid rafts. *J Neurosci Res,* 90, 870-877.

326. Hama, E., Shirotani, K., Iwata, N. and Saido, T.C. (2004) Effects of neprilysin chimeric proteins targeted to subcellular compartments on amyloid beta peptide clearance in primary neurons. *J Biol Chem,* 279, 30259-30264.

327. Stefani, M. and Liguri, G. (2009) Cholesterol in Alzheimer's disease: unresolved questions. *Curr Alzheimer Res,* 6, 15-29.

328. Lee, C.Y., Tse, W., Smith, J.D. and Landreth, G.E. (2012) Apolipoprotein E promotes beta-amyloid trafficking and degradation by modulating microglial cholesterol levels. *J Biol Chem,* 287, 2032-2044.

329. Jick, H., Zornberg, G.L., Jick, S.S., Seshadri, S. and Drachman, D.A. (2000) Statins and the risk of dementia. *Lancet,* 356, 1627-1631.

330. Wolozin, B., Kellman, W., Ruosseau, P., Celesia, G.G. and Siegel, G. (2000) Decreased prevalence of Alzheimer disease associated with 3-hydroxy-3-methyglutaryl coenzyme A reductase inhibitors. *Arch Neurol,* 57, 1439-1443.

331. Rockwood, K., Kirkland, S., Hogan, D.B., MacKnight, C., Merry, H., Verreault, R., Wolfson, C. and McDowell, I. (2002) Use of lipid-lowering agents, indication bias, and the risk of dementia in community-dwelling elderly people. *Arch Neurol,* 59, 223-227.

332. Yaffe, K., Barrett-Connor, E., Lin, F. and Grady, D. (2002) Serum lipoprotein levels, statin use, and cognitive function in older women. *Arch Neurol,* 59, 378-384.

333. Friedhoff, L.T., Cullen, E.I., Geoghagen, N.S. and Buxbaum, J.D. (2001) Treatment with controlled-release lovastatin decreases serum concentrations of human beta-amyloid (A beta) peptide. *Int J Neuropsychopharmacol,* 4, 127-130.

334. Vega, G.L., Weiner, M.F., Lipton, A.M., Von Bergmann, K., Lutjohann, D., Moore, C. and Svetlik, D. (2003) Reduction in levels of 24S-hydroxycholesterol by statin treatment in patients with Alzheimer disease. *Arch Neurol,* 60, 510-515.

335. Ostrowski, S.M., Wilkinson, B.L., Golde, T.E. and Landreth, G. (2007) Statins reduce amyloid-beta production through inhibition of protein isoprenylation. *J Biol Chem,* 282, 26832-26844.

336. Fonseca, A.C., Resende, R., Oliveira, C.R. and Pereira, C.M. (2010) Cholesterol and statins in Alzheimer's disease: current controversies. *Exp Neurol,* 223, 282-293.

337. Bate, C. and Williams, A. (2007) Squalestatin protects neurons and reduces the activation of cytoplasmic phospholipase A2 by Abeta(1-42). *Neuropharmacology,* 53, 222-231.

338. Paris, D., Townsend, K.P., Humphrey, J., Obregon, D.F., Yokota, K. and Mullan, M. (2002) Statins inhibit A beta-neurotoxicity in vitro and A beta-induced vasoconstriction and inflammation in rat aortae. *Atherosclerosis,* 161, 293-299.

339. Salins, P., Shawesh, S., He, Y., Dibrov, A., Kashour, T., Arthur, G. and Amara, F. (2007) Lovastatin protects human neurons against Abeta-induced toxicity and causes activation of beta-catenin-TCF/LEF signaling. *Neurosci Lett,* 412, 211-216.

340. Chauhan, N.B., Siegel, G.J. and Feinstein, D.L. (2004) Effects of lovastatin and pravastatin on amyloid processing and inflammatory response in TgCRND8 brain. *Neurochem Res,* 29, 1897-1911.

341. Arvanitakis, Z., Schneider, J.A., Wilson, R.S., Bienias, J.L., Kelly, J.F., Evans, D.A. and Bennett, D.A. (2008) Statins, incident Alzheimer disease, change in cognitive function, and neuropathology. *Neurology,* 70, 1795-1802.

342. Li, Y., Tacey, K., Doil, L., van Luchene, R., Garcia, V., Rowland, C., Schrodi, S., Leong, D., Lau, K., Catanese, J. *et al.* (2004) Association of ABCA1 with late-onset Alzheimer's disease is not observed in a case-control study. *Neurosci Lett,* 366, 268-271.

343. Rea, T.D., Breitner, J.C., Psaty, B.M., Fitzpatrick, A.L., Lopez, O.L., Newman, A.B., Hazzard, W.R., Zandi, P.P., Burke, G.L., Lyketsos, C.G. *et al.* (2005) Statin

use and the risk of incident dementia: the Cardiovascular Health Study. *Arch Neurol,* 62, 1047-1051.

344. Zandi, P.P., Sparks, D.L., Khachaturian, A.S., Tschanz, J., Norton, M., Steinberg, M., Welsh-Bohmer, K.A. and Breitner, J.C. (2005) Do statins reduce risk of incident dementia and Alzheimer disease? The Cache County Study. *Arch Gen Psychiatry,* 62, 217-224.

345. Kandiah, N. and Feldman, H.H. (2009) Therapeutic potential of statins in Alzheimer's disease. *J Neurol Sci,* 283, 230-234.

346. Heverin, M., Meaney, S., Lutjohann, D., Diczfalusy, U., Wahren, J. and Bjorkhem, I. (2005) Crossing the barrier: net flux of 27-hydroxycholesterol into the human brain. *J Lipid Res,* 46, 1047-1052.

347. Glebov, K. and Walter, J. (2012) Statins in unconventional secretion of insulin-degrading enzyme and degradation of the amyloid-β peptide. *Neurodegener Dis,* 10, 309-312.

348. Kuipers, H.F., Rappert, A.A., Mommaas, A.M., van Haastert, E.S., van der Valk, P., Boddeke, H.W., Biber, K.P. and van den Elsen, P.J. (2006) Simvastatin affects cell motility and actin cytoskeleton distribution of microglia. *Glia,* 53, 115-123.

349. Pahan, K., Sheikh, F.G., Namboodiri, A.M. and Singh, I. (1997) Lovastatin and phenylacetate inhibit the induction of nitric oxide synthase and cytokines in rat primary astrocytes, microglia, and macrophages. *J Clin Invest,* 100, 2671-2679.

350. Shishehbor, M.H., Brennan, M.L., Aviles, R.J., Fu, X., Penn, M.S., Sprecher, D.L. and Hazen, S.L. (2003) Statins promote potent systemic antioxidant effects through specific inflammatory pathways. *Circulation,* 108, 426-431.

351. Tanaka, K., Honda, M. and Takabatake, T. (2004) Anti-apoptotic effect of atorvastatin, a 3-hydroxy-3-methylglutaryl coenzyme a reductase inhibitor, on cardiac myocytes through protein kinase C activation. *Clin Exp Pharmacol Physiol,* 31, 360-364.

352. Zacco, A., Togo, J., Spence, K., Ellis, A., Lloyd, D., Furlong, S. and Piser, T. (2003) 3-hydroxy-3-methylglutaryl coenzyme A reductase inhibitors protect cortical neurons from excitotoxicity. *J Neurosci,* 23, 11104-11111.

353. Youssef, S., Stuve, O., Patarroyo, J.C., Ruiz, P.J., Radosevich, J.L., Hur, E.M., Bravo, M., Mitchell, D.J., Sobel, R.A., Steinman, L. *et al.* (2002) The HMG-CoA reductase inhibitor, atorvastatin, promotes a Th2 bias and reverses paralysis in central nervous system autoimmune disease. *Nature,* 420, 78-84.

354. Eckert, G.P., Kirsch, C. and Mueller, W.E. (2001) Differential effects of lovastatin treatment on brain cholesterol levels in normal and apoE-deficient mice. *Neuroreport,* 12, 883-887.

355. Huttunen, H.J., Havas, D., Peach, C., Barren, C., Duller, S., Xia, W., Frosch, M.P., Hutter-Paier, B., Windisch, M. and Kovacs, D.M. (2010) The acyl-coenzyme A: cholesterol acyltransferase inhibitor CI-1011 reverses diffuse brain amyloid pathology in aged amyloid precursor protein transgenic mice. *J Neuropathol Exp Neurol,* 69, 777-788.

356. Bhattacharyya, R. and Kovacs, D.M. (2010) ACAT inhibition and amyloid beta reduction. *Biochim Biophys Acta,* 1801, 960-965.

357. Burns, M.P., Vardanian, L., Pajoohesh-Ganji, A., Wang, L., Cooper, M., Harris, D.C., Duff, K. and Rebeck, G.W. (2006) The effects of ABCA1 on cholesterol efflux and Abeta levels in vitro and in vivo. *J Neurochem,* 98, 792-800.

358. Loane, D.J., Washington, P.M., Vardanian, L., Pocivavsek, A., Hoe, H.S., Duff, K.E., Cernak, I., Rebeck, G.W., Faden, A.I. and Burns, M.P. (2010) Modulation of ABCA1 by an LXR agonist reduces β-amyloid levels and improves outcome after traumatic brain injury. *J Neurotrauma,* 28, 225-236.

359. Riddell, D.R., Zhou, H., Comery, T.A., Kouranova, E., Lo, C.F., Warwick, H.K., Ring, R.H., Kirksey, Y., Aschmies, S., Xu, J. *et al.* (2007) The LXR agonist TO901317 selectively lowers hippocampal Abeta42 and improves memory in the Tg2576 mouse model of Alzheimer's disease. *Mol Cell Neurosci,* 34, 621-628.

360. Zelcer, N., Khanlou, N., Clare, R., Jiang, Q., Reed-Geaghan, E.G., Landreth, G.E., Vinters, H.V. and Tontonoz, P. (2007) Attenuation of neuroinflammation and Alzheimer's disease pathology by liver x receptors. *Proc Natl Acad Sci U S A,* 104, 10601-10606.

361. Shafaati, M., O'Driscoll, R., Bjorkhem, I. and Meaney, S. (2009) Transcriptional regulation of cholesterol 24-hydroxylase by histone deacetylase inhibitors. *Biochem Biophys Res Commun,* 378, 689-694.

362. Qing, H., He, G., Ly, P.T., Fox, C.J., Staufenbiel, M., Cai, F., Zhang, Z., Wei, S., Sun, X., Chen, C.H. *et al.* (2008) Valproic acid inhibits Abeta production, neuritic plaque formation, and behavioral deficits in Alzheimer's disease mouse models. *J Exp Med,* 205, 2781-2789.

363. Vanier, M.T. (2010) Niemann-Pick disease type C. *Orphanet J Rare Dis,* 5, 16.

364. Walkley, S.U. and Suzuki, K. (2004) Consequences of NPC1 and NPC2 loss of function in mammalian neurons. *Biochim Biophys Acta,* 1685, 48-62.

365. Saito, Y., Suzuki, K., Nanba, E., Yamamoto, T., Ohno, K. and Murayama, S. (2002) Niemann-Pick type C disease: accelerated neurofibrillary tangle formation and amyloid beta deposition associated with apolipoprotein E epsilon 4 homozygosity. *Ann Neurol,* 52, 351-355.

366. Higgins, M.E., Davies, J.P., Chen, F.W. and Ioannou, Y.A. (1999) Niemann-Pick C1 is a late endosome-resident protein that transiently associates with lysosomes and the trans-Golgi network. *Mol Genet Metab,* 68, 1-13.

367. Neufeld, E.B., Wastney, M., Patel, S., Suresh, S., Cooney, A.M., Dwyer, N.K., Roff, C.F., Ohno, K., Morris, J.A., Carstea, E.D. *et al.* (1999) The Niemann-Pick C1 protein resides in a vesicular compartment linked to retrograde transport of multiple lysosomal cargo. *J Biol Chem,* 274, 9627-9635.

368. Carstea, E.D., Morris, J.A., Coleman, K.G., Loftus, S.K., Zhang, D., Cummings, C., Gu, J., Rosenfeld, M.A., Pavan, W.J., Krizman, D.B. *et al.* (1997) Niemann-Pick C1 disease gene: homology to mediators of cholesterol homeostasis. *Science,* 277, 228-231.

369. Davies, J.P. and Ioannou, Y.A. (2000) Topological analysis of Niemann-Pick C1 protein reveals that the membrane orientation of the putative sterol-sensing domain is identical to those of 3-hydroxy-3-methylglutaryl-CoA reductase and sterol regulatory element binding protein cleavage-activating protein. *J Biol Chem,* 275, 24367-24374.

370. Ohgami, N., Ko, D.C., Thomas, M., Scott, M.P., Chang, C.C. and Chang, T.Y. (2004) Binding between the Niemann-Pick C1 protein and a photoactivatable cholesterol analog requires a functional sterol-sensing domain. *Proc Natl Acad Sci U S A,* 101, 12473-12478.

371. Greer, W.L., Dobson, M.J., Girouard, G.S., Byers, D.M., Riddell, D.C. and Neumann, P.E. (1999) Mutations in NPC1 highlight a conserved NPC1-specific cysteine-rich domain. *Am J Hum Genet,* 65, 1252-1260.

372. Ioannou, Y.A. (2000) The structure and function of the Niemann-Pick C1 protein. *Mol Genet Metab,* 71, 175-181.

373. Watari, H., Blanchette-Mackie, E.J., Dwyer, N.K., Glick, J.M., Patel, S., Neufeld, E.B., Brady, R.O., Pentchev, P.G. and Strauss, J.F., 3rd (1999) Niemann-Pick C1 protein: obligatory roles for N-terminal domains and lysosomal targeting in cholesterol mobilization. *Proc Natl Acad Sci U S A,* 96, 805-810.

374. Watari, H., Blanchette-Mackie, E.J., Dwyer, N.K., Watari, M., Burd, C.G., Patel, S., Pentchev, P.G. and Strauss, J.F., 3rd (2000) Determinants of NPC1 expression and action: key promoter regions, posttranscriptional control, and the importance of a "cysteine-rich" loop. *Exp Cell Res,* 259, 247-256.

375. Watari, H., Blanchette-Mackie, E.J., Dwyer, N.K., Watari, M., Neufeld, E.B., Patel, S., Pentchev, P.G. and Strauss, J.F., 3rd (1999) Mutations in the leucine zipper motif and sterol-sensing domain inactivate the Niemann-Pick C1 glycoprotein. *J Biol Chem,* 274, 21861-21866.

376. Kwon, H.J., Abi-Mosleh, L., Wang, M.L., Deisenhofer, J., Goldstein, J.L., Brown, M.S. and Infante, R.E. (2009) Structure of N-terminal domain of NPC1 reveals distinct subdomains for binding and transfer of cholesterol. *Cell,* 137, 1213-1224.

377. Infante, R.E., Wang, M.L., Radhakrishnan, A., Kwon, H.J., Brown, M.S. and Goldstein, J.L. (2008) NPC2 facilitates bidirectional transfer of cholesterol between NPC1 and lipid bilayers, a step in cholesterol egress from lysosomes. *Proc Natl Acad Sci U S A,* 105, 15287-15292.

378. Willenborg, M., Schmidt, C.K., Braun, P., Landgrebe, J., von Figura, K., Saftig, P. and Eskelinen, E.L. (2005) Mannose 6-phosphate receptors, Niemann-Pick C2 protein, and lysosomal cholesterol accumulation. *J Lipid Res,* 46, 2559-2569.

379. Cheruku, S.R., Xu, Z., Dutia, R., Lobel, P. and Storch, J. (2006) Mechanism of cholesterol transfer from the Niemann-Pick type C2 protein to model membranes supports a role in lysosomal cholesterol transport. *J Biol Chem,* 281, 31594-31604.

380. Okamura, N., Kiuchi, S., Tamba, M., Kashima, T., Hiramoto, S., Baba, T., Dacheux, F., Dacheux, J.L., Sugita, Y. and Jin, Y.Z. (1999) A porcine homolog of the major secretory protein of human epididymis, HE1, specifically binds cholesterol. *Biochim Biophys Acta,* 1438, 377-387.

381. Xu, S., Benoff, B., Liou, H.L., Lobel, P. and Stock, A.M. (2007) Structural basis of sterol binding by NPC2, a lysosomal protein deficient in Niemann-Pick type C2 disease. *J Biol Chem,* 282, 23525-23531.

382. Friedland, N., Liou, H.L., Lobel, P. and Stock, A.M. (2003) Structure of a cholesterol-binding protein deficient in Niemann-Pick type C2 disease. *Proc Natl Acad Sci U S A,* 100, 2512-2517.

383. Ko, D.C., Binkley, J., Sidow, A. and Scott, M.P. (2003) The integrity of a cholesterol-binding pocket in Niemann-Pick C2 protein is necessary to control lysosome cholesterol levels. *Proc Natl Acad Sci U S A,* 100, 2518-2525.

384. Wang, M.L., Motamed, M., Infante, R.E., Abi-Mosleh, L., Kwon, H.J., Brown, M.S. and Goldstein, J.L. (2010) Identification of surface residues on Niemann-Pick C2 essential for hydrophobic handoff of cholesterol to NPC1 in lysosomes. *Cell Metab,* 12, 166-173.

385. Loftus, S.K., Morris, J.A., Carstea, E.D., Gu, J.Z., Cummings, C., Brown, A., Ellison, J., Ohno, K., Rosenfeld, M.A., Tagle, D.A. *et al.* (1997) Murine model of Niemann-Pick C disease: mutation in a cholesterol homeostasis gene. *Science,* 277, 232-235.

386. Miyawaki, S., Yoshida, H., Mitsuoka, S., Enomoto, H. and Ikehara, S. (1986) A mouse model for Niemann-Pick disease. Influence of genetic background on disease expression in spm/spm mice. *J Hered,* 77, 379-384.

387. Morris, M.D., Bhuvaneswaran, C., Shio, H. and Fowler, S. (1982) Lysosome lipid storage disorder in NCTR-BALB/c mice. I. Description of the disease and genetics. *Am J Pathol,* 108, 140-149.

388. Sleat, D.E., Wiseman, J.A., El-Banna, M., Price, S.M., Verot, L., Shen, M.M., Tint, G.S., Vanier, M.T., Walkley, S.U. and Lobel, P. (2004) Genetic evidence for nonredundant functional cooperativity between NPC1 and NPC2 in lipid transport. *Proc Natl Acad Sci U S A,* 101, 5886-5891.

389. March, P.A., Thrall, M.A., Brown, D.E., Mitchell, T.W., Lowenthal, A.C. and Walkley, S.U. (1997) GABAergic neuroaxonal dystrophy and other cytopathological alterations in feline Niemann-Pick disease type C. *Acta Neuropathol,* 94, 164-172.

390. Somers, K.L., Wenger, D.A., Royals, M.A., Carstea, E.D., Connally, H.E., Kelly, T., Kimball, R. and Thrall, M.A. (1999) Complementation studies in human and feline Niemann-Pick type C disease. *Mol Genet Metab,* 66, 117-121.

391. Vite, C.H., Ding, W., Bryan, C., O'Donnell, P., Cullen, K., Aleman, D., Haskins, M.E. and Van Winkle, T. (2008) Clinical, electrophysiological, and serum biochemical measures of progressive neurological and hepatic dysfunction in feline Niemann-Pick type C disease. *Pediatr Res,* 64, 544-549.

392. Huang, X., Suyama, K., Buchanan, J., Zhu, A.J. and Scott, M.P. (2005) A Drosophila model of the Niemann-Pick type C lysosome storage disease: dnpc1a is required for molting and sterol homeostasis. *Development,* 132, 5115-5124.

393. Malathi, K., Higaki, K., Tinkelenberg, A.H., Balderes, D.A., Almanzar-Paramio, D., Wilcox, L.J., Erdeniz, N., Redican, F., Padamsee, M., Liu, Y. *et al.* (2004) Mutagenesis of the putative sterol-sensing domain of yeast Niemann Pick C-related protein reveals a primordial role in subcellular sphingolipid distribution. *J Cell Biol,* 164, 547-556.

394. Zhang, S., Ren, J., Li, H., Zhang, Q., Armstrong, J.S., Munn, A.L. and Yang, H. (2004) Ncr1p, the yeast ortholog of mammalian Niemann Pick C1 protein, is dispensable for endocytic transport. *Traffic,* 5, 1017-1030.

395. Vanier, M.T. and Millat, G. (2003) Niemann-Pick disease type C. *Clin Genet,* 64, 269-281.

396. Coxey, R.A., Pentchev, P.G., Campbell, G. and Blanchette-Mackie, E.J. (1993) Differential accumulation of cholesterol in Golgi compartments of normal and Niemann-Pick type C fibroblasts incubated with LDL: a cytochemical freeze-fracture study. *J Lipid Res,* 34, 1165-1176.

397. Liscum, L., Ruggiero, R.M. and Faust, J.R. (1989) The intracellular transport of low density lipoprotein-derived cholesterol is defective in Niemann-Pick type C fibroblasts. *J Cell Biol,* 108, 1625-1636.

398. Wojtanik, K.M. and Liscum, L. (2003) The transport of low density lipoprotein-derived cholesterol to the plasma membrane is defective in NPC1 cells. *J Biol Chem,* 278, 14850-14856.

399. Pentchev, P.G., Comly, M.E., Kruth, H.S., Tokoro, T., Butler, J., Sokol, J., Filling-Katz, M., Quirk, J.M., Marshall, D.C., Patel, S. *et al.* (1987) Group C Niemann-Pick disease: faulty regulation of low-density lipoprotein uptake and cholesterol storage in cultured fibroblasts. *FASEB J,* 1, 40-45.

400. Pentchev, P.G., Comly, M.E., Kruth, H.S., Vanier, M.T., Wenger, D.A., Patel, S. and Brady, R.O. (1985) A defect in cholesterol esterification in Niemann-Pick disease (type C) patients. *Proc Natl Acad Sci U S A,* 82, 8247-8251.

401. Sokol, J., Blanchette-Mackie, J., Kruth, H.S., Dwyer, N.K., Amende, L.M., Butler, J.D., Robinson, E., Patel, S., Brady, R.O., Comly, M.E. *et al.* (1988) Type C Niemann-Pick disease. Lysosomal accumulation and defective intracellular mobilization of low density lipoprotein cholesterol. *J Biol Chem,* 263, 3411-3417.

402. Cruz, J.C. and Chang, T.Y. (2000) Fate of endogenously synthesized cholesterol in Niemann-Pick type C1 cells. *J Biol Chem,* 275, 41309-41316.

403. Shamburek, R.D., Pentchev, P.G., Zech, L.A., Blanchette-Mackie, J., Carstea, E.D., VandenBroek, J.M., Cooper, P.S., Neufeld, E.B., Phair, R.D., Brewer, H.B., Jr. *et al.* (1997) Intracellular trafficking of the free cholesterol derived from LDL cholesteryl ester is defective in vivo in Niemann-Pick C disease: insights on normal metabolism of HDL and LDL gained from the NP-C mutation. *J Lipid Res,* 38, 2422-2435.

404. Liu, B., Xie, C., Richardson, J.A., Turley, S.D. and Dietschy, J.M. (2007) Receptor-mediated and bulk-phase endocytosis cause macrophage and cholesterol accumulation in Niemann-Pick C disease. *J Lipid Res,* 48, 1710-1723.

405. Karten, B., Peake, K.B. and Vance, J.E. (2009) Mechanisms and consequences of impaired lipid trafficking in Niemann-Pick type C1-deficient mammalian cells. *Biochim Biophys Acta,* 1791, 659-670.

406. Lloyd-Evans, E. and Platt, F.M. (2010) Lipids on trial: the search for the offending metabolite in Niemann-Pick type C disease. *Traffic,* 11, 419-428.

407. Choudhury, A., Sharma, D.K., Marks, D.L. and Pagano, R.E. (2004) Elevated endosomal cholesterol levels in Niemann-Pick cells inhibit rab4 and perturb membrane recycling. *Mol Biol Cell,* 15, 4500-4511.

408. Ganley, I.G. and Pfeffer, S.R. (2006) Cholesterol accumulation sequesters Rab9 and disrupts late endosome function in NPC1-deficient cells. *J Biol Chem,* 281, 17890-17899.

409. Lombardi, D., Soldati, T., Riederer, M.A., Goda, Y., Zerial, M. and Pfeffer, S.R. (1993) Rab9 functions in transport between late endosomes and the trans Golgi network. *EMBO J,* 12, 677-682.

410. Zerial, M. and McBride, H. (2001) Rab proteins as membrane organizers. *Nat Rev Mol Cell Biol,* 2, 107-117.

411. Kobayashi, T., Beuchat, M.H., Lindsay, M., Frias, S., Palmiter, R.D., Sakuraba, H., Parton, R.G. and Gruenberg, J. (1999) Late endosomal membranes rich in lysobisphosphatidic acid regulate cholesterol transport. *Nat Cell Biol,* 1, 113-118.

412. Miwako, I., Yamamoto, A., Kitamura, T., Nagayama, K. and Ohashi, M. (2001) Cholesterol requirement for cation-independent mannose 6-phosphate receptor exit from multivesicular late endosomes to the Golgi. *J Cell Sci*, 114, 1765-1776.

413. Ohashi, M., Miwako, I., Yamamoto, A. and Nagayama, K. (2000) Arrested maturing multivesicular endosomes observed in a Chinese hamster ovary cell mutant, LEX2, isolated by repeated flow-cytometric cell sorting. *J Cell Sci,* 113 (Pt 12), 2187-2205.

414. Ikeda, K., Hirayama, M., Hirota, Y., Asa, E., Seki, J. and Tanaka, Y. (2008) Drug-induced phospholipidosis is caused by blockade of mannose 6-phosphate receptor-mediated targeting of lysosomal enzymes. *Biochem Biophys Res Commun,* 377, 268-274.

415. Choudhury, A., Dominguez, M., Puri, V., Sharma, D.K., Narita, K., Wheatley, C.L., Marks, D.L. and Pagano, R.E. (2002) Rab proteins mediate Golgi transport of caveola-internalized glycosphingolipids and correct lipid trafficking in Niemann-Pick C cells. *J Clin Invest,* 109, 1541-1550.

416. Narita, K., Choudhury, A., Dobrenis, K., Sharma, D.K., Holicky, E.L., Marks, D.L., Walkley, S.U. and Pagano, R.E. (2005) Protein transduction of Rab9 in Niemann-Pick C cells reduces cholesterol storage. *FASEB J,* 19, 1558-1560.

417. Walter, M., Davies, J.P. and Ioannou, Y.A. (2003) Telomerase immortalization upregulates Rab9 expression and restores LDL cholesterol egress from Niemann-Pick C1 late endosomes. *J Lipid Res,* 44, 243-253.

418. Linder, M.D., Uronen, R.L., Holtta-Vuori, M., van der Sluijs, P., Peranen, J. and Ikonen, E. (2007) Rab8-dependent recycling promotes endosomal cholesterol removal in normal and sphingolipidosis cells. *Mol Biol Cell,* 18, 47-56.

419. Kaptzan, T., West, S.A., Holicky, E.L., Wheatley, C.L., Marks, D.L., Wang, T., Peake, K.B., Vance, J., Walkley, S.U. and Pagano, R.E. (2009) Development of a Rab9 transgenic mouse and its ability to increase the lifespan of a murine model of Niemann-Pick type C disease. *Am J Pathol,* 174, 14-20.

420. Goldman, S.D. and Krise, J.P. (2010) Niemann-Pick C1 functions independently of Niemann-Pick C2 in the initial stage of retrograde transport of membrane-impermeable lysosomal cargo. *J Biol Chem*, 285, 4983-4994.

421. Gong, Y., Duvvuri, M., Duncan, M.B., Liu, J. and Krise, J.P. (2006) Niemann-Pick C1 protein facilitates the efflux of the anticancer drug daunorubicin from cells according to a novel vesicle-mediated pathway. *J Pharmacol Exp Ther*, 316, 242-247.

422. Reddy, J.V., Ganley, I.G. and Pfeffer, S.R. (2006) Clues to neuro-degeneration in Niemann-Pick type C disease from global gene expression profiling. *PLoS One*, 1, e19.

423. Amritraj, A., Peake, K., Kodam, A., Salio, C., Merighi, A., Vance, J.E. and Kar, S. (2009) Increased activity and altered subcellular distribution of lysosomal enzymes determine neuronal vulnerability in Niemann-Pick type C1-deficient mice. *Am J Pathol*, 175, 2540-2556.

424. Liao, G., Yao, Y., Liu, J., Yu, Z., Cheung, S., Xie, A., Liang, X. and Bi, X. (2007) Cholesterol accumulation is associated with lysosomal dysfunction and autophagic stress in Npc1 -/- mouse brain. *Am J Pathol*, 171, 962-975.

425. Yu, W., Gong, J.S., Ko, M., Garver, W.S., Yanagisawa, K. and Michikawa, M. (2005) Altered cholesterol metabolism in Niemann-Pick type C1 mouse brains affects mitochondrial function. *J Biol Chem*, 280, 11731-11739.

426. Wang, B., Nguyen, M., Chang, N.C. and Shore, G.C. (2011) Fis1, Bap31 and the kiss of death between mitochondria and endoplasmic reticulum. *EMBO J*, 30, 451-452.

427. Charman, M., Kennedy, B.E., Osborne, N. and Karten, B. (2010) MLN64 mediates egress of cholesterol from endosomes to mitochondria in the absence of functional Niemann-Pick Type C1 protein. *J Lipid Res*, 51, 1023-1034.

428. Zhang, M., Liu, P., Dwyer, N.K., Christenson, L.K., Fujimoto, T., Martinez, F., Comly, M., Hanover, J.A., Blanchette-Mackie, E.J. and Strauss, J.F., 3rd (2002) MLN64 mediates mobilization of lysosomal cholesterol to steroidogenic mitochondria. *J Biol Chem*, 277, 33300-33310.

429. Mari, M., Caballero, F., Colell, A., Morales, A., Caballeria, J., Fernandez, A., Enrich, C., Fernandez-Checa, J.C. and Garcia-Ruiz, C. (2006) Mitochondrial free cholesterol loading sensitizes to TNF- and Fas-mediated steatohepatitis. *Cell Metab*, 4, 185-198.

430. Griffin, L.D., Gong, W., Verot, L. and Mellon, S.H. (2004) Niemann-Pick type C disease involves disrupted neurosteroidogenesis and responds to allopregnanolone. *Nat Med*, 10, 704-711.

431. Wraith, J.E., Baumgartner, M.R., Bembi, B., Covanis, A., Levade, T., Mengel, E., Pineda, M., Sedel, F., Topcu, M., Vanier, M.T. *et al.* (2009) Recommendations on the diagnosis and management of Niemann-Pick disease type C. *Mol Genet Metab,* 98, 152-165.

432. Erickson, R.P., Garver, W.S., Camargo, F., Hossain, G.S. and Heidenreich, R.A. (2000) Pharmacological and genetic modifications of somatic cholesterol do not substantially alter the course of CNS disease in Niemann-Pick C mice. *J Inherit Metab Dis,* 23, 54-62.

433. Patterson, M.C. and Platt, F. (2004) Therapy of Niemann-Pick disease, type C. *Biochim Biophys Acta,* 1685, 77-82.

434. Zidovetzki, R. and Levitan, I. (2007) Use of cyclodextrins to manipulate plasma membrane cholesterol content: evidence, misconceptions and control strategies. *Biochim Biophys Acta,* 1768, 1311-1324.

435. Davis, M.E. and Brewster, M.E. (2004) Cyclodextrin-based pharmaceutics: past, present and future. *Nat Rev Drug Discov,* 3, 1023-1035.

436. Liu, B., Turley, S.D., Burns, D.K., Miller, A.M., Repa, J.J. and Dietschy, J.M. (2009) Reversal of defective lysosomal transport in NPC disease ameliorates liver dysfunction and neurodegeneration in the npc1-/- mouse. *Proc Natl Acad Sci U S A,* 106, 2377-2382.

437. Liu, B., Ramirez, C.M., Miller, A.M., Repa, J.J., Turley, S.D. and Dietschy, J.M. (2010) Cyclodextrin overcomes the transport defect in nearly every organ of NPC1 mice leading to excretion of sequestered cholesterol as bile acid. *J Lipid Res,* 51, 933-944.

438. Davidson, C.D., Ali, N.F., Micsenyi, M.C., Stephney, G., Renault, S., Dobrenis, K., Ory, D.S., Vanier, M.T. and Walkley, S.U. (2009) Chronic cyclodextrin treatment of murine Niemann-Pick C disease ameliorates neuronal cholesterol and glycosphingolipid storage and disease progression. *PLoS One,* 4, e6951.

439. Ramirez, C.M., Liu, B., Taylor, A.M., Repa, J.J., Burns, D.K., Weinberg, A.G., Turley, S.D. and Dietschy, J.M. (2010) Weekly cyclodextrin administration normalizes cholesterol metabolism in nearly every organ of the Niemann-Pick type C1 mouse and markedly prolongs life. *Pediatr Res,* 68, 309-315.

440. Rosenbaum, A.I., Zhang, G., Warren, J.D. and Maxfield, F.R. (2010) Endocytosis of beta-cyclodextrins is responsible for cholesterol reduction in Niemann-Pick type C mutant cells. *Proc Natl Acad Sci U S A,* 107, 5477-5482.

441. Peake, K.B. and Vance, J.E. (2012) Normalization of cholesterol homeostasis by 2-hydroxypropyl-beta-cyclodextrin in neurons and glia from Niemann-Pick C1 (NPC1)-deficient mice. *J Biol Chem,* 287, 9290-9298.

442. Abi-Mosleh, L., Infante, R.E., Radhakrishnan, A., Goldstein, J.L. and Brown, M.S. (2009) Cyclodextrin overcomes deficient lysosome-to-endoplasmic reticulum transport of cholesterol in Niemann-Pick type C cells. *Proc Natl Acad Sci U S A,* 106, 19316-19321.

443. Rajewski, R.A. and Stella, V.J. (1996) Pharmaceutical applications of cyclodextrins. 2. In vivo drug delivery. *J Pharm Sci,* 85, 1142-1169.

444. Monnaert, V., Tilloy, S., Bricout, H., Fenart, L., Cecchelli, R. and Monflier, E. (2004) Behavior of alpha-, beta-, and gamma-cyclodextrins and their derivatives on an in vitro model of blood-brain barrier. *J Pharmacol Exp Ther,* 310, 745-751.

445. Yanjanin, N.M., Velez, J.I., Gropman, A., King, K., Bianconi, S.E., Conley, S.K., Brewer, C.C., Solomon, B., Pavan, W.J., Arcos-Burgos, M. *et al.* (2010) Linear clinical progression, independent of age of onset, in Niemann-Pick disease, type C. *Am J Med Genet B Neuropsychiatr Genet,* 153B, 132-140.

446. Auer, I.A., Schmidt, M.L., Lee, V.M., Curry, B., Suzuki, K., Shin, R.W., Pentchev, P.G., Carstea, E.D. and Trojanowski, J.Q. (1995) Paired helical filament tau (PHFtau) in Niemann-Pick type C disease is similar to PHFtau in Alzheimer's disease. *Acta Neuropathol,* 90, 547-551.

447. Distl, R., Treiber-Held, S., Albert, F., Meske, V., Harzer, K. and Ohm, T.G. (2003) Cholesterol storage and tau pathology in Niemann-Pick type C disease in the brain. *J Pathol,* 200, 104-111.

448. Love, S., Bridges, L.R. and Case, C.P. (1995) Neurofibrillary tangles in Niemann-Pick disease type C. *Brain,* 118 (Pt 1), 119-129.

449. Ohm, T.G., Treiber-Held, S., Distl, R., Glockner, F., Schonheit, B., Tamanai, M. and Meske, V. (2003) Cholesterol and tau protein--findings in Alzheimer's and Niemann Pick C's disease. *Pharmacopsychiatry,* 36 Suppl 2, S120-126.

450. Suzuki, K., Parker, C.C., Pentchev, P.G., Katz, D., Ghetti, B., D'Agostino, A.N. and Carstea, E.D. (1995) Neurofibrillary tangles in Niemann-Pick disease type C. *Acta Neuropathol,* 89, 227-238.

451. Mattsson, N., Zetterberg, H., Bianconi, S., Yanjanin, N.M., Fu, R., Mansson, J.E., Porter, F.D. and Blennow, K. (2011) Gamma-secretase-dependent amyloid-beta is increased in Niemann-Pick type C: a cross-sectional study. *Neurology,* 76, 366-372.

452. Kagedal, K., Kim, W.S., Appelqvist, H., Chan, S., Cheng, D., Agholme, L., Barnham, K., McCann, H., Halliday, G. and Garner, B. (2010) Increased expression of the lysosomal cholesterol transporter NPC1 in Alzheimer's disease. *Biochim Biophys Acta,* 1801, 831-838.

453. Kivipelto, M., Helkala, E.L., Laakso, M.P., Hanninen, T., Hallikainen, M., Alhainen, K., Iivonen, S., Mannermaa, A., Tuomilehto, J., Nissinen, A. *et al.* (2002) Apolipoprotein E epsilon4 allele, elevated midlife total cholesterol level, and high

midlife systolic blood pressure are independent risk factors for late-life Alzheimer disease. *Ann Intern Med*, 137, 149-155.

454. Notkola, I.L., Sulkava, R., Pekkanen, J., Erkinjuntti, T., Ehnholm, C., Kivinen, P., Tuomilehto, J. and Nissinen, A. (1998) Serum total cholesterol, apolipoprotein E epsilon 4 allele, and Alzheimer's disease. *Neuroepidemiology*, 17, 14-20.

Chapter2: Alterations in Gene Expression in Mutant Amyloid Precursor Protein Transgenic Mice Lacking Niemann-Pick Type C1 Protein

A version of this chapter has been accepted for publication. Maulik M, Thinakaran G and Kar S (2012) PLOS ONE.

2.1 Introduction

Niemann-Pick type C (NPC) disease is an autosomal recessive neurovisceral disorder caused predominantly by mutations in the *NPC1* gene and less frequently in the *NPC2* gene. The *NPC1* gene encodes for a 1278 amino acid polytopic membrane protein harboring a sterol sensing domain, whereas the *NPC2* gene encodes for a soluble cholesterol binding protein. The loss of function of either protein leads to intracellular accumulation of unesterified cholesterol and glycosphingolipids in many tissues, including the brain. These defects in cholesterol sequestration trigger widespread neurological deficits such as ataxia, dystonia, seizures and dementia, leading to premature death (1-3). In addition to cholesterol accumulation, NPC disease is neuropathologically characterized by the presence of tau-positive neurofibrillary tangles, gliosis, demyelination and loss of neurons in selected brain regions (2, 4, 5). Moreover, NPC patients carrying Apolipoprotein E (*APOE*) ε4 alleles develop extracellular cerebral deposition of β-amyloid (Aβ) peptides (6), a characteristic pathological feature of Alzheimer's disease (AD), the most common type of senile dementia affecting the elderly (7, 8). Some recent studies have also reported increased levels of Aβ-related peptides in vulnerable neurons as well as in the cerebrospinal fluid of NPC patients (9, 10). Although overall increase in the level or intracellular accumulation of cholesterol is known to trigger generation of Aβ peptides by proteolytic processing of amyloid precursor protein (APP), the functional significance of these peptides in NPC pathology remains unclear (11-13).

Earlier studies have shown that BALB/c-*Npc1*^{nih} mice, which do not express Npc1 protein (Npc1-null) due to a spontaneous mutation in the *Npc1* gene, can recapitulate most of the pathological features associated with human NPC disease, with the exception of neurofibrillary tangles (14-17). These Npc1-null mice are usually asymptomatic at birth but gradually develop tremor and ataxia, and die prematurely at ~3 months of age. At the cellular level, these mice exhibit intracellular accumulation of cholesterol, activation of microglia and astrocytes as well as loss of myelin sheath throughout the central nervous system. Progressive loss of neurons is also evident in selected brain regions including cerebellum, whereas the hippocampus is relatively

spared (17-19). These mice exhibit increased levels of intracellular Aβ-related peptides in distinct brain regions (9), but the significance of Aβ in the development and/or progression of NPC disease pathology remain unclear. To evaluate the potential role of Aβ peptides in pathological abnormalities related to NPC disease, we have recently developed a new line of bigenic ANPC mice by crossing heterozygous Npc1-deficient mice with mutant human APP transgenic (APP-Tg) mice which exhibit extracellular Aβ deposits and spatial learning deficits but no overt loss of neurons in any brain region. These bigenic mice clearly show that APP overexpression can increase the rate of mortality and exacerbate behavioral as well as neuropathological abnormalities associated with Npc1-null phenotype (20). Thus, these mice provide a model system to evaluate how expression of human APP in the absence of functional Npc1 protein can influence pathological abnormalities related to AD and NPC disease. Here, we used a gene expression profiling approach to probe the molecular basis underlying the accelerated development of pathological abnormalities in ANPC mice. Specifically, we focused on the expression of 86 selected genes that are involved in APP and Aβ metabolism, cholesterol homeostasis, intracellular vesicular trafficking and cell death mechanisms in the affected cerebellar and relatively spared hippocampal regions of ANPC, Npc1-null, APP-Tg and double heterozygous (Dhet) mice compared to wild-type (WT) controls. The alterations in gene expression profiles were validated using Western blotting. Our results clearly show that Npc1-null and ANPC mice exhibit marked alterations in the expression profiles of a number of genes in both hippocampus and cerebellum, while the changes in APP-Tg and Dhet mice are limited to only few genes, mostly in the hippocampus, compared to WT mice. Furthermore, the alterations in Npc1-null and ANPC mice, consistent with the severity of disease pathology, are more pronounced in the affected cerebellar region than the hippocampus.

2.2. Materials and Methods

Materials: 4-12% NuPAGE Bis-Tris gels, Prolong Gold Antifade and Alexa Fluor-488/594 conjugated secondary antisera were purchased from Life Technologies Corp. (Burlington, ON, Canada). The bicinchoninic acid protein assay kit and enhanced chemiluminescence (ECL) kit were obtained from Thermo Fisher Scientific (Montreal, QC, Canada). DNA isolation kit, RNeasy lipid tissue mini kit, SABiosciences' RT^2 First Strand Kit, RT^2 SYBR Green/Fluorescein qPCR master mix and 96-well RT^2 Custom Profiler^{TM} PCR Array were all from Qiagen Inc. (Mississauga, ON, Canada). Sources of all primary antibodies used in the study are listed in Table 2.1. All horseradish peroxidase-conjugated secondary antibodies were from Santa Cruz Biotechnology, Inc (Paso Robles, CA). All other chemicals were from Sigma-Aldrich or Thermo Fisher Scientific.

Generation of Transgenic mice: Mutant human $APP_{KM670/671NL+V717F}$ Tg mice (APP-Tg) maintained on a C3H/C57BL6 background (21) and heterozygous Npc1-null mice (16) maintained on a Balb/cNctr-*Npc1*^{m1N}/J background were from our breeding colony. These mutant mice were first crossed to produce *APP*$^{+/0}$*Npc1*$^{+/-}$ and *APP*$^{0/0}$*Npc1*$^{+/-}$ off-springs, which were subsequently crossed to generate the following five lines of mice: bigenic *APP*$^{+/0}$*Npc1*$^{-/-}$ (ANPC), *APP*$^{+/0}$*Npc1*$^{+/+}$ (APP-Tg), *APP*$^{0/0}$*Npc1*$^{-/-}$ (Npc1-null), *APP*$^{+/0}$*Npc1*$^{+/-}$ (Dhet) and *APP*$^{0/0}$*Npc1*$^{+/+}$ (wildtype: WT). All animals were bred and housed with access to food and water *ad libitum* in accordance with the Institutional and Canadian Council on Animal Care guidelines. Different lines of transgenic mice were genotyped by PCR analysis of tail DNA as described earlier (16, 21).

***Histology and Immunohistochemistry*:** WT, APP-Tg, Dhet, Npc1-null and ANPC mice (n = 4-5 per genotype) of 7 weeks of age were transcardially perfused and the brains fixed in 4% paraformaldehyde. Brains were sectioned on a cryostat (20 μm) and then processed as described earlier (18). To determine cholesterol accumulation, hippocampal and cerebellar sections from all five genotypes were incubated with 25 μg/ml of filipin in phosphate-buffered saline (PBS) for 30 min in the dark under agitation (18). For immunohistochemistry, brain sections were incubated overnight at 4^{o}C with anti-

Calbindin-D-28k or anti-NeuN antibodies at dilutions listed in Table 2.1. Subsequently, sections were processed with Alexa Fluor 488/594 conjugated secondary antibodies (1:1000) for immunofluorescence methods and examined using a Zeiss Axioskop-2 microscope (Carl Zeiss Canada Ltd.).

RNA extraction for PCR array: Total RNA was isolated from hippocampal and cerebellar tissues of 7 week old ANPC, Dhet, Npc1-null, APP-Tg and WT mice (4 animals per genotype for each brain region studied) using RNeasy lipid tissue mini kit following manufacturer's instructions (Qiagen Inc., Mississauga, ON, Canada) and stored at -80°C. RNA concentrations were determined using a Nanodrop 1000 spectrophotometer (Thermo Fisher Scientific) and 260/230 nm and 260/280 nm absorbance ratios were analyzed to determine RNA purity.

RT^2 Profiler^{TM} PCR Array: At first 1µg of total RNA was treated with genomic DNA elimination buffer at 42°C for 5 mins to remove possible genomic DNA contamination. Following the elimination step, reverse transcription was carried out using the RT^2 First Strand Kit in accordance with the manufacturer's protocol (SuperArray Biosciences Corp., MD). The resulting complementary DNA (cDNA) was diluted and combined with RT^2 SYBR Green/Fluorescein qPCR master mix and loaded onto a 96-well RT^2 Custom Profiler^{TM} PCR Array designed to profile the expression of 84 genes representative of biological pathways involved in cholesterol and APP metabolism, intracellular trafficking and cell death. All real-time PCR reactions were performed in a final volume of 25µl using a MyiQ^{TM} Real-Time PCR Detection System (Bio-rad Laboratories, Inc., Canada) using a two-step cycling program: 10 min at 95°C (one cycle), 15 s at 95°C, followed by 1 min at 60°C (40 cycles). Data collection was performed during the annealing step (58°C) of each cycle and data were PCR-baseline subtracted and curve fitted. Threshold cycle (Ct) values were calculated using the instrument's MyiQ optical software (Bio-rad Laboratories, Inc.).

PCR Data Normlization and Analysis: The data were analyzed using the SABiosciences' PCR Array Data analysis software based on the comparative Ct method

and expressed as relative fold differences in APP-Tg, Dhet, Npc1-null or ANPC mice compared to WT mice. All Ct values ≥35 were considered a negative call. Quality control tests for PCR reproducibility, reverse transcription efficiency, and level of genomic DNA contamination were included in each plate and monitored as per the supplier's instructions. The expression level of three housekeeping genes included in the PCR array: *Hprt1*, *Gapdh* and *Actb* were used for normalization. The ΔCt for each gene in each plate was first calculated by subtracting the Ct value of the gene of interest from the average Ct value of the three housekeeping genes. Then, the average ΔCt value of each gene was calculated across the four replicate arrays for each animal group within the same brain region and ΔΔCt values were obtained by subtracting the ΔCt values of WT group from the respective ΔCt values of APP-Tg, Dhet, Npc1-null or ANPC mice. The fold change for each gene from WT to APP-Tg, Dhet, Npc1-null or ANPC mice was calculated as $2^{(-\Delta\Delta Ct)}$. Finally the "fold change" for each gene was converted to "fold regulation" as follows. For fold-change values greater than 1, which indicated a positive or an up-regulation, the fold-regulation was equal to the fold-change. For fold-change values less than 1 indicating a negative or down-regulation, the fold-regulation was calculated as the negative inverse of the fold-change. *P*-values were calculated using the Student's t-test. A fold difference of ≥1.2 with a *p*-value <0.05 was considered as significant differential gene expression.

***Western blotting*:** Hippocampal and cerebellar regions of 7 week old ANPC mice and their age-matched siblings (n = 4-6 animals/genotype) were processed for Western blotting as described earlier (18). In brief, tissues were homogenized in RIPA lysis buffer and equal amounts of proteins were separated on 4-12% NuPAGE Bis-Tris gels. The proteins were transferred to PVDF membranes and incubated overnight at 4°C with anti-Aplp1, anti-Ide, anti-Igf2r, anti-Gsk3β, anti-neprilysin, anti-Npc2, anti-Abca1, anti-Apoe, anti-tau, anti-cathepsin B, anti-cathepsin D or anti-β-glucoronidase antisera at dilutions listed in Table 2.1. Membranes were then exposed to respective secondary antibodies and visualized using an ECL detection kit. Blots were reprobed with anti-β-actin and/or anti-GAPDH and quantified using a MCID image analyzer (Imaging Research, Inc.) as described earlier (18). The data are expressed as mean ± S.E.M and statistically analyzed

using one-way ANOVA followed by Newman-Keuls post-hoc analysis with significance set at $p < 0.05$. All statistical analyses were performed using GraphPad Prism (GraphPad software, Inc., CA, USA).

Table 2.1: Details of the primary antibodies used in this study

Antibody	Type	IHC/IF dilution	WB dilution	Source
ATP-binding cassette, sub-family A, member 1 (Abca1)	Polyclonal	n/a	1:500	[1]Dr. S. Sipione
Tau (clone Tau 5)	Monoclonal	n/a	1:2000	EMD Millipore Corp.
Amyloid precursor-like protein 1 (Aplp1)	Polyclonal	n/a	1:1000	[2]Dr. G. Thinakaran
Apolipoprotein E (Apoe)	Polyclonal	n/a	1:5000	[1]Dr. J.E. Vance
β-glucuronidase (Gusb)	Polyclonal	n/a	1:1000	Novus Biologicals
Calbindin-D28K	Monoclonal	1:7000	n/a	Sigma-Aldrich Co.
Cathepsin B (CatB)	Polyclonal	n/a	1:500	Santa Cruz Biotech., Inc.
Cathepsin D (CatD)	Polyclonal	n/a	1:500	Santa Cruz Biotech., Inc.
Glyceraldehyde-3-phosphate dehydrogenase (GAPDH)	Monoclonal	n/a	1:1000	Sigma-Aldrich, Inc.
Glycogen synthase kinase 3β (Gsk3β)	Monoclonal	n/a	1:5000	BD Transduction Labs™
Insulin degrading enzyme (Ide)	Polyclonal	n/a	1:500	Abcam Inc.
Insulin-like growth factor 2 receptor (Igf2r)	Polyclonal	n/a	1:5000	[3]Dr. C. Scott
Neprilysin	Monoclonal	n/a	1:500	Abcam Inc.
Neuronal Nuclei (NeuN)	Monoclonal	1:25,000	n/a	EMD Millipore Corp.
Niemann-Pick type C2 (Npc2)	Polyclonal	n/a	1:500	[4]Dr. P. Lobel
β-actin	Monoclonal	n/a	1:5000	Sigma-Aldrich, Inc.

IHC/IF, Immunohistochemistry/Immunofluorescence; WB, western blotting; n/a, not used in that specific application; [1]University of Alberta, AB, Canada; [2]The University of Chicago, IL, USA; [3]Kolling Institute of Medical Research, New South Wales, Australia; [4]University of Medicine and Dentistry of New Jersey, NJ, USA

2.3 Results

***RT^2 Profiler PCR array analysis of gene expression*:** The mutant APP-Tg mice used in this study exhibit extracellular Aβ deposits and cognitive behavioral deficits, but no overt loss of neurons or neurofibrillary tangles in any brain region by 3 months of age (21, 22). The Npc1-null mice, on the other hand, exhibit intracellular cholesterol accumulation and loss of cerebellar Purkinje cells, but lack extracellular Aβ deposits. These mice survive for 12-16 weeks after birth and do not exhibit any significant loss of neurons in the hippocampal region (15-17). The bigenic ANPC mice, in our colony, survived for ~11 weeks after birth, but their mortality rate increased considerably from the 8^{th} week onwards. These mice exhibited significant cognitive and motor deficits by 7 weeks of age compared to other littermates (20). At the cellular level, ANPC mice accumulate filipin-labeled unesterified cholesterol in most neurons of the hippocampus and cerebellum as observed in Npc1-null mice. No cholesterol accumulation was apparent in the brains of WT, APP-Tg or Dhet littermates (Fig. 2.1). We also observed the presence of degenerating neurons (i.e., Purkinje cells) in the cerebellum, but not in the hippocampus, of ANPC and Npc1-null mouse brains (Fig. 2.1). Age-matched WT, APP-Tg or Dhet mice did not show cell loss either in the hippocampus or cerebellum. Accompanying these changes, ANPC mice showed profound activation of astrocytes and microglia in a manner which exceeded the level and intensity of staining noted in other genotypes (20).

In order to gain molecular insights into the exacerbated neuropathological changes observed in ANPC mice, we analyzed the expression profiles of 86 selected genes involved in APP and Aβ metabolism, cholesterol homeostasis, intracellular vesicular trafficking and cell death mechanisms in the affected cerebellar and relatively spared hippocampal regions at 7-week of age (when distinct neuropathological and behavioral abnormalities are evident) from five different genotypes (i.e., WT, APP-Tg, Dhet, Npc1-null and ANPC mice) (Table 2.2). Our results of the RT^2 Profiler PCR array analysis showed significant alterations in the relative expression of a wide-spectrum of transcripts in the brain regions of APP-Tg, Dhet, Npc1-null and ANPC mice compared to the WT controls [see Fig. 2.2; Tables 2.3-2.10 (Supplementary Tables 1-8)]. The changes observed in APP-Tg and Dhet mice were limited to only a few transcripts, whereas Npc1-

null and ANPC mice showed striking alterations in the expression profiles of a number of genes in both hippocampus and cerebellum compared to WT mice [see Fig. 2.2; Tables 2.3-2.10 (Supplementary Tables 1-8)]. Intriguingly, ANPC and Npc1-null mice with the exception of some subtle differences, exhibited more or less similar changes, *albeit* the magnitude of alteration differs between the affected cerebellar *vs* relatively spared hippocampal regions [see Fig. 2.2; Tables 2.3-2.10 (Supplementary Tables 1-8)]. Of the 86 genes evaluated, 14 transcripts (i.e., *Ctsb*, *Ctsd*, *Gusb*, *A2m*, *Npc2*, *Apoe*, *Mme*, *Clu*, *Plat*, *Plau*, *Cyp46a1*, *Srebf1*, *Pmaip1* and *Bid*) were significantly ($p < 0.05$) up-regulated (Figs. 2.3-2.5) and 4 genes (i.e., *Anax6*, *Klc2*, *Aph1b* and *Mapt*) were significantly ($p < 0.05$) down-regulated (Fig. 2.6) in the cerebellum of ANPC and Npc1-null mice compared to WT mice. In contrast to cerebellum, expression of only 6 genes (i.e, *Ctsd*, *Gusb*, *A2m*, *Npc2*, *Apoe* and *Abca1*) were significantly ($p < 0.05$) up-regulated (Figs. 2.3-2.6) and one gene (i.e., *Tubb4*) is significantly ($p < 0.05$) down-regulated in the hippocampus of ANPC and Npc1-null mice as compared with WT mice. Apart from the similarities, expression profiles of selected genes were found to be differentially altered in Npc1-null *vs* ANPC mice. For example, while the expression of *Abca1*, *Park2* and *Shisa5* genes were significantly ($p < 0.05$) up-regulated in the cerebellum and that of *Dhcr24* down regulated in the hippocampus of Npc1-null mice as compared with WT mice, no such alteration was observed in ANPC mice (Fig. 2.6). With regard to ANPC mice, we observed down-regulation of *Cyp46a1*, *Rabggta* and *Kif1c* and up-regulation of *Ctsb* in the hippocampus compared to WT controls. However, expression of these genes was not significantly altered in Npc1-null mice (Fig. 2.4).

The gene expression profiles that were selectively altered in APP-Tg mice compared to WT mice include up-regulation of *Acat2*, *Sqle*, *Fdps*, *Fdft1* and *Dhcr24* in the hippocampus but not in the cerebellum. The genes that were down-regulated in APP-Tg mice include *Cyp46a1* in the hippocampus and *Park2* in the cerebellum. The Dhet mice, on the other hand, showed significant ($p < 0.05$) up-regulation of *Fdft1*, *Dhcr24* and *Sqle* and down-regulation of *Ctsb*, *Srebf1* and *Cyp46a1* in the hippocampus, whereas no alteration of any gene was evident in the cerebellum. The majority of the differentially expressed genes in our data set showed 1.2 - 2 fold changes, whereas only a few genes

such as *Ctsd*, *Gusb*, *A2m*, *Npc2*, *Apoe*, *Plau* and *Bid*, displayed more than 2 fold changes compared to WT mice. These changes were found in Npc1-null or ANPC mice. The majority of the 86 transcripts evaluated in our study, including *Aplp1*, *Ide*, *Igf2r* and *Gsk3β*, however, did not exhibit any alterations either in the hippocampus or cerebellum among fives lines of mice.

***Validation of altered gene expression profiles by Western blotting*:** To validate the observed changes in the gene expressions, we evaluated the steady-state protein levels of selected transcripts in both the hippocampus and cerebellum of all five lines of mice by immunoblot analysis. In keeping with up-regulated transcript levels, we observed significant ($p < 0.05$) increases in the levels of Apoe, Npc2, cathepsin B, cathepsin D and β-glucoronidase (encoded by *Apoe*, *Npc2*, *Ctsb*, *Ctsd* and *Gusb*, respectively) in both the hippocampus and cerebellum of ANPC and Npc1-null mice compared with APP-Tg, Dhet and WT mice (Figs. 2.3-2.5). In addition, the levels of tau (encoded by *Mapt*) were significantly ($p < 0.05$) decreased and the levels of neprilysin (encoded by *Mme*) were markedly increased in the cerebellum, but not in the hippocampus, of ANPC and Npc1-null mice compared to littermates of other genotypes (Figs. 2.5 and 2.6). Consistent with *Abca1* transcripts, the protein levels were significantly ($p < 0.05$) enhanced in the hippocampus of Npc1-null and ANPC mice as well as in the cerebellum of Npc1-null mice compared to WT mice (Fig. 2.6). Interestingly, certain proteins such as Apoe and neprilysin, but not their transcripts, are found to be enhanced more predominantly in ANPC than Npc1-null mice, suggesting potential translational control or post-translational modifications of the peptide levels (Figs. 2.3 and 2.5). As expected from the relative fold change quantified from RT^2 Profiler PCR array data, immunoblot analysis showed more prominent changes for proteins such as cathepsin D, neprilysin, tau and β-glucoronidase in the affected cerebellum than hippocampus in both ANPC and Npc1-null mice (Figs. 2.4-2.6). Consistent with unaltered transcript levels, no significant changes were evident in the levels of Bace1, Cdk-5 (encoded by *Bace1* and *Cdk-5*, respectively; data not shown), Aplp1, Gsk3β, Ide and Igf2r (encoded by *Aplp1*, *Gsk3β*, *Ide* and *Igf2r*, respectively; Figs. 2.7 and 2.8) either in the hippocampus or cerebellum of ANPC and Npc1-null mice compared with age-matched APP-Tg, Dhet and WT mice.

Table 2.2: List of selected genes for the RT^2 Mouse Custom Profiler PCR array

NCBI Ref Seq#	Gene Symbol	Official Gene Name
A. Selected genes related to APP/Aβ metabolism		
NM_175628	*A2m*	Alpha-2-macroglobulin
NM_007399	*Adam10*	A disintegrin and metallopeptidase domain 10
NM_009615	*Adam17*	A disintegrin and metallopeptidase domain 17
NM_146104	*Aph1a*	Anterior pharynx defective 1a homolog (C. elegans)
NM_177583	*Aph1b*	Anterior pharynx defective 1b homolog (C. elegans)
NM_007467	*Aplp1*	Amyloid beta (A4) precursor-like protein 1
NM_011792	*Bace1*	Beta-site APP cleaving enzyme 1
NM_019517	*Bace2*	Beta-site APP-cleaving enzyme 2
NM_031156	*Ide*	Insulin degrading enzyme
NM_008604	*Mme*	Membrane metallo endopeptidase
NM_021607	*Ncstn*	Nicastrin
NM_008872	*Plat*	Plasminogen activator, tissue
NM_008873	*Plau*	Plasminogen activator, urokinase
NM_008877	*Plg*	Plasminogen
NM_008943	*Psen1*	Presenilin 1
NM_011183	*Psen2*	Presenilin 2
NM_025498	*Psenen*	Presenilin enhancer 2 homolog (C. elegans)
NM_013697	*Ttr*	Transthyretin
B. Selected genes involved in cholesterol metabolism		
NM_013454	*Abca1*	ATP-binding cassette, sub-family A (ABC1), member 1
NM_031884	*Abcg5*	ATP-binding cassette, sub-family G (WHITE), member 5
NM_009338	*Acat2*	Acetyl-Coenzyme A acetyltransferase 2
NM_009696	*Apoe*	Apolipoprotein E
NM_013492	*Clu*	Clusterin
NM_010010	*Cyp46a1*	Cytochrome P450, family 46, subfamily a, polypeptide 1
NM_053272	*Dhcr24*	24-dehydrocholesterol reductase
NM_010191	*Fdft1*	Farnesyl diphosphate farnesyl transferase 1
NM_134469	*Fdps*	Farnesyl diphosphate synthetase
NM_008255	*Hmgcr*	3-hydroxy-3-methylglutaryl-Coenzyme A reductase
NM_010700	*Ldlr*	Low density lipoprotein receptor
NM_008512	*Lrp1*	Low density lipoprotein receptor-related protein 1
NM_207242	*Npc1l1*	NPC1-like 1
NM_023409	*Npc2*	Niemann Pick type C2
NM_009473	*Nr1h2*	Nuclear receptor subfamily 1, group H, member 2
NM_001001144	*Scap*	SREBF chaperone
NM_009270	*Sqle*	Squalene epoxidase
NM_011480	*Srebf1*	Sterol regulatory element binding transcription factor 1

NM_033218	*Srebf2*	Sterol regulatory element binding factor 2

C. Selected genes involved in intracellular trafficking

NM_013472	*Anxa6*	Annexin A6
NM_015740	*Bloc1s1*	Biogenesis of lysosome-related organelles complex-1, subunit 1
NM_021538	*Cope*	Coatomer protein complex, subunit epsilon
NM_007864	*Dlg4*	Discs, large homolog 4 (Drosophila)
NM_010064	*Dync1i2*	Dynein cytoplasmic 1 intermediate chain 2
NM_010515	*Igf2r*	Insulin-like growth factor 2 receptor
NM_153103	*Kif1c*	Kinesin family member 1C
NM_008451	*Klc2*	Kinesin light chain 2
NM_010684	*Lamp1*	Lysosomal-associated membrane protein 1
NM_010749	*M6pr*	Mannose-6-phosphate receptor, cation dependent
NM_010838	*Mapt*	Microtubule-associated protein tau
NM_025887	*Rab5a*	RAB5A, member RAS oncogene family
NM_009005	*Rab7*	RAB7, member RAS oncogene family
NM_019773	*Rab9*	RAB9, member RAS oncogene family
NM_145522	*Rabepk*	Rab9 effector protein with kelch motifs
NM_019519	*Rabggta*	Rab geranylgeranyl transferase, a subunit
NM_009294	*Stx4a*	Syntaxin 4A (placental)
NM_009305	*Syp*	Synaptophysin
NM_009451	*Tubb4*	Tubulin, beta 4

D. Selected genes implicated in cell death/survival pathways

NM_009652	*Akt1*	Thymoma viral proto-oncogene 1
NM_026217	*Atg12*	Autophagy-related 12 (yeast)
NM_053069	*Atg5*	Autophagy-related 5 (yeast)
NM_028835	*Atg7*	Autophagy-related 7 (yeast)
NM_007527	*Bax*	Bcl2-associated X protein
NM_009741	*Bcl2*	B-cell leukemia/lymphoma 2
NM_019584	*Becn1*	Beclin 1, autophagy related
NM_007544	*Bid*	BH3 interacting domain death agonist
NM_133926	*Camk1*	Calcium/calmodulin-dependent protein kinase I
NM_007602	*Capn5*	Calpain 5
NM_009810	*Casp3*	Caspase 3
NM_009817	*Cast*	Calpastatin
NM_007668	*Cdk5*	Cyclin-dependent kinase 5
NM_007798	*Ctsb*	Cathepsin B
NM_009983	*Ctsd*	Cathepsin D
NM_010234	*Fos*	FBJ osteosarcoma oncogene
NM_019827	*Gsk3b*	Glycogen synthase kinase 3 beta
NM_010368	*Gusb*	Glucuronidase, beta
NM_010514	*Igf2*	Insulin-like growth factor 2
NM_026160	*Map1lc3b*	Microtubule-associated protein 1 light chain 3 beta

NM_011949	*Mapk1*	Mitogen-activated protein kinase 1
NM_011952	*Mapk3*	Mitogen-activated protein kinase 3
NM_016700	*Mapk8*	Mitogen-activated protein kinase 8
NM_016694	*Park2*	Parkinson disease (autosomal recessive, juvenile) 2, parkin
NM_181414	*Pik3c3*	Phosphoinositide-3-kinase, class 3
NM_008839	*Pik3ca*	Phosphatidylinositol 3-kinase, catalytic, alpha polypeptide
NM_023371	*Pin1*	Protein (peptidyl-prolyl cis/trans isomerase) NIMA-interacting 1
NM_021451	*Pmaip1*	Phorbol-12-myristate-13-acetate-induced protein 1
NM_011563	*Prdx2*	Peroxiredoxin 2
NM_025858	*Shisa5*	Shisa homolog 5 (Xenopus laevis)

Table 2.3: *Supplementary Table-1*. Expression profiles of genes related to APP/Aβ metabolism in the hippocampus of APP-Tg, Dhet, Npc1-null and ANPC compared to the WT mice

Gene Symbol	APP-Tg		Dhet		Npc1-null		ANPC	
	Fold Regulation	p-value	Fold Regulation	p-value	Fold Regulation	p-value	Fold Regulation	p-value
A2m	1.45	0.073	-1.07	0.640	1.84	0.001	2.08	0.010
Adam10	-1.03	0.789	-1.05	0.470	-1.14	0.044	-1.15	0.103
Adam17	-1.06	0.693	-1.35	0.124	-1.25	0.218	-1.39	0.118
Aph1a	1.01	0.894	-1.05	0.660	1.03	0.881	1.05	0.766
Aph1b	1.12	0.417	1.10	0.379	-1.20	0.204	1.02	0.898
Aplp1	1.20	0.129	1.09	0.248	-1.32	0.108	-1.11	0.359
Bace1	-1.11	0.318	-1.09	0.226	-1.12	0.153	-1.23	0.064
Bace2	1.12	0.357	-1.31	0.189	1.26	0.053	-1.13	0.243
Ide	1.17	0.024	-1.06	0.570	-1.06	0.203	-1.15	0.038
Mme	-1.39	0.470	-1.10	0.451	1.08	0.600	1.01	0.948
Ncstn	-1.07	0.561	-1.17	0.090	1.04	0.448	1.01	0.834
Plat	1.21	0.064	1.04	0.756	1.03	0.833	1.10	0.306
Plau	1.03	0.788	1.04	0.755	1.37	0.163	1.54	0.061
Plg	1.12	0.429	-1.15	0.397	-1.15	0.678	-1.19	0.360
Psen1	-1.05	0.618	-1.14	0.302	-1.11	0.247	-1.18	0.258
Psen2	1.14	0.361	1.06	0.642	1.07	0.519	1.10	0.421
Psenen	1.06	0.532	1.03	0.518	-1.11	0.068	-1.04	0.452
Ttr	-2.47	0.306	-2.50	0.342	3.99	0.975	1.34	0.416

Table 2.4: *Supplementary Table-2*. Expression profiles of genes related to APP/Aβ metabolism in the cerebellum of APP-Tg, Dhet, Npc1-null and ANPC compared to the WT mice

Gene Symbol	APP-Tg		Dhet		Npc1-null		ANPC	
	Fold Regulation	p-value	Fold Regulation	p-value	Fold Regulation	p-value	Fold Regulation	p-value
A2m	1.02	0.787	1.03	0.680	1.43	0.009	1.64	0.002
Adam10	1.03	0.915	-1.03	0.842	-1.29	0.110	-1.26	0.177
Adam17	-1.15	0.266	-1.19	0.234	-1.16	0.287	-1.33	0.236
Aph1a	1.00	0.965	-1.02	0.832	1.04	0.713	-1.02	0.753
Aph1b	-1.00	0.981	1.00	0.945	-1.24	0.019	-1.27	0.016
Aplp1	-1.11	0.297	1.01	0.886	-1.05	0.436	-1.07	0.650
Bace1	1.01	0.915	1.00	0.987	-1.22	0.062	-1.17	0.072
Bace2	-1.23	0.104	-1.15	0.311	1.06	0.598	1.01	0.910
Ide	-1.11	0.113	-1.08	0.197	-1.07	0.274	-1.10	0.241
Mme	-1.17	0.572	1.05	0.822	1.96	0.006	1.99	0.003
Ncstn	-1.02	0.933	1.00	0.999	-1.00	0.985	-1.11	0.180
Plat	1.11	0.399	1.12	0.423	1.51	0.008	1.69	0.001
Plau	1.19	0.445	1.15	0.529	13.82	0.000	10.50	0.000
Plg	-1.19	0.703	-1.04	0.786	-1.05	0.731	1.20	0.326
Psen1	1.02	0.800	-1.07	0.378	-1.11	0.165	-1.18	0.031
Psen2	1.05	0.659	1.01	0.996	1.04	0.702	-1.08	0.650
Psenen	-1.00	0.949	-1.04	0.610	-1.00	0.987	-1.15	0.186
Ttr	-6.75	0.961	-1.48	0.928	-1.90	0.323	-37.36	0.039

Table 2.5: *Supplementary Table-3*. Expression profiles of genes involved in cholesterol metabolism in the hippocampus of APP-Tg, Dhet, Npc1-null and ANPC compared to the WT mice

Gene Symbol	APP-Tg		Dhet		Npc1-null		ANPC	
	Fold Regulation	p-value	Fold Regulation	p-value	Fold Regulation	p-value	Fold Regulation	p-value
Abca1	1.04	0.724	-1.09	0.348	1.43	0.003	1.44	0.012
Abcg5	1.26	0.489	-1.45	0.137	1.35	0.403	-1.23	0.342
Acat2	1.50	0.021	1.23	0.235	1.10	0.407	1.28	0.063
Apoe	1.12	0.600	1.21	0.331	1.60	0.048	1.76	0.048
Clu	1.10	0.466	-1.04	0.699	1.12	0.197	1.15	0.155
Cyp46a1	-1.42	0.006	-1.24	0.010	-1.15	0.135	-1.27	0.039
Dhcr24	1.34	0.011	1.31	0.02	-1.23	0.013	-1.03	0.819
Fdft1	1.26	0.02	1.39	0.019	1.01	0.885	1.33	0.096
Fdps	1.51	0.047	1.31	0.179	-1.06	0.607	1.11	0.376
Hmgcr	1.42	0.071	1.12	0.314	-1.15	0.450	1.01	0.836
Ldlr	1.57	0.081	1.41	0.079	-1.00	0.925	-1.00	0.819
Lrp1	1.11	0.319	1.04	0.716	1.23	0.169	1.20	0.176
Npc1l1	-1.66	0.079	-1.46	0.173	-1.30	0.199	1.06	0.720
Npc2	1.00	0.905	-1.04	0.477	1.42	0.001	1.50	0.002
Nr1h2	1.21	0.051	-1.10	0.349	-1.14	0.250	-1.01	0.994
Scap	1.08	0.600	-1.10	0.413	-1.01	0.863	1.01	0.944
Sqle	1.53	0.037	1.34	0.035	1.05	0.709	1.12	0.396
Srebf1	-1.15	0.115	-1.32	0.006	1.01	0.909	-1.06	0.471
Srebf2	1.17	0.180	1.18	0.099	-1.01	0.952	-1.04	0.842

Table 2.6: *Supplementary Table-4*. Expression profiles of genes involved in cholesterol metabolism in the cerebellum of APP-Tg, Dhet, Npc1-null and ANPC compared to the WT mice

Gene Symbol	APP-Tg		Dhet		Npc1-null		ANPC	
	Fold Regulation	p-value	Fold Regulation	p-value	Fold Regulation	p-value	Fold Regulation	p-value
Abca1	1.02	0.781	-1.04	0.738	1.34	0.043	1.18	0.402
Abcg5	-1.74	0.144	-1.15	0.826	-1.11	0.693	-1.38	0.355
Acat2	-1.09	0.484	1.01	0.922	1.21	0.253	1.19	0.406
Apoe	-1.20	0.425	1.09	0.770	2.43	0.012	2.10	0.013
Clu	-1.04	0.763	-1.02	0.799	1.47	0.012	1.43	0.037
Cyp46a1	1.04	0.608	1.18	0.094	1.23	0.040	1.38	0.032
Dhcr24	-1.04	0.513	1.04	0.612	1.16	0.141	1.20	0.069
Fdft1	-1.08	0.103	1.02	0.667	1.10	0.275	1.20	0.074
Fdps	-1.08	0.499	-1.02	0.802	1.11	0.379	1.11	0.466
Hmgcr	-1.17	0.049	-1.12	0.060	-1.07	0.455	1.03	0.648
Ldlr	-1.19	0.059	-1.19	0.112	-1.10	0.241	-1.00	0.838
Lrp1	1.11	0.459	1.06	0.706	1.12	0.391	1.17	0.286
Npc1l1	-1.37	0.228	-1.21	0.499	1.05	0.788	1.37	0.377
Npc2	-1.06	0.647	-1.06	0.671	2.03	0.000	1.65	0.039
Nr1h2	-1.02	0.883	1.02	0.865	-1.13	0.238	-1.10	0.490
Scap	-1.01	0.786	-1.06	0.345	-1.06	0.377	-1.06	0.595
Sqle	-1.05	0.425	1.00	0.906	1.02	0.746	1.19	0.018
Srebf1	-1.10	0.334	-1.06	0.514	1.26	0.009	1.30	0.022
Srebf2	-1.00	0.961	-1.02	0.823	-1.05	0.604	-1.03	0.755

Table 2.7: *Supplementary Table-5*. Expression profiles of genes involved in intracellular trafficking in the hippocampus of APP-Tg, Dhet, Npc1-null and ANPC compared to the WT mice

Gene Symbol	APP-Tg		Dhet		Npc1-null		ANPC	
	Fold Regulation	p-value	Fold Regulation	p-value	Fold Regulation	p-value	Fold Regulation	p-value
Anxa6	-1.00	0.956	1.01	0.902	-1.18	0.049	-1.17	0.017
Bloc1s1	1.21	0.083	1.01	0.856	1.02	0.688	-1.01	0.934
Cope	1.20	0.053	-1.02	0.901	-1.00	0.995	1.02	0.818
Dlg4	-1.11	0.561	1.07	0.600	-1.05	0.745	-1.16	0.263
Dync1i2	1.05	0.350	-1.11	0.271	-1.17	0.064	-1.21	0.078
Igf2r	-1.07	0.145	-1.19	0.082	1.01	0.807	-1.03	0.884
Kif1c	-1.30	0.070	-1.21	0.126	-1.25	0.19	-1.42	0.038
Klc2	-1.12	0.316	-1.06	0.465	-1.16	0.051	-1.23	0.096
Lamp1	1.16	0.164	-1.02	0.785	1.07	0.362	1.04	0.506
M6pr	1.09	0.199	-1.01	0.971	-1.02	0.889	-1.01	1.000
Mapt	1.00	0.926	-1.07	0.511	-1.16	0.139	-1.23	0.092
Rab5a	1.06	0.597	-1.23	0.243	-1.11	0.233	-1.06	0.523
Rab7	1.07	0.527	1.05	0.609	1.04	0.574	1.08	0.433
Rab9	1.19	0.067	1.03	0.661	-1.04	0.617	-1.02	0.861
Rabepk	1.21	0.170	1.20	0.054	-1.03	0.875	-1.09	0.563
Rabggta	-1.06	0.295	-1.11	0.093	-1.12	0.028	-1.23	0.001
Stx4a	1.09	0.412	1.00	0.985	-1.06	0.552	-1.11	0.407
Syp	-1.11	0.361	-1.02	0.894	-1.09	0.426	-1.13	0.226
Tubb4	-1.00	0.969	-1.05	0.488	-1.45	0.001	-1.60	0.000

Table 2.8: *Supplementary Table-6*. Expression profiles of genes involved in intracellular trafficking in the cerebellum of APP-Tg, Dhet, Npc1-null and ANPC compared to the WT mice

Gene Symbol	APP-Tg		Dhet		Npc1-null		ANPC	
	Fold Regulation	p-value	Fold Regulation	p-value	Fold Regulation	p-value	Fold Regulation	p-value
Anxa6	1.00	0.995	-1.04	0.634	-1.25	0.028	-1.37	0.022
Bloc1s1	1.11	0.499	1.08	0.643	1.03	0.913	-1.03	0.805
Cope	1.00	0.993	-1.05	0.222	-1.00	0.988	-1.07	0.353
Dlg4	1.01	0.901	1.02	0.782	-1.11	0.349	-1.01	0.957
Dync1i2	-1.11	0.003	-1.08	0.243	-1.10	0.010	-1.07	0.550
Igf2r	1.02	0.734	-1.04	0.633	-1.07	0.465	1.01	0.803
Kif1c	-1.10	0.460	-1.14	0.458	1.15	0.304	-1.19	0.236
Klc2	1.06	0.463	1.02	0.783	-1.28	0.002	-1.27	0.015
Lamp1	-1.12	0.147	-1.09	0.174	1.18	0.091	1.12	0.379
M6pr	1.00	0.998	1.05	0.735	1.06	0.670	1.21	0.194
Mapt	-1.04	0.476	-1.06	0.494	-1.29	0.03	-1.24	0.013
Rab5a	-1.04	0.463	-1.11	0.192	-1.08	0.310	1.03	0.669
Rab7	1.05	0.547	1.00	0.982	-1.60	0.180	1.08	0.292
Rab9	-1.01	0.743	-1.07	0.083	-1.13	0.117	-1.08	0.255
Rabepk	-1.06	0.634	-1.03	0.760	-1.06	0.536	-1.12	0.432
Rabggta	-1.01	0.729	-1.01	0.813	-1.02	0.547	1.02	0.682
Stx4a	-1.08	0.403	-1.07	0.356	-1.04	0.628	-1.12	0.243
Syp	-1.03	0.798	-1.01	0.909	-1.12	0.171	-1.05	0.635
Tubb4	1.03	0.761	-1.07	0.435	-1.14	0.196	-1.20	0.133

Table 2.9: *Supplementary Table-7*. Expression profiles of genes implicated in cell death/survival in the hippocampus of APP-Tg, Dhet, Npc1-null and ANPC compared to the WT mice

Gene Symbol	APP-Tg		Dhet		Npc1-null		ANPC	
	Fold Regulation	p-value	Fold Regulation	p-value	Fold Regulation	p-value	Fold Regulation	p-value
Akt1	-1.22	0.229	-1.15	0.128	-1.06	0.652	-1.17	0.163
Atg12	1.07	0.582	1.07	0.591	-1.02	0.824	-1.08	0.559
Atg5	-1.04	0.445	-1.01	0.878	-1.04	0.458	-1.02	0.564
Atg7	-1.17	0.454	1.00	0.966	1.06	0.652	-1.26	0.117
Bax	1.02	0.784	-1.04	0.432	-1.05	0.391	-1.15	0.077
Bcl2	-1.03	0.760	-1.19	0.265	1.01	0.946	-1.16	0.315
Becn1	1.14	0.150	1.08	0.281	-1.04	0.490	-1.12	0.338
Bid	-1.02	0.740	-1.01	0.783	1.25	0.067	1.21	0.066
Camk1	1.19	0.313	1.03	0.908	1.10	0.593	1.04	0.818
Capn5	1.15	0.337	-1.04	0.648	-1.16	0.114	-1.03	0.850
Casp3	-1.06	0.483	-1.10	0.256	-1.15	0.054	-1.20	0.056
Cast	1.22	0.174	1.06	0.682	1.30	0.149	1.14	0.319
Cdk5	1.14	0.340	1.00	0.999	-1.26	0.08	-1.29	0.097
Ctsb	-1.09	0.199	-1.26	0.006	1.13	0.111	1.25	0.011
Ctsd	1.14	0.382	-1.04	0.681	2.20	0.000	2.38	0.000
Fos	1.85	0.472	1.05	0.940	-1.43	0.378	-1.11	0.571
Gsk3b	1.07	0.511	-1.04	0.592	-1.06	0.088	-1.13	0.061
Gusb	1.11	0.252	-1.08	0.424	1.53	0.002	1.54	0.001
Igf2	-1.47	0.229	-1.35	0.318	1.13	0.574	-1.36	0.348
Map1lc3b	1.02	0.812	1.02	0.821	-1.01	0.900	-1.04	0.554
Mapk1	-1.01	0.970	1.06	0.178	1.02	0.677	1.06	0.297
Mapk3	-1.11	0.708	-1.08	0.447	-1.06	0.284	-1.07	0.156
Mapk8	-1.01	0.981	1.06	0.630	-1.02	0.873	-1.06	0.674
Park2	1.02	0.986	-1.07	0.603	1.18	0.251	1.06	0.742
Pik3c3	1.13	0.315	-1.08	0.323	-1.15	0.029	-1.05	0.658
Pik3ca	-1.05	0.745	-1.05	0.391	-1.08	0.218	-1.11	0.273
Pin1	1.12	0.075	1.00	0.961	-1.03	0.615	-1.04	0.407
Pmaip1	1.27	0.137	1.13	0.442	1.15	0.270	1.12	0.400
Prdx2	1.24	0.109	-1.00	0.897	-1.07	0.523	-1.06	0.730
Shisa5	1.14	0.395	1.04	0.678	1.10	0.412	1.05	0.658

Table 2.10: *Supplementary Table-8*. Expression profiles of genes implicated in cell death/survival in cerebellum of APP-Tg, Dhet, Npc1-null and ANPC compared to the WT mice

Gene Symbol	APP-Tg		Dhet		Npc1-null		ANPC	
	Fold Regulation	p-value	Fold Regulation	p-value	Fold Regulation	p-value	Fold Regulation	p-value
Akt1	-1.03	0.731	-1.06	0.488	-1.11	0.249	-1.01	0.926
Atg12	1.08	0.519	1.08	0.587	-1.01	0.908	1.03	0.789
Atg5	-1.03	0.735	-1.04	0.777	-1.11	0.353	-1.08	0.189
Atg7	-1.04	0.736	-1.05	0.683	-1.06	0.485	1.08	0.628
Bax	1.05	0.485	-1.02	0.737	-1.01	0.886	-1.11	0.205
Bcl2	1.11	0.370	1.04	0.708	-1.04	0.872	1.04	0.653
Becn1	-1.07	0.533	-1.11	0.309	-1.14	0.189	-1.06	0.648
Bid	-1.01	0.870	1.09	0.546	2.25	0.007	2.56	0.001
Camk1	-1.10	0.396	-1.09	0.717	1.00	0.965	-1.02	0.987
Capn5	-1.17	0.024	-1.15	0.312	-1.12	0.228	1.06	0.624
Casp3	-1.04	0.744	-1.01	0.859	1.13	0.206	-1.01	0.963
Cast	1.02	0.731	1.00	0.934	1.01	0.761	-1.01	0.908
Cdk5	-1.02	0.807	1.03	0.758	-1.19	0.061	-1.19	0.247
Ctsb	-1.13	0.127	-1.05	0.466	1.50	0.003	1.72	0.035
Ctsd	-1.13	0.227	-1.05	0.272	6.29	0.000	4.14	0.002
Fos	-1.25	0.412	1.54	0.852	1.16	0.454	1.14	0.605
Gsk3b	-1.08	0.091	-1.11	0.259	-1.09	0.052	-1.05	0.380
Gusb	-1.09	0.324	-1.13	0.218	3.59	0.001	3.06	0.000
Igf2	-1.11	0.884	-1.01	0.951	-1.07	0.633	-1.29	0.342
Map1lc3b	1.04	0.701	1.11	0.390	1.13	0.304	1.20	0.158
Mapk1	1.06	0.183	-1.01	0.808	-1.07	0.163	-1.06	0.356
Mapk3	1.08	0.455	-1.03	0.775	1.00	0.972	1.04	0.680
Mapk8	1.00	0.992	1.06	0.732	1.05	0.741	-1.00	0.972
Park2	-1.22	0.032	-1.18	0.068	1.28	0.005	1.19	0.267
Pik3c3	1.07	0.194	-1.09	0.219	-1.19	0.049	-1.17	0.241
Pik3ca	-1.32	0.306	-1.11	0.360	-1.15	0.044	-1.19	0.022
Pin1	1.03	0.697	-1.04	0.543	-1.06	0.459	-1.02	0.840
Pmaip1	1.02	0.927	1.10	0.501	1.43	0.036	1.31	0.041
Prdx2	-1.11	0.530	-1.09	0.213	-1.14	0.091	-1.21	0.313
Shisa5	-1.07	0.612	1.02	0.883	1.36	0.039	1.23	0.262

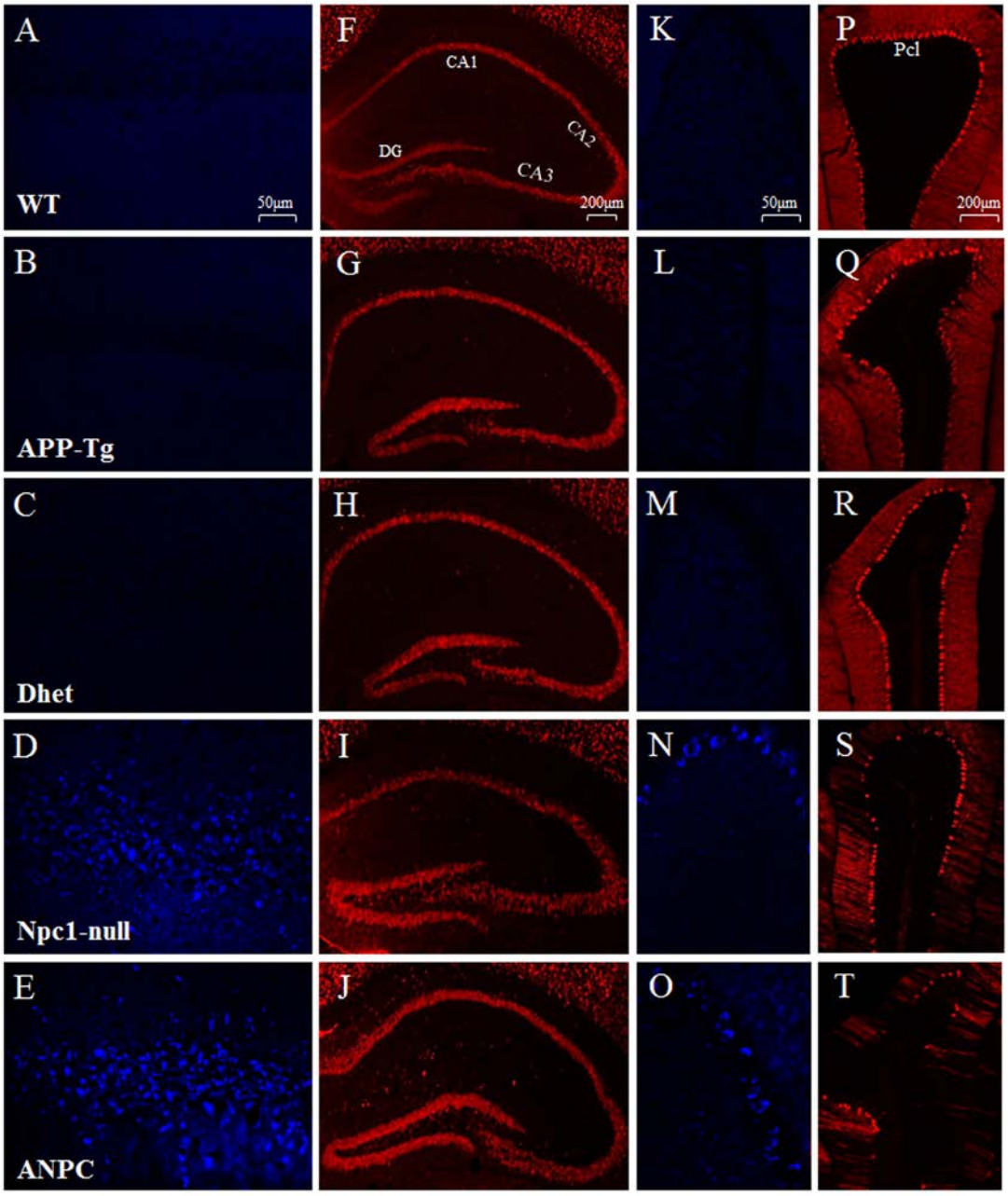

Figure 2.1: Cholesterol accumulation and neurodegeneration in Npc1-null and ANPC mice compared to other genotypes. **A-E,** Photomicrographs showing filipin staining of unesterified cholesterol in the hippocampus of WT, APP-Tg, Dhet, Npc1-null and ANPC mice. Cholesterol accumulation is evident only in the hippocampal neurons of Npc1-null (**D**) and ANPC (**E**) mice but not in WT (**A**), APP-Tg (**B**) or Dhet (**C**) littermates. **F-J,** Photomicrographs showing NeuN labeled hippocampal sections from mice of different genotypes. No apparent loss of neurons was evident in the hippocampus of Npc1-null (**I**) or ANPC (**J**) mice compared to WT (**F**), APP-Tg (**G**) and Dhet (**H**) littermates. **K-O,** Photomicrographs showing filipin staining in the cerebellum of WT, APP-Tg, Dhet, Npc1-null and ANPC mice. Accumulation of cholesterol is evident only in the cerebellar neurons of Npc1-null (**N**) and ANPC (**O**) mice but not in WT (**K**), APP-Tg (**L**) or Dhet (**M**) mice. **P-T**, Photomicrographs showing calbindin-positive cerebellar Purkinje cell layer (Pcl) in mice from different genotypes. Note the relative loss of Purkinje cells in Npc1-null (**S**) and ANPC (**T**) mice compared to WT (**P**), APP-Tg (**Q**) and Dhet (**R**) littermates. All photomicrographs of each column are of same magnification. CA1-CA3, Cornu Ammonis1-3 subfields of the Ammon's horn; DG, dentate gyrus; Pcl, Purkinje cell layer.

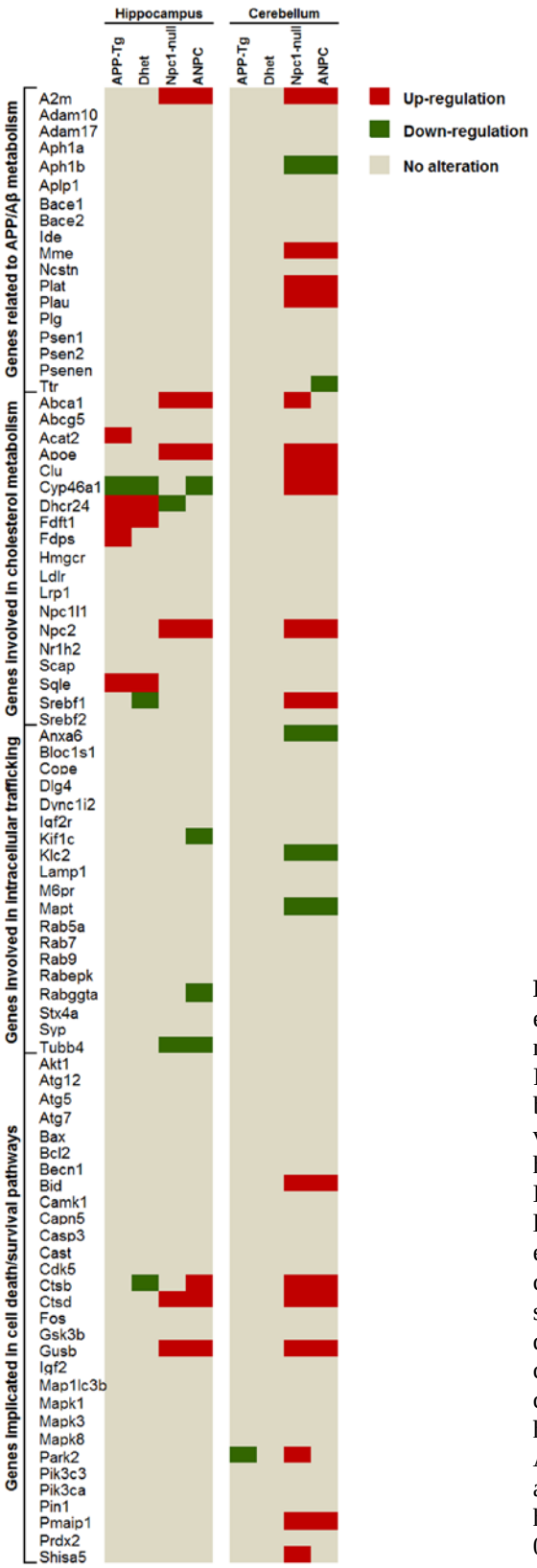

Figure 2.2: Heatmap diagram showing gene expression profiles in five lines of mice. The figure represents data obtained using RT^2 Mouse Custom Profiler PCR array of 86 selected genes involved in brain cholesterol and APP metabolisms, intracellular vesicular trafficking and cell death pathways in the hippocampus and cerebellum of 7-week-old APP-Tg, Dhet, Npc1-null and ANPC mice compared with WT littermates. Each row represents a single gene and each column represents a mouse genotype combination. Expression levels are colored red for significant up-regulations, green for significant down-regulations and grey for no alteration compared with the WT mice. As shown, the major changes in gene expression occurred in the hippocampus and cerebellum of Npc1-null and ANPC mice while changes in APP-Tg and Dhet mice are limited to only a few genes mainly in the hippocampus. A fold difference of ≥1.2 with a $p < 0.05$ was considered to be a significant dysregulation.

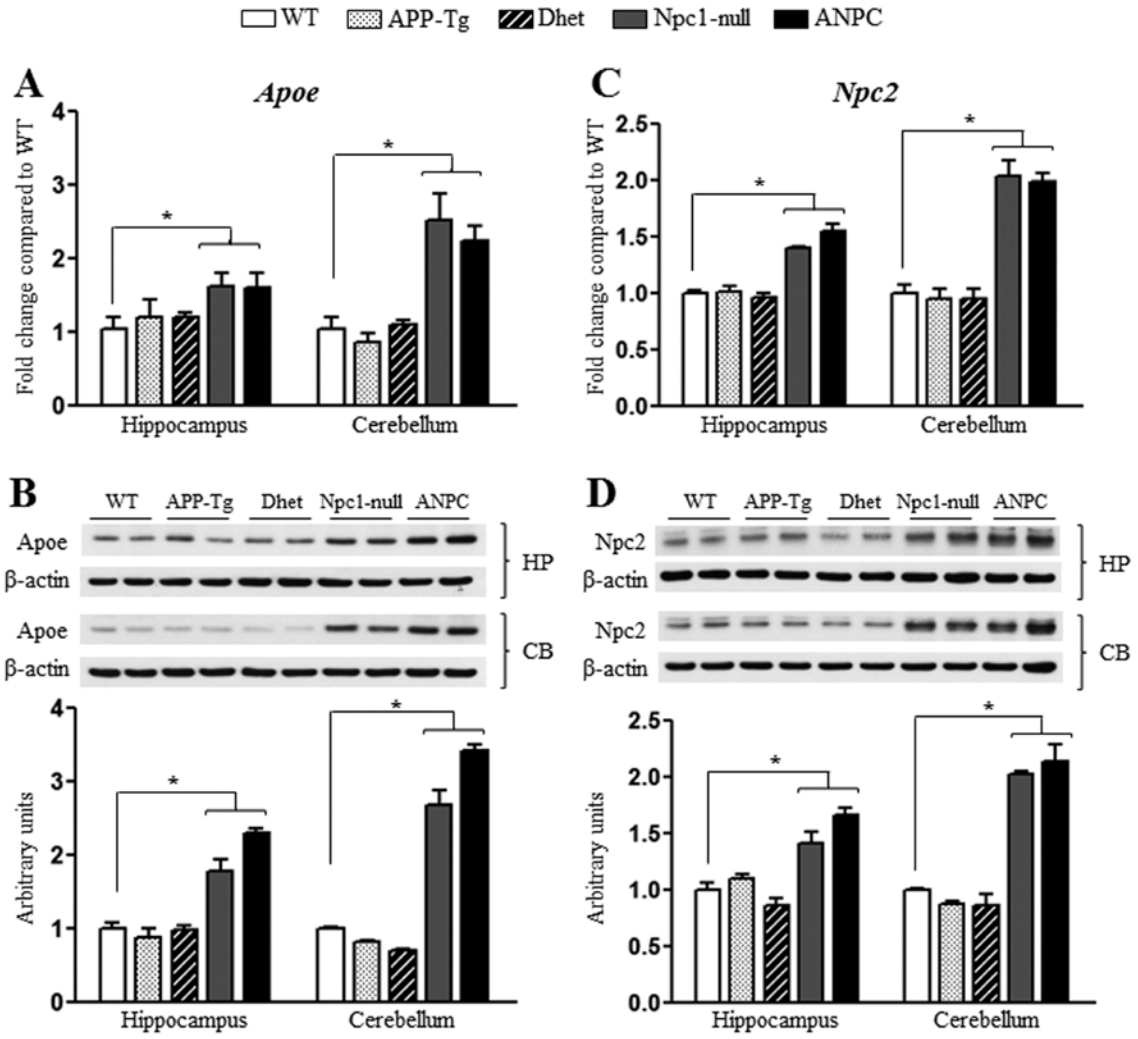

Figure 2.3: Expression levels of Apoe (**A**, **B**) and Npc2 (**C**, **D**) in the hippocampus and cerebellum of five lines of mice. **(A, C)** Histograms showing increased mRNA levels for *Apoe* (**A**) and *Npc2* (**C**) in the hippocampus and cerebellum of Npc1-null and ANPC mice compared with WT mice as obtained using RT^2 Mouse Custom Profiler PCR array. **(B, D)** Immunoblots and respective histograms validating increased levels of Apoe (**B**) and Npc2 (**D**) in the hippocampus and cerebellum of Npc1-null and ANPC mice compared with age-matched WT mice. The protein levels of Apoe and Npc2 were normalized to the β-actin and the values (n = 4 animals per genotype) are expressed as means ± SEM. *, $p < 0.05$.

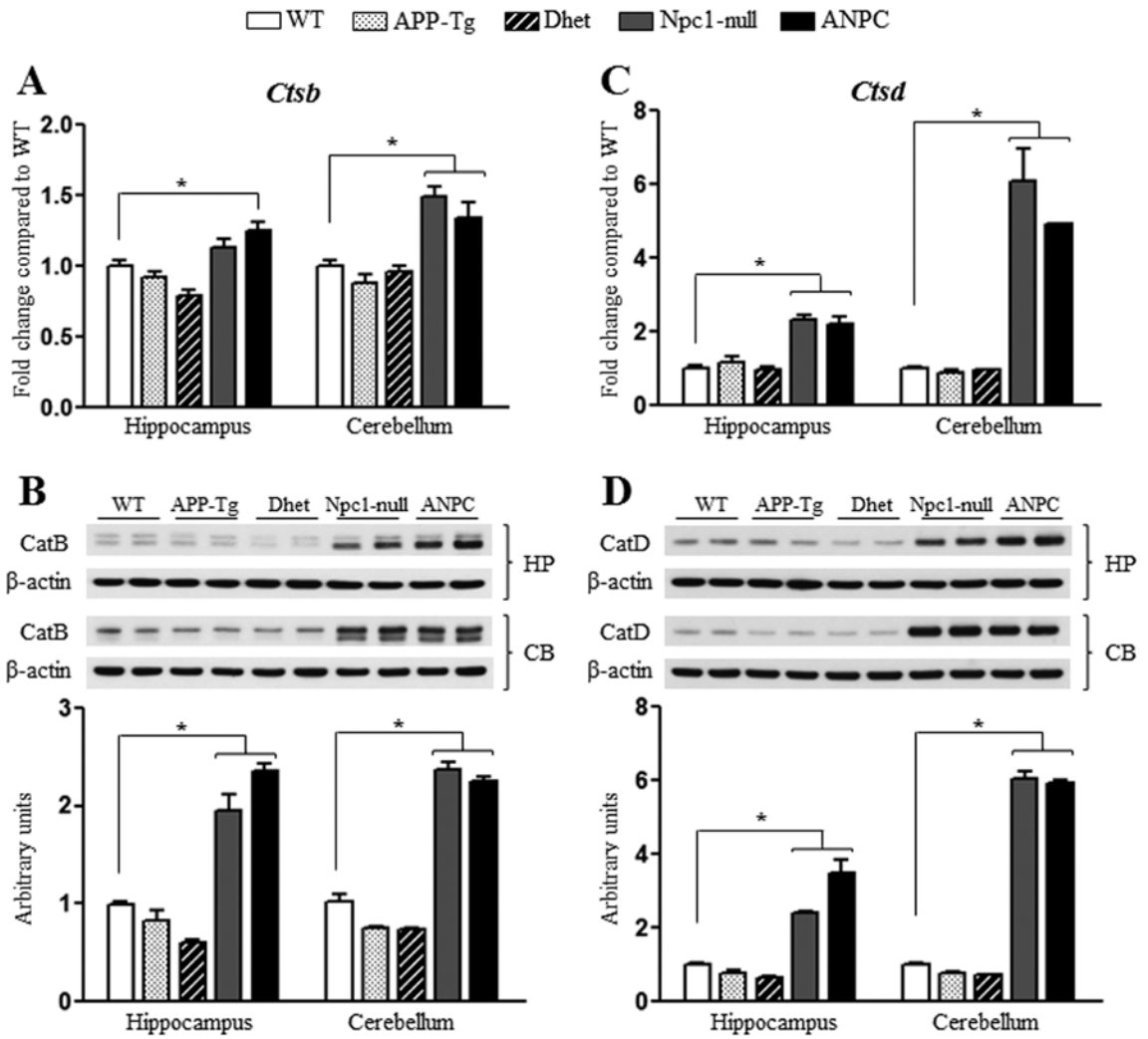

Figure 2.4: Expression levels of cathepsin B (**A**, **B**) and cathepsin D (**C**, **D**) in the hippocampus and cerebellum of five lines of mice. **(A, C)** Histograms showing increased mRNA levels for *Ctsb* (encoding cathepsin B, **A**) and *Ctsd* (encoding cathepsin D**, C**) in the hippocampus and cerebellum of Npc1-null and ANPC mice compared with WT control mice as obtained using RT^2 Mouse Custom Profiler PCR array. **(B, D)** Immunoblotting performed to validate data obtained by PCR arrays revealed increased levels of cathepsin B (**B**) and cathepsin D (**D**) in the hippocampus and cerebellum of Npc1-null and ANPC mice compared with the WT mice. APP-Tg and Dhet mice showed no alteration in transcript or protein expression levels of cathepsin B and cathepsin D compared with WT mice. The protein levels of cathepsin B and cathepsin D were normalized to the β-actin and the values (n = 4 animals/ genotype) are expressed as means ± SEM. *, $p < 0.05$. CatB, cathepsin B; CatD, cathepsin D.

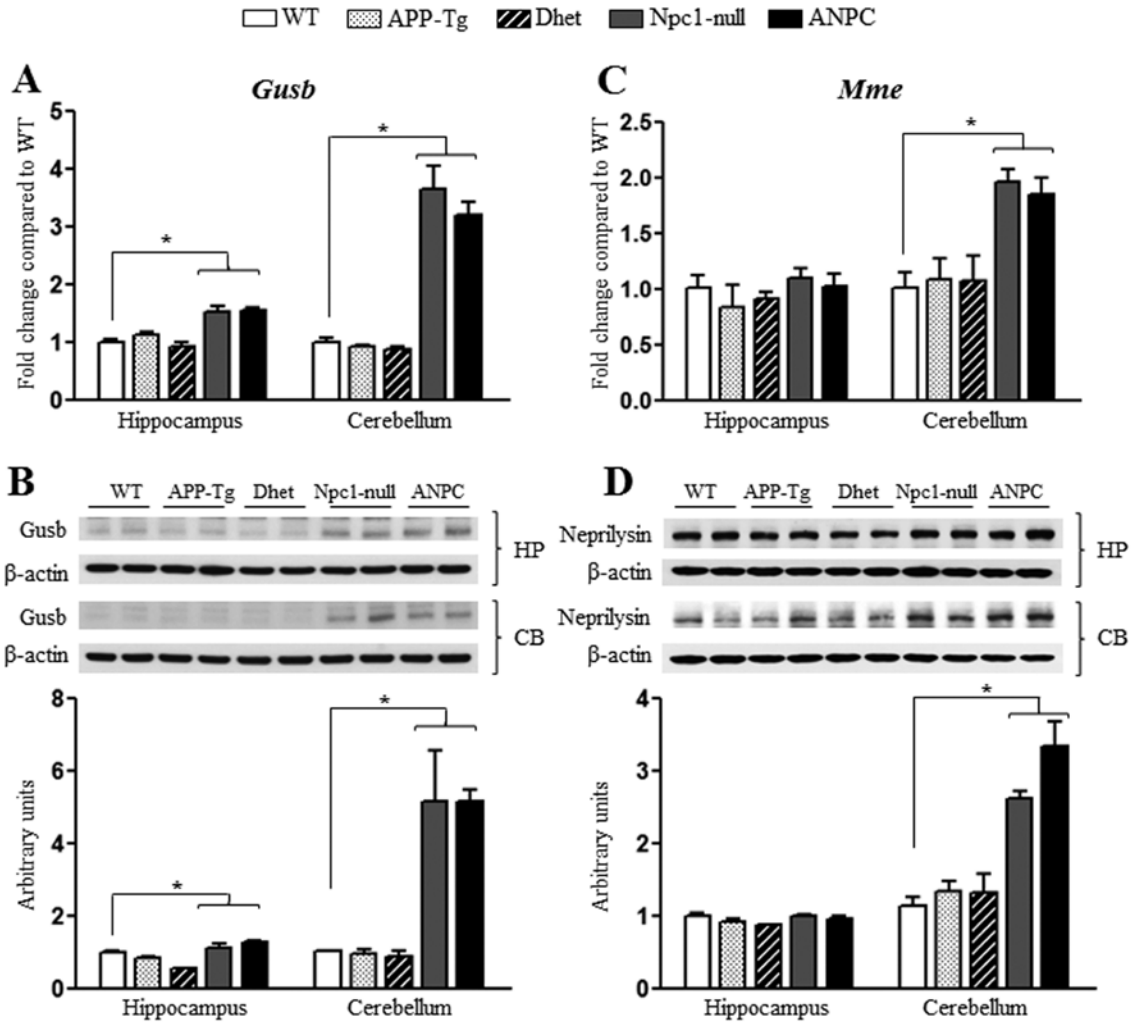

Figure 2.5: Expression levels of β-glucoronidase (Gusb; **A**, **B**) and neprilysin (**C**, **D**) in the hippocampus and cerebellum of five lines of mice. **(A, C)** Histograms showing increased mRNA levels for *Gusb* (**A**) in both hippocampus and cerebellum and *Mme* (encoding neprilysin**, C**) in the cerebellum of Npc1-null and ANPC mice compared with WT control mice as obtained using RT^2 Mouse Custom Profiler PCR array. **(B, D)** Immunoblotting performed to validate data obtained by PCR arrays revealed increased levels of Gusb (**B**) in both the hippocampus and cerebellum and neprilysin (**D**) in the cerebellum of Npc1-null and ANPC mice compared with WT mice. APP-Tg and Dhet mice showed no significant alteration in transcript or protein expression levels of Gusb (**A**, **B**) or neprilysin (**C**, **D**) compared with the WT mice. The protein levels of Gusb and neprilysin were normalized to the β-actin and the values (n = 4 animals per genotype) are expressed as means ± SEM. *, $p < 0.05$.

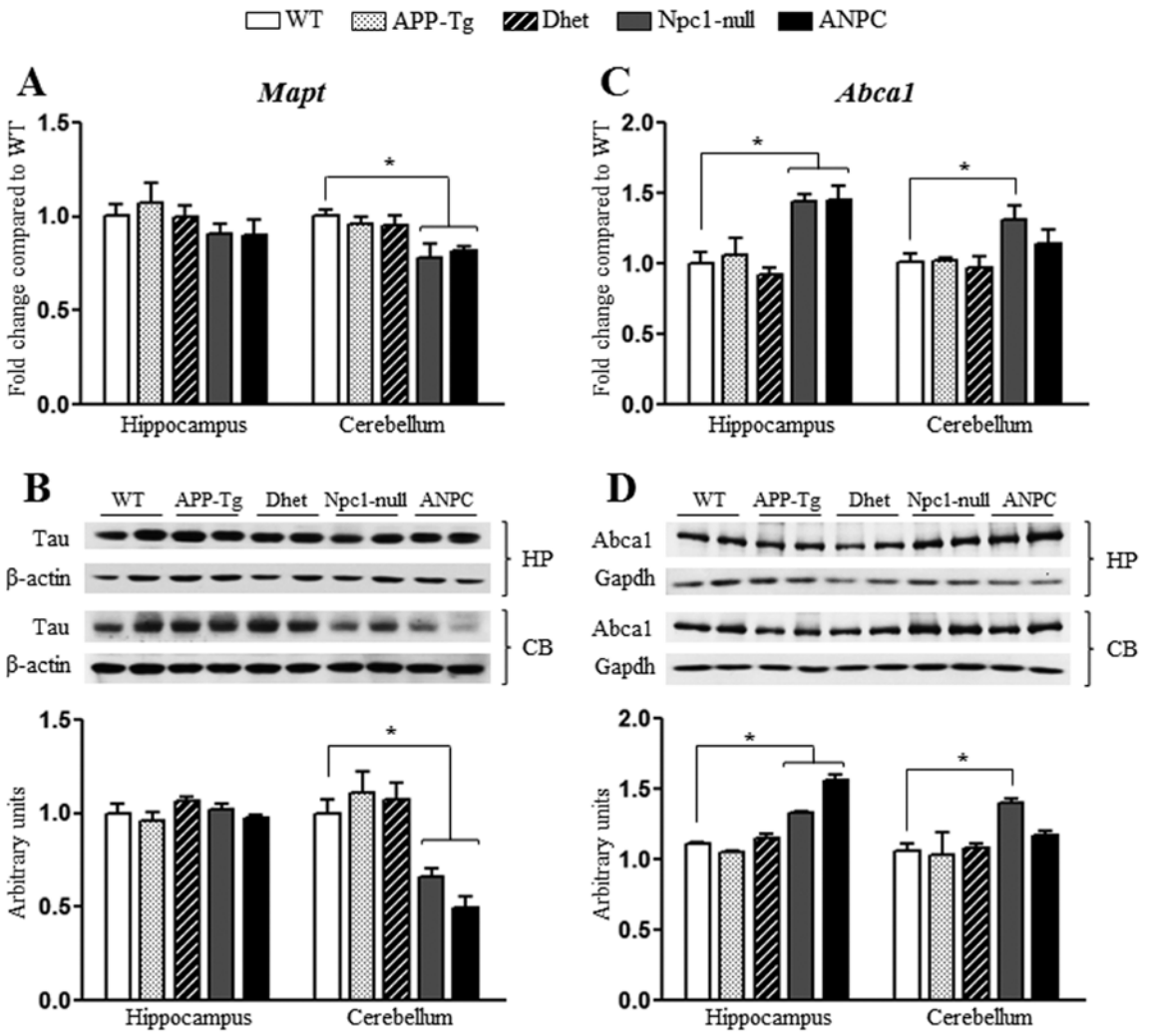

Figure 2.6: Expression levels of tau (**A**, **B**) and Abca1 (**C**, **D**) in the hippocampus and cerebellum of five lines of mice. **(A)** Histograms showing decreased *Mapt* mRNA (encoding tau) level in the cerebellum but not in hippocampus of Npc1-null and ANPC mice compared with WT mice as obtained using RT^2 Mouse Custom Profiler PCR array. **(B)** Immunoblots and respective histograms validating the decreased levels of tau in the cerebellum of Npc1-null and ANPC mice compared with age-matched WT. **(C)** Histograms showing increased *Abca1* mRNA level in the hippocampus of Npc1-null and ANPC mice and in the cerebellum of Npc1-null mice compared with WT as obtained using RT^2 Mouse Custom Profiler PCR array. **(D)** Immunoblotting performed to validate data obtained by PCR arrays revealed significant up-regulations in the Abca1 protein level in Npc1-null and ANPC mice in the respective brain regions compared with WT mice. The protein levels of tau and Abca1 were normalized to the β-actin and Gapdh respectively, and the values (n = 4 animals per genotype) are expressed as means ± SEM. *, $p < 0.05$.

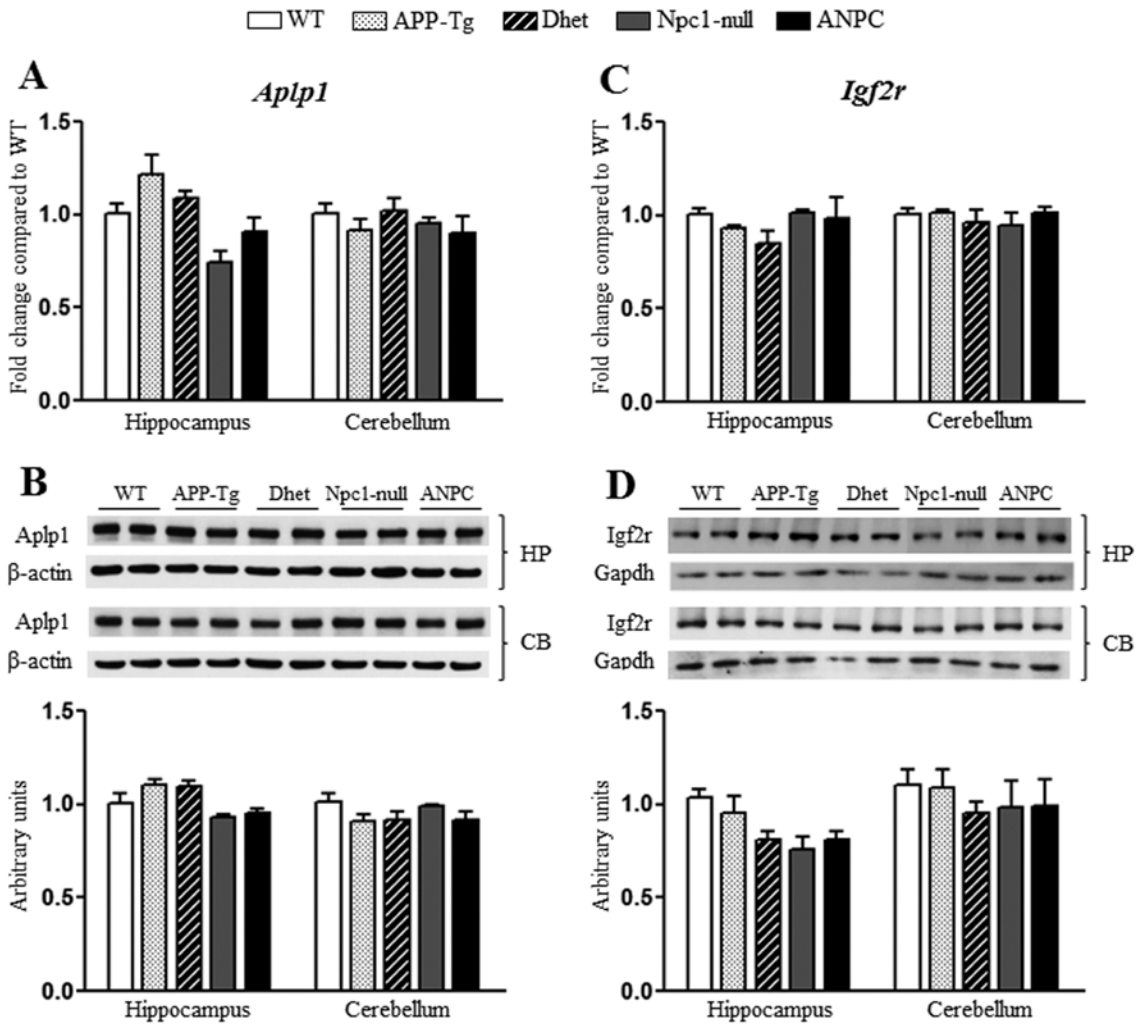

Figure 2.7: Expression levels of Aplp1 (**A**, **B**) and Igf2r (**C**, **D**) in the hippocampus and cerebellum of five lines of mice. **(A, C)** Histograms showing no significant alteration in *Aplp1* (**A**) and *Igf2r* (**C**) mRNA levels in the hippocampus and cerebellum of APP-Tg, Dhet, Npc1-null and ANPC mice compared with the WT mice as obtained using RT^2 Mouse Custom Profiler PCR array. **(B, D)** Immunoblots and respective histograms showing no significant alteration in Aplp1 (**B**) and Igf2r (**D**) protein levels in the hippocampus or cerebellum of the different genotype combinations compared with the WT mice consistent with the transcript levels. The protein levels of Aplp1 and Igf2r were normalized to the β-actin and Gapdh respectively, and the values (n = 4 animals per genotype) are expressed as means ± SEM. *, $p < 0.05$.

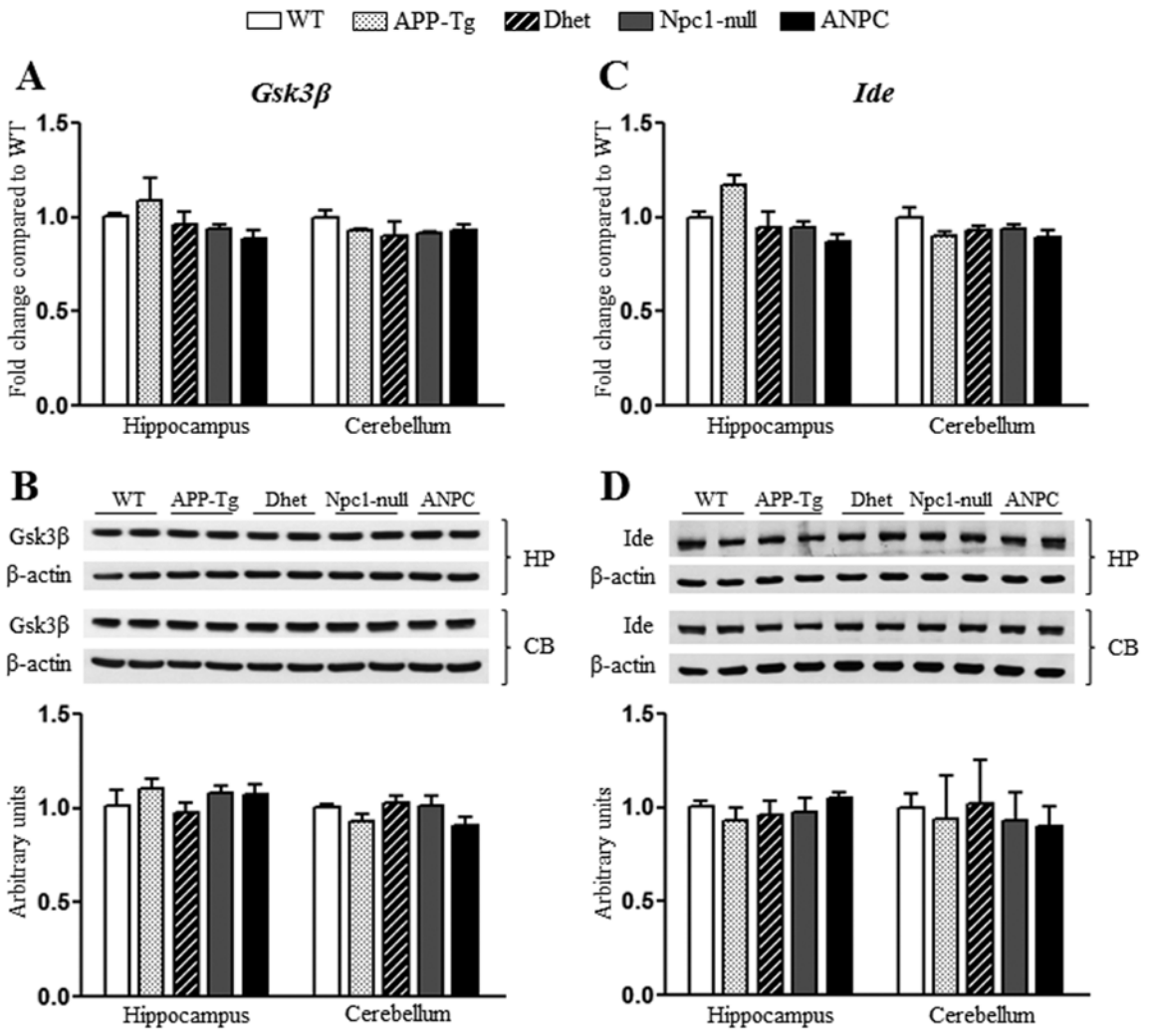

Figure 2.8: Expression levels of Gsk3β (**A**, **B**) and Ide (**C**, **D**) in the hippocampus and cerebellum of five lines of mice. **(A, C)** Histograms showing no significant alteration in *Gsk3β* (**A**) and *Ide* (**C**) mRNA levels in the hippocampus and cerebellum of APP-Tg, Dhet, Npc1-null and ANPC mice compared with the WT mice as obtained using RT^2 Mouse Custom Profiler PCR array. **(B, D)** Immunoblots and respective histograms showing no significant alteration in Gsk3β (**B**) and Ide (**D**) protein levels in the hippocampus or cerebellum of the different genotype combinations compared with the WT mice consistent with the transcript levels. The protein levels of Gsk3β and Ide were normalized to β-actin and the values (n = 4 animals per genotype) are expressed as means ± SEM. *, $p < 0.05$.

2.4 Discussion

The present study demonstrates several genes as evident by RT^2 Profiler PCR arrays are selectively altered in the brains of ANPC, Npc1-null, APP-Tg and Dhet mice compared to WT mouse brains. While the Npc1-null and ANPC mice showed marked alterations in the expression profiles of multiple genes, the changes in APP-Tg and Dhet mice were limited to only few genes in both the hippocampus and cerebellum compared to WT mice. Interestingly, ANPC and Npc1-null mice, with the exception of a few genes, exhibited more or less similar changes, although more genes were differentially expressed in the affected cerebellar region than the relatively spared hippocampal formation. The altered gene profiles were found to match with the corresponding alterations in the protein levels. Collectively, these results suggest that intracellular cholesterol accumulation due to Npc1 deficiency can alter the expression of certain genes in selected brain regions, which may be involved either directly or indirectly in NPC pathogenesis, whereas transgenic expression of mutant human APP in Npc1-null background exacerbates pathology mostly by amplifying the observed changes that are already altered by Npc1-deficiency rather than instigating expression of additional genes.

Our analysis of gene profiles is validated by two lines of evidence. First, the genes that are known to be enhanced by Npc1-deficiency such as *Npc2*, *Abca1* and *Ctsb* were found to be up-regulated in our experiments (23). Second, the altered gene profiles exhibited corresponding changes in the levels of proteins. Nevertheless, it is important to note that the absolute fold changes in the level of a specific transcript need not be highly altered to have a significant consequence on cell physiology. Additionally, post-translational modification of proteins can have an important role in regulating neuropathology and phenotype of a mouse line. Given the evidence from earlier reports (14, 24), it is likely that some of the changes observed in the present study such as increased cathepsin B and cathespin D levels may underlie the cause rather than be a consequence of disease pathology.

***Cholesterol metabolism*:** As a major component of the cell membrane, cholesterol plays a key role in fluidity and ion permeability which in turn regulates a multitude of vesicular

trafficking steps and intracellular signaling events that are crucial for neuronal differentiation, growth and survival (25). Cytoplasmic cholesterol, on the other hand, can serve as a precursor for steroid hormones, vitamin D and oxysterols (26). The special need for cholesterol for normal neuronal function is apparent from two distinct lines of evidence: i) brain contains the highest amount of total cholesterol/gm tissue in the body (27) and ii) the cholesterol content of the brain is derived primarily from *de novo* synthesis (27, 28). Under normal conditions, brain cholesterol levels are tightly regulated by a number of mechanisms including synthesis, transport, uptake, storage and efflux of cholesterol. At the transcriptional level, sterol regulatory element-binding proteins regulate the expression profiles of multiple genes that are involved in monitoring the synthesis and uptake of cholesterol, fatty acids and phoshpholipids (29). With adequate cholesterol in the endoplasmic reticulum, genes involved in cholesterol synthesis and uptake are not activated by sterol regulatory element-binding proteins. Npc1-deficient cells do not to respond to the accumulation of unesterified cholesterol in the EL system, thus LDL receptor expression is not down-regulated and uptake of LDL-mediated cholesterol continues (30). Our RT^2 Profiler PCR array data reflect the dysregulation of cholesterol metabolism as we observed an up-regulation of *Apoe, Clu, Cyp46a1, Srebf1* and *Npc2* in the cerebellum and *Apoe, Abca1* and *Npc2* in the hippocampus of both Npc1-null and ANPC mice. There is evidence of selective up-regulation of *Abca1* in the cerebellum and down-regulation of *Dhcr24* in the hippocampus of Npc1-null mice. Consistent with the transcripts levels, we observed up-regulation of Abca1, Npc2 and Apoe in the cerebellum as well as hippocampus of ANPC and Npc1-null mice compared to WT mice by immunoblot analysis. The hippocampus of APP-Tg mice also showed increased expression of *Acat2, Fdps, Sqle* and *Dhcr24,* which may relate to alterations in the intracellular cholesterol homeostasis as a consequence of APP overexpression.

***APP and Aβ metabolisms*:** A number of recent studies have shown that NPC disease exhibits some striking parallels with AD pathology including i) the presence of tau-positive neurofibrillary tangles (4, 5), ii) the influence of ε4 isoform APOE in promoting disease pathology (6, 31), and iii) endosomal abnormalities associated with the accumulation of cleaved APP derivatives and/or Aβ peptides in vulnerable neurons (9,

32). However, consistent with previous analysis of NPC1-deficient human fibroblasts (23) and Npc1-deficient mouse cells (33), we did not observe any difference in the mRNA profiles of α-secretase (i.e., *Adam 10* and *Adam 17*), β-secretase (*Bace1* and *Bace2*) or most components of the γ-secretase complex (i.e., *Psen1*, *Psen2*, *Nicastrin*, *Pen2* and *Aph1a*) either in Npc1-null or ANPC mouse brains compared to WT mice. Only *Aph1b* showed down-regulation in the cerebellum of Npc1-null and ANPC mice, the significance of which remains to be established. At the protein level, no alteration was evident in the components of APP processing pathways, except increased levels of nicastrin and presenilin 1 which may relate to activity of the γ-secretase complex or other functions of these proteins in the cells (20, 34, 35). Interestingly, the levels of transcripts (i.e, *A2m*, *Plat*, *Plau* and *Mme*) and some of the corresponding proteins (i.e., neprilysin), which are known to be involved in the clearance of Aβ peptides (36, 37), were significantly up-regulated in the cerebellum of Npc1-null and ANPC mice. These results suggest that cholesterol accumulation may influence the clearance of Aβ peptides. However, we did not observe an alteration in the expression of *Ide*, which codes for one of the major enzymes involved in degradation of extracellular Aβ, either in ANPC or Npc1-null mouse brains. Thus, it remains to be determined whether increased expression of *A2m*, *Plat*, *Plau* and *Mme* is directly associated with degradation of Aβ or other proteins in Npc1-null and ANPC mice.

The formation of neurofibrillary tangles resulting from phosphorylation of tau protein, encoded by the *Mapt* gene, has been implicated in the loss of neurons in many taupathies including NPC and AD (38). Our results showed down-regulation of *Mapt* transcript in the cerebellum but not in the hippocampus of ANPC and Npc1-null mice as compared with WT mice. This corresponds rather well with the steady-state levels of tau protein observed by Western blot analysis. Since partial or complete loss of tau expression can reduce the life-span and exacerbate pathology (39) and inhibition of tau phosphorylation can attenuate the phenotype (40) in Npc1-null mice, it is likely that alterations in total tau levels in the cerebellum of ANPC and Npc1-null mice may be involved in the loss of neurons and the development of pathology associated with these mice.

***Altered trafficking*:** Cholesterol accumulation in NPC1-deficient cells has been shown to interfere with the transport of proteins between various cellular compartments. Consequently, proteins involved in membrane trafficking including those regulating biogenesis/function of lysosomes are up-regulated to compensate for the defects (41, 42). In keeping with these data, we observed a significant increase in the expression of genes encoding lysosomal enzymes such as *Ctsb*, *Ctsd* and *Gusb*, both at transcript and protein levels, in the Npc1-null and ANPC mouse brains. This is consistent with earlier studies, which reported elevated levels of cathepsin B and cathepsin D in NPC1-deficient cells as well as Npc1-null and ANPC mouse brains (14, 20, 23, 43, 44). These enzymes not only mediate the clearance of proteins but also regulate neuronal viability following their release into the cytosol. However, unlike the previous studies (23) we did not observe alterations in the levels of mRNA encoding *Igf2r*, which is involved in the trafficking of the lysosomal enzymes, either in Npc1-null or ANPC mouse brains. Additionally, we did not detect alterations in the expression of transcripts encoding Rab GTPase such as *Rab5*, *Rab7* and *Rab9* that are known to act as general regulators of membrane trafficking in the endosomal pathway (45, 46). Other components involved in the vesicular movement such as *Klc2*, *Kif1c* and *Anx6* were differentially down-regulated in the Npc1-null and ANPC mice, but not in APP-Tg or Dhet mouse brains, possibly as a consequence of the defects triggered by intracellular cholesterol accumulation.

***Cell death/survival pathways*:** Although the APP-Tg mouse model used in our study does not exhibit any overt loss of neurons (21, 22), there is evidence of neuronal loss in the cerebellum of Npc1-null mice (15, 17). Additionally, we showed that ANPC mice exhibited more severe loss of neurons than Npc1-null mice, thus suggesting that overexpression of APP may exacerbate neurodegeneration (20). At present, the mechanisms underlying selective degeneration of neurons remain unclear as events related to both apoptosis and autophagy have been observed in Npc1-null mouse brains (2, 44, 47, 48). The results of our study did not reveal any alterations in the expression of genes such as *Atg5*, *Atg7*, *Atg12*, *Becn1*, *Bcl2*, *Casp3* or *Bax*, which are known to regulate autophagy or apoptosis pathways, either in Npc1-null or ANPC mouse brains. The affected cerebellar region, however, showed a marked up-regulation of *Bid* and

Pmaip1 in both Npc1-null and ANPC mice, whereas expression of *Shisa5* was up-regulated only in Npc1-null mice. Although the significance of the differential expression of these genes remains to be established, we have recently reported that increased cytosolic levels of lysosomal enzymes resulting from lysosomal destabilization, such as cathepsin B and cathepsin D, as well as altered levels, phosophorylation and cleavage of tau protein, may be involved in triggering cell death *via* a caspase-dependent pathway in Npc1-null and ANPC mouse brains (14, 20). This is consistent with the up-regulation of *Ctsb* and *Ctsd*, and down-regulation of *Mapt* transcripts and their corresponding protein levels observed in the cerebellum of Npc1-null and ANPC mouse brains compared with WT mice.

***Conclusions*:** The present study reveals that the gene expression profile is differentially altered in APP-Tg, Dhet, Npc1-null and ANPC mouse brains when compared to WT mice. These changes are found to be more striking in Npc1-null and ANPC mice, which exhibit more severe pathology than APP-Tg or Dhet mice. Additionally, the changes in Npc1-null and ANPC mice were more pronounced in the affected cerebellar region than the relatively spared hippocampus.

2.5 References

1. Mukherjee, S. and Maxfield, F.R. (2004) Lipid and cholesterol trafficking in NPC. *Biochim Biophys Acta,* 1685, 28-37.

2. Pacheco, C.D. and Lieberman, A.P. (2008) The pathogenesis of Niemann-Pick type C disease: a role for autophagy? *Expert Rev Mol Med,* 10, e26.

3. Vanier, M.T. and Suzuki, K. (1998) Recent advances in elucidating Niemann-Pick C disease. *Brain Pathol,* 8, 163-174.

4. Auer, I.A., Schmidt, M.L., Lee, V.M., Curry, B., Suzuki, K., Shin, R.W., Pentchev, P.G., Carstea, E.D. and Trojanowski, J.Q. (1995) Paired helical filament tau (PHFtau) in Niemann-Pick type C disease is similar to PHFtau in Alzheimer's disease. *Acta Neuropathol,* 90, 547-551.

5. Ohm, T.G., Treiber-Held, S., Distl, R., Glockner, F., Schonheit, B., Tamanai, M. and Meske, V. (2003) Cholesterol and tau protein--findings in Alzheimer's and Niemann Pick C's disease. *Pharmacopsychiatry,* 36 Suppl 2, S120-126.

6. Saito, Y., Suzuki, K., Nanba, E., Yamamoto, T., Ohno, K. and Murayama, S. (2002) Niemann-Pick type C disease: accelerated neurofibrillary tangle formation and amyloid beta deposition associated with apolipoprotein E epsilon 4 homozygosity. *Ann Neurol,* 52, 351-355.

7. Nelson, P.T., Braak, H. and Markesbery, W.R. (2009) Neuropathology and cognitive impairment in Alzheimer disease: a complex but coherent relationship. *J Neuropathol Exp Neurol,* 68, 1-14.

8. Selkoe, D.J. (2008) Biochemistry and molecular biology of amyloid beta-protein and the mechanism of Alzheimer’s disease. In *Handb Clin Neurol* Vol. 89, pp. 245-260.

9. Jin, L.W., Shie, F.S., Maezawa, I., Vincent, I. and Bird, T. (2004) Intracellular accumulation of amyloidogenic fragments of amyloid-beta precursor protein in neurons with Niemann-Pick type C defects is associated with endosomal abnormalities. *Am J Pathol,* 164, 975-985.

10. Mattsson, N., Zetterberg, H., Bianconi, S., Yanjanin, N.M., Fu, R., Mansson, J.E., Porter, F.D. and Blennow, K. (2011) Gamma-secretase-dependent amyloid-beta is increased in Niemann-Pick type C: a cross-sectional study. *Neurology,* 76, 366-372.

11. Canevari, L. and Clark, J.B. (2007) Alzheimer's disease and cholesterol: the fat connection. *Neurochem Res,* 32, 739-750.

12. Hartmann, T. (2001) Cholesterol, Abeta and Alzheimer's disease. *Trends Neurosci,* 24, S45-48.

13. Martins, I.J., Berger, T., Sharman, M.J., Verdile, G., Fuller, S.J. and Martins, R.N.

(2009) Cholesterol metabolism and transport in the pathogenesis of Alzheimer's disease. *J Neurochem*, 111, 1275-1308.

14. Amritraj, A., Peake, K., Kodam, A., Salio, C., Merighi, A., Vance, J.E. and Kar, S. (2009) Increased activity and altered subcellular distribution of lysosomal enzymes determine neuronal vulnerability in Niemann-Pick type C1-deficient mice. *Am J Pathol*, 175, 2540-2556.

15. German, D.C., Quintero, E.M., Liang, C.L., Ng, B., Punia, S., Xie, C. and Dietschy, J.M. (2001) Selective neurodegeneration, without neurofibrillary tangles, in a mouse model of Niemann-Pick C disease. *J Comp Neurol*, 433, 415-425.

16. Loftus, S.K., Morris, J.A., Carstea, E.D., Gu, J.Z., Cummings, C., Brown, A., Ellison, J., Ohno, K., Rosenfeld, M.A., Tagle, D.A. *et al.* (1997) Murine model of Niemann-Pick C disease: mutation in a cholesterol homeostasis gene. *Science*, 277, 232-235.

17. Paul, C.A., Boegle, A.K. and Maue, R.A. (2004) Before the loss: neuronal dysfunction in Niemann-Pick Type C disease. *Biochim Biophys Acta*, 1685, 63-76.

18. Kodam, A., Maulik, M., Peake, K., Amritraj, A., Vetrivel, K.S., Thinakaran, G., Vance, J.E. and Kar, S. (2010) Altered levels and distribution of amyloid precursor protein and its processing enzymes in Niemann-Pick type C1-deficient mouse brains. *Glia*, 58, 1267-1281.

19. Li, H., Repa, J.J., Valasek, M.A., Beltroy, E.P., Turley, S.D., German, D.C. and Dietschy, J.M. (2005) Molecular, anatomical, and biochemical events associated with neurodegeneration in mice with Niemann-Pick type C disease. *J Neuropathol Exp Neurol*, 64, 323-333.

20. Maulik, M., Ghoshal, B., Kim, J., Wang, Y., Yang, J., Westaway, D. and Kar, S. (2012) Mutant Human APP Exacerbates Pathology in a Mouse Model of NPC and its Reversal by a beta-cyclodextrin. *Hum Mol Genet*, 21, 4857-4875.

21. Chishti, M.A., Yang, D.S., Janus, C., Phinney, A.L., Horne, P., Pearson, J., Strome, R., Zuker, N., Loukides, J., French, J. *et al.* (2001) Early-onset amyloid deposition and cognitive deficits in transgenic mice expressing a double mutant form of amyloid precursor protein 695. *J Biol Chem*, 276, 21562-21570.

22. Adalbert, R., Nogradi, A., Babetto, E., Janeckova, L., Walker, S.A., Kerschensteiner, M., Misgeld, T. and Coleman, M.P. (2009) Severely dystrophic axons at amyloid plaques remain continuous and connected to viable cell bodies. *Brain*, 132, 402-416.

23. Reddy, J.V., Ganley, I.G. and Pfeffer, S.R. (2006) Clues to neuro-degeneration in Niemann-Pick type C disease from global gene expression profiling. *PLoS One*, 1, e19.

24. Xie, X., Brown, M.S., Shelton, J.M., Richardson, J.A., Goldstein, J.L. and Liang, G. (2011) Amino acid substitution in NPC1 that abolishes cholesterol binding reproduces phenotype of complete NPC1 deficiency in mice. *Proc Natl Acad Sci U S A*, 108, 15330-15335.

25. Pfrieger, F.W. (2003) Cholesterol homeostasis and function in neurons of the central nervous system. *Cell Mol Life Sci*, 60, 1158-1171.

26. Martin, M., Dotti, C.G. and Ledesma, M.D. (2010) Brain cholesterol in normal and pathological aging. *Biochim Biophys Acta*, 1801, 934-944.

27. Dietschy, J.M. and Turley, S.D. (2004) Thematic review series: brain Lipids. Cholesterol metabolism in the central nervous system during early development and in the mature animal. *J Lipid Res*, 45, 1375-1397.

28. Bjorkhem, I. and Meaney, S. (2004) Brain cholesterol: long secret life behind a barrier. *Arterioscler Thromb Vasc Biol*, 24, 806-815.

29. Horton, J.D. (2002) Sterol regulatory element-binding proteins: transcriptional activators of lipid synthesis. *Biochem Soc Trans*, 30, 1091-1095.

30. Liscum, L. and Faust, J.R. (1987) Low density lipoprotein (LDL)-mediated suppression of cholesterol synthesis and LDL uptake is defective in Niemann-Pick type C fibroblasts. *J Biol Chem*, 262, 17002-17008.

31. Kim, J., Basak, J.M. and Holtzman, D.M. (2009) The role of apolipoprotein E in Alzheimer's disease. *Neuron*, 63, 287-303.

32. Nixon, R.A. (2004) Niemann-Pick Type C disease and Alzheimer's disease: the APP-endosome connection fattens up. *Am J Pathol*, 164, 757-761.

33. Runz, H., Rietdorf, J., Tomic, I., de Bernard, M., Beyreuther, K., Pepperkok, R. and Hartmann, T. (2002) Inhibition of intracellular cholesterol transport alters presenilin localization and amyloid precursor protein processing in neuronal cells. *J Neurosci*, 22, 1679-1689.

34. Zhang, Y.W., Luo, W.J., Wang, H., Lin, P., Vetrivel, K.S., Liao, F., Li, F., Wong, P.C., Farquhar, M.G., Thinakaran, G. *et al.* (2005) Nicastrin is critical for stability and trafficking but not association of other presenilin/gamma-secretase components. *J Biol Chem*, 280, 17020-17026.

35. Zhao, G., Liu, Z., Ilagan, M.X. and Kopan, R. (2010) Gamma-secretase composed of PS1/Pen2/Aph1a can cleave notch and amyloid precursor protein in the absence of nicastrin. *J Neurosci*, 30, 1648-1656.

36. Eckman, E.A. and Eckman, C.B. (2005) Abeta-degrading enzymes: modulators of Alzheimer's disease pathogenesis and targets for therapeutic intervention. *Biochem Soc Trans*, 33, 1101-1105.

37. Miners, J.S., Baig, S., Palmer, J., Palmer, L.E., Kehoe, P.G. and Love, S. (2008) Abeta-degrading enzymes in Alzheimer's disease. *Brain Pathol,* 18, 240-252.

38. Morris, M., Maeda, S., Vossel, K. and Mucke, L. (2011) The many faces of tau. *Neuron,* 70, 410-426.

39. Pacheco, C.D., Elrick, M.J. and Lieberman, A.P. (2009) Tau deletion exacerbates the phenotype of Niemann-Pick type C mice and implicates autophagy in pathogenesis. *Hum Mol Genet,* 18, 956-965.

40. Zhang, M., Li, J., Chakrabarty, P., Bu, B. and Vincent, I. (2004) Cyclin-dependent kinase inhibitors attenuate protein hyperphosphorylation, cytoskeletal lesion formation, and motor defects in Niemann-Pick Type C mice. *Am J Pathol,* 165, 843-853.

41. Ganley, I.G. and Pfeffer, S.R. (2006) Cholesterol accumulation sequesters Rab9 and disrupts late endosome function in NPC1-deficient cells. *J Biol Chem,* 281, 17890-17899.

42. Karten, B., Peake, K.B. and Vance, J.E. (2009) Mechanisms and consequences of impaired lipid trafficking in Niemann-Pick type C1-deficient mammalian cells. *Biochim Biophys Acta,* 1791, 659-670.

43. Cluzeau, C.V., Watkins-Chow, D.E., Fu, R., Borate, B., Yanjanin, N., Dail, M.K., Davidson, C.D., Walkley, S.U., Ory, D.S., Wassif, C.A. *et al.* (2012) Microarray expression analysis and identification of serum biomarkers for Niemann-Pick disease, type C1. *Hum Mol Genet,* 21, 3632-3646.

44. Liao, G., Yao, Y., Liu, J., Yu, Z., Cheung, S., Xie, A., Liang, X. and Bi, X. (2007) Cholesterol accumulation is associated with lysosomal dysfunction and autophagic stress in Npc1 -/- mouse brain. *Am J Pathol,* 171, 962-975.

45. Li, G. (2011) Rab GTPases, membrane trafficking and diseases. *Curr Drug Targets,* 12, 1188-1193.

46. Pfeffer, S.R. (2007) Unsolved mysteries in membrane traffic. *Annu Rev Biochem,* 76, 629-645.

47. Alvarez, A.R., Klein, A., Castro, J., Cancino, G.I., Amigo, J., Mosqueira, M., Vargas, L.M., Yevenes, L.F., Bronfman, F.C. and Zanlungo, S. (2008) Imatinib therapy blocks cerebellar apoptosis and improves neurological symptoms in a mouse model of Niemann-Pick type C disease. *FASEB J,* 22, 3617-3627.

48. Wu, Y.P., Mizukami, H., Matsuda, J., Saito, Y., Proia, R.L. and Suzuki, K. (2005) Apoptosis accompanied by up-regulation of TNF-alpha death pathway genes in the brain of Niemann-Pick type C disease. *Mol Genet Metab,* 84, 9-17.

Chapter 3: Mutant Human APP Exacerbates Pathology in a Mouse Model of NPC and its Reversal by a β-Cyclodextrin

A version of this chapter has been published. Maulik M, Ghoshal B, Kim J, Wang Y, Yang J, Westaway D and Kar S (2012) Hum Mol Genet, 21: 4857-4875.

3.1 Introduction

Niemann-Pick type C (NPC) disease is an autosomal recessive neurovisceral disorder characterized by abnormal accumulation of unesterified cholesterol and glycosphingolipids within the endosomal-lysosomal system in a number of tissues including the brain. These defects in cholesterol sequestration trigger widespread neurological deficits such as ataxia, seizures and dementia that eventually lead to premature death (1, 2). In majority of the cases, NPC disease is caused by loss-of-function mutations in the *NPC1* gene, which encodes a transmembrane glycoprotein implicated in the intracellular transport of cholesterol (3, 4). Neuropathologically, NPC is characterized by the accumulation of unesterified cholesterol, activation of glial cells and presence of intracellular tau-positive neurofibrillary tangles (NFTs). Loss of neurons is evident primarily in the prefrontal cortex, thalamus and cerebellum but not in the hippocampus (5, 6). Some studies have also shown that levels of β-amyloid (Aβ)-related peptides are increased in the vulnerable brain regions (7) as well as cerebrospinal fluid (8), while extracellular deposition of the peptide was apparent in patients with ε4 genotype of apolipoprotein E (APOE), which serves as a protein carrier for cholesterol (9). Interestingly, Balb/cNctr-Npc$^{N/N}$ mice due to spontaneous mutations in the *Npc1* gene (Npc1-null) are found to recapitulate most of the human pathology excepting for the formation of NFTs (10, 11).

A number of recent studies have shown that NPC disease exhibits some intriguing parallels with the Alzheimer's disease (AD), the most common type of senile dementia affecting elderly people. Neuropathologically, AD is characterized by the presence of NFTs, Aβ-containing neuritic plaques, gliosis and the loss of neurons primarily in the hippocampus, cortex and certain subcellular nuclei such as basal forebrain cholinergic neurons (12-14). The pathological changes observed in AD brains are believed to be triggered by *in vivo* accumulation of Aβ peptide derived from amyloid precursor protein (APP). The AD pathology, unlike NPC disease, is not associated with widespread intracellular accumulation of free cholesterol or loss of neurons in the cerebellum. Additionally, development of AD which occurs mostly after 65 years of age does not lead to ataxia as observed in NPC disease (2, 6, 13, 14). Notwithstanding the differences, the

striking parallels that exist between AD with NPC include: i) the presence of structurally and immunologically similar tau-positive NFTs (15, 16), ii) influence of ε4 isoform of APOE in promoting disease pathology (9, 17, 18), and iii) endosomal abnormalities associated with accumulation of cleaved APP and/or Aβ peptides in vulnerable neurons (19). Recently, alteration of NPC1 mRNA/protein has been reported in vulnerable regions of AD brains indicating a functional link between NPC1 dysfunction and AD (20). Although cholesterol is not sequestered in AD as observed in NPC pathology, there is evidence that high cholesterol levels increase the risk of AD (21, 22) and neurons bearing NFTs exhibit higher levels of free cholesterol in AD brains (23). Many lines of experimental evidence further suggest that alteration in cholesterol homeostasis can influence APP metabolism, whereas changes in the levels/expression of APP can also lead to altered cholesterol metabolism (24-27). A*lbeit* these results suggest convergence of factors regulating NPC and AD pathologies, very little is currently known about the interaction between the NPC1 and APP.

Transgenic mice overexpressing mutant APP are known to recapitulate amyloid deposits and spatial learning deficits but do not exhibit overt loss of neurons as seen in AD brains (28-31). Earlier studies have shown that up-regulating cholesterol levels can exacerbate behavior and cellular pathology, whereas decreasing cholesterol levels can have the opposite effects in these mice (24, 27). However, it remains unclear how APP overexpression can influence behavior and pathological features, particularly the tau-pathology and neurodegeneration that lie downstream of altered APP and cholesterol metabolism, in Npc1-null mice. We addressed this issue by using a new line of bigenic ANPC mice generated by crossing mutant human APP transgenic mice (29) with heterozygous Npc1-deficient mice (32). Our results clearly show that overexpression of APP in the presence of intracellular cholesterol accumulation can decrease longevity, accelerate the onset of behavioral abnormalities and exacerbate glial pathology as well as degeneration of neurons that show preferential vulnerability to cholesterol accumulation in NPC disease. To establish the significance of cholesterol, we treated ANPC mice with the sterol binding agent 2-hydroxypropyl-β-cyclodextrin (2-HPC) that has been shown to promote movement of the sequestered cholesterol from lysosomes to the metabolically

active pool in various experimental paradigms (33-35). Our results clearly reveal that dispersal of cholesterol by 2-HPC treatment can not only prolong the lifespan but also can significantly reverse the behavioral and pathological abnormalities in ANPC mice, thus providing a strong functional link between APP and NPC1 genes that may interact in regulating both AD and NPC pathologies.

3.2 Materials and Methods

Materials: 4-20% Tris-Glycine gels, 4-12% NuPAGE Bis-Tris gels, NeuroTrace red fluorescent Nissl stain (BrainStain^{TM} Imaging Kit), Alexa Fluor 488/594 conjugated secondary antibodies and ProLong Gold antifade reagent were all purchased from Life Technologies. The DNA isolation kit and Qproteome cell compartment kit were from Qiagen Inc. Filipin, the cathepsin D assay kit and 2-HPC (product H107) were obtained from Sigma-Aldrich, Inc. The bicinchoninic acid (BCA) protein assay kit and enhanced chemiluminescence (ECL) kit were obtained from ThermoFisher Scientific. Sources of all the primary antibodies used in the study are listed in Table 3.1. All horseradish peroxidase (HRP)-conjugated secondary antibodies were purchased from Santa Cruz Biotechnology, Inc. All other chemicals were from Sigma-Aldrich or ThermoFisher Scientific.

Generation of Transgenic mice: Mutant human $APP_{KM670/671NL+V717F}$ transgenic mice (APP-Tg) maintained on a C3H/C57BL6 background (29) were obtained from our breeding colony. Heterozygous Npc1-deficient ($Npc1^{+/-}$) mice (32) maintained on a BALB/c background were purchased from Jackson Laboratories. Mutant APP-Tg mice were first crossed to $Npc1^{+/-}$ mice to produce $APP^{+/0}Npc1^{+/-}$ and $APP^{0/0}Npc1^{+/-}$ off-springs. These two lines of mice were subsequently crossed to generate the following five lines of mice: bigenic $APP^{+/0}Npc1^{-/-}$ (ANPC), $APP^{+/0}Npc1^{+/+}$ (APP-Tg), $APP^{0/0}Npc1^{-/-}$ (Npc1-null), $APP^{+/0}Npc1^{+/-}$ (double heterozygous: Dhet) and $APP^{0/0}Npc1^{+/+}$ (wild-type: WT), all on a C3H/C57BL6/BALB/c background. Animals of different genotypes used in a given experiment were obtained from the same breeding pairs. All animals, maintained on a 12 h light/dark cycle, were bred and housed with access to food and water *ad libitum*. The probability of survival was determined by the Kaplan-Meier technique using GraphPad Prism software. The maintenance of the breeding colony and the experiments involving these animals were performed in accordance with Institutional and Canadian Council on Animal Care guidelines. All transgenic mice were identified by a unique ear notching pattern and genotyped by PCR analysis of tail DNA as described earlier (29, 32).

Behavioral tests: WT, APP-Tg, Dhet, Npc1-null and ANPC mice were examined at 4, 7 and 10 weeks of age for their object recognition memory and sensorimotor performance as described earlier (36). All these mice were generated from the same breeding on a C3H/C57BL6/BALB/c background thus making it likely that behavioral changes observed in any of these lines may be associated with altered expression of APP and/or Npc1 rather than to the background strains. For the object recognition memory test, mice were first habituated for five consecutive days and on the sixth day their exploratory behavior towards a familiar and novel object was quantified using a memory index (MI), wherein "t_o" represents time exploring an object during the original exposure and "t_n" represents time spent exploring an object that is novel on re-exposure: MI = $(t_n - t_o)/ (t_n + t_o)$. The motor function of mice from different genotypes was tested by measurement of latency to fall from a Rotamex-5 accelerating rotarod (Columbus Instruments). All mice were examined 5 min each 4 times per day with an inter-trial interval of 30 min for five consecutive days. A score of 300 s was assigned to a mouse that stayed on the rod for the full 5 min test period. Gait analysis of the animals was done from their footprints as described earlier (37). Stride lengths and hind limb widths were measured manually as the distance between two paw prints. Mice of different genotypes were also tested for their open-field activity over a 5-min test session. Durations of walking, pausing and rearing were analyzed as indices of spontaneous locomotor activity as described earlier (36).

Cellular cholesterol Assay: Hippocampus and cerebellum of 4-, 7- and 10-week mice of all five genotypes (n = 4 per genotype/age group) were homogenized and mass of cholesterol was determined using gas-liquid chromatography as described earlier (38).

***Histology and Immunohistochemistry*:** WT, APP-Tg, Dhet, Npc1-null and ANPC mice of 4-, 7- and 10-weeks (n = 4-5 per genotype/age group) were transcardially perfused and fixed in 4% paraformaldehyde. Brains were sectioned on a cryostat (20 μm) and then processed as described earlier (5). To determine cholesterol accumulation, brain sections from all five genotypes were incubated with 25 μg/ml of filipin in PBS for 30 min in the dark under agitation (5). For immunohistochemistry, sections were incubated overnight at 4^oC with the anti-GFAP, anti-Iba1, anti-CNPase, anti-Calbindin-D-28k, anti-cleaved

caspase 3 or anti-Tau, caspase cleaved antibodies at dilutions listed in Table 3.1. Subsequently, sections were incubated with appropriate HRP-conjugated secondary antibodies (1:400) for enzyme-linked immunohistochemistry or Alexa Fluor 488/594 conjugated secondary antibodies (1:1000) for immunofluorescence methods. Immunostained sections were examined and photographed using a Zeiss Axioskop-2 microscope (Carl Zeiss Canada Ltd.).

Neuronal cell counting: For neuronal quantification, every sixth section from the hippocampus and cerebellum of 7 week old mice of different genotypes were used (n = 3-4 per genotype). Hippocampal sections were stained with NeuroTrace 530/616 red fluorescent Nissl stain (1:300), whereas cerebellar Purkinje cells were labeled using anti-calbindin D-28k antiserum as mentioned above. Cell counts were normalized to the CA1 area or the Purkinje layer length and expressed as neuronal density as described earlier (39).

Western blotting: Hippocampal and cerebellar brain regions were homogenized in ice-cold RIPA lysis buffer and protein content was determined using a BCA protein assay kit as described earlier (5). Equal amounts of protein samples were separated on 4-20% Tris-Glycine gels or 4-12% NuPAGE Bis-Tris gels and transferred to nitrocellulose membranes, blocked with 5% non-fat milk and then incubated overnight at 4^{o}C with either anti-APP, anti-NPC1, anti-GFAP, anti-Iba1, anti-CNPase, anti-PSD95, anti-synaptophysin, anti-cathepsin D, anti-AT100, anti-PHF1, anti-AT8, anti-AT180, anti-AT270, anti-Tau5, anti-Tau1, anti-Tau (caspase cleaved), anti-phospho-Thr^{202}/Tyr^{204} ERK1/2, anti-ERK1/2, anti-Cdk5, anti-p35, anti-phospho-Tyr^{216}GSK3 or anti-total GSK-3β antisera at dilutions listed in Table 3.1. On the following day, membranes were washed, incubated with appropriate HRP-conjugated secondary antibodies (1:5000) and immunoreactive proteins were visualized using an ECL detection kit. All Blots were re-probed with anti-β-actin antibody and quantified using a MCID image analyzer.

Cathepsin D activity assay: Hippocampus and cerebellum of 7 week old WT, APP-Tg, Dhet, Npc1-null and ANPC mice (n = 4-8 per genotype) were homogenized and centrifuged at 4°C for 10 minutes. The supernatant was assayed to determine the protein

content and then used to measure the cathepsin D activity using a fluorogenic assay kit according to the manufacturer's instructions.

Subcellular fractionation: Hippocampus and cerebellum of 7-week old WT, APP-Tg, Dhet, Npc1-null and ANPC mice (n = 3-4 per genotype) were homogenized in ice-cold PBS and fractionated using the Qproteome Cell Compartment kit into cytosol, membrane, and nuclear fractions. Protein content of different fractions was determined using a BCA protein assay kit and equal amounts of protein were separated by SDS-PAGE. Immunoblotting was performed with anti-cathepsin D, anti-cytochrome c, anti-Bax and anti-AIF antisera as mentioned earlier (38). All blots were re-probed with anti-GAPDH, anti-N-cadherin and anti-histone antibodies to check for equal protein loading for the cytosolic, membrane and nuclear fractions, respectively.

***2-HPC treatment*:** A subset of WT, Npc1-null and ANPC mice were administered a single subcutaneous injection of either 2-HPC (4000mg/kg body weight; 20% wt./vol. in saline solution; n = 14-16 per genotype) or normal saline (n = 9-12 per genotype) at 7 days of age at the scruff of the neck as described recently (34). Following treatment, a subset of mice from saline- and 2HPC-treated groups were kept to determine their longevity, whereas another subgroup was tested for object recognition memory and rotarod performance using protocols described above. In parallel, brains from saline- and drug-treated mice were collected and processed for histology, immunohistochemistry or immunoblotting as described above.

***Statistical analysis*:** All data are presented as means ± S.E.M. Statistical differences between different genotype combinations were tested using one-way ANOVA followed by Newman-Keuls multiple comparison post-hoc analysis (Graph-Pad Software, Inc.) with significance set at $p < 0.05$. Differences among survival curves were determined using the Log-rank test, whereas statistical differences between saline and 2-HPC-treated Npc1-null or ANPC mice were tested using the unpaired Student's t-test with significance set at $p < 0.05$.

Table 3.1: Details of the primary antibodies used in this study

Antibody	Type	IHC/IF dilution	WB dilution	Source
Apoptosis inducing factor (AIF)	Polyclonal	n/a	1:200	Santa Cruz Biotech., Inc.
Amyloid precursor protein (APP, clone Y188)	Monoclonal	n/a	1:5000	Abcam Inc.
AT-8	Monoclonal	n/a	1:1000	ThermoFisher Scientific
AT-100	Monoclonal	n/a	1:1000	ThermoFisher Scientific
AT-180	Monoclonal	n/a	1:1000	ThermoFisher Scientific
AT-270	Monoclonal	n/a	1:1000	ThermoFisher Scientific
Bcl-2-associated X protein (Bax)	Monoclonal	n/a	1:200	Santa Cruz Biotech., Inc.
Calbindin-D-28K	Monoclonal	1:7000	n/a	Sigma-Aldrich, Inc.
Cathepsin D	Polyclonal	n/a	1:200	Santa Cruz Biotech., Inc.
Cleaved caspase 3	Monoclonal	1:200	n/a	Cell Signaling Tech., Inc.
2'3'-cyclic nucleotide 3'-phosphodiesterase (CNPase)	Monoclonal	1:500	1:1000	EMD Millipore, Co.
Cyclin dependent kinase 5 (Cdk5)	Monoclonal	n/a	1:200	Santa Cruz Biotech., Inc.
Cytochrome c	Monoclonal	n/a	1:1000	BD Transduction Labs™
Glial fibrillary acidic protein (GFAP)	Polyclonal	1:1000	1:1000	Dako
Glyceraldehyde-3-phosphate dehydrogenase (GAPDH)	Monoclonal	n/a	1:1000	Sigma-Aldrich, Inc.
Glycogen synthase kinase-3β (GSK-3β)	Monoclonal	n/a	1:5000	BD Transduction Labs.™
Histone H3	Polyclonal	n/a	1:500	Santa Cruz Biotech., Inc.
Ionizing calcium-binding adaptor molecule 1 (Iba1)	Polyclonal	1:3000	1:1000	Wako Chemicals, Inc.
N-cadherin	Polyclonal	n/a	1:200	Santa Cruz Biotech., Inc.
Niemann-Pick Type C1 (NPC1) protein	Polyclonal	n/a	1:1000	Abcam Inc.
p35	Polyclonal	n/a	1:200	Santa Cruz Biotech., Inc.
Extracellular-signal regulated kinase 1/2 (ERK1/2)	Monoclonal	n/a	1:2000	Cell Signaling Tech., Inc.
PHF1 Tau	Monoclonal	n/a	1:1000	Kind gift from Dr. Peter Davis
phospho-Thr^{202}/Tyr^{204} ERK1/2 (Phospho-ERK1/2)	Polyclonal	n/a	1:1000	Cell Signaling Tech., Inc.
phospho-Tyr^{216}GSK-3	Monoclonal	n/a	1:1000	Upstate Biotechnology Inc.
Postsynaptic density protein 95 (PSD 95)	Monoclonal	n/a	1:500	EMD Millipore, Co.
Synaptophysin	Monoclonal	n/a	1:3000	Sigma-Aldrich, Inc.
Tau, caspase cleaved	Monoclonal	1:100	1:1000	EMD Millipore, Co.
Tau1	Monoclonal	n/a	1:1000	EMD Millipore, Co.
Tau5	Monoclonal	n/a	1:2000	EMD Millipore, Co.
β-actin	Monoclonal	n/a	1:5000	Sigma-Aldrich, Inc.

IHC/IF, Immunohistochemistry/Immunofluorescence; WB, western blotting; n/a, not used in that specific application

3.3 Results

***Generation of bigenic ANPC mice*:** To determine how overexpression of APP can influence pathological changes triggered by intracellular accumulation of cholesterol, we generated a novel bigenic ANPC mouse line (APP-Tg and Npc1-null: $APP^{+/0}Npc1^{-/-}$) by crossing mutant human APP transgenic (APP-Tg: $APP^{+/0}Npc1^{+/+}$) with heterozygous Npc1-deficient ($APP^{0/0}Npc1^{+/-}$) mice (Fig. 3.1A). Our immunoblotting analysis revealed that APP holoprotein levels in ANPC mice were similar to APP-Tg and double heterozygous (Dhet: $APP^{+/0}Npc1^{+/-}$) mice but were markedly higher compared to wild-type (WT: $APP^{0/0}Npc1^{+/+}$) and homozygous Npc1-null mice (Npc1-null: $APP^{0/0}Npc1^{-/-}$), as expected (Fig. 3.1B). Npc1 protein levels did not differ between WT and APP-Tg mice, and, as anticipated, the Dhet mice showed ~50% reduction, while Npc1-null and ANPC mice did not exhibit detectable levels of this protein (Fig. 3.1B). ANPC mice had a maximum life-span of 77-days, with mortality rate increasing drastically from 55-days onward (Fig. 3.1C). Npc1-null mice, as reported earlier (40), exhibited a reduced life-span with only ~30% of the animals alive past the 90-day censor date in our colony. The majority (>90%) of APP-Tg and Dhet mice, on the other hand, survived past the censor date, whereas the WT mice had no recorded deaths within the study period. Thus the bigenic ANPC mice had a significantly reduced life-span compared to WT, APP-Tg, Dhet or Npc1-null mutants (Fig. 3.1C). Additionally, the ANPC mice reached a maximum body weight of ~12g by 6 weeks, which was ~30% less compared to other lines of mice, and then declined progressively until death (Fig. 3.1D).

***Accelerated object recognition memory and motor deficits*:** To determine whether overexpression of APP in Npc1-null mice can influence cognitive performance, we evaluated all 5 genotypes at 4, 7 and 10 weeks of age in an object recognition memory test (Fig. 3.2A). The performance of WT, APP-Tg, Dhet, Npc1-null and ANPC mice did not differ significantly at 4 weeks of age (data not shown). ANPC mice, however, exhibited significant deficits in the object memory index at 7 and 10 weeks, whereas APP-Tg, Dhet and Npc1-null mice showed reduced memory index only at 10 weeks (Fig. 3.2A). Loss of Npc1 function is known to impair motor ability in Npc1-null mice (41). To examine this effect we first tested mice of all 5 genotypes at 4, 7 and 10 weeks of age

for their spontaneous locomotor activity (walking, rearing and periods of inactivity) in open-field tests [Fig. 3.16A-C (i.e. Suppl. Fig.1)]. No significant variation was apparent in the sensorimotor behavior between the genotypes at 4 weeks of age (data not shown). The ANPC mice exhibited significantly reduced locomotor activity and increased periods of inactivity in our open-field tests at both 7 and 10 weeks age, whereas Npc1-null mice showed these deficits mostly at the later age of 10 weeks only. The APP-Tg and Dhet mice did not show any difference from WT at any age [Fig. 3.16A-C (i.e.Suppl. Fig.1)]. Furthermore, rotarod performance and gait co-ordination analysis revealed that motor co-ordination in Npc1-null mice was impaired at 10 weeks but not at 4 or 7 weeks of age. The ANPC mice, on the other hand, displayed a significant impairment in their motor function at 7 weeks, which was further exacerbated by 10 weeks. The APP-Tg and Dhet mice did not show any motor deficit compared to WT mice at any age (Fig. 3.2B,C).

***Intracellular accumulation of unesterified cholesterol*:** We assessed intracellular cholesterol accumulation across the genotypes by filipin staining which binds unesterified cholesterol [Fig. 3.17A-J (i.e. Suppl. Fig.2)]. Filipin-labeled cholesterol was evident in almost all neurons of the hippocampus and cerebellum in Npc1-null [Fig. 3.17D,I (i.e. Suppl. Fig.2)] and ANPC [Fig. 3.17E,J (i.e. Suppl. Fig.2)] mice at 4, 7 and 10 weeks of age. By contrast, no cholesterol accumulation was evident in WT, APP-Tg or Dhet littermates at any age group [Fig. 3.17A-H (i.e. Suppl. Fig.2)]. Interestingly, total cholesterol content in the hippocampus and cerebellum of ANPC and Npc1-null mice at 4, 7 and 10 weeks of age, as detected by gas-liquid chromatography, did not exhibit any alteration compared to age-matched WT, APP-Tg or Dhet mice [Fig. 3.17K-M (i.e.Suppl. Fig.2)].

***Aggravated glial activation and demyelination*:** At the cellular level, ANPC mice showed a profound increase in the number and activation of GFAP-labeled astrocytes in both the hippocampus and cerebellum compared to WT, APP-Tg, Dhet and Npc1-null mice (Fig. 3.3A-J). Our western blot analysis also revealed a significant increase in GFAP levels in the hippocampus and cerebellum of 4, 7 and 10 weeks old ANPC mice compared to WT, APP-Tg and Dhet mice (Fig. 3.3K,L). The Npc1-null mice displayed a significant increase in GFAP levels over the WT, APP-Tg and Dhet mice, mostly at later

stages. The relative increase in ANPC over Npc1-null mice was evident at 4 weeks but not at later stages.

Consistent with the alteration in astrocytes, ANPC mice showed profound microglial activation in both the hippocampus and cerebellum compared to all other genotypes (Fig. 3.4A-L). At the cellular levels, Iba1-labeled microglial cells in WT, APP-Tg and Dhet mouse brains displayed small cell bodies with few ramified processes typical of resident microglia (Fig. 3.4A-C, F-H). In contrast, the ANPC mice showed numerous intensely stained phagocytic, amoeboid microglia primarily in the hippocampus, whereas fully activated, hypertrophic microglia were apparent in the cerebellum (Fig. 3.4E,J). Age-matched Npc1-null mice, on the other hand, revealed fewer activated microglia in both the hippocampus and cerebellum than those observed in ANPC mice (Fig. 3.4D,I). Our western blot analysis also showed a significant increase in Iba1 levels in the hippocampus and cerebellum of 4, 7 and 10 week old ANPC mice compared to WT, APP-Tg and Dhet mice (Fig. 3.4K,L). The increase over the Npc1-null mice was evident only at 4 weeks in the cerebellum. Interestingly, the relative increase in Iba1 levels was found to be more profound in the cerebellum than hippocampus of ANPC and Npc1-null mice than the other lines of mice.

Immunohistochemical staining with the oligodendrocyte marker CNPase showed dramatic loss of myelin fiber tracts in the ANPC hippocampus/cortex and cerebellum compared to the other lines of mice (Fig. 3.5A-J). This was substantiated by our western blot data showing striking decreases in CNPase levels in ANPC hippocampus and cerebellum at 4, 7 and 10 weeks (Fig. 3.5K,L). Npc1-null mice, as reported earlier (42), also showed significant demyelination at various ages, but this was found to be less severe than ANPC mice at earlier stages. Additionally, the levels of CNPase in the hippocampus, but not in the cerebellum, were depleted in APP-Tg and Dhet mice at later stages compared to age-matched WT mice (Fig. 3.5K,L).

***Loss of neurons and synaptic markers*:** Our APP-Tg mice, as reported for most other lines of mutant APP mice, do not exhibit frank losses of neurons in any brain region (28, 29). The Npc1-null mice, on the other hand, show progressive loss of neurons in selected

brain regions such as thalamus and cerebellum but not in the hippocampus (5, 6). In keeping with these results, we observed a significant decrease in the number of cerebellar Purkinje cells in ANPC and Npc1-null mice compared to WT, APP-Tg and Dhet mice (Fig. 3.6A-L). The magnitude of cell loss was found to be more pronounced in ANPC than in the Npc1-null mice (Fig. 3.6L). Labeling of degenerating neurons with cleaved-caspase-3 suggested the possible involvement of apoptosis in triggering the loss of neurons (Fig. 3.6M-R). The hippocampus, on the other hand, did not exhibit any significant neuronal loss either in APP-Tg, Dhet, ANPC or Npc1-null mouse brains compared to the WT (Fig. 3.6A-E,K). The levels of presynaptic marker synaptophysin and postsynaptic marker PSD95 were markedly decreased in 7- and/or 10-week-old Npc1-null and ANPC cerebellum compared to WT, APP-Tg and Dhet mice. In the hippocampus, however, no alteration in synaptophysin levels was evident at any age, whereas the levels of PSD-95 were decreased in 10-week-old Npc1-null and ANPC mice compared to other lines [Fig. 3.187A-D (i.e. Suppl. Fig.3)].

***Activation of tau-kinases and phosphorylation of tau*:** Although florid tau pathology is not apparent in either APP-Tg or Npc1-null mice, there is evidence that altered cholesterol levels can regulate tau phosphorylation under *in vitro* conditions (43). To determine whether overexpression of APP together with intracellular cholesterol accumulation can influence tau phosphorylation under *in vivo* paradigm, we first evaluated tau kinases in all lines of mice. Our results clearly demonstrated a significant up-regulation of phospho-ERK1/2 in the cerebellum, but not in the hippocampus, of Npc1-null or ANPC mice (Fig. 3.7A-D). Additionally, the steady-state levels of p35 were found to be decreased in the cerebellum, but not hippocampus, of Npc1-null and ANPC compared to other lines of mice (Fig. 3.7A-D). In contrast, the levels of phosphoGSK-3β did not alter in ANPC or Npc1-null mice [Fig. 3.19A-B (i.e. Suppl. Fig.4)]. As a follow up, we measured the levels of total-tau using Tau1 and Tau5 antibodies and phospho-tau using various epitope specific antibodies in the hippocampus and cerebellum of five different lines of mice (Fig. 3.8A-D). Our results clearly showed that total tau levels were strikingly decreased in the cerebellum, but not hippocampus, of ANPC and Npc1-null mice compared to other lines. Interestingly, the levels of phospho-tau remain unaltered in

both brain regions of ANPC and Npc1-null mice with respect to other genotypes. Thus, it is evident that phosphorylation of tau is selectively increased in the affected cerebellar region, which is more pronounced in ANPC than Npc1-null mice. More recently, a number of studies have indicated that proteolytic cleavage of tau protein, in addition to enhanced phosphorylation, may have a role in the degeneration of neurons (44-46). Our results showed that levels of caspase-cleaved tau are markedly increased in the cerebellum, but not hippocampus, of ANPC and Npc1-null mice (Fig. 3.8A-D). The relative change, however, was more obvious in ANPC than Npc1-null mice. At the cellular level, cleaved tau immunoreactivity was evident only in the Purkinje cells of the ANPC and Npc1-null mice but not in WT, APP-Tg or Dhet mice (Fig. 3.8E-G).

***Increased activity and cytosolic levels of cathepsin D*:** Several studies have shown that up-regulation of lysosomal enzymes within lysosomes can prevent sub-lethal damage (47), whereas lysosomal rupture leading to sustained release of enzymes into the cytosol can induce cell death *via* cytochrome c release from mitochondria (38, 48, 49). To determine the potential involvement of the lysosomal enzymes in ANPC mice, we measured the level/activity and subcellular distribution of cathepsin D in all five lines of mice [(Figs. 3.9A-F, 3.20A,B (i.e. Suppl. Fig.5)]. Our results clearly showed that cathepsin D levels and activity were significantly higher in the hippocampus and even more pronounced in the cerebellum of ANPC and Npc1-null mice compared to other lines of mice (Fig. 3.9A-D). It is of interest to note that the activity of this enzyme was found to be increased more profoundly in ANPC cerebellum compared to Npc1-null mice (Fig. 3.9D). Our subcellular fractionation results further revealed that cytosolic cathepsin D levels were higher in the cerebellum of ANPC and Npc1-null mice compared to WT mice (Fig. 3.9F). Similar to cathepsin D, the levels of cytochrome c and Bax, but not AIF, were increased in the cerebellar cytosolic fraction of ANPC and Npc1-null mice compared to other lines [(Figs. 3.9F, 3.20B (i.e. Suppl. Fig.5)]. The relative change was found to be more obvious in the ANPC than Npc1-null mice (Fig. 3.9F). In contrast to the cerebellum, alterations in hippocampal cytosolic cathepsin D, cytochrome c and Bax levels were less apparent in ANPC and Npc1-null mice compared to WT mice [(Figs. 3.9E, 3.20A (i.e. Suppl. Fig.5)]. It is also of interest to note that changes observed in the

hippocampus did not reveal as much variation between ANPC and Npc1-null mice as evident in the cerebellum. The cytosolic levels of cathepsin D, cytochrome c and Bax in APP-Tg and Dhet mice did not differ from the WT mice in either brain regions [(Fig. 3.20A,B (i.e. Suppl. Fig.5)].

***Effect of 2-HPC treatment*:** To determine whether lowering cholesterol accumulation can attenuate the aforementioned abnormalities, we injected WT, Npc1-null and ANPC mice with 2-HPC or saline at postnatal day 7 and then evaluated their behavioral and pathological features at 4 or 7 weeks of age. The ANPC and Npc1-null mice treated with 2-HPC lived significantly longer than their respective saline-injected mice (ANPC median survival: 103 days *vs.* 69 days; Npc1-null median survival: 107 days *vs.* 85 days) (Fig. 3.10A). Additionally, our results clearly showed that 2-HPC treatment can lead to significant improvement in the motor and cognitive performances of 7-week-old ANPC and Npc1-null mice compared to the respective saline-treated genotypes (Fig. 3.10B,C).

At the cellular level, we observed that 2-HPC treatment was able to sequester filipin-labeled cholesterol accumulation in most neurons in 4-week old ANPC and Npc1-null mice (Fig. 3.11A-H). Accompanying these changes, the number of surviving Purkinje cells in treated ANPC and Npc1-null mice, *albeit* significantly lower than WT mice, was found to be doubled compared to the saline-injected ANPC and Npc1-null mice (Fig. 3.12A-E). Our immunohistochemical analysis further showed a significant decrease in the activation of GFAP-labeled astrocytes and Iba1-labeled microglia in both hippocampus and cerebellum of 2-HPC-treated ANPC and Npc1-null mice compared to respective saline-treated animals (Fig. 3.13A-P). The beneficial effects of 2-HPC were also reflected with a substantial increase in CNPase immunoreactivity, suggesting preservation of brain myelination (Fig. 3.13Q-X). Interestingly, 2-HPC treatment, as evident from our western blot analysis, markedly attenuated the enhanced levels of phospho-ERK1/2 in the cerebellum of ANPC and Npc1-null mice (Fig. 3.14A,B). This was accompanied by a parallel increase in total tau and a decrease in cleaved tau levels in the cerebellum of 2-HPC-treated ANPC and Npc1-null animals compared to the respective saline-injected genotypes (Fig. 3.15A-B).

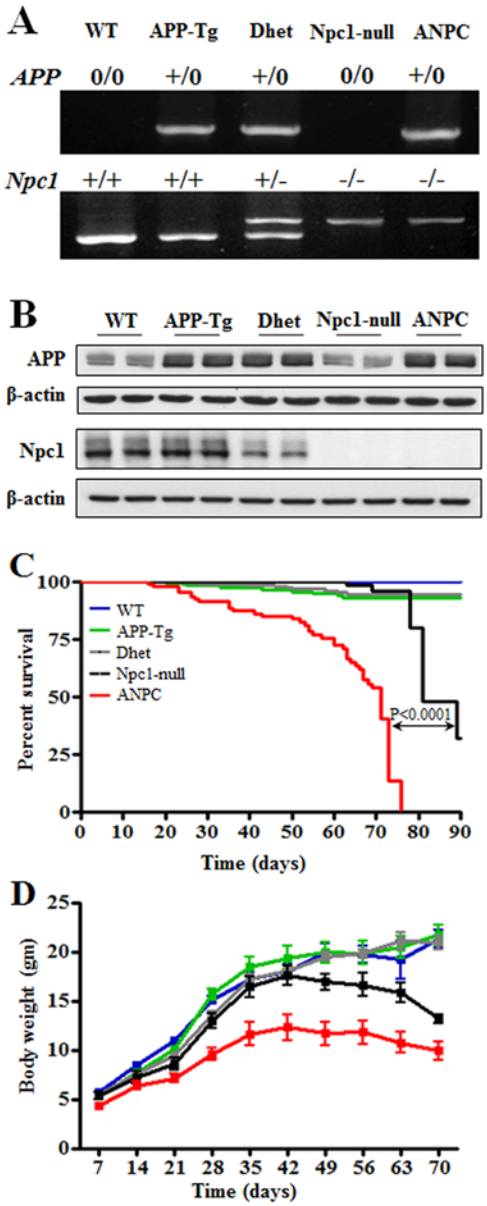

Figure 3.1: A, PCR analysis of tail biopsy DNA from WT (lane 1), APP-Tg (lane 2), Dhet (lane 3), Npc1-null (lane 4) and ANPC (lane 5) mice for human *APP* transgene (upper panel) and mouse *Npc1* gene (lower panel). In *APP* PCR, presence of a band indicates the presence of the transgene while its absence indicates lack of the human transgene. For *Npc1* PCR, presence of the lower band indicates the wild-type allele and the upper band indicates the knocked-out allele. **B**, Immunoblotting showing profiles of APP and Npc1 expression in different genotypes as detected with APP C-terminal (Y188) antibody reactive against mouse and human APP (upper panel) and C-terminal Npc1 antibody (lower panel), respectively. The APP-Tg, Dhet and ANPC mice, as expected, exhibit higher levels of APP expression over WT and Npc1-null mice harboring only the mouse APP holoprotein. Immunoblotting with the Npc1 antibody revealed the presence of normal levels of Npc1 protein in WT and APP-Tg mice, ~50% of the normal levels in Dhet mice and its absence in ANPC and Npc1-null mice. Anti β-actin antibody was used to monitor an equal loading of proteins. **C**, Percent survival curves (Kaplan-Meier survival analysis) of different genotypes (WT=205, APP-Tg =186, Dhet=198, Npc1-null=126 and ANPC=106 animals) showing that ANPC mice have a significantly ($P<0.0001$) reduced survival compared to mice of other genotypes. **D**, Weight curves for WT, APP-Tg, Dhet, Npc1-null and ANPC assessed between 7-70 days of age. ANPC mice show a significantly reduced body weight compared to other genotypes.

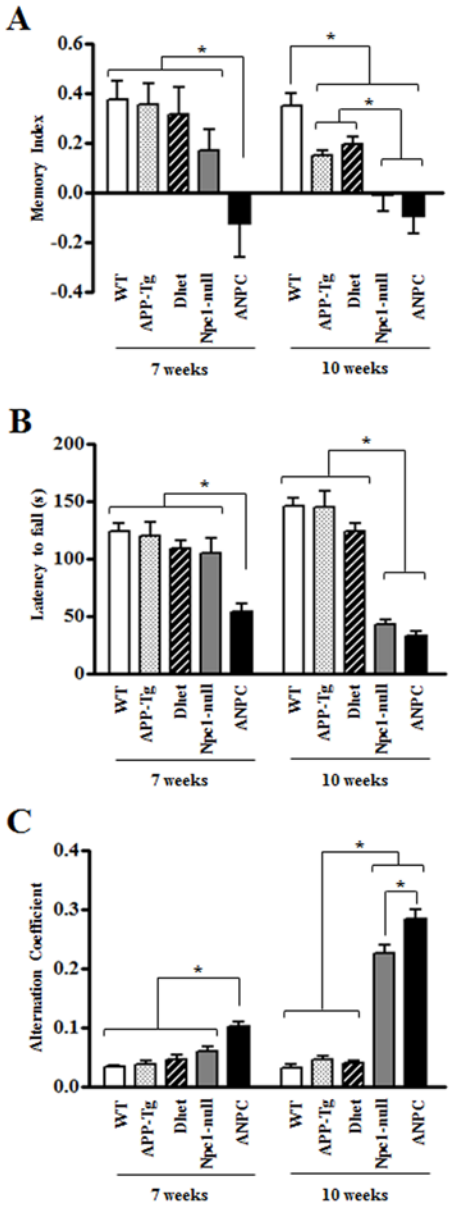

Figure 3.2: A-C, Cognitive and motor behavioral analysis at 7- and 10-weeks of age in WT, APP-Tg, Dhet, Npc1-null and ANPC mice. **A**, ANPC mice exhibit a profound deficit in 3-hr object recognition memory test at 7 and 10 weeks of age, whereas the APP-Tg, Dhet and Npc1-null mice show a significant deficit only at 10 weeks of age. Values are means ± SEM of memory index scores, with n=6-10 for each genotype. **B**, Histograms showing the average latency to fall from an accelerating rotarod for WT, APP-Tg, Dhet, Npc1-null and ANPC mice at 7- and 10-weeks of age. ANPC mice exhibited significant motor impairment at 7 weeks which progressively worsened by 10 weeks. Npc1-null mice exhibit significant motor impairment only at 10 weeks, whereas APP-Tg and Dhet mice did not display any impairment at either 7 or 10 weeks of age. Data are means ± SEM of all trials performed on final test day, with n = 6-10 for each genotype. **C**, Histograms showing alternation coefficient representing gait asymmetry in all five genotypes of mice as assessed by measurement of right hind paw stride length. The WT, APP-Tg and Dhet mice exhibited a normal alternating gait at both 7 and 10 weeks of age. The ANPC mice showed severe gait abnormalities at 7 and 10 weeks of age, whereas Npc1-null mice displayed gait disturbances only at 10-weeks. Data are means ± SEM of alternation coefficients, with n = 6-10 for each genotype. *, $P<0.05$.

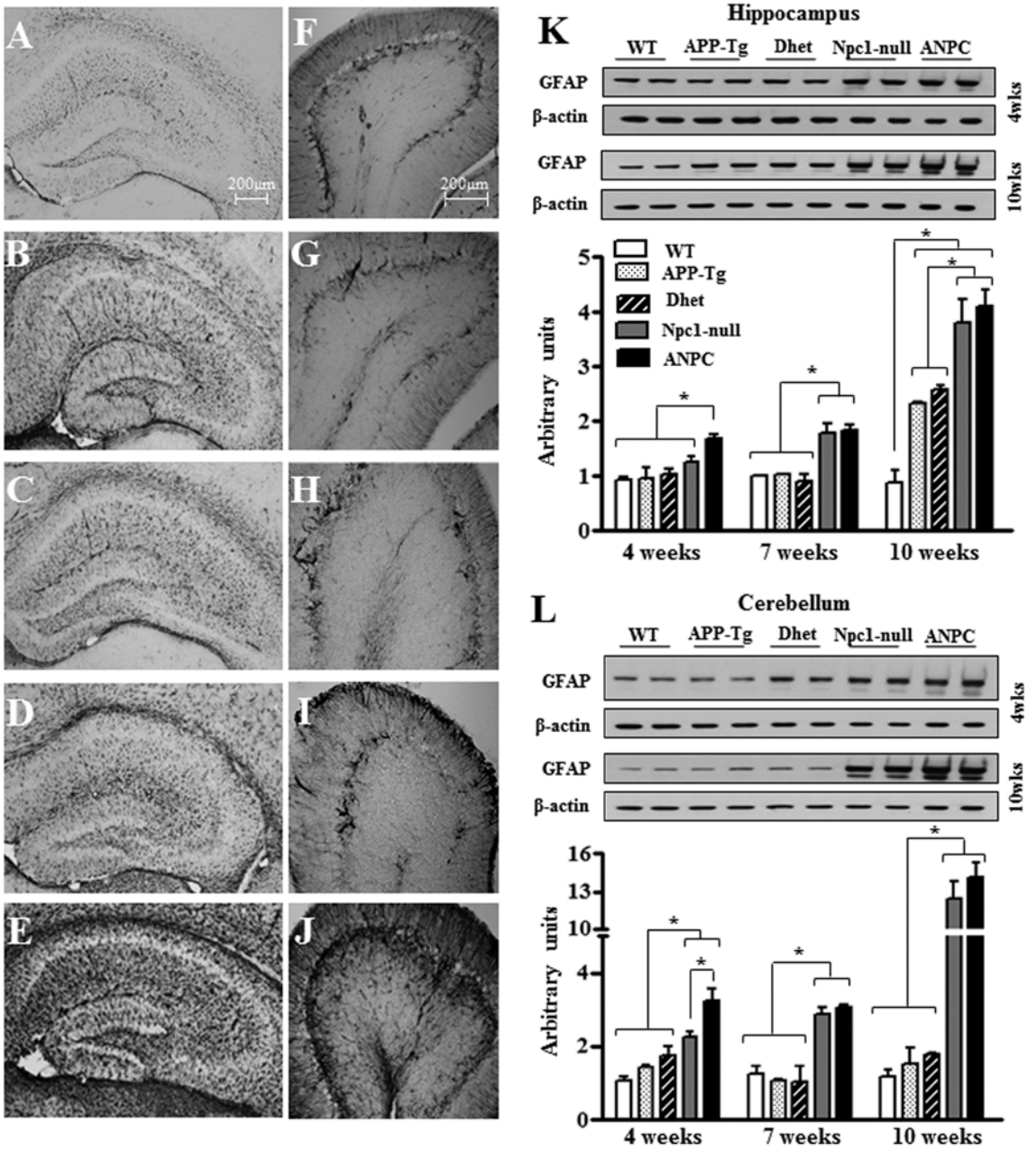

Figure 3.3: A-J, Bright-field photomicrographs showing GFAP-positive astrocytes in the hippocampus (A-E) and cerebellum (F-J) of 4-week old WT (A, F), APP-Tg (B, G), Dhet (C, H), Npc1-null (D, I) and ANPC (E, J) mice. Note the relative increase in intensity of GFAP immunoreactivity in the hippocampus and cerebellum of ANPC compared to other genotypes. **K-L**, Immunoblots and respective histograms showing GFAP levels in the hippocampus (K) and cerebellum (L) of 4-, 7- and 10-week old WT, APP-Tg, Dhet, Npc1-null and ANPC mice. Protein levels were normalized to β-actin. Note the relative increase in hippocampal and cerebellar GFAP levels in ANPC mice over other genotypes at different age groups. Values are means ± SEM; n = 4-6 animals per genotype and age group. *, $P<0.05$.

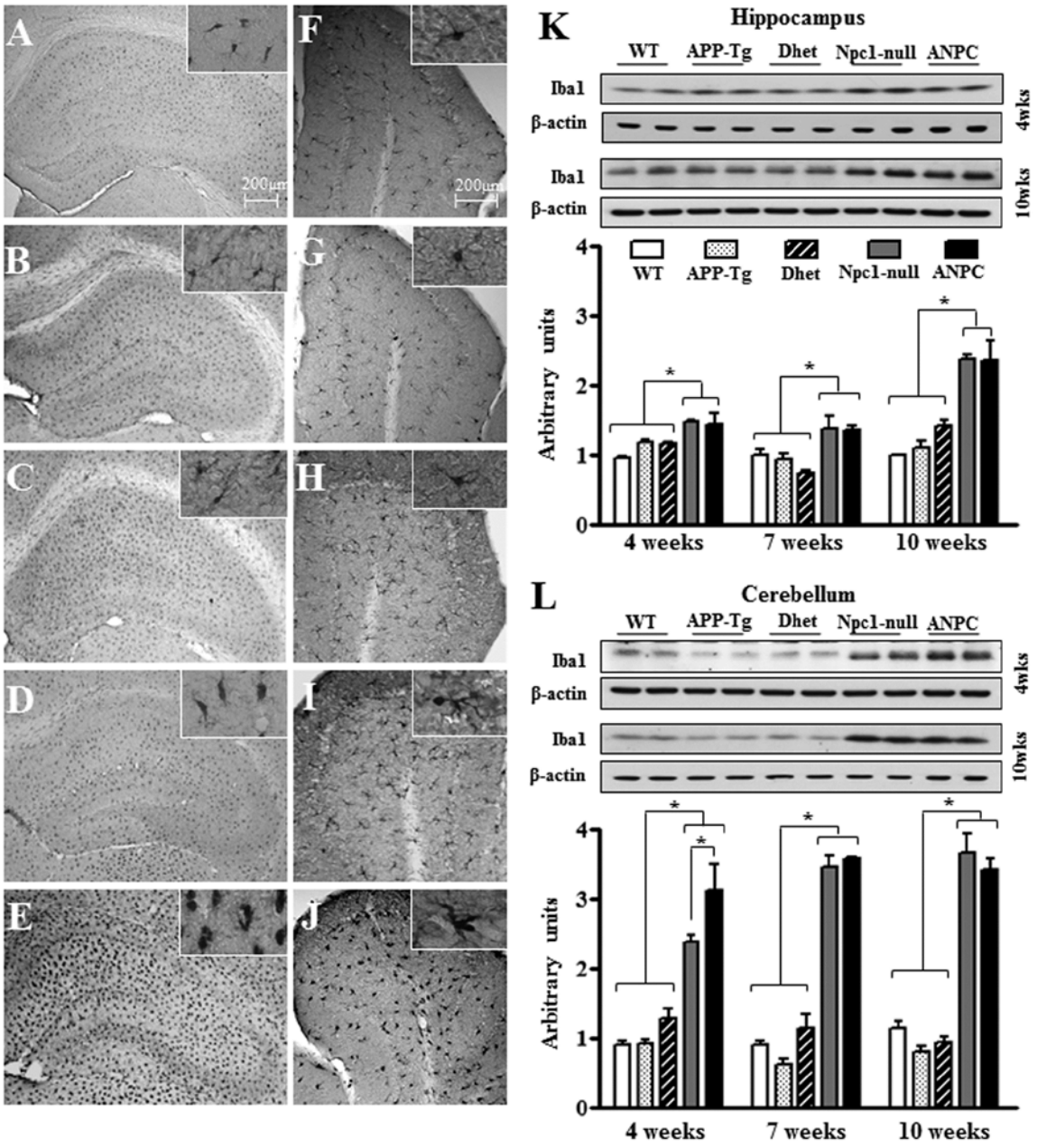

Figure 3.4: A-J, Bright-field photomicrographs showing Iba1-positive microglia in the hippocampus (A-E) and cerebellum (F-J) of 4-week old WT (A, F), APP-Tg (B, G), Dhet (C, H), Npc1-null (D, I) and ANPC (E, J) mice. Note the relative change in intensity and morphology of microglia in the hippocampus and cerebellum of ANPC compared to other genotypes. **K-L**, Immunoblots and respective histograms showing Iba1levels in the hippocampus (K) and cerebellum (L) of 4-, 7-, and 10-week old WT, APP-Tg, Dhet, Npc1-null and ANPC mice. Protein levels were normalized to β-actin. Note the relative increase in hippocampal and cerebellar Iba1 levels in ANPC mice over other genotypes at different age groups. Values are means ± SEM; n = 4-6 animals per genotype and age group. *, P<0.05.

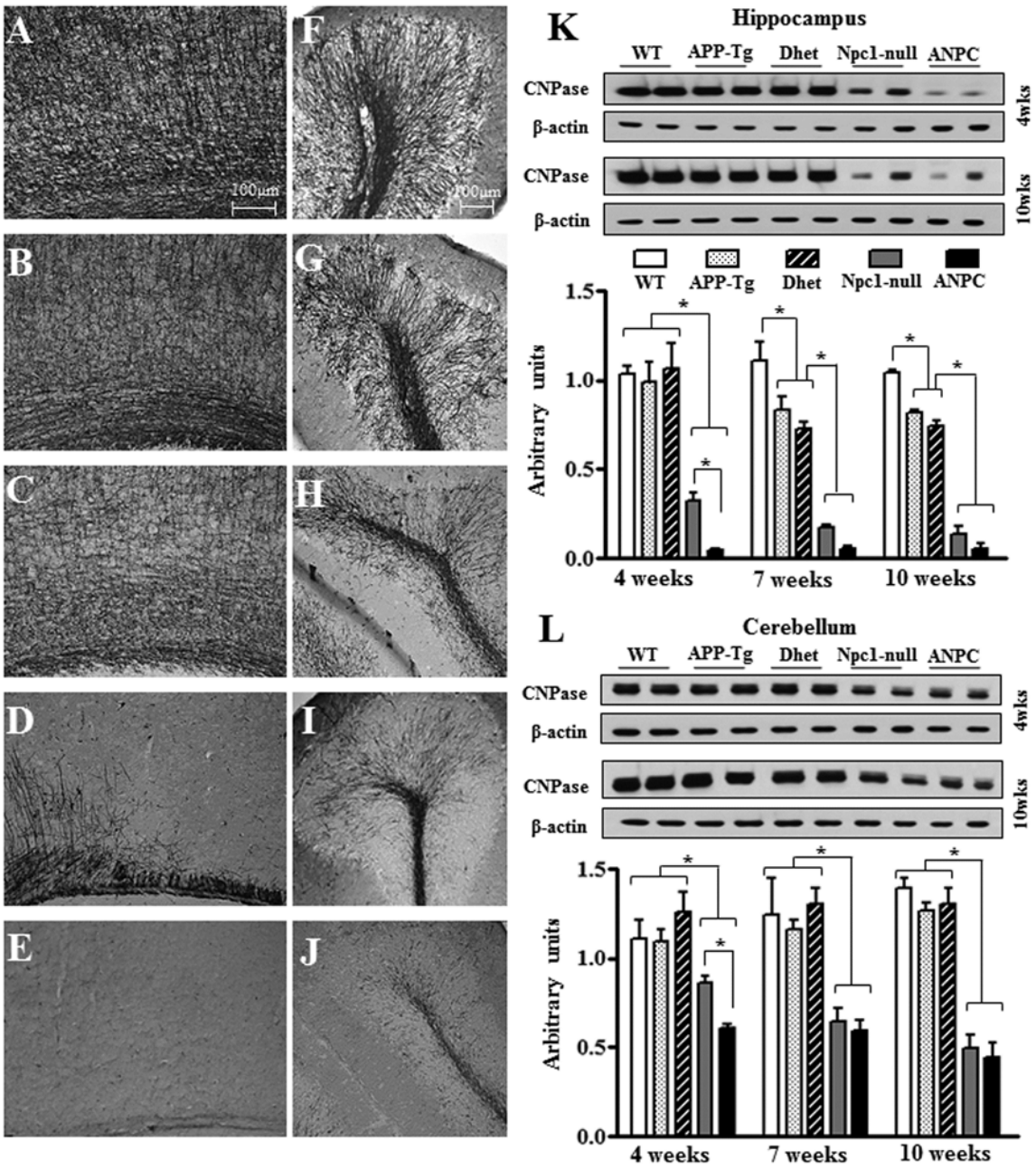

Figure 3.5: A-J, Bright-field photomicrographs showing CNPase-positive oligodendrocytes in the hippocampus/cortex (A-E) and cerebellum (F-J) of 4-week old WT (A, F), APP-Tg (B, G), Dhet (C, H), Npc1-null (D, I) and ANPC (E, J) mice. Note the relative decrease in intensity of CNPase immunoreactivity in the hippocampus/cortex and cerebellum of ANPC compared to WT, APP-Tg, Dhet and Npc1-null mouse brains. **K-L**, Immunoblots and respective histograms showing CNPase levels in the hippocampus (K) and cerebellum (L) of 4-, 7-, and 10-week old WT, APP-Tg, Dhet, Npc1-null and ANPC mice. Protein levels were normalized to β-actin. Note the relative decrease in CNPase levels in the hippocampus/cortex and cerebellum of ANPC mice compared to other genotypes at different age groups. Values are means ± SEM; n = 4-6 animals per genotype and age group. *, $P<0.05$.

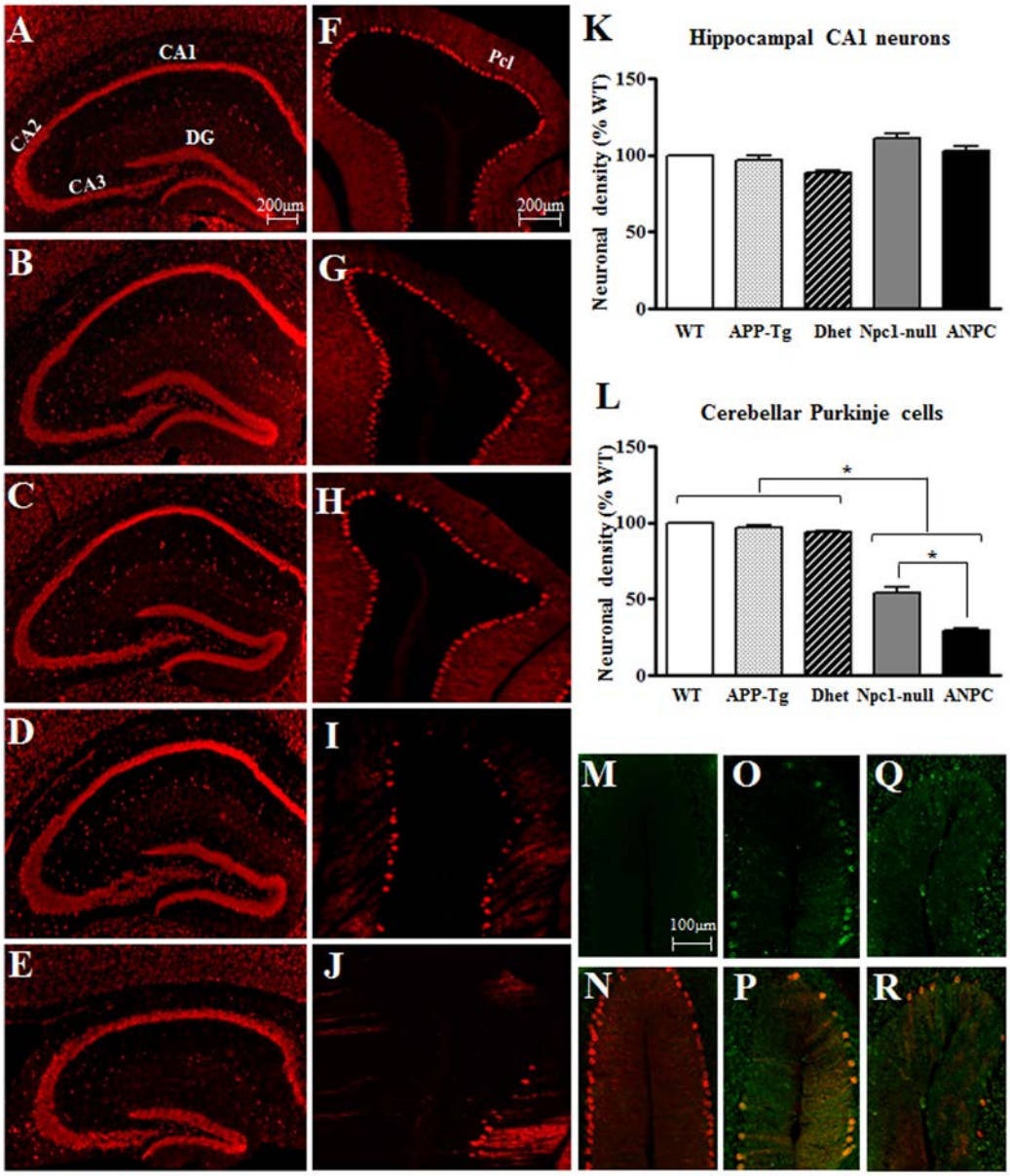

Figure 3.6: A-E, Photomicrographs showing NeuroTrace-labeled hippocampal sections from mice of different genotypes at 7 weeks of age. No apparent loss of neurons was evident in the hippocampus of ANPC (E) compared to WT (A), APP-Tg (B), Dhet (C) and Npc1-null (D) littermates. **F-J**, Photomicrographs showing calbindin-positive cerebellar Purkinje cell layer (Pcl) from 7 week old mice of different genotypes. Note the relative loss of Purkinje cells in Npc1-null (I) and ANPC (J) mice compared to WT (F), APP-Tg (G), Dhet (H) mice. **K-L**, Quantitative analysis of neuronal density in the hippocampal CA1 region (K) and cerebellar Pcl (L) of APP-Tg, Dhet, Npc1-null and ANPC brains expressed as percentage of WT. Note the significant loss of cerebellar Purkinje cells (L) but no alteration in the hippocampal neurons (K) in Npc1-null and ANPC mice compared to other genotypes. The magnitude of Purkinje cell loss was more profound in ANPC than age-matched Npc1-null mice. **M-R,** Photomicrographs showing co-localization of cleaved caspase-3 (green) with calbindin-positive (red) Purkinje cells in WT, Npc1-null and ANPC cerebellum. M, O and Q represent the cleaved caspase-3 labeling in WT, Npc1-null and ANPC respectively, while N, P, R are the merged images. CA1-CA3, Cornu Ammonis 1-3; DG, Dentate Gyrus. Values are means ± SEM.*, $P<0.001$.

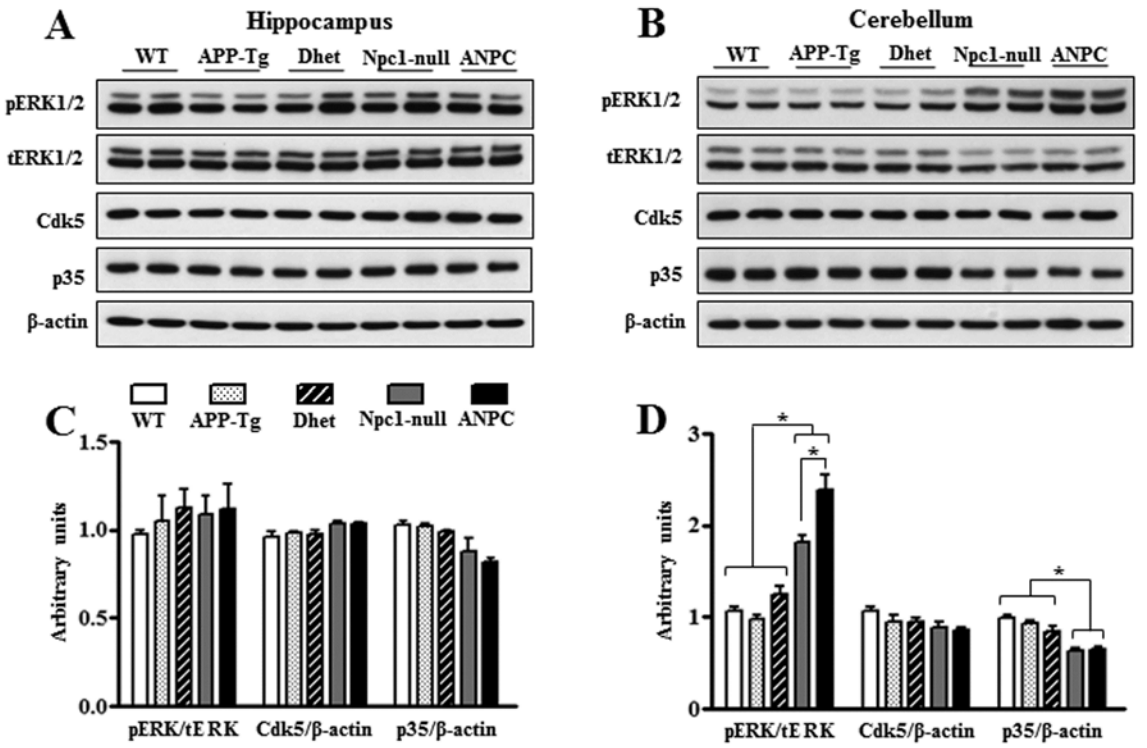

Figure 3.7: A-D, Immunoblot analysis of tau kinases in the hippocampus (A, C) and cerebellum (B, D) of 7-week old WT, APP-Tg, Dhet, Npc1-null and ANPC mice. Phospho-ERK1/2 levels were significantly increased in the cerebellum (B, D) but not in the hippocampus (A, C) of ANPC mice compared to other genotypes. The cerebellum of Npc1-null mice also showed a significant increase in phospho-ERK1/2 levels compared to other genotypes but is less pronounced than ANPC mice (B, D). Quantitative analysis of Cdk5 levels normalized to β-actin showed no significant alteration between the genotypes either in the hippocampal (A, C) or cerebellar (B, D) brain regions. Immunoblotting using p35 antibody indicate a decrease in p35 levels in the cerebellum of ANPC and Npc1-null mice relative to WT, APP-Tg and Dhet mice (B, D). No alteration in p35 levels was observed in the hippocampus between the genotypes (A, C). Values are means ± SEM; n = 4-6 animals per genotype. *, $P<0.05$.

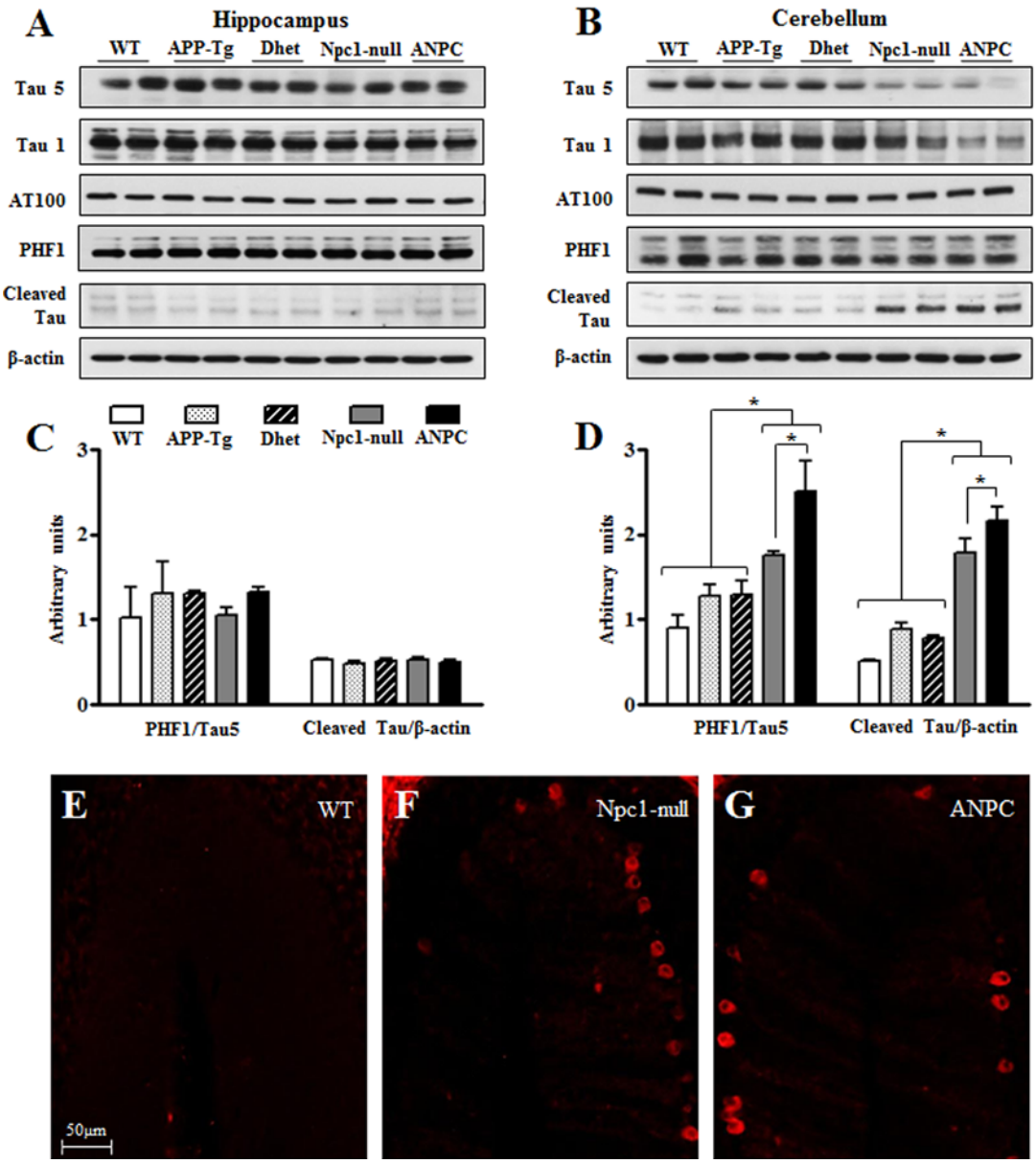

Figure 3.8: A-D, Immunoblot analysis of total, phospho and cleaved tau levels in the hippocampus (A, C) and cerebellum (B, D) of 7-week old WT, APP-Tg, Dhet, Npc1-null and ANPC mice. Total tau was detected by Tau-5 (phospho-independent anti-tau antibody) and Tau-1(dephosphorylated tau at serines 195, 198, 199 and 202) antibodies, whereas phospho-tau was detected using AT 100 (T212, S214 and T217) and PHF1 (S396/S404) antibodies. Note the decrease in total tau levels in the cerebellum (B) but not in the hippocampus (A) of Npc1-null and ANPC mice compared to WT, APP-Tg and Dhet mice. Quantitative analysis of phospho-tau levels normalized to total tau showed hyperphosphorylation of tau protein specifically in the cerebellum of Npc1-null and ANPC mice compared to other genotypes (C, D). The increased level of phospho-tau was more pronounced in the ANPC than Npc1-null mice. Caspase cleaved tau level showed marked increase in the cerebellum (B, D) but not in the hippocampus (A, C) of Npc1-null and ANPC mice than WT, APP-Tg and Dhet mice. The alteration in the levels of cleaved tau was found to be more pronounced in ANPC mice than Npc1-null mice. E-G, Representative images from WT (E), Npc1-null (F) and ANPC (G) cerebellar sections showing immunolabeling for cleaved Tau. Values are means ± SEM; n = 4-6 animals per genotype. *, $P<0.05$.

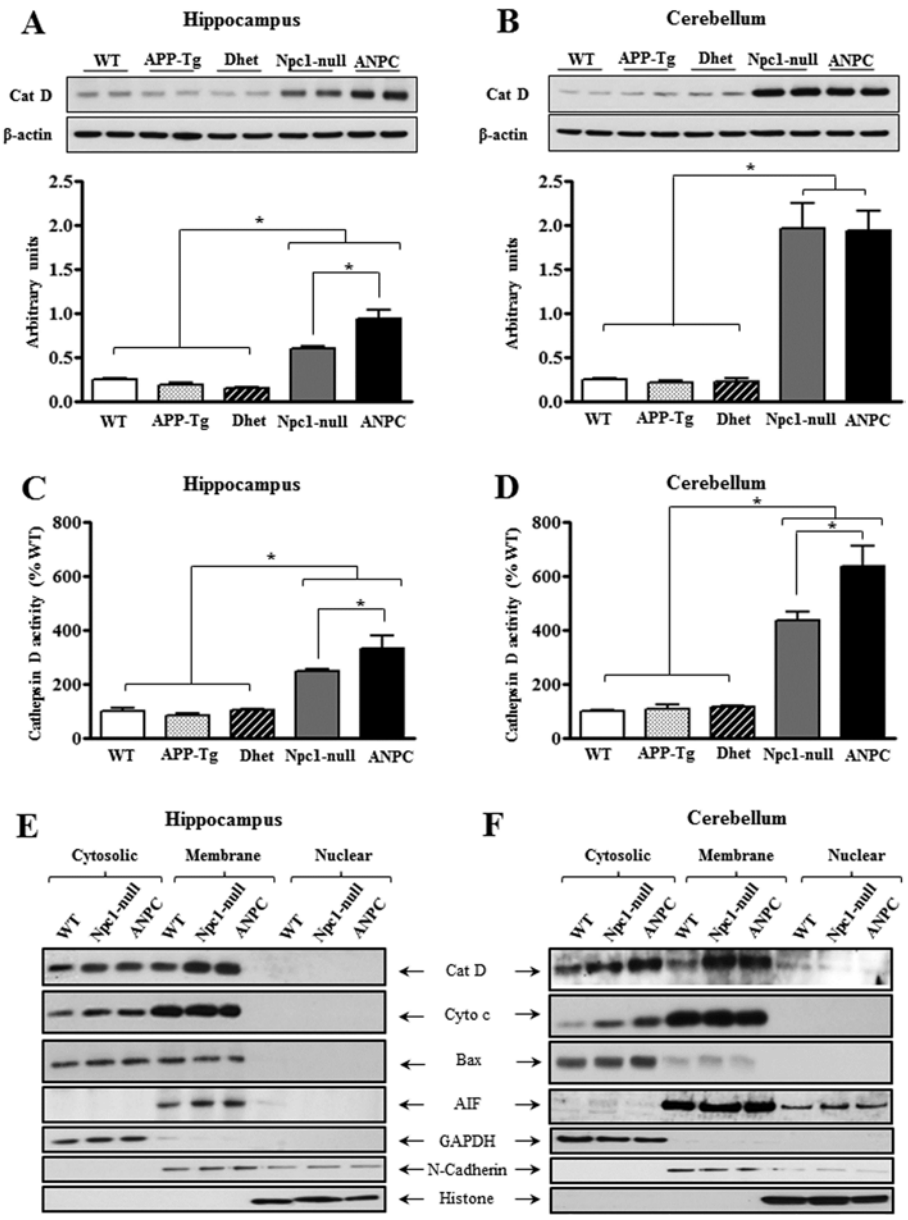

Figure 3.9: A-B, Immunoblots and respective histograms showing increased mature Cat D levels in the hippocampus (A) and cerebellum (B) of 7-week old ANPC and Npc1-null mice compared to age-matched WT, APP-Tg and Dhet mice. Note the relatively greater fold increase in Cat D levels in the cerebellum than the hippocampus of ANPC and Npc1-null mice compared to other genotypes. Protein levels were normalized to β-actin. **C-D**, Histograms showing Cat D enzyme activity in the hippocampus (C) and cerebellum (D) of 7-week old APP-Tg, Dhet, Npc1-null and ANPC mice expressed as percentage of activity in WT. Note the relatively greater increase in Cat D activity in the hippocampus and cerebellum of ANPC mice compared to other genotypes. **E-F**, Representative immunoblots showing subcellular distribution of Cat D, Cyto c, Bax and AIF in the hippocampus (E) and cerebellum (F) of 7-week old WT, Npc1-null and ANPC mice. Note the relatively higher cytosolic levels of Cat D, Cyto c, and Bax in the cerebellum than the hippocampus of Npc1-null and ANPC mice compared to WT. Immunoblots for GAPDH, N-cadherin and Histone 3 represent the loading controls for the cytosolic, membrane and nuclear fractions respectively. Cat D, Cathepsin D; Cyto c, Cytochrome c; Bax, Bcl-2-associated X protein; AIF, Apoptosis Inducing Factor; GAPDH, Glyceraldehyde-3-Phosphate Dehydrogenase. Histograms values represent means ± SEM; n = 4-6 animals per genotype. *, $P<0.05$.

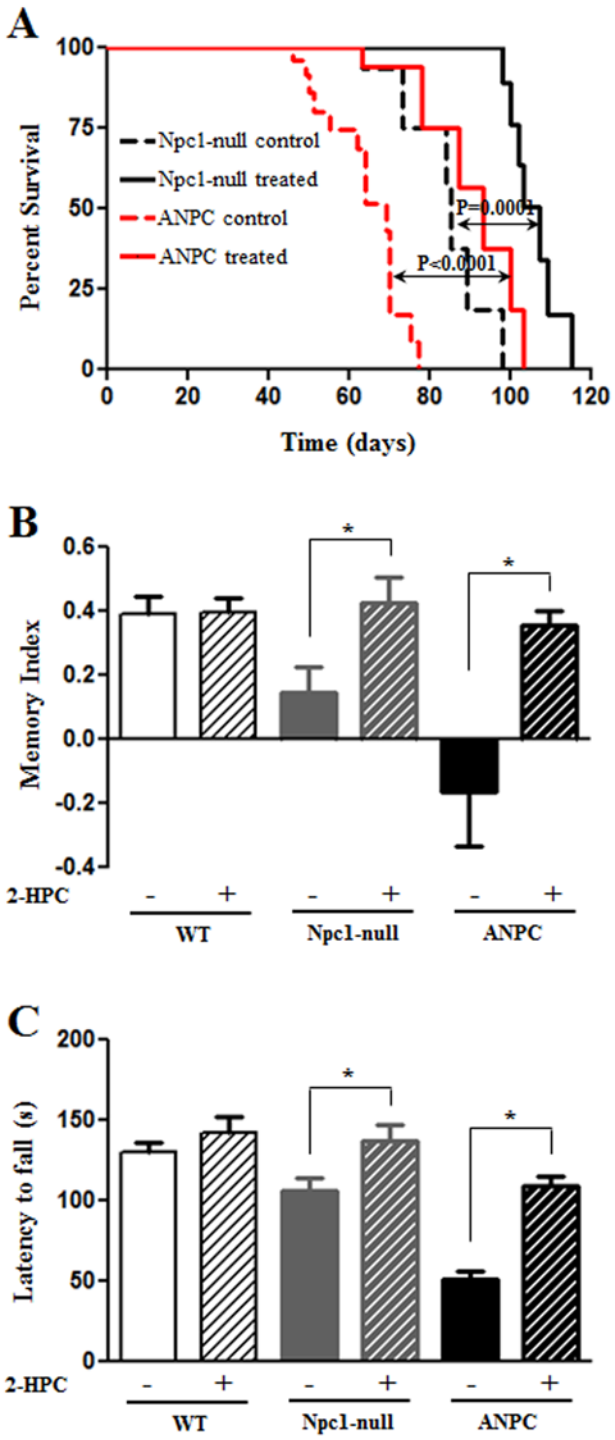

Figure 3.10: A-C, Effect of 2-hydroxypropyl-β-cyclodextrin (2-HPC) treatment on survival, cognitive and motor analysis in ANPC and Npc1-null mice. **A**, Survival curve showing that 2-HPC treatment significantly prolonged the life of both ANPC and Npc1-null mice ($p \leq 0.0001$ by log rank test) compared to saline-treated mice. **B** and **C**, Histograms showing that 2-HPC treatment significantly improved the performance of Npc1-null and ANPC mice in 3-hr object recognition memory (B) and rotarod (C) tests compared to their respective saline-treated control groups but had no effect on the WT animals. Values are means± SEM, with n = 6-10 for each group. *, $P<0.05$.

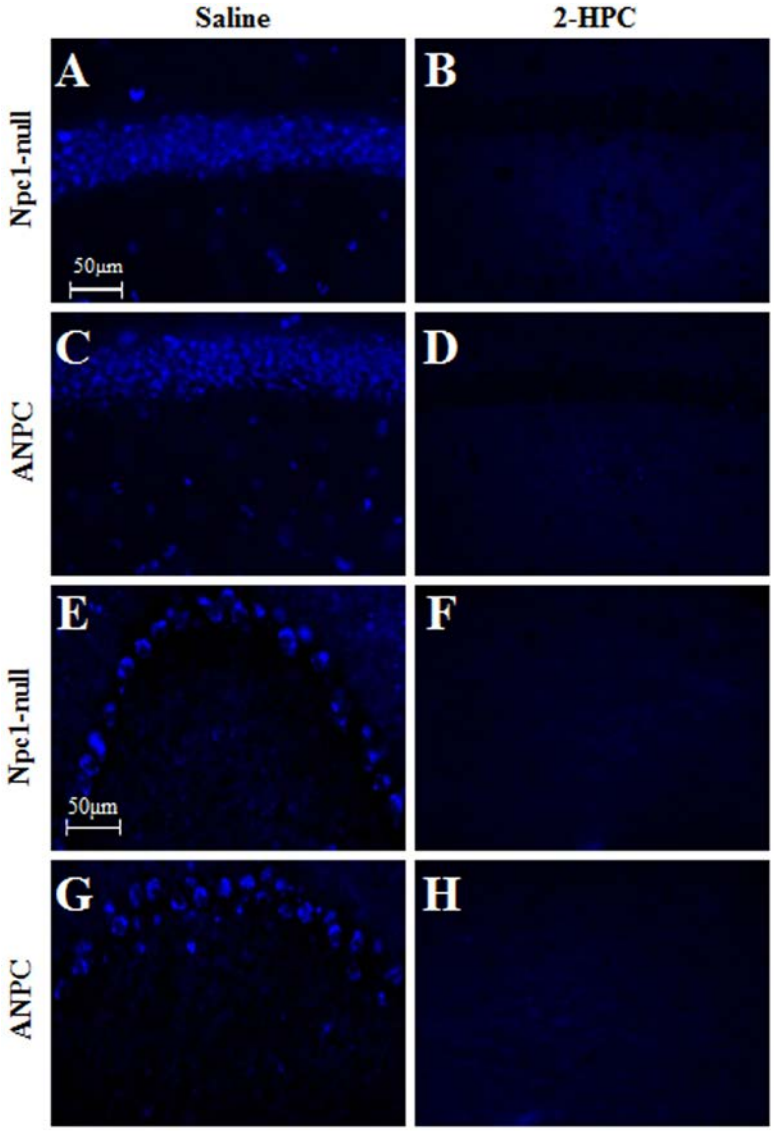

Figure 3.11: A-H, Effect of 2-hydroxypropyl-β-cyclodextrin (2-HPC) treatment on cholesterol accumulation in Npc1-null and ANPC mice. Filipin labeling in the hippocampal (A, B, C, D) and cerebellar (E, F, G, H) brain sections of Npc1-null (A, B, E, F) and ANPC (C, D, G, H) mice revealed no apparent cholesterol accumulation in 2-HPC-treated mice compared to saline-treated control mice. n = 3-4 animals per treatment group.

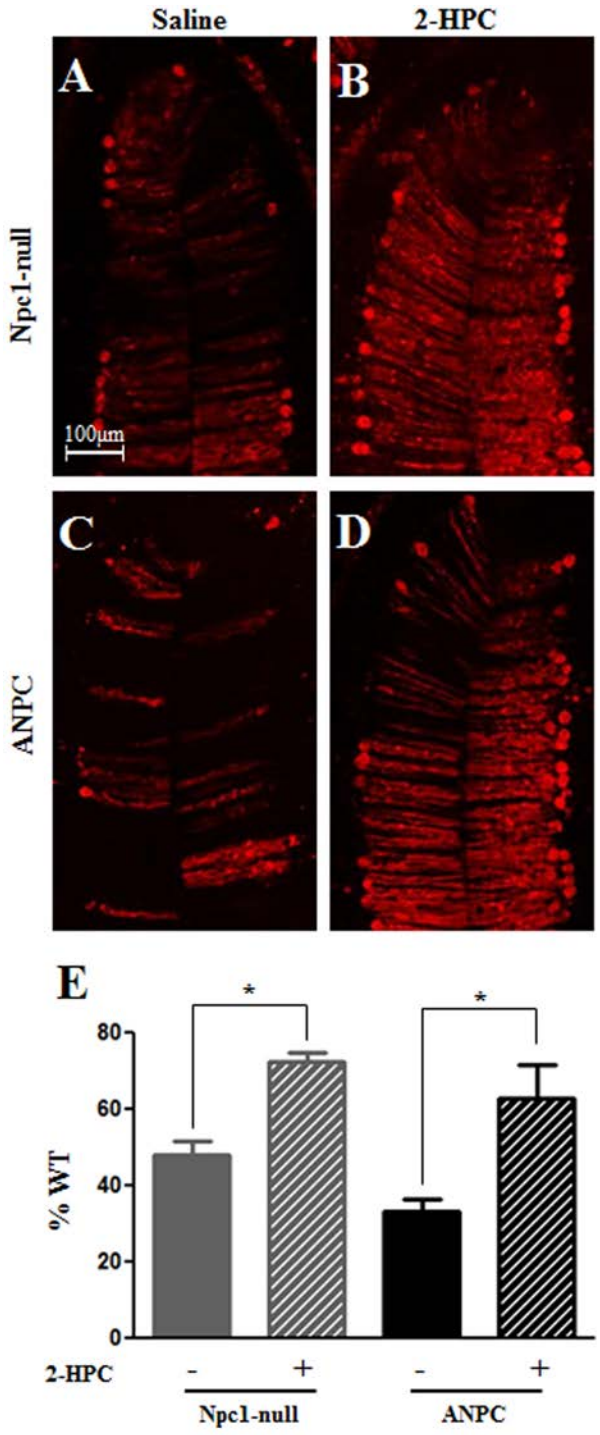

Figure 3.12: A-E, Photomicrographs and histograms showing the effect of 2-hydroxypropyl-β-cyclodextrin (2-HPC) treatment on the cerebellar Purkinje cell viability in Npc1-null and ANPC mice. **A-D,** Representative cerebellar sections from 7 week old saline- (A, C) and 2-HPC- (B, D) treated Npc1-null (A, B) and ANPC (C, D) mice showing calbindin-positive Purkinje cell layer. **E,** Quantitative analysis revealed a significant increase in the survival of cerebellar Purkinje cells in 2-HPC-treated Npc1-null and ANPC mice compared to respective saline-treated control mice. Values are means ± SEM, with n = 3-4 animals for each group. *, $P<0.05$.

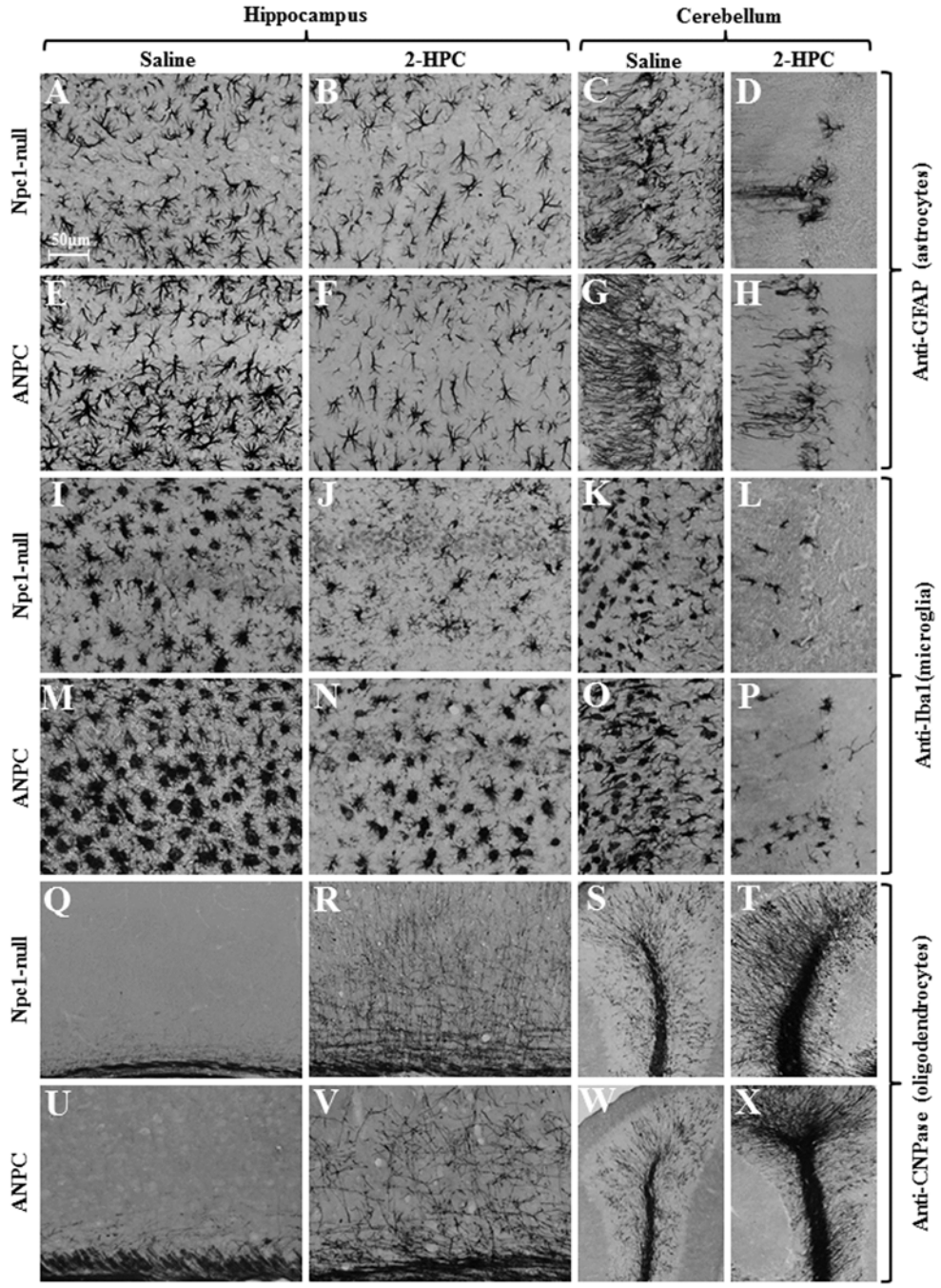

Figure 3.13: A-X, Photomicrographs showing the effect of 2-hydroxypropyl-β-cyclodextrin (2-HPC) treatment on different glial markers in the hippocampus and cerebellum of Npc1-null and ANPC mice. Note the attenuation in the proliferation/activation of GFAP-labeled astrocytes (A-H) and Iba1-labeled microglia (I-P) in the hippocampus (A, B, E, F, I, J, M, N) and cerebellum (C, D, G, H, K, L, O, P) of 2-HPC-treated Npc1-null (B, D, J, L) and ANPC (F, H, N, P) mice compared to respective saline-treated control (A, C, E, G, I, K, M, O) mice. The expression of CNPase-immunoreactive oligodendrocytes was found to be increased in the hippocampus (Q, R, U, V) and cerebellum (S, T, W, X) of 2-HPC-treated Npc1-null (R, T) and ANPC (V, X) mice compared to respective saline-treated control (Q, S, U, W) mice. n = 3-4 animals per treatment group.

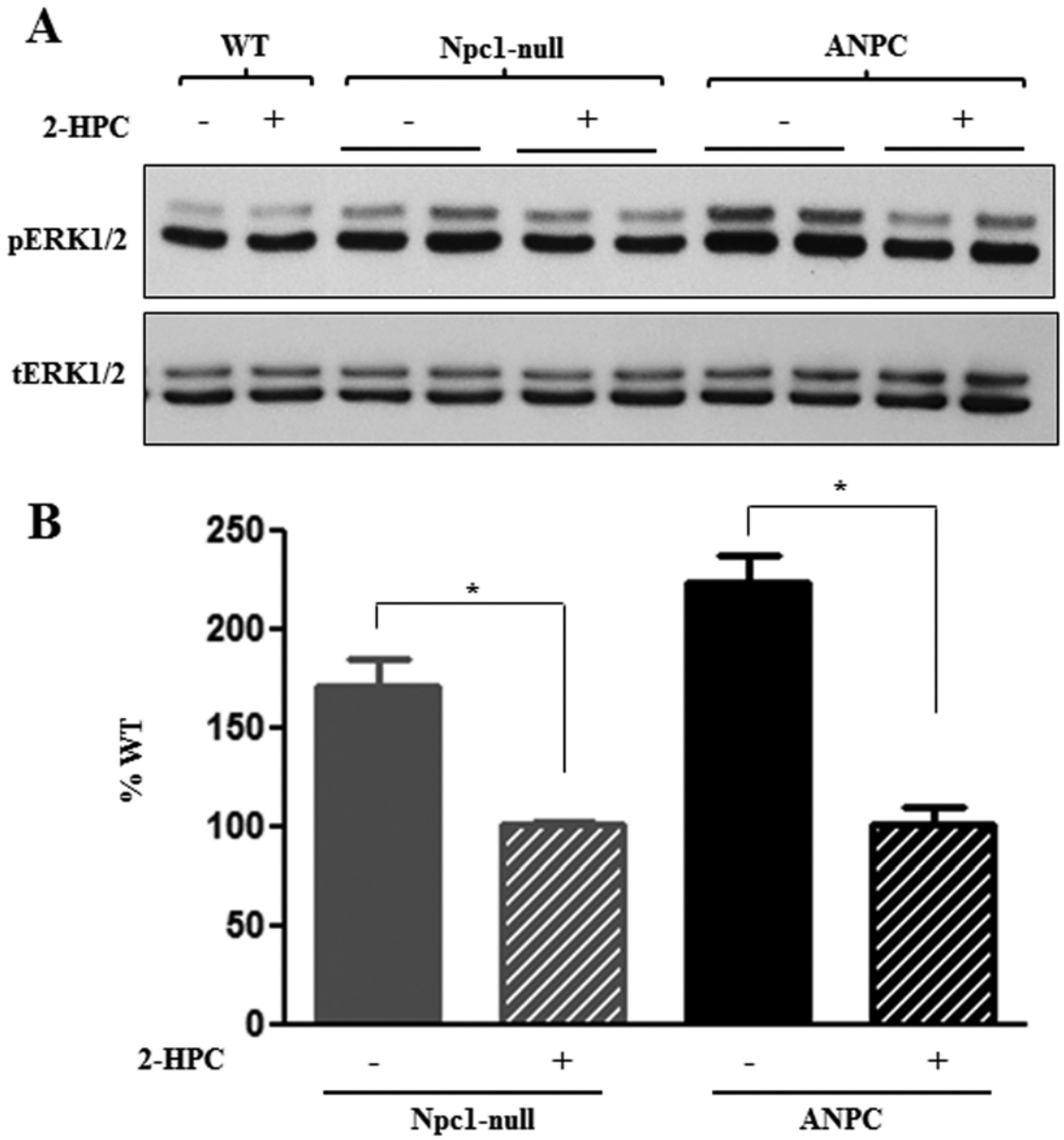

Figure 3.14: **A** and **B**, Immunoblot analysis showing the effect of 2-hydroxypropyl-β-cyclodextrin (2-HPC) treatment on phospho-ERK1/2 levels in Npc1-null and ANPC mice. **A**, Representative immunoblots illustrating reversal in the increase of phospho-ERK1/2 levels in 7 week old Npc1-null and ANPC cerebellum following 2-HPC treatment. **B**, Quantitative analysis of phospho-ERK1/2 normalized to total ERK levels illustrating significant down-regulation in phosho-ERK1/2 levels in 2-HPC-treated Npc1-null and ANPC compared to their respective saline-treated groups. Values are means ± SEM, with n = 4 for each group. *, $P<0.05$.

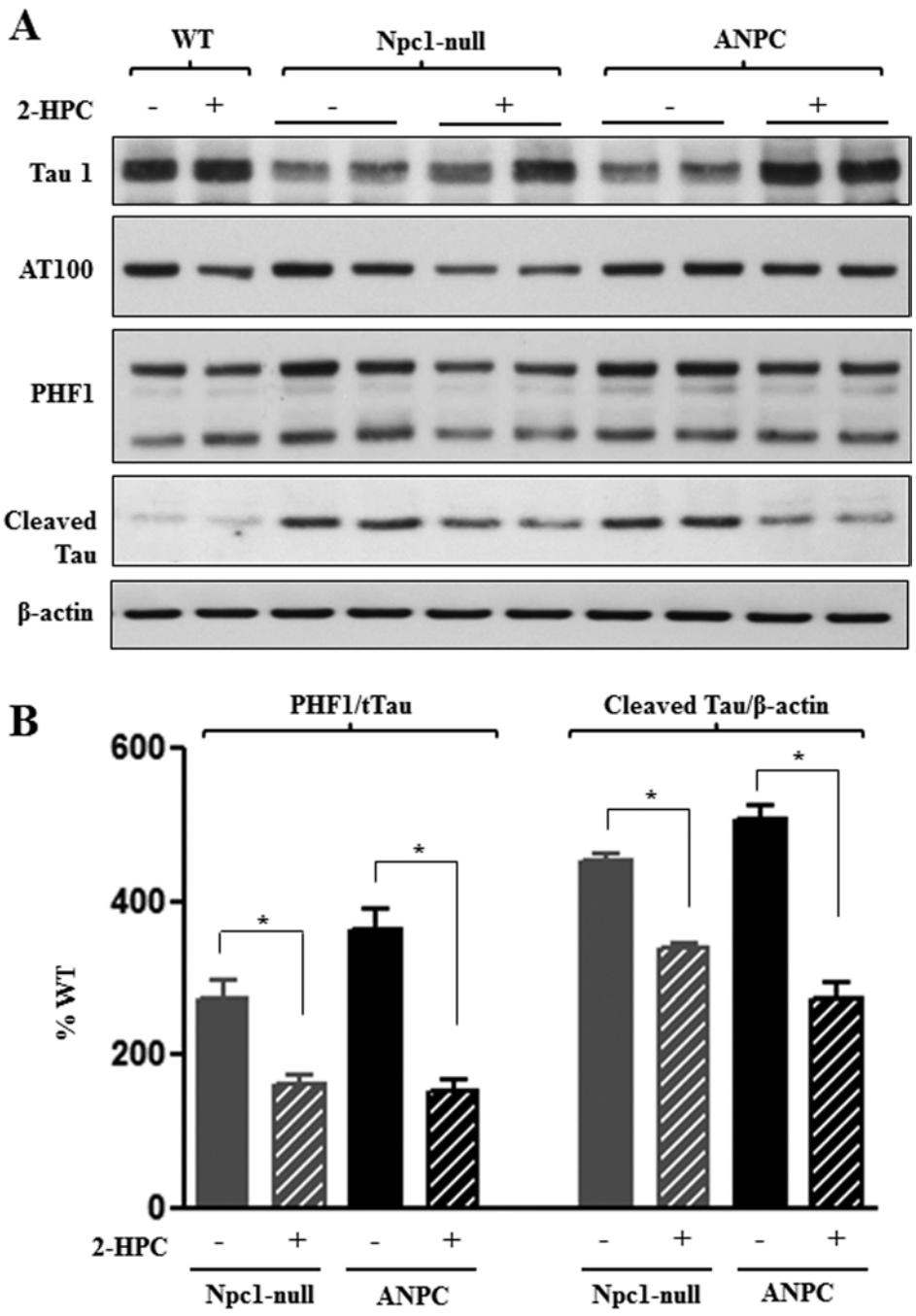

Figure 3.15: A and **B,** Immunoblot analysis showing the effect of 2-hydroxypropyl-β-cyclodextrin (2-HPC) treatment on total, phospho and cleaved tau levels in Npc1-null and ANPC mice. **A**, Representative immunoblots illustrating reversal in the decrease of total tau but no alterations in phospho-tau levels in 7 weeks old Npc1-null and ANPC cerebellum following 2-HPC treatment. Increased levels of caspase-cleaved tau were also attenuated in 2-HPC-treated Npc1-null and ANPC mice compared to their respective saline treated control mice. **B**, Quantitative analysis showing reduced phospho-tau/total tau ratio and cleaved tau products in the cerebellum of 2-HPC-treated 7 week old Npc1-null and ANPC compared to their respective saline-treated groups. Values are means ± SEM, with n = 4 for each group. *, $P<0.05$.

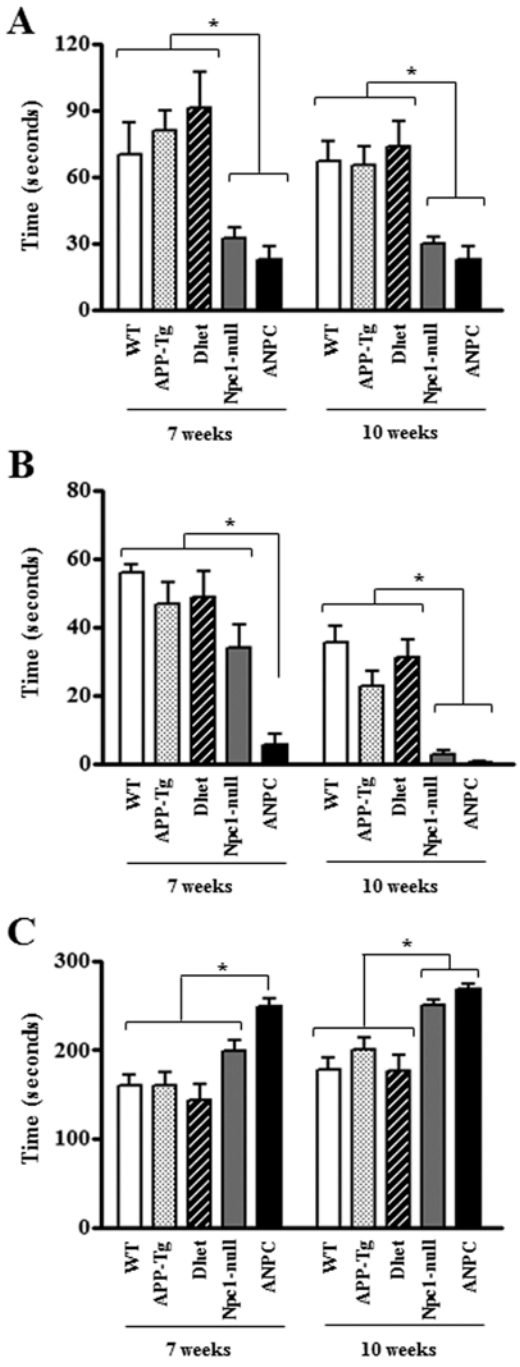

Figure 3.16: *Suppl. Figure 1;* **A-C**, Open-field activity assessed at 7- and 10-weeks of age in WT, APP-Tg, Dhet, Npc1-null and ANPC mice. **(A)** Walking was significantly reduced in ANPC and Npc1-null mice compared to other genotypes both at 7 and 10 weeks of age. **(B)** Rearing was significantly decreased in 7 and 10 week old ANPC mice as well as 10 week old Npc1-null mice compared to WT, APP-Tg and Dhet genotypes. **(C)** Period of inactivity was significantly enhanced in ANPC mice at both 7 and 10 weeks of age. Npc1-null mice showed significantly enhanced periods of inactiveness during the test period only at 10 weeks but not at 7 weeks compared to WT, APP-Tg and Dhet genotypes. Data represent means ± SEM with n = 6-10 for each genotype. *, $P<0.05$.

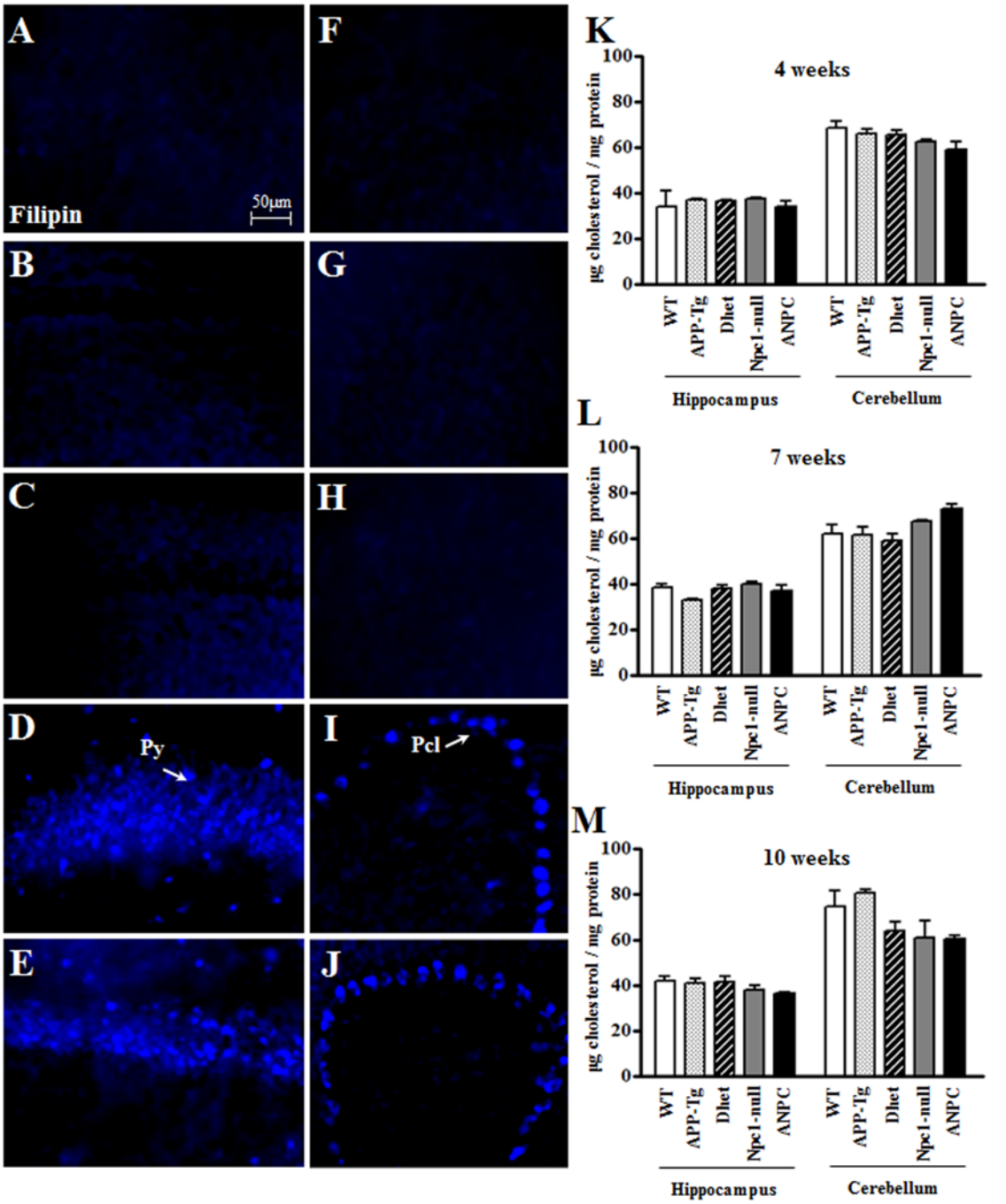

Figure 3.17: *Suppl. Figure 2;* **A-J**, Photomicrographs showing filipin staining of unesterified cholesterol in the hippocampal pyramidal (Py) neurons (A-E) and cerebellar Purkinje cell layer (Pcl) (F-J) of 4-week old WT, APP-Tg, Dhet, Npc1-null and ANPC mice. Accumulation of unesterified cholesterol is evident in the hippocampus and cerebellum of Npc1-null (D, I) and ANPC (E, J) mice but not in WT (A, F), APP-Tg (B, G) or Dhet (C, H) mice. **K-M,** Histograms showing total cholesterol levels in the hippocampus and cerebellum of 4-, 7-, and 10-week old WT, APP-Tg, Dhet, Npc1-null and ANPC mice as measured by gas chromatography. No significant alteration in cholesterol levels was evident in any brain region between different lines of mice at any age-group. Values are means ± SEM; n = 4 animals per genotype and age group.

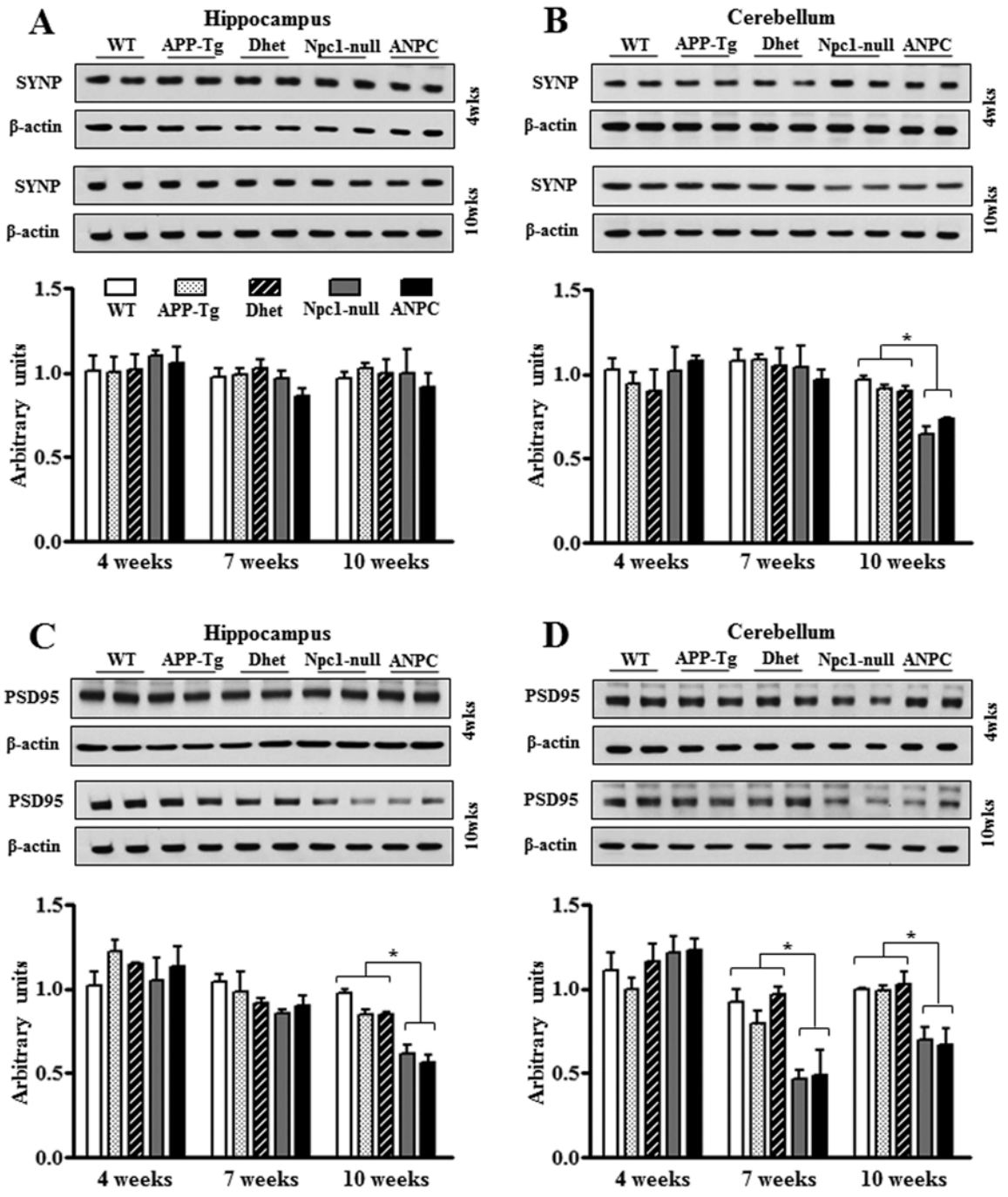

Figure 3.18: *Suppl. Figure 3;* **A** and **B**, Immunoblots and respective histograms depicting synaptophysin (SYNP) levels in the hippocampus (A) and cerebellum (B) of 4-, 7- and 10-week old WT, APP-Tg and Dhet, Npc1-null and ANPC mice. Note the significant decrease in SYNP levels in Npc1-null and ANPC cerebellum at 10-weeks compared to other lines of mice. **C** and **D**, Immunoblots and respective histograms showing the decreased levels of PSD-95 in 10-week hippocampus (C) and 7- and 10-week cerebellum (D) of Npc1-null and ANPC mice compared to age-matched WT, APP-Tg and Dhet mice. Values are means ± SEM; n = 4-6 animals per genotype and age group.

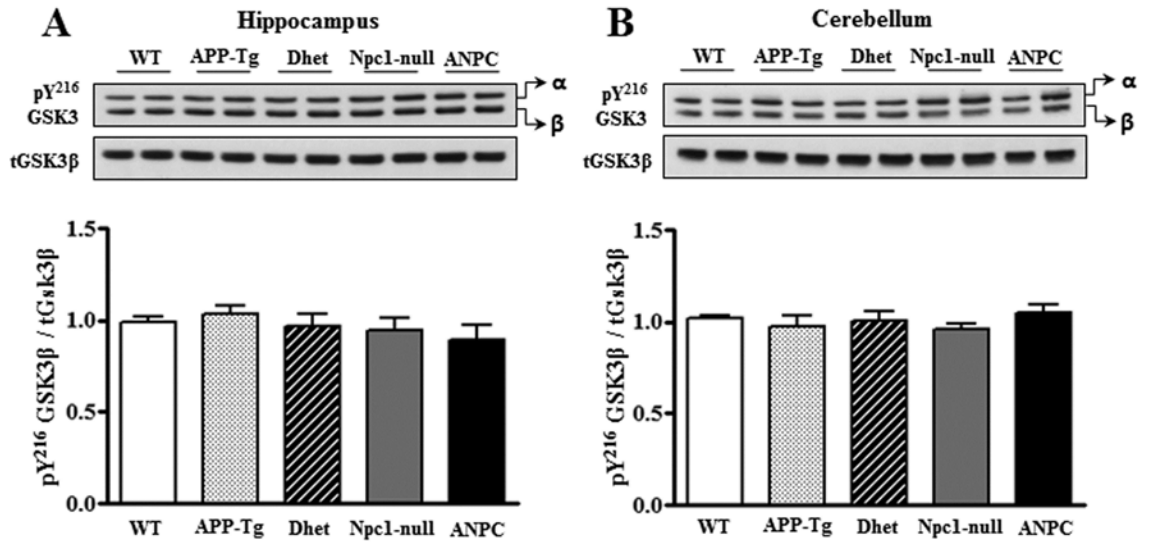

Figure 3.19: *Suppl. Figure 4;* **A** and **B**, Immunoblot analysis of phospho-Tyr^{216}GSK-3β and anti-GSK-3β levels in 7-week old WT, APP-Tg and Dhet, Npc1-null and ANPC mice hippocampus (A) and cerebellum (B). Quantitative analysis revealed no significant alteration in phospho-Tyr^{216}GSK-3β level in the hippocampus or cerebellum between the different genotype combinations. Values are means ± SEM; n = 4-6 animals per genotype and age group. *, P<0.05.

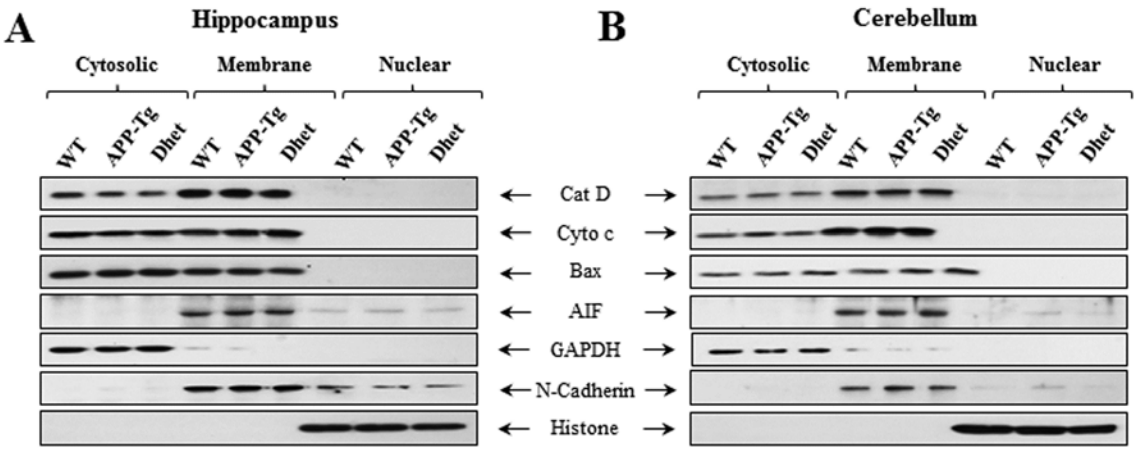

Figure 3.20: *Suppl. Figure 5;* **A** and **B**, Immunoblots showing subcellular distribution of Cat D, Cyto c, Bax and AIF in the hippocampus (A) and cerebellum (B) of 7-week old WT, APP-Tg and Dhet mice. None of these proteins show any alteration in their levels in the different subcellular compartments when compared between the genotypes. Immunoblots for GAPDH, N-cadherin and Histone represent the loading controls for the cytosolic, membrane and nuclear fractions respectively. Cat D, Cathepsin D; Cyto c, Cytochrome c; Bax, Bcl-2-associated X ptotein; AIF, Apoptosis Inducing Factor; GAPDH, Glyceraldehyde-3-Phosphate Dehydrogenase.

3.4 Discussion

Using a new line of bigenic ANPC mice, the present study shows that overexpression of APP in the absence of functional Npc1 protein can significantly decrease longevity, impair motor and object recognition memory functions, exacerbate glial pathology and accelerate degeneration of neurons. This is accompanied by altered function of the endosomal-lysosomal system and increased phosphorylation and cleavage of tau protein. Neuropathological abnormalities are more profound in the cerebellum, exhibiting a significant loss of neurons compared to the relatively spared hippocampus in ANPC mice. This is supported by results which showed that: i) proliferation of astrocytes and microglia and loss of myelin are notably higher in the cerebellum than the hippocampus, ii) phosphorylation and cleavage of tau protein are selectively enhanced in the cerebellum and iii) cytosolic levels of cathepsin D, cytochrome c and Bax are increased more predominantly in the cerebellum than the hippocampus. It is also of interest to note that cerebellar dysfunctions in ANPC mice are conspicuously more severe than in Npc1-null, Dhet, APP-Tg and WT mice. Reversal of accumulated cholesterol by 2-HPC treatment not only prolongs life-span but also attenuates behavioral and glial pathology in ANPC mice. This is accompanied by enhanced survival of neurons and decreased phosphorylation/cleavage of tau protein. Collectively, these results suggest that overexpression of APP in Npc1-null mice can influence longevity as well as a wide spectrum of behavioral and neuronal abnormalities associated with NPC disease, whereas reversal of cholesterol accumulation is beneficial in attenuating these abnormalities.

Multiple lines of evidence have shown that elevated cholesterol levels can influence APP metabolism as well as AD-related pathology (50). Conversely, APP-Tg mice exhibit altered levels of lipids surrounding plaque cores that may have a role in the dynamic of amyloid aggregation (51). The present study clearly reveals that APP overexpression did not elicit any obvious alterations in either intracellular accumulation or total levels of cholesterol in Npc1-null mice. This could possibly reflect a compensatory adjustment where increased cholesterol levels in the cell bodies are obscured by its reduction in myelin, the major repository of cholesterol in the central nervous system (26). Overexpression of APP, however, drastically reduces the life-span

of Npc1-null mice along with a progressive decline in their body weight. This is interesting in context of the results which showed that decreasing *de novo* cholesterol synthesis/turnover by deleting the 24-hydroxylase gene can prolong the life-span of APP-Tg mice (52). Accompanying the mortality rate, object recognition memory and a spectrum of sensorimotor functions including locomotor activity and gait coordination are impaired earlier in ANPC mice than Npc1-null, APP-Tg, Dhet and WT mice. Given the evidence that all these mice were generated on the same outbred genetic background, the behavioral changes observed in ANPC mice most likely reflect the influence of APP overexpression in the context of an Npc1-null genotype, rather than the coincident segregation of (hypothetical) modifier genes. Prior studies have reported motor impairments in Npc1-null mice (41) and object memory deficits in APP-Tg mice without any evidence of motor dysfunction (30). Our results, however, reveal that overexpression of APP induces early motor and object memory deficits in Npc1-null mice compared to other littermates. While object memory relies on the integrity of entorhinal-hippocampal circuitry (53), the cerebellum is known to play a critical role in regulating normal motor activity (39, 54). The early manifestation of behavioral deficits in ANPC mice possibly relates to their neuropathological abnormalities that precede those found in Npc1-null and APP-Tg mice.

Earlier studies have shown activation of both astrocytes and microglia in APP-Tg and Npc1-null mice, but loss of myelin only in Npc1-null mice (5, 10, 55). The overall glial pathology in ANPC mice is markedly exacerbated at the earlier stages compared to other littermates, whereas at the later stages it varies from other genotypes except Npc1-null mice. This suggests that APP overexpression may induce early glial activation in Npc1-null mice which can subsequently influence disease pathology. This is partly reflected in the loss of cerebellar Purkinje cells which is more severe in ANPC than in Npc1-null mice. Interestingly, hippocampal neurons, even though they accumulate cholesterol, are found to be relatively spared in ANPC mice as observed in Npc1-null mice. It is possible that these neurons are being protected against toxic insult by an up-regulation of survival mechanisms as demonstrated in mutant APP-Tg mice (56) or they might be vulnerable if the animals would have lived longer.

Most APP-Tg mice do not exhibit any overt loss of neurons, but there is evidence that defective steroidogenesis (57), abnormal lipid trafficking (58) and production of inflammatory molecules (10) from glia can negatively affect NPC disease progression and neuronal viability. This is supported by the observation that an astrocyte-targeted Npc1 transgene can enhance lifespan and decrease neurodegeneration in Npc1-null mice (59). However, two independent studies using a mouse chimera (60) or a conditional knock-out of Npc1 (39) have demonstrated cell autonomous death of Purkinje neurons. Additionally, neuron-targeted Npc1 gene expression was able to protect neurons and prolong life-span in Npc1-null mice (61), suggesting the loss of Npc1 function in neurons rather than glia may be responsible for the loss of neurons in ANPC mice.

At present, the precise mechanism that may underlie degeneration of neurons in either AD or NPC brain remains unclear, but there is evidence of up-regulation of lysosomal enzymes in “at-risk” neurons in both the diseases (7, 62). This is substantiated by our study which shows an increased level and activity of the cathepsin D both in the hippocampus and cerebellum of ANPC and Npc1-null mice. Our subcellular data, on the other hand, show that cytosolic levels of cathepsin D are markedly increased in the cerebellum, but only slightly increased in the relatively spared hippocampus of Npc1-null and ANPC mice compared to WT controls. This is accompanied by a parallel increase in the cytosolic levels of cytochrome c and Bax in the cerebellum of Npc1-null and ANPC mice. The magnitude of cytosolic cathepsin D level, in keeping with the loss of neurons, is found to be markedly higher in ANPC than Npc1-null mice. There is evidence that increased activity of enzymes within lysosomes or limited release of enzymes into the cytosol can prevent sub-lethal damage, whereas sustained release of the enzymes into the cytosol can induce cell death (47, 48). Thus, it is likely that enhanced levels of cathepsin D in the hippocampus may counter cellular abnormalities resulting from APP overexpression/cholesterol accumulation or may not reach levels necessary to mediate cell death. On the other hand, larger increases in cytosolic levels of the enzyme in the cerebellum, resulting from lysosomal destabilization, may lead to death of neurons. This is supported by two lines of evidence: i) Purkinje cells, but not hippocampal neurons, are labeled with cleaved caspase-3 in ANPC and Npc1-null mice and ii) cytosolic cathepsin

D levels did not differ in hippocampus or cerebellum among APP-Tg, Dhet and WT mice, which do not exhibit any loss of neurons.

Apart from lysosomal dysfunction the presence of tau-positive NFTs represents a striking similarity between AD and NPC pathologies (15, 16). The formation of tangles resulting from phosphorylation of tau protein has been implicated in the degeneration of neurons in many taupathies including NPC and AD brains by triggering loss of microtubule binding and impaired axonal transport (63). Tau phosphorylation is usually mediated in a site-specific manner by various kinases including ERK1/2, GSK-3β and Cdk-5 (64, 65). Although tau is known to be phosphorylated in APP-Tg and Npc1-null mice there is no evidence of its association to the loss of neurons or tangle formation in any regions of the brain (66-68). Our results clearly show that while the total tau levels are decreased, phospho-tau levels in relation to total tau are increased in the cerebellum but not in the hippocampus of ANPC and Npc1-null mice. These changes are significantly higher in ANPC than Npc1-null mice and are accompanied by an increase in phospho-ERK1/2 and a decrease in p35 levels. Since partial or complete loss of tau expression can reduce life-span and exacerbate pathology in Npc1-null mice (69) and inhibitors of Cdk-5 can attenuate tau phosphorylation as well as the phenotype in Npc1-null mice (41, 70), it is likely that alterations in the levels and phosphorylation of tau in the cerebellum of ANPC and Npc1-null mice may be involved in the loss of Purkinje neurons. Additionally, we showed that caspase-cleaved tau levels are selectively increased and expressed in the Purkinje neurons of ANPC and Npc1-null mice. Since truncated tau generated by caspases tends to assemble more rapidly into filaments than full-length tau (71, 72) and is able to trigger neurodegeneration by reducing the pool of full length tau available for binding to microtubules (44-46), it is likely that cleaved tau in ANPC and Npc1-null mice may also contribute to the loss of Purkinje neurons.

Since neuropathological abnormalities in mutant ANPC mice were evident primarily in brain regions that are preferentially vulnerable to cholesterol accumulation in NPC pathology, we treated the animals with 2-HPC - which binds to cholesterol and facilitates its exit from lysosomes even in the absence of functional Npc1 protein (73). A

number of recent studies have shown that single or repeated administration of 2-HPC can increase life-span, delay motor impairments and reduce neuronal cholesterol accumulation in Npc1-null mice. Additionally, 2-HPC treatment is able to attenuate degeneration of neurons as well as glial pathology in Npc1-null mice (33-35, 74). Our results also clearly show that single systemic administration of 2-HPC at postnatal day 7 can not only prevent cholesterol accumulation but can also prolong the life-span and attenuate both motor and object recognition memory deficits in ANPC and Npc1-null mice. Additionally, a marked reduction in the glial pathology and protection of Purkinje cells are apparent in 2-HPC-treated ANPC and Npc1-null mice compared to respective saline-treated mice. These cellular changes are accompanied by significant reversal of phospho-ERK1/2 levels as well as phosphorylation and cleavage of tau in the cerebellum of ANPC and Npc1-null mice. Given the beneficial effects of a single injection, it would be of interest to determine whether repeated injections of 2-HPC over time can completely prevent the dysfunction associated with ANPC mice. Nevertheless, our results clearly show that overexpression of APP in Npc1-null mice can negatively influence longevity as well as a spectrum of behavioral and neuropathological features that can be reversed markedly by 2-HPC treatment. Additionally, this study raises the possibility of a functional interaction between APP and NPC1 that may have a role in the development of both AD and NPC diseases.

3.5 References

1. Mukherjee, S. and Maxfield, F.R. (2004) Lipid and cholesterol trafficking in NPC. *Biochim Biophys Acta,* 1685, 28-37.

2. Pacheco, C.D. and Lieberman, A.P. (2008) The pathogenesis of Niemann-Pick type C disease: a role for autophagy? *Expert Rev Mol Med,* 10, e26.

3. Carstea, E.D., Morris, J.A., Coleman, K.G., Loftus, S.K., Zhang, D., Cummings, C., Gu, J., Rosenfeld, M.A., Pavan, W.J., Krizman, D.B. *et al.* (1997) Niemann-Pick C1 disease gene: homology to mediators of cholesterol homeostasis. *Science,* 277, 228-231.

4. Walkley, S.U. and Suzuki, K. (2004) Consequences of NPC1 and NPC2 loss of function in mammalian neurons. *Biochim Biophys Acta,* 1685, 48-62.

5. Kodam, A., Maulik, M., Peake, K., Amritraj, A., Vetrivel, K.S., Thinakaran, G., Vance, J.E. and Kar, S. (2010) Altered levels and distribution of amyloid precursor protein and its processing enzymes in Niemann-Pick type C1-deficient mouse brains. *Glia,* 58, 1267-1281.

6. Li, H., Repa, J.J., Valasek, M.A., Beltroy, E.P., Turley, S.D., German, D.C. and Dietschy, J.M. (2005) Molecular, anatomical, and biochemical events associated with neurodegeneration in mice with Niemann-Pick type C disease. *J Neuropathol Exp Neurol,* 64, 323-333.

7. Jin, L.W., Shie, F.S., Maezawa, I., Vincent, I. and Bird, T. (2004) Intracellular accumulation of amyloidogenic fragments of amyloid-beta precursor protein in neurons with Niemann-Pick type C defects is associated with endosomal abnormalities. *Am J Pathol,* 164, 975-985.

8. Mattsson, N., Zetterberg, H., Bianconi, S., Yanjanin, N.M., Fu, R., Mansson, J.E., Porter, F.D. and Blennow, K. (2011) Gamma-secretase-dependent amyloid-beta is increased in Niemann-Pick type C: a cross-sectional study. *Neurology,* 76, 366-372.

9. Saito, Y., Suzuki, K., Nanba, E., Yamamoto, T., Ohno, K. and Murayama, S. (2002) Niemann-Pick type C disease: accelerated neurofibrillary tangle formation and amyloid beta deposition associated with apolipoprotein E epsilon 4 homozygosity. *Ann Neurol,* 52, 351-355.

10. Baudry, M., Yao, Y., Simmons, D., Liu, J. and Bi, X. (2003) Postnatal development of inflammation in a murine model of Niemann-Pick type C disease: immunohistochemical observations of microglia and astroglia. *Exp Neurol,* 184, 887-903.

11. German, D.C., Quintero, E.M., Liang, C.L., Ng, B., Punia, S., Xie, C. and Dietschy, J.M. (2001) Selective neurodegeneration, without neurofibrillary tangles, in a mouse model of Niemann-Pick C disease. *J Comp Neurol,* 433, 415-425.

12. Goate, A. and Hardy, J. (2012) Twenty years of Alzheimer's disease-causing mutations. *J Neurochem*, 120 Suppl 1, 3-8.

13. Selkoe, D.J. (2008) Biochemistry and molecular biology of amyloid beta-protein and the mechanism of Alzheimer's disease. In *Handb Clin Neurol* Vol. 89, pp. 245-260.

14. St George-Hyslop, P.H., McLaurin, J. and Fraser, P.E. (2000) Neuropathological, biochemical and genetic alterations in AD. *Drug News Perspect*, 13, 281-288.

15. Auer, I.A., Schmidt, M.L., Lee, V.M., Curry, B., Suzuki, K., Shin, R.W., Pentchev, P.G., Carstea, E.D. and Trojanowski, J.Q. (1995) Paired helical filament tau (PHFtau) in Niemann-Pick type C disease is similar to PHFtau in Alzheimer's disease. *Acta Neuropathol*, 90, 547-551.

16. Ohm, T.G., Treiber-Held, S., Distl, R., Glockner, F., Schonheit, B., Tamanai, M. and Meske, V. (2003) Cholesterol and tau protein--findings in Alzheimer's and Niemann Pick C's disease. *Pharmacopsychiatry*, 36 Suppl 2, S120-126.

17. Kim, J., Basak, J.M. and Holtzman, D.M. (2009) The role of apolipoprotein E in Alzheimer's disease. *Neuron*, 63, 287-303.

18. Poirier, J., Davignon, J., Bouthillier, D., Kogan, S., Bertrand, P. and Gauthier, S. (1993) Apolipoprotein E polymorphism and Alzheimer's disease. *Lancet*, 342, 697-699.

19. Nixon, R.A. (2004) Niemann-Pick Type C disease and Alzheimer's disease: the APP-endosome connection fattens up. *Am J Pathol*, 164, 757-761.

20. Kagedal, K., Kim, W.S., Appelqvist, H., Chan, S., Cheng, D., Agholme, L., Barnham, K., McCann, H., Halliday, G. and Garner, B. (2010) Increased expression of the lysosomal cholesterol transporter NPC1 in Alzheimer's disease. *Biochim Biophys Acta*, 1801, 831-838.

21. Kivipelto, M., Helkala, E.L., Laakso, M.P., Hanninen, T., Hallikainen, M., Alhainen, K., Iivonen, S., Mannermaa, A., Tuomilehto, J., Nissinen, A. *et al.* (2002) Apolipoprotein E epsilon4 allele, elevated midlife total cholesterol level, and high midlife systolic blood pressure are independent risk factors for late-life Alzheimer disease. *Ann Intern Med*, 137, 149-155.

22. Notkola, I.L., Sulkava, R., Pekkanen, J., Erkinjuntti, T., Ehnholm, C., Kivinen, P., Tuomilehto, J. and Nissinen, A. (1998) Serum total cholesterol, apolipoprotein E epsilon 4 allele, and Alzheimer's disease. *Neuroepidemiology*, 17, 14-20.

23. Distl, R., Meske, V. and Ohm, T.G. (2001) Tangle-bearing neurons contain more free cholesterol than adjacent tangle-free neurons. *Acta Neuropathol*, 101, 547-554.

24. Fassbender, K., Simons, M., Bergmann, C., Stroick, M., Lutjohann, D., Keller, P.,

Runz, H., Kuhl, S., Bertsch, T., von Bergmann, K. *et al.* (2001) Simvastatin strongly reduces levels of Alzheimer's disease beta -amyloid peptides Abeta 42 and Abeta 40 in vitro and in vivo. *Proc Natl Acad Sci U S A*, 98, 5856-5861.

25. Grimm, M.O., Grimm, H.S., Tomic, I., Beyreuther, K., Hartmann, T. and Bergmann, C. (2008) Independent inhibition of Alzheimer disease beta- and gamma-secretase cleavage by lowered cholesterol levels. *J Biol Chem*, 283, 11302-11311.

26. Martin, M., Dotti, C.G. and Ledesma, M.D. (2010) Brain cholesterol in normal and pathological aging. *Biochim Biophys Acta*, 1801, 934-944.

27. Refolo, L.M., Pappolla, M.A., LaFrancois, J., Malester, B., Schmidt, S.D., Thomas-Bryant, T., Tint, G.S., Wang, R., Mercken, M., Petanceska, S.S. *et al.* (2001) A cholesterol-lowering drug reduces beta-amyloid pathology in a transgenic mouse model of Alzheimer's disease. *Neurobiol Dis*, 8, 890-899.

28. Adalbert, R., Nogradi, A., Babetto, E., Janeckova, L., Walker, S.A., Kerschensteiner, M., Misgeld, T. and Coleman, M.P. (2009) Severely dystrophic axons at amyloid plaques remain continuous and connected to viable cell bodies. *Brain*, 132, 402-416.

29. Chishti, M.A., Yang, D.S., Janus, C., Phinney, A.L., Horne, P., Pearson, J., Strome, R., Zuker, N., Loukides, J., French, J. *et al.* (2001) Early-onset amyloid deposition and cognitive deficits in transgenic mice expressing a double mutant form of amyloid precursor protein 695. *J Biol Chem*, 276, 21562-21570.

30. Francis, B.M., Kim, J., Barakat, M.E., Fraenkl, S., Yucel, Y.H., Peng, S., Michalski, B., Fahnestock, M., McLaurin, J. and Mount, H.T. (2012) Object recognition memory and BDNF expression are reduced in young TgCRND8 mice. *Neurobiol Aging*, 33, 555-563.

31. Reddy, P.H. (2011) Abnormal tau, mitochondrial dysfunction, impaired axonal transport of mitochondria, and synaptic deprivation in Alzheimer's disease. *Brain Res*, 1415, 136-148.

32. Loftus, S.K., Morris, J.A., Carstea, E.D., Gu, J.Z., Cummings, C., Brown, A., Ellison, J., Ohno, K., Rosenfeld, M.A., Tagle, D.A. *et al.* (1997) Murine model of Niemann-Pick C disease: mutation in a cholesterol homeostasis gene. *Science*, 277, 232-235.

33. Davidson, C.D., Ali, N.F., Micsenyi, M.C., Stephney, G., Renault, S., Dobrenis, K., Ory, D.S., Vanier, M.T. and Walkley, S.U. (2009) Chronic cyclodextrin treatment of murine Niemann-Pick C disease ameliorates neuronal cholesterol and glycosphingolipid storage and disease progression. *PLoS One*, 4, e6951.

34. Liu, B., Turley, S.D., Burns, D.K., Miller, A.M., Repa, J.J. and Dietschy, J.M. (2009) Reversal of defective lysosomal transport in NPC disease ameliorates liver

dysfunction and neurodegeneration in the npc1-/- mouse. *Proc Natl Acad Sci U S A,* 106, 2377-2382.

35. Ramirez, C.M., Liu, B., Taylor, A.M., Repa, J.J., Burns, D.K., Weinberg, A.G., Turley, S.D. and Dietschy, J.M. (2010) Weekly cyclodextrin administration normalizes cholesterol metabolism in nearly every organ of the Niemann-Pick type C1 mouse and markedly prolongs life. *Pediatr Res,* 68, 309-315.

36. Vaucher, E., Fluit, P., Chishti, M.A., Westaway, D., Mount, H.T. and Kar, S. (2002) Object recognition memory and cholinergic parameters in mice expressing human presenilin 1 transgenes. *Exp Neurol,* 175, 398-406.

37. D'Hooge, R., Hartmann, D., Manil, J., Colin, F., Gieselmann, V. and De Deyn, P.P. (1999) Neuromotor alterations and cerebellar deficits in aged arylsulfatase A-deficient transgenic mice. *Neurosci Lett,* 273, 93-96.

38. Amritraj, A., Peake, K., Kodam, A., Salio, C., Merighi, A., Vance, J.E. and Kar, S. (2009) Increased activity and altered subcellular distribution of lysosomal enzymes determine neuronal vulnerability in Niemann-Pick type C1-deficient mice. *Am J Pathol,* 175, 2540-2556.

39. Elrick, M.J., Pacheco, C.D., Yu, T., Dadgar, N., Shakkottai, V.G., Ware, C., Paulson, H.L. and Lieberman, A.P. (2010) Conditional Niemann-Pick C mice demonstrate cell autonomous Purkinje cell neurodegeneration. *Hum Mol Genet,* 19, 837-847.

40. Liu, B., Li, H., Repa, J.J., Turley, S.D. and Dietschy, J.M. (2008) Genetic variations and treatments that affect the lifespan of the NPC1 mouse. *J Lipid Res,* 49, 663-669.

41. Hao, Y., Pan, D., Zhang, M., Xu, J., Li, L., Wei, J. and Wang, X. (2009) The neuroprotective effects of cyclin-dependent kinase-5 inhibition in mice with Niemann-Pick disease type C. *J Huazhong Univ Sci Technolog Med Sci,* 29, 324-329.

42. Ahmad, I., Lope-Piedrafita, S., Bi, X., Hicks, C., Yao, Y., Yu, C., Chaitkin, E., Howison, C.M., Weberg, L., Trouard, T.P. *et al.* (2005) Allopregnanolone treatment, both as a single injection or repetitively, delays demyelination and enhances survival of Niemann-Pick C mice. *J Neurosci Res,* 82, 811-821.

43. Ohm, T.G. and Meske, V. (2006) Cholesterol, statins and tau. *Acta Neurol Scand Suppl,* 185, 93-101.

44. Guillozet-Bongaarts, A.L., Glajch, K.E., Libson, E.G., Cahill, M.E., Bigio, E., Berry, R.W. and Binder, L.I. (2007) Phosphorylation and cleavage of tau in non-AD tauopathies. *Acta Neuropathol,* 113, 513-520.

45. Park, S.Y. and Ferreira, A. (2005) The generation of a 17 kDa neurotoxic fragment: an alternative mechanism by which tau mediates beta-amyloid-induced

neurodegeneration. *J Neurosci,* 25, 5365-5375.

46. Wang, Y., Garg, S., Mandelkow, E.M. and Mandelkow, E. (2010) Proteolytic processing of tau. *Biochem Soc Trans,* 38, 955-961.

47. Bendiske, J. and Bahr, B.A. (2003) Lysosomal activation is a compensatory response against protein accumulation and associated synaptopathogenesis--an approach for slowing Alzheimer disease? *J Neuropathol Exp Neurol,* 62, 451-463.

48. Chwieralski, C.E., Welte, T. and Buhling, F. (2006) Cathepsin-regulated apoptosis. *Apoptosis,* 11, 143-149.

49. Turk, B., Stoka, V., Rozman-Pungercar, J., Cirman, T., Droga-Mazovec, G., Oresic, K. and Turk, V. (2002) Apoptotic pathways: involvement of lysosomal proteases. *Biol Chem,* 383, 1035-1044.

50. Martins, I.J., Berger, T., Sharman, M.J., Verdile, G., Fuller, S.J. and Martins, R.N. (2009) Cholesterol metabolism and transport in the pathogenesis of Alzheimer's disease. *J Neurochem,* 111, 1275-1308.

51. Kuzyk, A., Kastyak, M., Agrawal, V., Gallant, M., Sivakumar, G., Rak, M., Del Bigio, M.R., Westaway, D., Julian, R. and Gough, K.M. (2010) Association among amyloid plaque, lipid, and creatine in hippocampus of TgCRND8 mouse model for Alzheimer disease. *J Biol Chem,* 285, 31202-31207.

52. Halford, R.W. and Russell, D.W. (2009) Reduction of cholesterol synthesis in the mouse brain does not affect amyloid formation in Alzheimer's disease, but does extend lifespan. *Proc Natl Acad Sci U S A,* 106, 3502-3506.

53. Burwell, R.D., Saddoris, M.P., Bucci, D.J. and Wiig, K.A. (2004) Corticohippocampal contributions to spatial and contextual learning. *J Neurosci,* 24, 3826-3836.

54. Middleton, F.A. and Strick, P.L. (1998) Cerebellar output: motor and cognitive channels. *Trends Cogn Sci,* 2, 348-354.

55. German, D.C., Liang, C.L., Song, T., Yazdani, U., Xie, C. and Dietschy, J.M. (2002) Neurodegeneration in the Niemann-Pick C mouse: glial involvement. *Neuroscience,* 109, 437-450.

56. Stein, T.D. and Johnson, J.A. (2002) Lack of neurodegeneration in transgenic mice overexpressing mutant amyloid precursor protein is associated with increased levels of transthyretin and the activation of cell survival pathways. *J Neurosci,* 22, 7380-7388.

57. Chen, G., Li, H.M., Chen, Y.R., Gu, X.S. and Duan, S. (2007) Decreased estradiol release from astrocytes contributes to the neurodegeneration in a mouse model of Niemann-Pick disease type C. *Glia,* 55, 1509-1518.

58. Lloyd-Evans, E., Morgan, A.J., He, X., Smith, D.A., Elliot-Smith, E., Sillence, D.J., Churchill, G.C., Schuchman, E.H., Galione, A. and Platt, F.M. (2008) Niemann-Pick disease type C1 is a sphingosine storage disease that causes deregulation of lysosomal calcium. *Nat Med*, 14, 1247-1255.

59. Zhang, M., Strnatka, D., Donohue, C., Hallows, J.L., Vincent, I. and Erickson, R.P. (2008) Astrocyte-only Npc1 reduces neuronal cholesterol and triples life span of Npc1-/- mice. *J Neurosci Res*, 86, 2848-2856.

60. Ko, D.C., Milenkovic, L., Beier, S.M., Manuel, H., Buchanan, J. and Scott, M.P. (2005) Cell-autonomous death of cerebellar purkinje neurons with autophagy in Niemann-Pick type C disease. *PLoS Genet*, 1, 81-95.

61. Lopez, M.E., Klein, A.D., Dimbil, U.J. and Scott, M.P. (2011) Anatomically defined neuron-based rescue of neurodegenerative Niemann-Pick type C disorder. *J Neurosci*, 31, 4367-4378.

62. Nixon, R.A. and Cataldo, A.M. (2006) Lysosomal system pathways: genes to neurodegeneration in Alzheimer's disease. *J Alzheimers Dis*, 9, 277-289.

63. Morris, M., Maeda, S., Vossel, K. and Mucke, L. (2011) The many faces of tau. *Neuron*, 70, 410-426.

64. Ballatore, C., Lee, V.M. and Trojanowski, J.Q. (2007) Tau-mediated neurodegeneration in Alzheimer's disease and related disorders. *Nat Rev Neurosci*, 8, 663-672.

65. Dolan, P.J. and Johnson, G.V. (2010) The role of tau kinases in Alzheimer's disease. *Curr Opin Drug Discov Devel*, 13, 595-603.

66. Bellucci, A., Rosi, M.C., Grossi, C., Fiorentini, A., Luccarini, I. and Casamenti, F. (2007) Abnormal processing of tau in the brain of aged TgCRND8 mice. *Neurobiol Dis*, 27, 328-338.

67. Bu, B., Li, J., Davies, P. and Vincent, I. (2002) Deregulation of cdk5, hyperphosphorylation, and cytoskeletal pathology in the Niemann-Pick type C murine model. *J Neurosci*, 22, 6515-6525.

68. Sawamura, N., Gong, J.S., Garver, W.S., Heidenreich, R.A., Ninomiya, H., Ohno, K., Yanagisawa, K. and Michikawa, M. (2001) Site-specific phosphorylation of tau accompanied by activation of mitogen-activated protein kinase (MAPK) in brains of Niemann-Pick type C mice. *J Biol Chem*, 276, 10314-10319.

69. Pacheco, C.D., Elrick, M.J. and Lieberman, A.P. (2009) Tau deletion exacerbates the phenotype of Niemann-Pick type C mice and implicates autophagy in pathogenesis. *Hum Mol Genet*, 18, 956-965.

70. Zhang, M., Li, J., Chakrabarty, P., Bu, B. and Vincent, I. (2004) Cyclin-dependent

kinase inhibitors attenuate protein hyperphosphorylation, cytoskeletal lesion formation, and motor defects in Niemann-Pick Type C mice. *Am J Pathol,* 165, 843-853.

71. Liu, M.C., Kobeissy, F., Zheng, W., Zhang, Z., Hayes, R.L. and Wang, K.K. (2011) Dual vulnerability of tau to calpains and caspase-3 proteolysis under neurotoxic and neurodegenerative conditions. *ASN Neuro,* 3, e00051.

72. Rissman, R.A., Poon, W.W., Blurton-Jones, M., Oddo, S., Torp, R., Vitek, M.P., LaFerla, F.M., Rohn, T.T. and Cotman, C.W. (2004) Caspase-cleavage of tau is an early event in Alzheimer disease tangle pathology. *J Clin Invest,* 114, 121-130.

73. Rosenbaum, A.I. and Maxfield, F.R. (2011) Niemann-Pick type C disease: molecular mechanisms and potential therapeutic approaches. *J Neurochem,* 116, 789-795.

74. Aqul, A., Liu, B., Ramirez, C.M., Pieper, A.A., Estill, S.J., Burns, D.K., Repa, J.J., Turley, S.D. and Dietschy, J.M. (2011) Unesterified cholesterol accumulation in late endosomes/lysosomes causes neurodegeneration and is prevented by driving cholesterol export from this compartment. *J Neurosci,* 31, 9404-9413.

Chapter 4: Endolysosomal Cholesterol Sequestration Affects Generation and Clearance of Amyloidogenic Peptides of Alzheimer's Disease

4.1 Introduction

Alzheimer's disease (AD), the most common form of dementia affecting the elderly, is characterized by the presence of intracellular tau-positive neurofibrillary tangles, extracellular β-amyloid (Aβ)-containing neuritic plaques and the loss of neurons in selected brain regions such as hippocampus, cortex and certain subcortical nuclei (1, 2). Studies of the pathological changes, and several other lines of evidence, indicate that *in vivo* accumulation of Aβ peptide may contribute to/trigger the loss of neurons and development of pathology associated with the AD brain (3). These peptides are generated from the amyloid precursor protein (APP) which is processed either by non-amyloidogenic α-secretase or amyloidogenic β-secretase pathways (2, 4). The α-secretase cleaves APP within the Aβ domain, yielding soluble APPα and a 10kD C-terminal fragment (α-CTF) that can be further processed by γ-secretase to generate $A\beta_{17-40}$/$A\beta_{17-42}$ fragments. The β-secretase, on the other hand, cleaves APP to generate soluble APPβ and an Aβ-containing C-terminal fragment (β-CTF), which is subsequently processed *via* γ-secretase to yield full-length $A\beta_{1-40}$/$A\beta_{1-42}$ peptides. While α-secretase processing occurs mostly in the secretory pathway, the endosomal-lysosomal system is known to play a critical role in the production of Aβ peptides. The alternative processing of APP can be regulated by multiple factors that influence not only the generation of Aβ peptide but also the development and/or progression of AD pathology (4).

A number of earlier studies have indicated that cholesterol can influence APP processing leading to the generation of Aβ peptides. This is supported by evidence that i) an increase in cellular cholesterol up-regulates, whereas a decrease down-regulates, Aβ generation in cultured neurons/cell lines (5, 6) and ii) a high-cholesterol diet can increase brain Aβ levels and deposition, whereas a low-cholesterol diet can decrease levels and deposition of Aβ peptides in mutant APP transgenic (Tg) mice (5, 7, 8). In contrast to the amyloidogenic processing of APP, some studies have found that increased plasma cholesterol may be associated with unchanged (9) or reduced (10, 11) Aβ levels, while lowering plasma cholesterol may either not affect (12) or elevate (13, 14) brain Aβ levels. These paradoxical results were obtained either under *in vitro* conditions or using *in vivo* models where cholesterol levels were modulated by dietary intake. Since cholesterol in

the brain is synthesized *de novo* and plasma-lipoproteins are unable to cross the blood-brain barrier, it is important to determine how alterations in cholesterol level and its subcellular distribution within neurons can influence production/secretion of Aβ-related peptides.

Under normal conditions, mature neurons depend on exogenous cholesterol derived from astrocytes to maintain its function. Cholesterol taken up by neurons is first delivered to the EL system where it is hydrolyzed by acid lipase resulting in the release of free cholesterol. Subsequently, cholesterol exits the EL system *via* a Niemann-Pick type C (NPC) 1 and 2 protein-dependent mechanism and distributed to other compartments including the endoplasmic reticulum and plasma membrane. Given the evidence that EL system acts as a major site of APP metabolism and exhibits marked changes in "at risk" neurons prior to extracellular Aβ deposition in AD brains, it is of critical relevance to establish how alteration in the cholesterol levels within the EL system can influence production and clearance of Aβ peptides. In this study, we have addressed this issue by using a new line of transgenic mice as well as stable cell lines which express mutant human APP in the absence of Npc1 protein that is required for normal intracellular cholesterol transport. Mice deficient in Npc1 protein not only accumulate cholesterol within the EL system but also exhibit progressive loss of neurons in selected brain regions, most predominantly in the cerebellum – thus providing a suitable model to evaluate how accumulation of cholesterol can regulate APP levels and processing under *in vivo* conditions. In parallel, we used the stable cell line to define the mechanisms by which cholesterol accumulation can influence APP metabolism at the cellular level. Our results clearly show that cholesterol accretion within EL system did not affect APP levels but increased APP-CTFs and Aβ levels that can render the cells vulnerable to toxicity. Additionally, we observed that cholesterol accumulation can impair autophagosomal but not proteasomal clearance of APP-CTFs and Aβ-related peptides.

4.2 Materials and Methods

Reagents: NuPAGE 4-12% Bis-Tris gels, Alexa Fluor 488/594 conjugated secondary antibodies, ProLong Gold antifade reagent, DNase I, oligo(dT)$_{12-18}$ primers, SuperScript^{TM} II Reverse Trancriptase and ELISA kits for the detection of human Aβ_{1-40} and Aβ_{1-42} were purchased from Life technologies, Corp. (Burlington, ON, Canada). The DNA and RNA isolation kits were from Qiagen, Inc. (Missisauga, ON, Canada), whereas iQ^{TM} SybrGreen supermix was from Bio-Rad Laboratories, Ltd. (Missisauga, ON, Canada). All genotyping and real-time PCR primers were from Integrated DNA Technologies, Inc. (Coralville, IA, USA). Filipin, chloroquine and γ-secretase inhibitors (DAPT and L-685,458) were obtained from Sigma-Aldrich, Co. LLC. (Oakville, ON, Canada). The bicinchoninic acid (BCA) protein assay kit and enhanced chemiluminescence (ECL) kit were from ThermoFisher Scientific Inc. (Nepean, ON, Canada). Vivaspin filtration columns were from GE Healthcare Ltd. (Missisauga, ON, Canada), Oxyblot^{TM} protein oxidation kit, BIV BACE1 inhibitor and proteasomal inhibitor (MG132) were from EMD Millipore Corp (Billerica, MA, USA). Proteasome fluorogenic substrates were from Enzo Life Sciences, Inc. (Ann Arbor, MI, USA). Sources of all the primary antibodies used in the study are listed in Table 4.1. All horseradish peroxidase (HRP)-conjugated secondary antibodies were purchased from Santa Cruz Biotechnology (Paso Robles, CA, USA). All other chemicals were from Sigma-Aldrich or ThermoFisher Scientific.

Mice: Mutant human APP$_{KM670/671NL+V717F}$ Tg mice (APP-Tg) maintained on a C3H/C57BL6 background (15) were crossed with heterozygous Npc1-deficient mice maintained on a BALB/c background (16, 17) to generate bigenic *APP*$^{+/0}$*Npc1*$^{-/-}$ (APP-Tg and Npc1-null: ANPC), *APP*$^{+/0}$*Npc1*$^{+/-}$ (Double heterozygous: Dhet), *APP*$^{+/0}$*Npc1*$^{+/+}$ (APP-Tg) and *APP*$^{-/-}$*Npc1*$^{+/+}$ (Wild-type: WT) mice on a C3H/C57BL6/BALB/c background as described recently (18). Both males and females of different genotypes obtained from the same breeding pairs were used in the study. All animals, maintained on a 12h light/dark cycle, were bred and housed in our own colony with access to food and water *ad libitum*. The maintenance of the breeding colony and experiments involving these animals were performed in accordance with Institutional and Canadian Council of

Animal Care guidelines. All mice were genotyped by PCR analysis of tail DNA twice, initially at weaning at 21 days of age and later confirmed at euthanisation before being used for a given experiment as described earlier (18).

***Cell culture, development of stable cell lines and drug treatments*:** Mouse Neuro2a (N2a) neuroblastoma cells stably overexpressing human Swedish mutant (K670N, M671L) APP (N2aAPPsw, clone Swe.10) were the generous gift of Dr. G. Thinakaran (The University of Chicago, IL, USA). The cells were maintained in N2a growth medium in 5% CO_2/95% air at 37°C as described earlier (19). Stable N2aAPPsw cell lines expressing reduced levels of Npc1 protein (referred to as N2a-ANPC) were generated by targeting the mRNA with Npc1 shRNA lentiviral particles and puromycin selection according to manufacturer's instructions (Santa Cruz Biotechnology). As for controls, N2aAPPsw cells were transduced with shRNA lentiviral construct enconding a scrambled sequence, referred to hereafter as N2a-APP cell lines. Stable shRNA expression clones were maintained in puromycin (5μg/ml) containing N2a growth medium. Cultured N2a-APP and N2a-ANPC cells were treated with H_2O_2 (0-500μM), MG132 (10μM), chloroquine (50μM), γ-secretase inhibitor DAPT (1μM) or BACE1 inhibitor BIV (10μM) in the growth medium for different periods of time. In some experiments, cultured cells were first treated with BIV (10μM) and/or DAPT (1μM) for 24h and then exposed to 0-500μM H_2O_2 for 3h. After treatments, cells were harvested according to specific experimental protocol or stored at -80°C until further use.

***Real-time PCR*:** Cellular RNA from cerebellar tissues of different mouse genotypes (i.e., WT, APP-Tg, Dhet and ANPC mice) or cultured N2a-APP as well as N2a-ANPC cells was isolated using an RNeasy lipid tissue mini kit and an RNeasy RNA extraction kit, respectively. RNA concentrations were determined using a Nanodrop spectrophotometer. A total of 2μg extracted RNA was DNaseI-treated and reverse transcribed using oligo$(dT)_{12\text{-}18}$ primers and SuperScript™ II Reverse Trancriptase. Quantitative real-time PCR was carried out with the iQ™ SybrGreen supermix using a MyiQ™ Cycler with iQ5 real-time detection system (Bio-rad Laboratories Ltd., Missisauga, ON, Canada). Primer sequences used in the study are as follows: APP (forward, 5'-GCCAAAGAGACATGCA

GTGA-3' and reverse, 5'-CCAGACATCCGAGTCATCCT-3'), Npc1 (forward, 5'-CACCAATCCTGTAGAGCTCTG-3' and reverse, 5'-GGAAGGTGATCACAAGCG CGG-3') and β-actin (forward, 5'-AGCCATGTACGTAGCCATCC-3' and reverse, 5'-CTCTCAGCTGTGGTGGTGAA-3'). Real-time PCR primers were designed to span regions of both human and mouse APP and were synthesized by the Integrated DNA Technologies, Inc (Coralville, IA, USA). Each sample was assayed in duplicate and the levels of mRNA were normalized to β-actin mRNA levels.

Western blotting: Western blotting was performed on brain cerebellar regions of 4 and 10 week old ANPC and their littermate genotypes (n = 4-6 animals/genotype/age group) and cultured cells as described earlier (18, 20). In brief, mouse cerebellar tissues and cultured cells were homogenized in ice-cold RIPA lysis buffer and protein content was determined using a BCA kit. A total of 15-20μg protein was separated on 7-17% polyacrylamide or NuPAGE 4-12% Bis-Tris gels, transferred to polyvinylidene fluoride membranes and then incubated overnight at 4°C with either anti-APP, anti-ADAM10, anti-BACE1, anti-nicastrin, anti-PS1, anti-Pen2, anti-APH1, anti-sAPPα, anti-sAPPβ, anti-β-amyloid (6E10), anti-LC3, anti-p62, anti-ubiquitin antisera at dilutions listed in Table 4.1. On the following day, membranes were incubated with appropriate HRP-conjugated secondary antibodies (1:5000) and immunoreactive proteins were visualized using an ECL detection kit. All Blots were re-probed with anti-β-actin antibody and quantified using a MCID image analyzer (Imaging Research, Inc., St Catherines, ON, Canada) as described earlier (18).

***Immunostaining and filipin labeling*:** Mice from different genotypes (i.e., WT, APP-Tg, Dhet and ANPC mice; 3-5 animals/genotype) were fixed by perfusion in 4% paraformaldehyde and their cerebellar sections (20μm) were processed using a free-floating procedure (18). For subcellular localization of antigens, brain sections were incubated overnight at 4°C with a combination of anti-APP or anti-Aβ and anti-Rab5, anti-Rab7 or anti-cathepsin D antibodies at dilutions listed in Table 4.1. The sections were then exposed to appropriate Alexa Fluor 488/594-conjugated secondary antibodies (1:1000) for 2 h, washed and mounted with ProLong Gold antifade medium. For triple

labeling with filipin, sections were incubated with 25µg/ml filipin in PBS for 30 min in the dark after the initial double labeling. Immunostained sections were visualized using a Zeiss LSM 710 confocal microscope and the images were acquired with a Zeiss confocal scanning laser using a 63x 1.4 numerical aperture Plan Apochromat oil-immersion lens. All images were deconvoluted using Huygens Elements XI software and % of co-localization was quantified using the Imaris 7.5.1 software.

For visualization of unesterified cholesterol accumulation in stable N2a-APP as well as N2a-ANPC clones, cells grown on coverslips were fixed in 4% PFA, washed in PBS and then incubated with 25µg/ml filipin in PBS for 1h in the dark at room temperature. Following washing, cells were mounted and examined using a Zeiss Axioskop-2 microscope (Carl Zeiss Canada Ltd).

***In vitro γ-secretase activity assays*:** The γ-secretase activity assay was performed on crude membrane fractions as described previously (21), with minor changes. Cultured cells or brain tissue were homogenized in 10mM Tris-HCl (pH 7.4) containing 1mM EDTA and protease inhibitor cocktail and then centrifuged to remove nuclei and cell debris. The supernatant was further centrifuged at 100,000 *g* for 1h at 4°C to separate the membrane fraction, which was solubilized in the homogenization buffer containing 1% CHAPSO at 4°C for 1h and then 50µg of protein was used to measure the γ-secretase activity. The assay was performed in 50mM Tris-HCl (pH 6.8), 2mM EDTA and 0.25% CHAPSO with 8µM fluorogenic γ-secretase substrate in a 200µl reaction volume. The fluorescence was measured at an excitation wavelength of 355nm and emission wavelength of 440nm at 37°C and the specific activity was determined by incubating a parallel set of samples with 100µM γ-secretase inhibitor L-658,458. All samples were assayed in duplicate and results presented were obtained from 3 independent experiments.

***ELISA for $A\beta_{1-40}$ and $A\beta_{1-42}$*:** Cellular Aβ in cultured cells or cerebellum of ANPC, APP-Tg, Dhet and WT mice were solubilized in 5M guanidine (Gdn)-HCl/50mM Tris-HCl (pH 8.0) buffer for 4h (15), centrifuged at 16,000g for 20mins and then assayed for human $A\beta_{1-40}$ or $A\beta_{1-42}$ levels using commercially available ELISA kits. For the

measurement of secreted Aβ in the conditioned media, cells were grown to 80-90% confluency, rinsed with PBS and incubated in 6ml of serum-free Opti-MEM I for 3h. Subsequently the conditioned media collected from these cells were concentrated using Vivaspin-6 filtration columns and then assayed for human $A\beta_{1-40}$ or $A\beta_{1-42}$ levels using the ELISA kits. All samples were assayed in duplicate and each experiment was repeated 2-3 times. The OD values obtained from each well were converted to pg/ml according to the respective standard curve.

***Viability of Cultured cells*:** Viability of N2a-APP and N2a-ANPC cells treated with H_2O_2 in the presence or absence of various drugs was determined using the colorimetric MTT assay (22). Control and drug-treated culture plates were first replaced with new medium containing 0.25% MTT and then incubated for 3h at 37°C. The reaction was terminated and measured spectrophotometrically at 570nm. The experiment was repeated three to four times in triplicate.

***Detection of proteasomal activities*:** Brain cerebellar tissue samples and cultured cells were homogenized in an ice-cold lysis buffer containing 20mM Tris-HCl (pH 7.2), 1mM EDTA, 1mM sodium azide, 1mM DTT, 0.1% NP40 and a cocktail of protease inhibitors. Homogenates were centrifuged and supernatants were used for determination of proteasome peptidase activities. Proteasome fluorogenic substrates i.e. Suc-LLVY-AMC, Boc-LRR-AMC and Z-LLE-AMC were used to estimate chymotryptic-like, tryptic-like and peptidyl-glutamyl peptide hydrolyzing (PGPH)-like proteasomal activities, respectively (23). Assays were carried out in a 150μL reaction volume containing 10μg proteasome extract and 13μM of the respective fluorogenic substrate for 30 min at 37°C. The cleavage rate of substrates was determined using an M5 plate reader at an excitation/emission wavelength of 390nm/460nm. All samples were assayed in triplicate and specific proteasome activity expressed as fluorescence units/μg protein/min was determined after subtracting the value obtained in the presence of 1μM proteasomal inhibitor MG132 (23).

Detection of oxidative stress: Cerebellar tissues from 4- and 10-week old WT, APP-Tg, Dhet and ANPC mouse brains were assayed for protein carbonyl content using the Oxyblot^{TM} protein oxidation detection kit (EMD Millipore, Co). Briefly, 20μg protein from each tissue extract homogenized in ice-cold RIPA lysis buffer were denatured with SDS, derivatized by incubation with 2,4-dinitrophenylhydrazine and then treated with neutralization solution. The samples were subsequently separated by electrophoresis and blotted onto membranes. Modified protein carbonyls were detected using rabbit anti-DNP antiserum and HRP-conjugated goat anti-rabbit IgG provided with the kit. All blots were re-probed with anti-β-actin to monitor equal protein loading.

***Statistical analysis*:** The data are expressed as mean ± S.E.M and were analyzed using one-way ANOVA followed by Newman-Keuls post-hoc analysis or using unpaired two-tailed Student's t-test with significance set at $p < 0.05$. All analyses were performed using GraphPad Prism software.

Table 4.1: Details of the primary antibodies used in the study

Antibody	Type	IF Dilution	WB Dilution	Source
ADAM10	Polyclonal	n/a	1:2000	EMD Millipore Co.
APH1	Polyclonal	n/a	1:500	[1]Dr. G.Thinakaran
APP (clone Y188)	Monoclonal	1:250	1:5000	Abcam Inc.
BACE1	Polyclonal	n/a	1:1000	Abcam Inc.
Cathepsin D (CatD)	Polyclonal	1:200	n/a	Santa Cruz Biotechnology, Inc.
LC3	Polyclonal	n/a	1:1000	MBL International Corp.
Nicastrin	Polyclonal	n/a	1:500	Santa Cruz Biotechnology, Inc.
p62 (Sequestosome-1)	Monoclonal	n/a	1:1000	EMD Millipore Co.
Pen2	Polyclonal	n/a	1:2000	[1]Dr. G.Thinakaran
PS1-N-terminal fragment (PS1-NTF)	Polyclonal	n/a	1:3000	[1]Dr. G.Thinakaran
Proteasome subunit beta type 2 (β2)	Monoclonal	n/a	1:1000	Abcam Inc.
Rab5	Polyclonal	1:200	n/a	Abcam Inc.
Rab7	Polyclonal	1:500	n/a	Sigma-Aldrich, Inc.
sAPPα (2B3)	Monoclonal	n/a	1:1000	IBL Co., Ltd
sAPPβ-sw (6A1)	Monoclonal	n/a	1:3000	IBL Co., Ltd
Ubiquitin	Polyclonal	n/a	1:200	Santa Cruz Biotechnology, Inc.
β-amyloid, 1-16 (6E10)	Monoclonal	1:1000	1:3000	Covance Corp.
β-amyloid, 17-24 (4G8)	Monoclonal	1:1000	n/a	Covance Corp.

IF, immunofluorescence; WB, western blotting; n/a, not used in that specific application; [1]The University of Chicago, IL, USA.

4.3 Results

Cholesterol sequestration causes accumulation of APP-CTFs and Aβ peptides: We have recently generated a bigenic ANPC mouse which overexpresses mutant human APP in the absence of Npc1 protein by crossing the well-established APP-Tg mice (i.e., TgCRND8) with heterozygous Npc1-deficient mice. These ANPC mice, like the TgCRND8 mice, exhibit cognitive deficits and extracellular Aβ deposits without any overt loss of hippocampal neurons. On the other hand, like the Npc1-null mice, these mice exhibit accumulation of unesterified cholesterol within the EL system and progressive loss of cerebellar Purkinje cells accompanied by severe motor impairments. These mice usually survive ~11 weeks, with mortality rates increasing drastically from the 8^{th} week onwards. The overall phenotype of ANPC mice was found to be more severe than either APP-Tg or Npc1-null mice. To determine how cholesterol accumulation within the EL system of ANPC mice could affect APP metabolism, we first determined APP mRNA and holoprotein expression in cerebellum of ANPC mice compared to WT, APP-Tg and Dhet littermates. Real-time qPCR analysis showed no significant alteration in APP mRNA level in ANPC mice compared to APP-Tg or Dhet littermates at any age (Fig. 4.1A). Consistent with these data, APP holoprotein levels measured using a C-terminal APP antibody (which recognizes both mouse and human APP) did not exhibit any variation between APP-Tg, Dhet or ANPC mice (Fig. 4.1B). The net level of APP holoprotein, as expected, was markedly higher in APP-Tg, Dhet and ANPC mice compared to WT mice.

In the absence of any alteration in APP expression, we evaluated levels of APP cleaved products in ANPC mouse brains compared to the other genotypes. Analysis of APP-CTFs generated by α- and β-secretase cleavage showed that levels of α-CTF were increased only at 10 weeks, while β-CTF levels were enhanced in both 4- and 10-week cerebellum of ANPC mice compared to other mouse lines (Fig. 4.1C). However, the levels of the soluble sAPPα or sAPPβ were not altered at any age group in ANPC mice compared to other lines (Fig. 4.1D). The levels of total human $A\beta_{1-40}$ (Fig. 4.1E) and $A\beta_{1-42}$ (Fig. 4.1F), as detected by ELISA, were significantly increased over time in the cerebellum of ANPC compared to age-matched APP-Tg and Dhet mice. However, no

Aβ-containing plaques were evident in the cerebellum of ANPC mice, *albeit* they were detected in the hippocampus as well as cortex at 10 weeks of age [Fig. 4.12A,B (i.e. Suppl. Fig.1)]. As anticipated, tissues from WT mice did not exhibit any Aβ signal above background. These results clearly revealed that cholesterol accumulation in the EL system in ANPC mouse cerebellum caused a progressive accumulation of APP-CTFs and Aβ peptides in the absence of any significant alteration in APP holoprotein or soluble APP levels.

At the cellular level, APP-CTF immunoreactivity, as detected by APP C-terminal antibody (clone Y188), exhibited diffuse, finely granular labeling in the cerebellar neurons of the WT, APP-Tg and Dhet mice, whereas in ANPC mice it is evident as coarse granules or larger patches. Our double labeling studies (Fig. 4.2A-J) showed that Y188 immunoreactivity mostly colocalized with Rab5- and Rab7-positive early-/late-endosomal compartments (Fig. 4.2,A,C) but not with cathepsin D-positive vesicles in APP-Tg (Fig. 4.2,E) as well as in WT and Dhet (not shown) mouse brains. In ANPC mice, Y188 immunoreactivity was evident mostly in Rab5-positive early-endosomes and to some extent in Rab7-positive late-endosomes (Fig. 4.2B,D). Interestingly, colocalization of Y188 immunoreactivity with Rab5-positive early endosomes was found to be significantly higher in ANPC mice compared to the APP-Tg mice (mean ± SEM: ANPC = 61.54 ± 3.932; APP-Tg = 43.33 ± 2.929; $p = 0.003$). The majority of cathepsin D-positive lysosomes were free of Y188-labeled APP-CTFs (Fig. 4.2F). Interestingly, filipin labeled unesterified cholesterol was found to be colocalized with cathepsin D but not with APP-CTFs (see Fig. 4.2H,J) in the cerebellum of ANPC mice. However, a subset of cathepsin D vesicles that were free of unesterified cholesterol showed APP-CTF immunoreactivity in the cerebellum of ANPC mice (Fig. 4.2F,H,J). At the cellular level, neurons of the cerebellum of ANPC mice, as detected by 4G8 antibody, exhibited more intense Aβ-immunoreactivity compared to WT, Dhet or APP-Tg mice, possibly due to increased levels of the peptides (Fig. 4.3A-H). Similar to APP-CTF immunoreactivity, our double labeling studies using 4G8 and antibodies for organelle-specific markers revealed that 4G8 immunoreactivity resided primarily in Rab5-positive early-endosomes (Fig. 4.3A,B) and to a lesser extent in Rab7-positive late-endosomes (Fig. 4.3C,D), but

rarely in cathepsin D-positive lysosomes (Fig. 4.3E,F) in the cerebellar neurons of APP-Tg as well as ANPC mice. Also similar to Y188 immunoreactivity, 4G8 immunoreactivity residing in the Rab5-positive early endosomal compartment was found to be significantly higher in ANPC mice compared to the APP-Tg littermates (mean ± SEM: ANPC = 44.17 ± 1.537; APP-Tg = 35.34 ± 1.591; p = 0.004). Moreover, 4G8-positive areas overlapped substantially with Y188-positive areas in ANPC cerebellar neurons but less so in APP-Tg mice, suggesting that the accumulated APP fragments contained both the Aβ domain and the extreme C-terminal fragments of APP. Considering the elevated levels of APP-CTFs and Aβ peptides in ANPC cerebellum in absence of any alteration in full-length APP levels, it is likely that accumulated 4G8 and Y188 antigen in our immunolabeling studies are Aβ and APP-CTFs, and not APP.

To determine the mechanisms by which cholesterol sequestration can alter APP metabolism, we knocked down Npc1 expression by sequence specific shRNAs in N2a cells stably overexpressing Swedish mutant APP. The knock down efficacy was validated by measuring Npc1 mRNA and protein levels in Npc1-shRNA (i.e. N2a-ANPC) *vs* control-shRNA (i.e. N2a-APP) transduced clones (Fig. 4.4A,B). Our filipin staining of unesterified cholesterol revealed bright, dense labeling in N2a-ANPC cells compared to the control N2a-APP cells, indicating that depletion of Npc1 triggers intracellular accumulation of cholesterol (Fig. 4.4C). Interestingly, the levels of APP-CTFs, but not full-length APP, were also significantly increased in N2a-ANPC cells as observed in ANPC mouse brains (Fig. 4.4D,E). ELISA-based analysis of the Aβ levels in the GnHCl extracted cell lysate preparations revealed a marked increase in intracellular $A\beta_{1-40}$ (~50%) as well as $A\beta_{1-42}$ (~30%) levels (Fig. 4.4F). However, we did not observe any alterations in the levels of sAPP (i.e., sAPPα and sAPPβ) or Aβ (i.e, $A\beta_{1-40}$ and $A\beta_{1-42}$) peptides in the conditioned media of N2a-ANPC *vs* N2a-APP cells, thus suggesting that cholesterol sequestration following Npc1 depletion did not influence secretion of soluble APP or Aβ-related peptides (Fig. 4.4G,H). These results complement our *in vivo* data showing that cholesterol accumulation induced by Npc1-deficiency might not affect APP processing in the secretory pathway.

***Cholesterol sequestration affects proteolytic processing of APP*:** The observation that Npc1 depletion resulted in differential levels of intracellular and secretory APP cleaved products led us to investigate its effect on the various secretases involved in APP processing (Fig. 4.5A-D). The steady state levels of α-secretase ADAM10, but not the β-secretase BACE1, was found to be significantly decreased in the cerebellum of 4- and 10-week ANPC mice compared to APP-Tg and Dhet mice (Fig. 4.5A,B). In cultured N2a-ANPC cells, however, we did not observe any significant alteration of either ADAM10 or BACE1 levels compared to control N2a-APP cells (Fig. 4.5C,D).

Since decreased levels/activity of γ-secretase could also lead to accumulation of APP-CTFs, we subsequently determined the impact of Npc1 depletion on the γ-secretase complex (Fig. 4.6A-E). The steady state levels of PS1 and nicastrin were significantly increased in the cerebellum of ANPC mice at both 4 and 10 weeks of age compared to APP-Tg and Dhet mice (Fig. 4.6A,B). Consistent with the steady state peptide levels, the activity of the γ-secretase complex was also significantly increased in ANPC mouse cerebellum compared to other genotypes at 10 weeks of age (Fig. 4.6D). Under *in vitro* conditions, however, we did not observe any alteration in the levels of nicastrin, PS1, APH1 or Pen2, in N2a-ANPC cells compared to N2a-APP cells (Fig. 4.6D). However, the activity of the γ-secretase complex showed a non-significant increasing trend in N2a-ANPC cells compared to the N2a-APP cells (Fig. 4.6E), suggesting that observed APP-CTFs accumulation in these cells is probably not mediated by inhibition of γ-secretase complex. These data, taken together, suggest that differential regulatory pathways may be involved in triggering accumulation of APP-CTFs observed under *in vivo* and *in vitro* conditions.

***Cholesterol sequestration does not affect the proteasomal activity*:** Previous studies have shown that APP-CTFs and many other core proteins involved in Aβ production are degraded by a ubiquitin-proteasome pathway - which plays an important role in the turnover of short-lived nuclear and cytosolic proteins (24, 25). To determine whether the increased accumulation of APP-CTFs was the consequence of impaired proteasomal activity, we measured chymotrypsin-like, trypsin-like or peptidyl-glutamyl peptide-

hydrolyzing (PGPH)-like activities in the cerebellum of WT, APP-Tg, Dhet and ANPC mice (Fig. 4.7A). However, no significant alteration was evident in ANPC mice compared to other genotypes. Additionally, we did not observe any variation in the catalytic β2 subunit levels of the ubiquitin proteasome system in either 4 or 10 week cerebellum of ANPC compared to WT, APP-Tg and Dhet mice (Fig. 4.7B). Under *in vitro* paradigms, we also did not observe any alterations in chymotrypsin-like, trypsin-like or PGPH-like activities between N2a-ANPC *vs* N2a-APP cells (Fig. 4.7C). Furthermore, N2a-APP and N2a-ANPC cells, when treated with the established proteasomal inhibitor MG132 for different periods (1h – 6h) of time, showed a time-dependent increase in the levels of ubiquitinated proteins without any significant difference between the two cell lines (Fig. 4.7D). Thus, accumulation of APP-CTFs or Aβ-related peptides observed under *in vivo* or *in vitro* paradigms following cholesterol sequestration may not be the consequence of decreased proteasomal activity.

***Influence of lysosomal and autophagosomal inhibition upon APP-CTFs levels*:** The autophagic-lysosomal system, the principal "self-clearance machinery" serves as a vital pathway for degrading normal and aggregated proteins within cells (26, 27). There is evidence of three types of autophagy that are involved in the clearance mechanism: macroautophagy, microautophagy and chaperone-mediated autophagy. The macroautophagy, hereafter referred to as autophagy, is characterized by the formation of a double-membrane autophagosome containing macromolecules and cell organelles that fuses with lysosomes to degrade its contents. In microautophagy, macromolecules and small organelles enter lysosomes through invagination of the membranes for degradation within the lumen, while in chaperone-mediated autophagy cytosolic proteins containing a KFERQ motif are transported by specific chaperone proteins to the lysosomal lumen for degradation. Interestingly, some recent studies have shown that certain ubiquitinated proteins are constitutively degraded by the autophagic-lysosomal pathway rather than the proteasomal system either due to misfolding, insolubility or other unknown reasons (26, 27). This is partly supported by evidence that some ubiquitinated proteins that are conjugated with p62, a protein involved in the formation of autophagosomes, are believed to be degraded by autophagy rather than by the proteasome (28).

Evidence accumulated from *in vitro* and *in vivo* studies suggests that altered function of the autophagic-lysosomal system may have a critical role in the generation and/or clearance of APP-CTFs and Aβ-related peptides observed in AD pathology (29). To determine whether increased accumulation of APP-CTFs and Aβ-related peptides are the consequence impaired activity of the autophagic-lysosomal system, we evaluated the steady state levels of the autophagic markers LC3-II and p62 in the cerebellum of WT, APP-Tg, Dhet and ANPC mice. While p62 levels were increased only at 10 weeks, LC3-II levels were enhanced in both 4- and 10-week cerebellum of ANPC mice compared to other mouse lines (Fig. 4.8A,B). Interestingly, the levels of LC3-II were found to be increased with age, thus raising a possibility of progressive accumulation of autophagic vacuoles – which could be due to decreased lysosomal flux and/or increased production of autophagosomes by cholesterol sequestration. Apart from autophagic markers, we also observed a significant increase in the levels of ubiquitinated proteins in the cerebellum of ANPC mice compared to APP-Tg and Dhet mice only at 10 weeks but not 4 weeks of age (Fig. 4.8C,D). Since proteasomal activity is not altered in the cerebellum of ANPC mice, it is likely that the accumulation of ubiquitinated proteins is the consequence of the abnormal autophagic-lysosomal system which is known to degrade certain ubiquitin-containing misfolded and/or aggregated proteins.

To determine whether impairment of autophagic-lysosomal function can lead to accumulation of APP-CTFs and Aβ peptides, we treated N2a-APP and N2a-ANPC cells for different times (2h – 10h) with chloroquine - a lysosomotropic agent which prevents the fusion of autophagosomes with lysosomes and subsequent autophagic degradation (30). As expected, chloroquine induced a time-dependent increase in LC3-II levels, suggesting decreased clearance of autophagic vacuoles associated with lysosomal dysfunction (Fig. 4.9A). In parallel, we observed a concomitant increase in APP-CTF levels in both cell lines, but the increase was evident earlier in N2a-APP cells (i.e., at 2h) than in N2a-ANPC cells (i.e., 5h and/or 10h) (Fig. 4.9A-C). Given the evidence that intracellular cholesterol accumulation can influence lysosomal acidification (31) as observed following chloroquine treatment (30), the delayed effects of the lysosomotropic

agent on APP-CTF levels in N2a-ANPC supports abnormalities in the lysosomal degradation pathway.

***Accumulation of APP-CTFs and Aβ increases vulnerability to toxic insults*:** Several lines of evidence suggest that oxidative stress may play a role in the degeneration of neurons observed in NPC as well as AD pathology (32-34). This is substantiated by our results from oxyblot experiments which showed a significant increase in levels of protein carbonyl, a marker of oxidative stress, in the cerebellar region of 10 weeks but not of 4 week old ANPC mice compared to age-matched WT, APP-Tg and Dhet mice (Fig. 4.10A,B). Although there is evidence that intracellular accumulation of Aβ-related peptides and β-CTFs can directly induce neurodegeneration or render cells vulnerable to toxicity (35-37), their potential involvement in cholesterol-induced oxidative stress remains unclear. Thus, as a first step, we measured the viability of cultured N2a-ANPC and N2a-APP cells following exposure to different doses of H_2O_2. Our results clearly showed that N2a-ANPC cells are significantly more vulnerable to oxidative stress than N2a-APP cells following 3h exposure to H_2O_2 (Fig. 4.11A). Additionally, we observed that toxicity induced by H_2O_2 was markedly attenuated when the cells were pre-treated for 24h with β-secretase or γ-secretase inhibitors (Fig. 4.11B,C) thus suggesting that accumulated APP-CTFs and Aβ-related peptides may have a critical role in mediating toxicity.

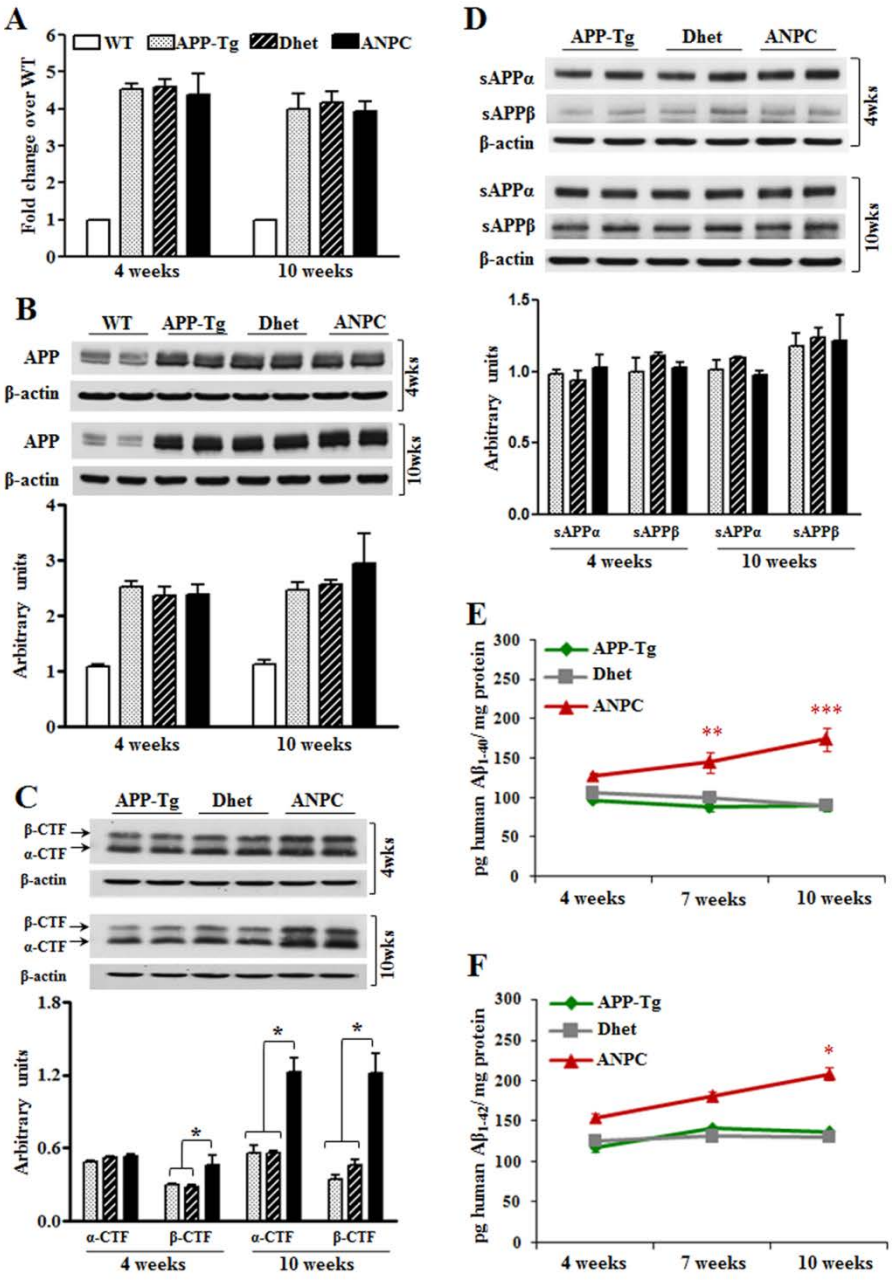

Figure 4.1: Enhanced levels of APP-CTFs and Aβ in ANPC mouse brains. **(A)** Real-time PCR analysis of APP mRNA levels in 4- and 10-week cerebellum showing no significant alteration in the APP transcript level in ANPC mice compared to APP-Tg or Dhet mice. **(B)** Representative immunoblots and histograms showing no significant change in APP holoprotein (~98 kD) expression as detected by APP C-terminal specific antibody (clone Y188) in the cerebellum of 4- and 10-week old WT, APP-Tg, Dhet and ANPC mice. **(C)** Immunoblots and respective histograms depicting an age-dependent increase in α-CTF (~10kDa) and β-CTF (~12 kDa) levels in the cerebellum of ANPC compared to APP-Tg and Dhet mice. **(D)** Immunoblots and respective histograms showing no change in soluble APPα (sAPPα) and soluble APPβ (sAPPβ) levels at 4- and 10-week cerebellum of ANPC mice compared to APP-Tg and Dhet mice. **(E, F)** Graphs showing an age-dependent increase in human $A\beta_{1\text{-}40}$ (E) and $A\beta_{1\text{-}42}$ (F) levels in ANPC cerebellum compared to APP-Tg and Dhet mice between 4 and 10 weeks of age as quantified by ELISA. All immunoblots were reprobed with β-actin antibody to monitor equal loading of proteins. Values represent the means ± SEM; n = 4-10 animals per genotype and age group. *, $p < 0.05$; **, $p < 0.01$; ***, $p < 0.001$.

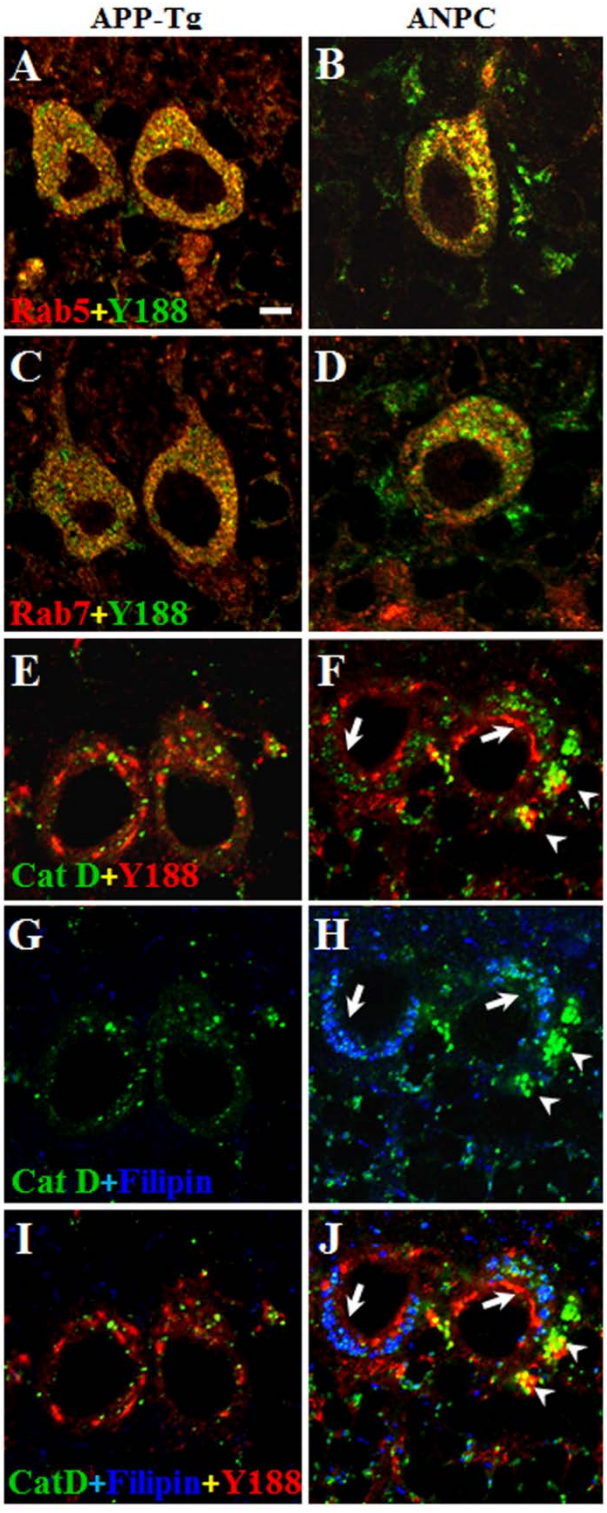

Figure 4.2: APP-CTFs accumulate in endosomal compartments but do not co-localize with filipin. **(A-D)** Representative confocal images of cerebellar Purkinje cells in APP-Tg and ANPC mice brains showing the localization of Y188-labeled APP-CTFs in Rab5- (A, B) and Rab7- (C, D) positive early- and late-endosomal vesicles, respectively. **(E-J)** Double/triple labeling of ANPC cerebellar neurons with Cathepsin D (Cat D), Y188 and filipin reveals that majority of the Cat D-containing vesicles accumulate filipin-labeled cholesterol but not APP-CTFs (F, H, J; arrows), whereas a subset of Cat D-containing vesicles which are free of filipin-labeled cholesterol contains APP-CTFs (F, H, J; arrowheads). Note that filipin-labeled cholesterol accumulation occurred only in ANPC but not in APP-Tg mouse brains. The fluorescence labeling of the primary antibodies used is indicated in respective font colors. Scale bar, 5 μm.

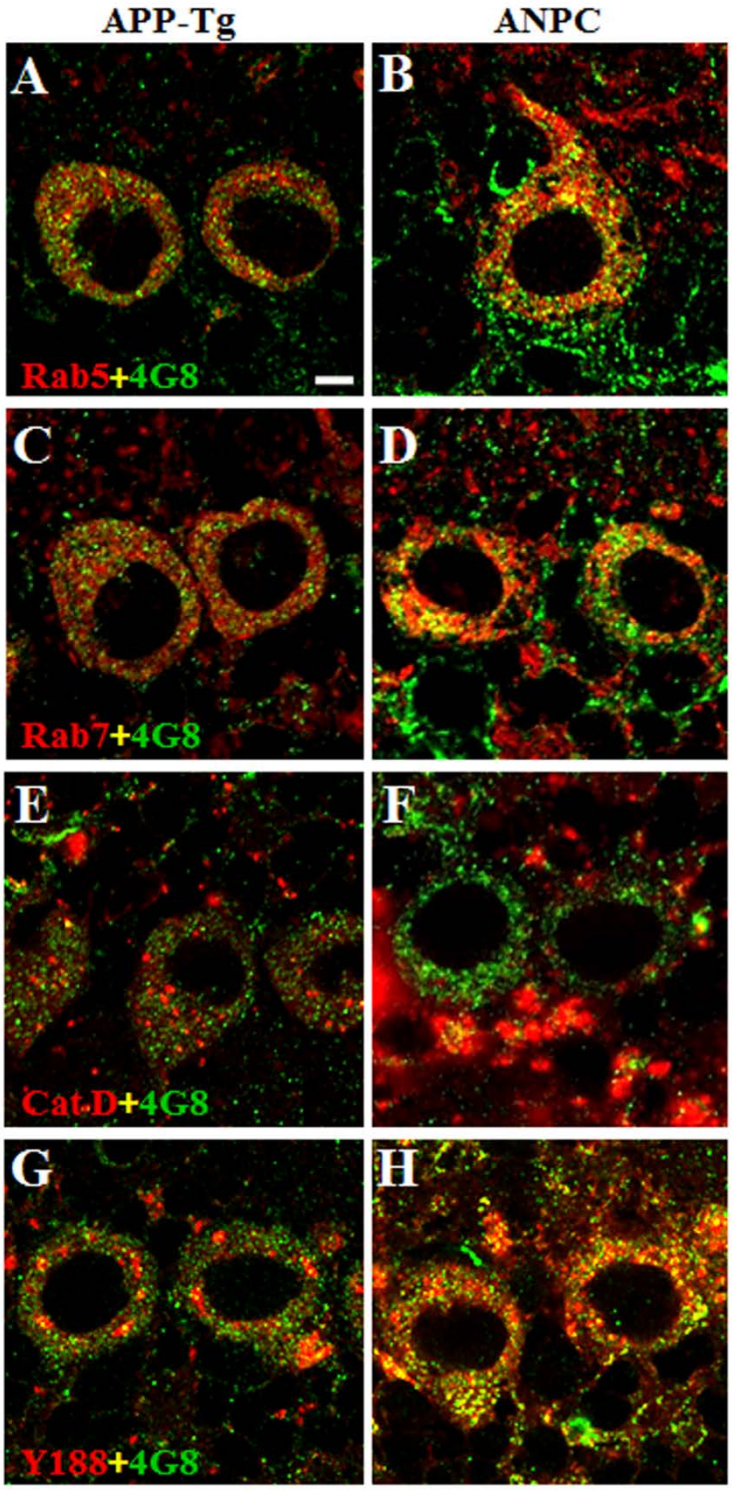

Figure 4.3: Aβ-deposits reside in endosomal compartments in association with APP-CTFs. **(A-F)** Representative confocal images of cerebellar Purkinje cells in APP-Tg and ANPC mouse brains showing the localization of 4G8-labeled Aβ peptides mostly in Rab5- (A, B) and Rab7- (C,D) positive early- and late-endosomal vesicles respectively, but not in Cathepsin D (Cat D)-positive (F, F) vesicles. **(G, H)** 4G8-labeled Aβ peptides were co-localized with Y-188-labeled APP-CTFs more predominantly in ANPC (H) compared to APP-Tg (G) cerebellar sections. The fluorescence labeling of the primary antibodies used is indicated in respective font colors. Scale bar, 5 μm.

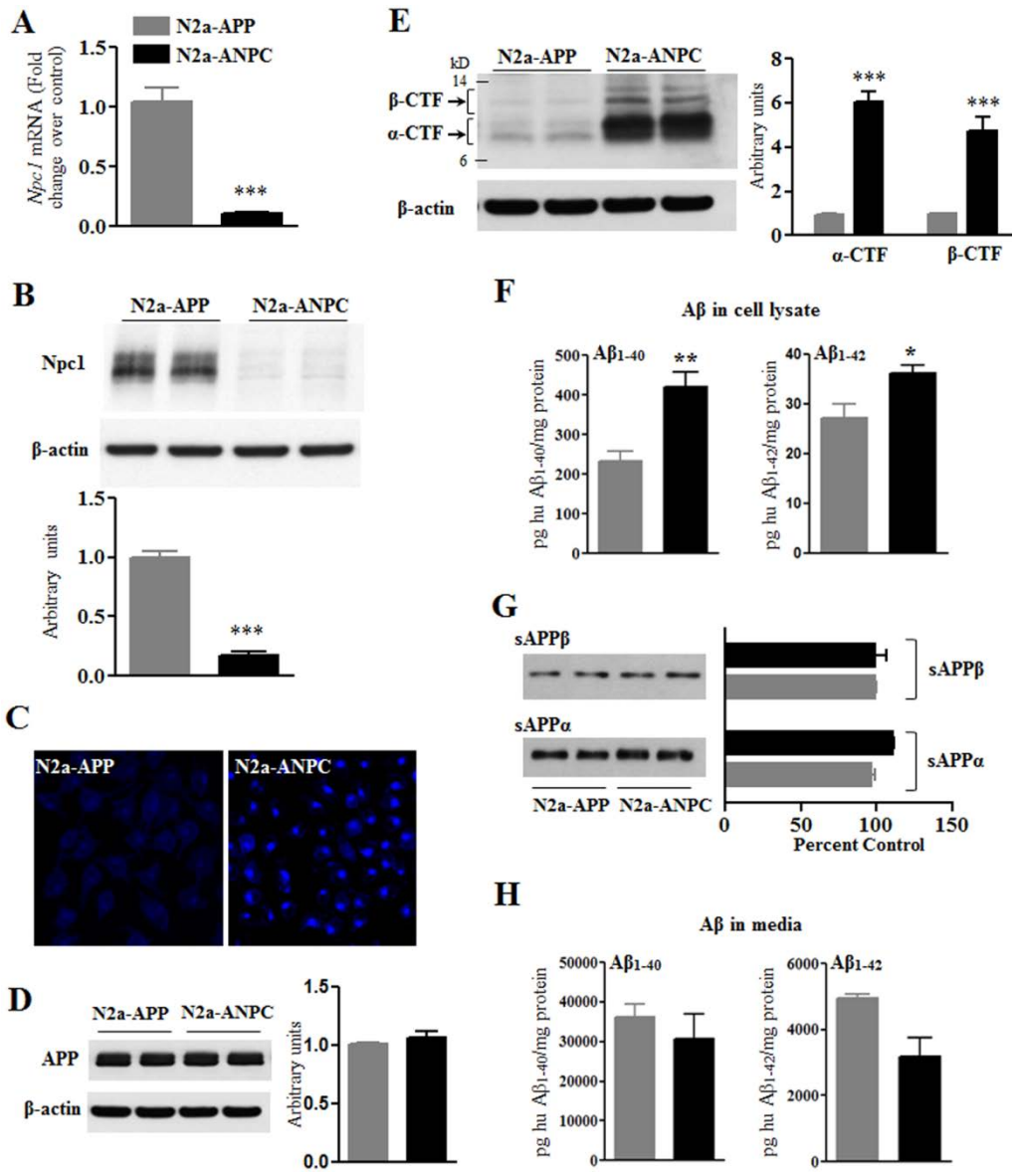

Figure 4.4: Npc1 knockdown in N2aAPP cells triggers cholesterol sequestration and enhanced the levels of APP-CTFs and Aβ without any alteration in APP holoprotein level. N2a cells overexpressing mutant human APP_{695} were transduced with shRNA lentiviral particles specifically directed against *Npc1*. **(A, B)** Npc1 mRNA (A) and protein levels (B) normalized to the respective β-actin levels in knocked down N2a-ANPC cells relative to control N2a-APP cells as determined by quantitative real-time PCR and western blot analysis respectively depicting the efficiency of shRNA reduction. **(C)** Filipin labeling showing sequestration of unesterified cholesterol following Npc1 reduction in N2a-ANPC cells compared to N2a-APP control cells. **(D)** Representative immunoblots and histograms showing no alteration in APP holoprotein level in N2a-APNC cells relative to N2a-APP cells. **(E)** Immunoblots and histograms illustrating an increase in α-CTF and β-CTF levels in N2a-APNC cells relative to N2a-APP cells. **(F)** Increased intracellular levels of human $A\beta_{1-40}$ and $A\beta_{1-42}$ in N2a-APNC cells relative to N2a-APP cells as detected by ELISA. **(G)** Immunoblots and histograms showing no alteration in secreted soluble APPα (sAPPα) and soluble APPβ (sAPPβ) levels in N2a-APNC cells relative to N2a-APP cells. **(H)** Histograms showing no significant alteration in secreted human $A\beta_{1-40}$ and $A\beta_{1-42}$ levels in N2a-APNC cells relative to N2a-APP cells as detected by ELISA. Values represent the means ± SEM of 3-4 independent experiments. *, $p < 0.05$; **, $p < 0.01$; ***, $p < 0.001$.

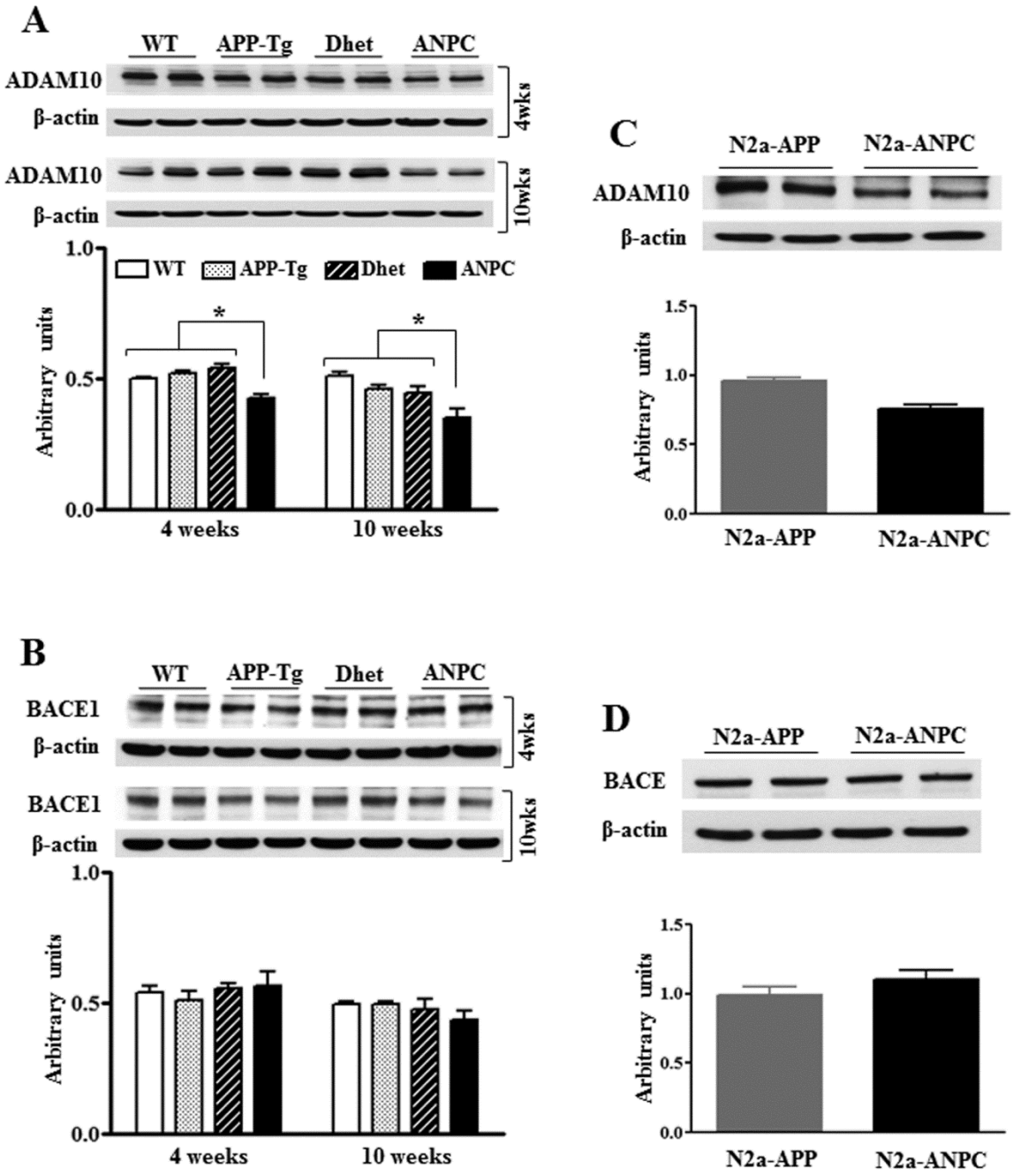

Figure 4.5: Effect of cholesterol accumulation on α- and β-secretases. **(A, B)** Immunoblots and respective histograms showing significant decrease in mature ADAM10 (~60 kDa; A) but no alteration in BACE1 (~70 kDa; B) steady-state levels in the cerebellum of 4- and 10-week old ANPC mice compared to WT, APP-Tg and Dhet mice. Values are means ± SEM from n = 4-6 animals per genotype/age group. **(C, D)** Immunoblots and respective histograms showing no significant alteration in mature ADAM10 (C) or BACE1 (D) levels in N2a-ANPC cells compared to N2a-APP controls. Protein levels were normalized to respective β-actin levels. Values are means ± SEM from 3 independent experiments. *, $p < 0.05$.

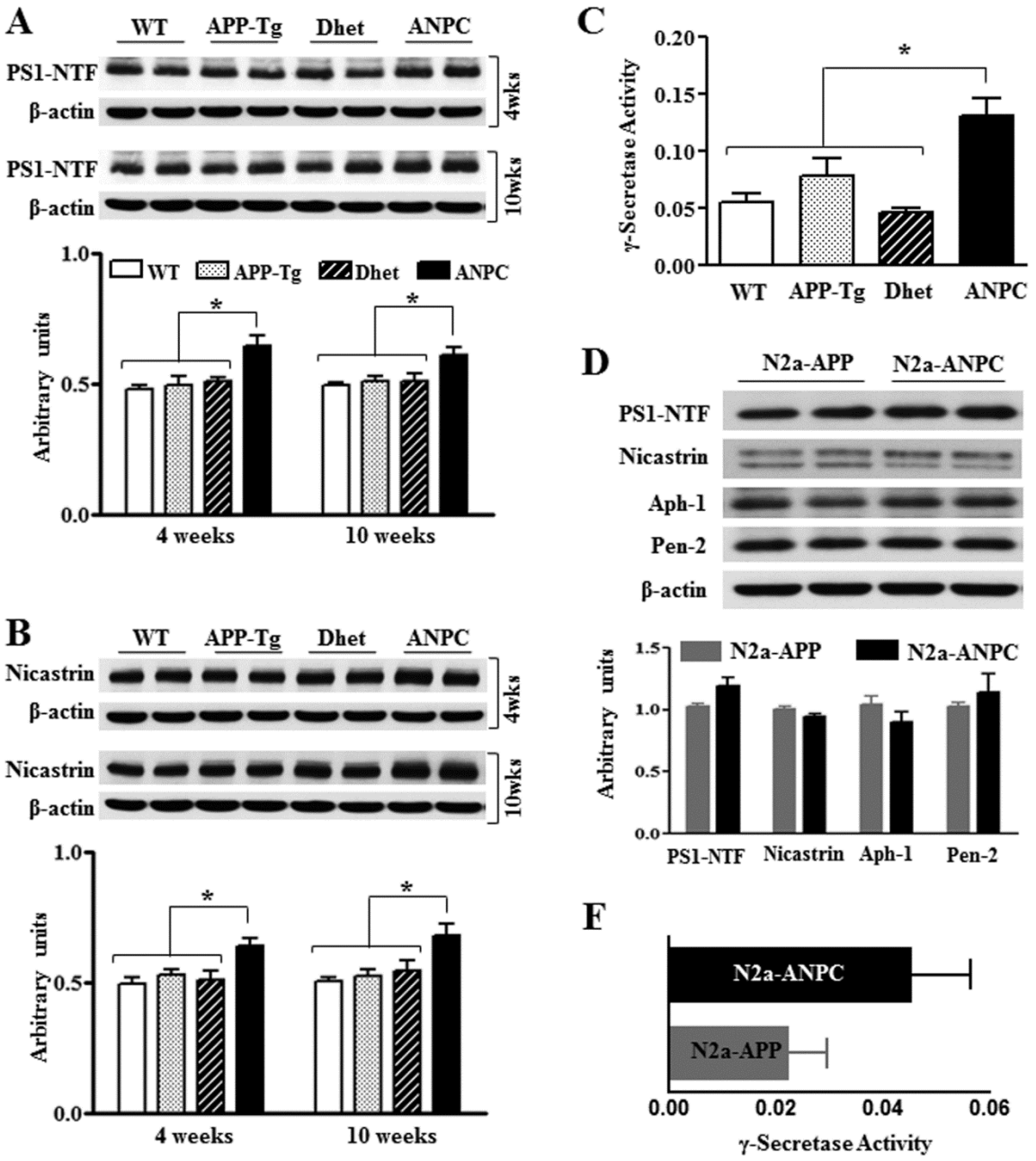

Figure 4.6: Effect of cholesterol sequestration on γ-secretase level and activity. **(A, B)** Immunoblots and respective histograms showing significant increase in presenilin 1 N-terminal fragment (PS1-NTF, ~27 kDa; A) and nicastrin (~110 kDa; B) steady-state levels in the cerebellum of 4- and 10-week old ANPC mice compared to WT, APP-Tg and Dhet mice. Protein levels were normalized to respective β-actin levels. **(C)** Histograms showing increased γ-secretase specific activity in cerebellar homogenates of ANPC mice at 10 weeks of age compared to the age-matched WT, APP-Tg and Dhet mice. Values are means ± SEM from n = 4 animals per genotype/age group. **(D)** Immunoblots and respective histograms showing no significant alteration in presenilin 1 (PS1-NTF), nicastrin, APh-1 or Pen-2 levels in N2a-ANPC cells compared to N2a-APP controls. Protein levels were normalized to respective β-actin levels. **(E)** Histograms showing an increasing trend (which did not reach statistical significance level) in γ-secretase activity in N2a-ANPC cells compared to N2a-APP controls. Values are means ± SEM from 3 independent experiments for culture studies. *, $p < 0.05$.

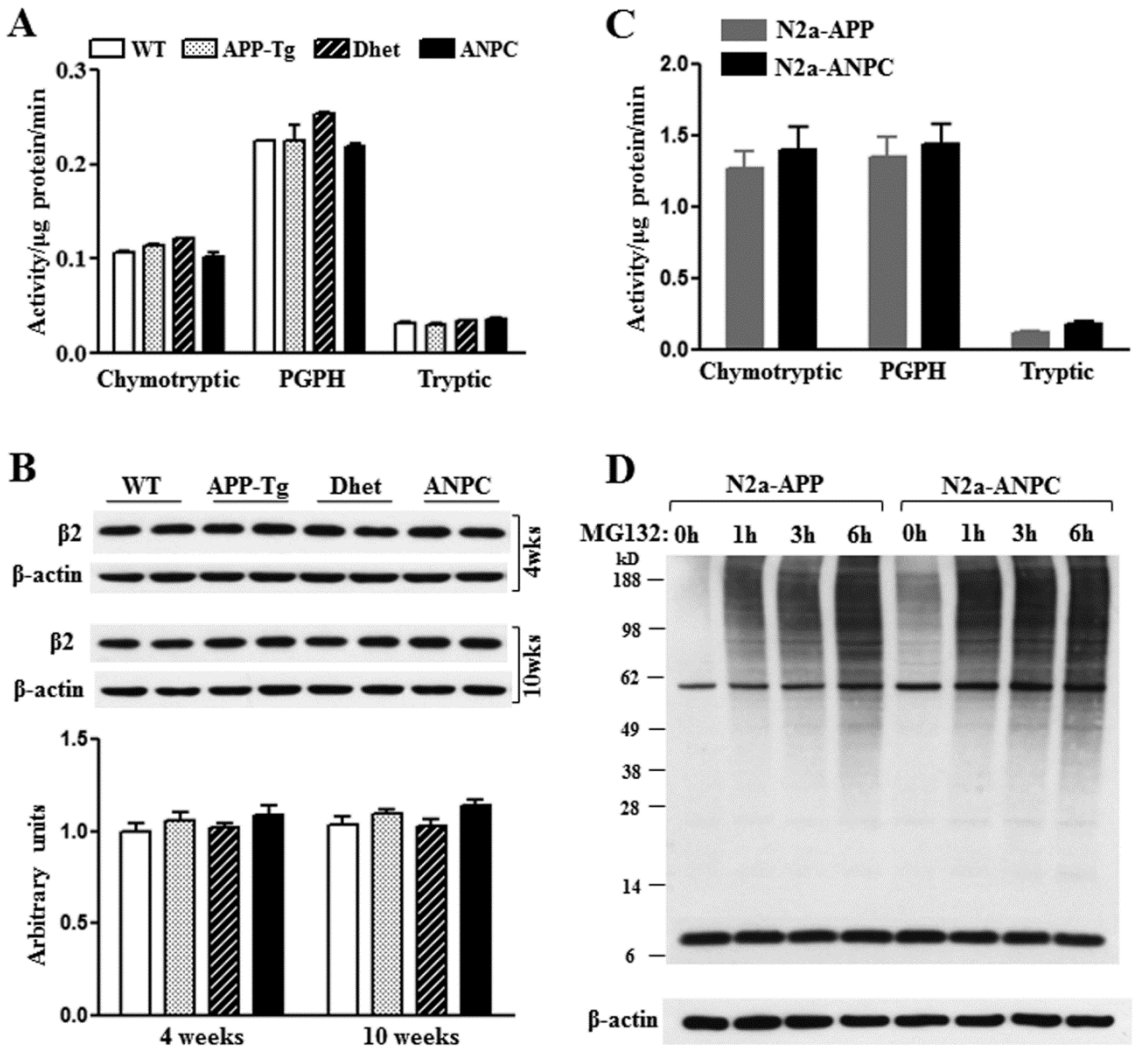

Figure 4.7: Proteasomal activity is not affected by cholesterol sequestration. **(A)** Histograms depicting the 20S proteasomal chymotrypsin-like, trypsin-like and PGPH activity in the cerebellar homogenates of 10 week old WT, APP-Tg, Dhet and ANPC mice without any significant variation between the genotypes. **(B)** Immunoblots and respective histograms showing no significant alteration in the proteasome β-2 subunit levels in the cerebellum of 4- and 10-week old ANPC mice compared to WT, APP-Tg and Dhet mice. Protein levels were normalized to respective β-actin levels. Values are means ± SEM from n = 4 animals per genotype/age group. **(C)** Histograms showing no significant alteration in the 20S proteasomal chymotrypsin-like, trypsin-like and PGPH activity in the N2a-ANPC cells compared to N2a-APP controls. Values are means ± SEM from 3 independent experiments. **(D)** Representative immunoblot from 3 independent experiments illustrating similar accumulation of ubiquitinated proteins in N2a-APP and N2a-ANPC cells following inhibition of proteasomal activity by MG132 (10µM) treatment for different periods of time. β-actin was used as a loading control.

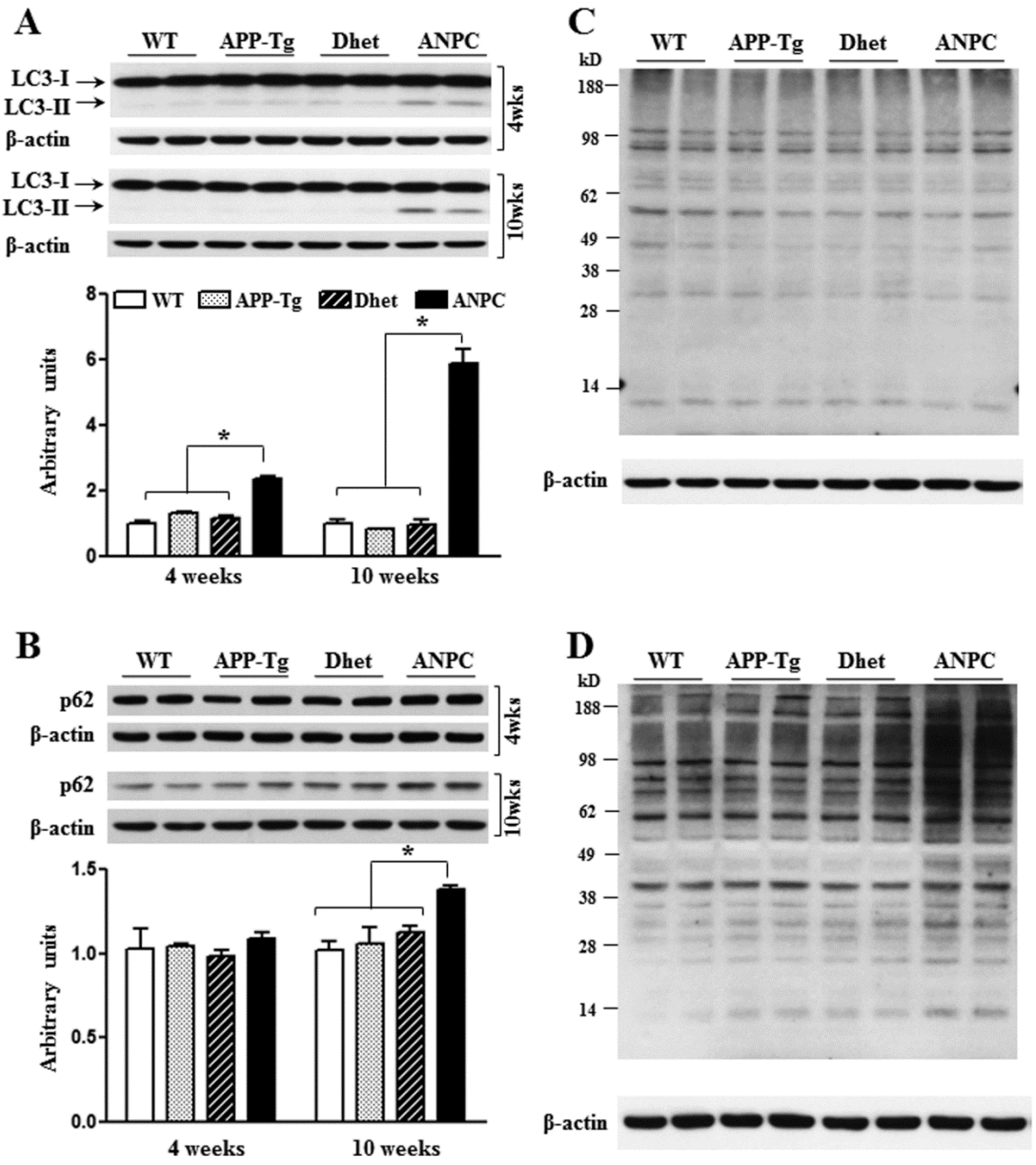

Figure 4.8: Impaired autophagic clearance in ANPC cerebellum. **(A, B)** Immunoblots and respective histograms showing progressive accumulation of LC3-II (~15 kDa; A) and p62 (~62 kDa; B) in the cerebellum of ANPC mice compared to WT, APP-Tg and Dhet mice between 4 and 10 weeks of age. Protein levels were normalized to respective β-actin levels. Values are means ± SEM from n = 4 animals per genotype/age group. **(C, D)** Representative immunoblots of cerebellar homogenates probed with anti-ubiquitin antibody showing increased levels of poly-ubiquitinated proteins in ANPC compared to WT, APP-Tg and Dhet mice at 10 weeks (D) but not at 4 weeks (C) of age. β-actin was used as a loading control. *, $p < 0.05$.

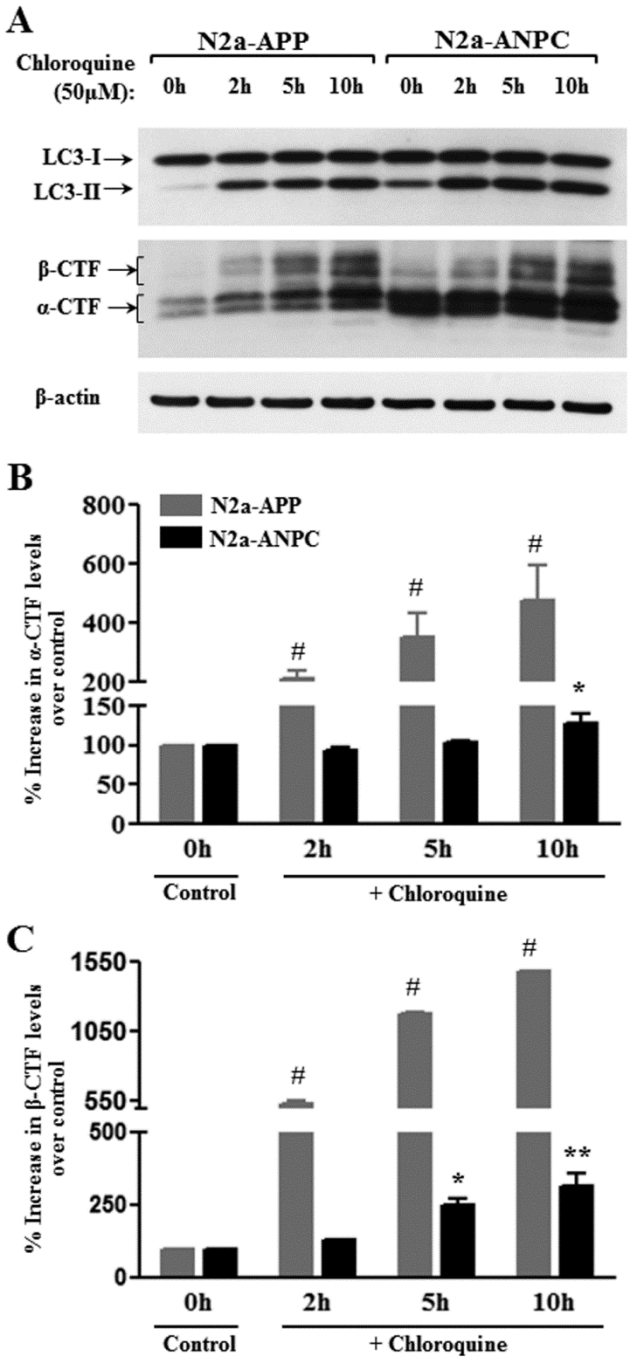

Figure 4.9: APP-CTF accumulation following cholesterol sequestration in N2aANPC cells is mediated by impaired lysosomal degradative activity. N2a-APP and N2a-ANPC cells were treated with chloroquine (50μM) for the specified time points. **(A)** Representative immunoblot showing LC3-I/II and APP-CTF levels at different time points following chloroquine treatment. **(B, C)** Histograms depicting α-CTF (B) and β-CTF (C) levels expressed as percentage of the respective controls at different time points following chloroquine treatment. Data represent means ± SEM from 3 independent experiments. Note that N2a-APP cells show a time-dependent (0h - 10h) increase in α-CTF and β-CTF levels, whereas the N2a-ANPC cells show an increase in CTF levels only at later time points (5h and/or 10h). Also, the percent increase of CTF levels above basal level (0h) is much less in N2a-ANPC cells compared to N2a-APP cells, suggesting impaired lysosomal clearance activity in N2a-ANPC cells. *, $p < 0.05$; ** $p < 0.01$; #, $p < 0.001$.

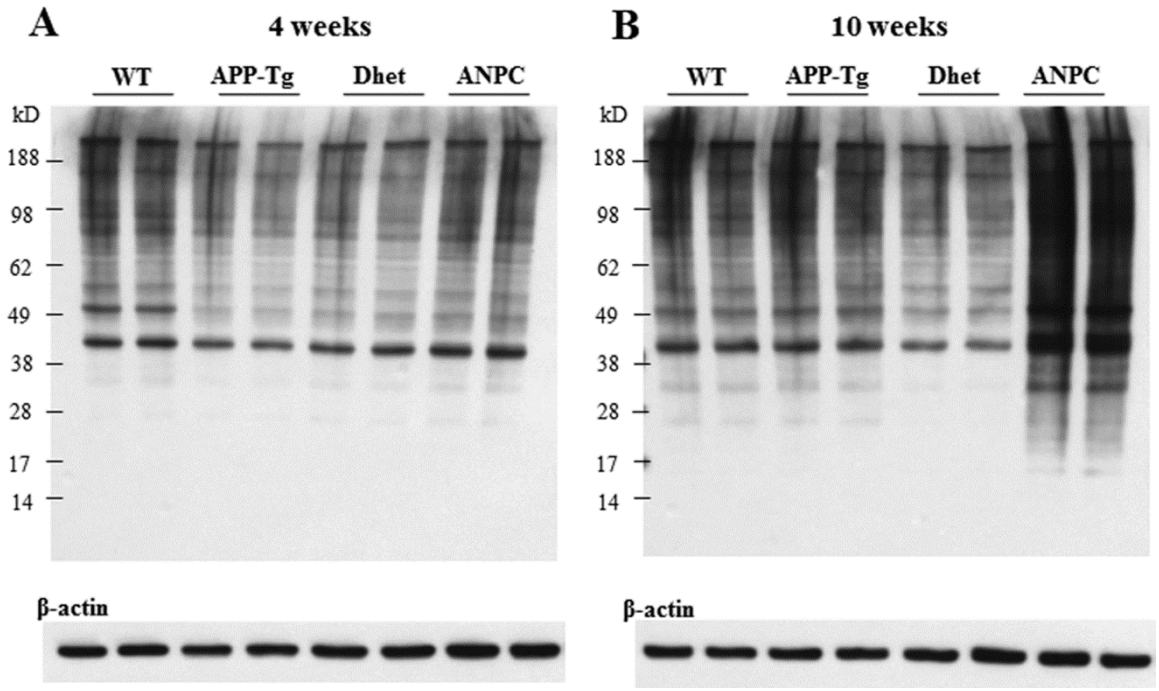

Figure 4.10: Age-dependent increase in oxidative stress in ANPC cerebellum. **(A, B)** Representative immunoblots showing increased protein carbonyl levels in ANPC cerebellar homogenates compared to those of WT, APP-Tg and Dhet mice at 10 weeks (B) but not at 4 weeks (A) of age. β-actin was used as a loading control.

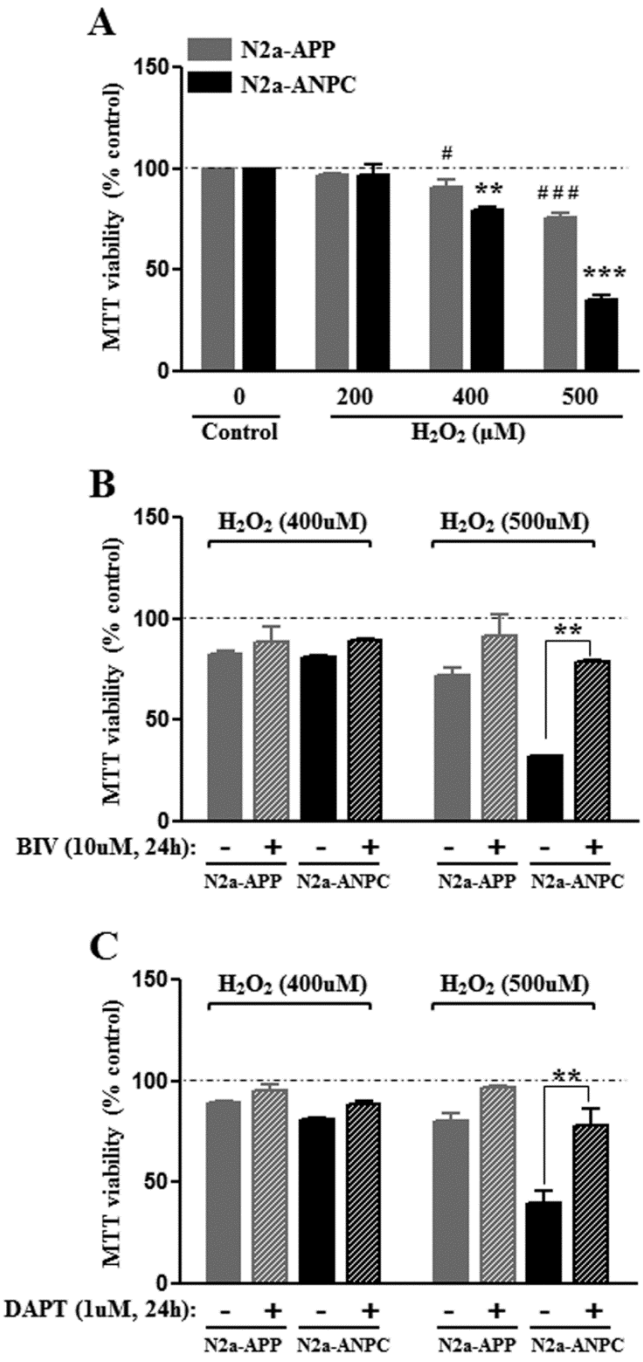

Figure 4.11: Involvement of the accumulated Aβ-related peptides in mediating oxidative stress-induced toxicity. **(A)** N2a-APP and N2a-ANPC cells were treated with different doses of H_2O_2 (0-500μM) for 3h and cell viability was determined by methyl thiazole tetrazolium (MTT) assay. Histograms showing decreased viability of N2a-ANPC cells to H_2O_2 treatment compared to N2a-APP cells. **(B, C)** Histograms showing reversal of H_2O_2-induced toxicity following 24 h pre-treatment of the cells with β-secretase (BIV - 10μM, B) or γ-secretase (DAPT - 1μM, C) inhibitor. Data are expressed as a percentage of control and represented as means ± SEM from 3 independent experiments. #, $p < 0.05$; ###, $p < 0.001$; **$p < 0.01$; ***$p < 0.001$

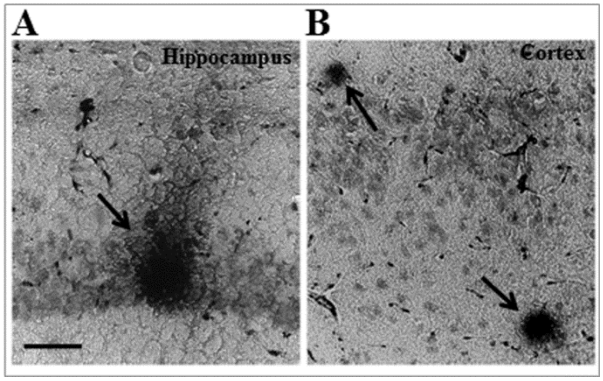

Figure 4.12: *Suppl Figure 1*; Representative images for extracellular Aβ deposits as seen in ANPC brain. **(A,B)** Photomicrographs showing 6E10-labeled extracellular Aβ deposits in the hippocampus (A) and cortex (B) of ANPC mice at 10 weeks of age. Scale bar, 50 μm.

4.4 Discussion

Using a new line of bigenic ANPC mice, the present study provides evidence that intracellular cholesterol accumulation can significantly increase APP-CTF and Aβ levels in the affected cerebellar region of the ANPC mice compared to APP-Tg and Dhet mice, *albeit* no changes in APP mRNA or protein levels were evident among the genotypes. Similar results were obtained in the stable N2a-ANPC cells that overexpress mutant human APP in the absence of Npc1 protein. While enhanced APP-CTF levels may be the consequence of decreased clearance, increased $A\beta_{1-40}$ and $A\beta_{1-42}$ levels are possibly derived from differential regulatory mechanisms. We also observed that cholesterol accumulation did not affect the ubiquitin-proteasome system but impaired the autophagic-lysosomal pathway both in ANPC mice and in N2a-ANPC cells. Additionally, our results revealed that increased levels of β-CTF and Aβ peptides rendered N2a-ANPC cells more vulnerable to oxidative injury than N2a-APP cells. These results, together with the observed increase in the protein carbonyls in the cerebellum of ANPC mice, suggest that enhanced levels of APP-CTFs and Aβ peptides can render neurons vulnerable to oxidative injury in NPC disease.

Earlier studies have shown that elevated cholesterol levels can increase Aβ production, whereas inhibition of cholesterol synthesis can lower Aβ levels (5, 6, 38, 39). The critical factor influencing Aβ production may depend not only on total levels but also on the compartmentalization of cholesterol within the cell (40). Considering the evidence that a subset of cellular APP, as well as β- and γ-secretases, are localized in cholesterol-rich lipid-raft domains (41-43), a number of *in vitro* studies have shown that increased levels or altered distribution of cholesterol can enhance APP levels and its processing *via* the amyloidogenic pathway, leading to increased Aβ production (39, 44, 45). However, our studies showed that cholesterol sequestration in the neuronal EL system by genetic means under *in vitro* as well as *in vivo* conditions does not influence either APP mRNA or holoprotein levels. This is consistent with recent data which show that cholesterol accretion in neurons following treatment with the cholesterol transport inhibitor U18666A (46) or decreased cholesterol synthesis in APP-Tg mice (47, 48) did not affect

APP levels. Thus cholesterol may influence Aβ levels/deposition by regulating Aβ production and/or clearance mechanisms rather than altering APP levels.

With regards to APP endoproteolysis, our results show that intracellular cholesterol accumulation within EL system can significantly increase α- and β-CTF levels in the cerebellum of ANPC mice as well as in N2a-ANPC cells. However, the levels of sAPPα or sAPPβ are not altered either in the cerebellum of ANPC mice or in the conditioned media of N2a-ANPC cultured cells. While these changes are accompanied by unaltered BACE1 levels, the ADAM10 levels are decreased in ANPC mice but not in cultured cells. Thus it is likely that enhanced levels of α- and β-CTFs may be the consequence of decreased clearance of the peptides rather than increased production. This is partly supported by the evidence that γ-secretase activity, which can regulate the levels of both α- and β-CTFs, is found to be either increased or unaltered in our experimental paradigms. Although an alteration in cholesterol levels can influence APP processing by regulating α- or β-secretase activity (49, 50), some animal models do not display any variation in levels/activity of either α- or β-secretases in spite of altered cholesterol levels (47, 51). Thus it remains to be established whether subcellular cholesterol distribution and/or factors other than cholesterol may influence APP processing by regulating level/activity of the α- or β-secretase.

In contrast to α and β-secretases, the levels of PS1 and nicastrin as well as activity of the γ-secretase are increased in the ANPC mouse cerebellum compared to other genotypes, thus raising the possibility that intracellular cholesterol accumulation may influence the functioning of the γ-secretase complex, as reported in Npc1-null mouse brains (20, 51). Although there is an increasing trend, we did not observe any significant alterations in the levels or activity of the γ-secretase complex in N2a-ANPC cells as reported in Chinese hamster ovary cells deficient in Npc1 protein and in neuronal cells exposed to the cholesterol transport-inhibiting agent U18666A (45). Whether the disparity relates to the presence or absence of mutant human APP, variation in cell types and/or other experimental paradigms remains to be determined. Nevertheless, our results clearly showed that levels of both $A\beta_{1-40}$ and $A\beta_{1-42}$ are enhanced in the cerebellum as

well as in the N2a-ANPC cells as reported in Npc1-null mice (39, 51) and cholesterol-accumulating cultured cells (39, 45, 46, 52). There is also evidence that partial depletion of NPC1 in mutant APP+PS1 double transgenic mice can increase Aβ levels and deposition, *albeit* intracellular accumulation of cholesterol remains unclear (53). The intracellular Aβ levels in N2a-ANPC cells, in the absence of any significant alteration in γ-secretase activity, most likely derived from decreased clearance rather than enhanced production. This is partially supported by the observation that the secretory pool of Aβ peptides was unaffected, as reported in some earlier studies (39, 46). In contrast to the cultured cells, increased levels of Aβ peptides in ANPC mouse cerebellum possibly originate from enhanced processing of β-CTFs by the γ-secretase complex. However, given the evidence that autophagic-lysosomal pathway, which is known to be impaired in NPC pathology (54, 55), plays a critical role in the clearance of Aβ-related peptides, it is likely that decreased clearance of the peptide may also partly contribute to the observed increase in $A\beta_{1\text{-}40}$ and $A\beta_{1\text{-}42}$ levels.

The ubiquitin-proteasome system plays important roles in a variety of cellular processes including the degradation of short-lived proteins. In this pathway, ubiquitin, a highly conserved 76 amino acid peptide, is first covalently conjugated to lysine residues of the substrate which are then transported to 26S proteasome and degraded by three different types of proteolytic activity: a chymotrpysin-like, a trypsin-like and a PGPH-like activity. Many of the core proteins involved in APP processing including the APP-CTFs (56), BACE1 (57) and γ-secretase complex (i.e., PS1, Pen2, nicastrin and APH1) (58-61) are known to be degraded by the proteasomal pathway. There is also evidence that a subset of APP holoprotein (62) and Aβ-related peptides (63) can be targeted to the proteasomal pathway. Notwithstanding the importance of this system in Aβ homeostasis, we did not observe any alteration of the chymotrypsin-like, trypsin-like or PGPH-like activity in ANPC mouse cerebellum or in N2a-ANPC cells. The catalytic β2 subunit levels of the ubiquitin proteasome system were also not affected in the cerebellum of ANPC mice compared to WT, APP-Tg and Dhet mice. Although ubiquitinated protein levels were not altered in N2a-ANPC cells, they are found to be markedly increased in the cerebellum of ANPC mice compared to other genotypes. In the absence of any

alteration in the proteasomal activity, this possibly reflects an abnormal autophagic-lysosomal system which is known to degrade certain p62-conjugated ubiquitinated proteins. Collectively, these results suggest that increased levels of APP-CTFs and Aβ-related peptides observed in ANPC mouse cerebellum as well as in N2a-ANPC cells are not the consequence of an abnormal ubiquitin-proteasome system.

The significance of the autophagic-lysosomal system in regulating the production and/or clearance of APP-CTFs and Aβ peptides remains controversial. Some studies have shown that inhibition of autophagy by 3-methyladenine treatment or down regulation of autophagy-related protein 5 (*Atg5*) can decrease APP-CTF and Aβ levels which can subsequently lead to cell survival (64, 65). In contrast, a number of studies have clearly demonstrated that induction of autophagy by overexpression of beclin1, an initiator of autophagy (66), or pharmacological treatments with rapamycin as well as a small molecule enhancer of rapamycin (SMER28) can decrease the levels of APP-CTFs and Aβ peptide and protect the cells from toxicity (67, 68). There is also evidence that an autophagy inducer can reduce Aβ pathology and ameliorate cognitive deficits in animal models of AD (69). Although the exact role of autophagy in Aβ homeostasis is still debated, there is convincing data that the autophagic-lysosomal system is impaired in NPC disease – reflected by an increased number of autophagosomes and lysosomes in the vulnerable neurons of the brain (54, 55). This is accompanied by up-regulation of the autophagic marker LC3-II as well as expression of lysosomal hydrolases such as cathepsins B and D within the cells (54, 55, 70). Consistent with these data we observed increased levels of LC3-II and/or p62 in the cerebellum of ANPC mice as well as N2a-ANPC cells. At the cellular levels both APP-CTFs and Aβ-related peptides, which showed intense immunoreactivity in ANPC mice compared to other genotypes, were localized mostly in endosomes rather than lysosomes. Given the unaltered BACE1, sAPPα and sAPPβ levels, it is likely that increased levels of APP-CTFs and Aβ peptides observed in our studies are the consequence of an impaired-autophagic-lysosomal system. This is partly supported by the evidence that chloroquine treatment enhanced APP-CTF levels somewhat earlier in N2a-APP cells than in N2a-ANPC cells. However, additional experiments are needed to establish whether induction of the autophagic

pathway or inhibition of autophagosome formation and its fusion with lysosomes can lead to clearance of APP-CTFs and Aβ-related peptides and cell survival.

Although there is evidence that accumulation of β-CTF and Aβ-related peptides can trigger degeneration of neurons both under *in vitro* and *in vivo* conditions (35-37), the significance of these peptides in NPC pathology remains unclear. Some earlier studies have shown that oxidative damage can play a critical role in the pathophysiology of NPC disease. This is supported by data showing that i) degeneration of neurons induced by U18666A, a class-II amphiphile that triggers an NPC-like cellular phenotype, is partly mediated by oxidative stress (71), ii) synthesis of an antioxidant enzyme (i.e., catalase) or molecules (i.e., allopregnanolone and glutathione) are substantially diminished, whereas oxidative stress markers (i.e., protein carbonyls) are increased in Npc1-deficient mice (72-74) and iii) treatments of Npc1-null mice with antioxidants such as allopregnanolone and curcumin have been shown to increase the life-span, delay the onset of neurological impairments and/or enhance viability of cerebellar Purkinje cells (74, 75). Interestingly, our results clearly showed that N2a-ANPC cells are not only more vulnerable to H_2O_2-induced toxicity than N2a-APP cells, but inhibiting β-secreatse or γ-secretase activity with specific inhibitors can significantly protect these cells against toxicity. Thus, it is likely that increased levels of β-CTF and/or Aβ-related peptides by activating oxidative stress pathways can trigger cell death mechanisms in NPC pathology. This is partly validated by the observation that the vulnerable cerebellar region of ANPC mice, which exhibits an up-regulation of β-CTF and Aβ levels, showed a parallel increase in carbonyl protein levels compared to other genotypes. In summary, the present study using a new line of bigenic ANPC mice as well as stable cell lines showed that cholesterol accretion within EL system did not affect APP levels but increased APP-CTF and Aβ levels that can render the cells vulnerable to oxidative injury. Additionally, we observed that up-regulation of APP-CTFs and Aβ peptides may possibly be the consequence of an impaired autophagic-lysosomal, but not proteasomal, clearance pathway.

4.5 References

1. Nelson, P.T., Braak, H. and Markesbery, W.R. (2009) Neuropathology and cognitive impairment in Alzheimer disease: a complex but coherent relationship. *J Neuropathol Exp Neurol,* 68, 1-14.

2. Selkoe, D.J. (2008) Biochemistry and molecular biology of amyloid beta-protein and the mechanism of Alzheimer's disease. In Vinken, P.J., Bruyn GW (ed.), *Handb Clin Neurol* Elsevier Inc., Vol. 89, pp. 245-260.

3. Hardy, J. (2009) The amyloid hypothesis for Alzheimer's disease: a critical reappraisal. *J Neurochem,* 110, 1129-1134.

4. Nathalie, P. and Jean-Noel, O. (2008) Processing of amyloid precursor protein and amyloid peptide neurotoxicity. *Curr Alzheimer Res,* 5, 92-99.

5. Fassbender, K., Simons, M., Bergmann, C., Stroick, M., Lutjohann, D., Keller, P., Runz, H., Kuhl, S., Bertsch, T., von Bergmann, K. *et al.* (2001) Simvastatin strongly reduces levels of Alzheimer's disease beta -amyloid peptides Abeta 42 and Abeta 40 in vitro and in vivo. *Proc Natl Acad Sci U S A,* 98, 5856-5861.

6. Simons, M., Keller, P., De Strooper, B., Beyreuther, K., Dotti, C.G. and Simons, K. (1998) Cholesterol depletion inhibits the generation of beta-amyloid in hippocampal neurons. *Proc Natl Acad Sci U S A,* 95, 6460-6464.

7. Refolo, L.M., Malester, B., LaFrancois, J., Bryant-Thomas, T., Wang, R., Tint, G.S., Sambamurti, K., Duff, K. and Pappolla, M.A. (2000) Hypercholesterolemia accelerates the Alzheimer's amyloid pathology in a transgenic mouse model. *Neurobiol Dis,* 7, 321-331.

8. Refolo, L.M., Pappolla, M.A., LaFrancois, J., Malester, B., Schmidt, S.D., Thomas-Bryant, T., Tint, G.S., Wang, R., Mercken, M., Petanceska, S.S. *et al.* (2001) A cholesterol-lowering drug reduces beta-amyloid pathology in a transgenic mouse model of Alzheimer's disease. *Neurobiol Dis,* 8, 890-899.

9. Fryer, J.D., Demattos, R.B., McCormick, L.M., O'Dell, M.A., Spinner, M.L., Bales, K.R., Paul, S.M., Sullivan, P.M., Parsadanian, M., Bu, G. *et al.* (2005) The low density lipoprotein receptor regulates the level of central nervous system human and murine apolipoprotein E but does not modify amyloid plaque pathology in PDAPP mice. *J Biol Chem,* 280, 25754-25759.

10. George, A.J., Holsinger, R.M., McLean, C.A., Laughton, K.M., Beyreuther, K., Evin, G., Masters, C.L. and Li, Q.X. (2004) APP intracellular domain is increased and soluble Abeta is reduced with diet-induced hypercholesterolemia in a transgenic mouse model of Alzheimer disease. *Neurobiol Dis,* 16, 124-132.

11. Howland, D.S., Trusko, S.P., Savage, M.J., Reaume, A.G., Lang, D.M., Hirsch, J.D., Maeda, N., Siman, R., Greenberg, B.D., Scott, R.W. *et al.* (1998) Modulation of secreted beta-amyloid precursor protein and amyloid beta-peptide in brain by cholesterol. *J Biol Chem,* 273, 16576-16582.

12. Fagan, A.M., Christopher, E., Taylor, J.W., Parsadanian, M., Spinner, M., Watson, M., Fryer, J.D., Wahrle, S., Bales, K.R., Paul, S.M. *et al.* (2004) ApoAI deficiency results in marked reductions in plasma cholesterol but no alterations in amyloid-beta pathology in a mouse model of Alzheimer's disease-like cerebral amyloidosis. *Am J Pathol,* 165, 1413-1422.

13. Abad-Rodriguez, J., Ledesma, M.D., Craessaerts, K., Perga, S., Medina, M., Delacourte, A., Dingwall, C., De Strooper, B. and Dotti, C.G. (2004) Neuronal membrane cholesterol loss enhances amyloid peptide generation. *J Cell Biol,* 167, 953-960.

14. Park, I.H., Hwang, E.M., Hong, H.S., Boo, J.H., Oh, S.S., Lee, J., Jung, M.W., Bang, O.Y., Kim, S.U. and Mook-Jung, I. (2003) Lovastatin enhances Abeta production and senile plaque deposition in female Tg2576 mice. *Neurobiol Aging,* 24, 637-643.

15. Chishti, M.A., Yang, D.S., Janus, C., Phinney, A.L., Horne, P., Pearson, J., Strome, R., Zuker, N., Loukides, J., French, J. *et al.* (2001) Early-onset amyloid deposition and cognitive deficits in transgenic mice expressing a double mutant form of amyloid precursor protein 695. *J Biol Chem,* 276, 21562-21570.

16. Karten, B., Vance, D.E., Campenot, R.B. and Vance, J.E. (2003) Trafficking of cholesterol from cell bodies to distal axons in Niemann Pick C1-deficient neurons. *J Biol Chem,* 278, 4168-4175.

17. Loftus, S.K., Morris, J.A., Carstea, E.D., Gu, J.Z., Cummings, C., Brown, A., Ellison, J., Ohno, K., Rosenfeld, M.A., Tagle, D.A. *et al.* (1997) Murine model of Niemann-Pick C disease: mutation in a cholesterol homeostasis gene. *Science,* 277, 232-235.

18. Maulik, M., Ghoshal, B., Kim, J., Wang, Y., Yang, J., Westaway, D. and Kar, S. (2012) Mutant human APP exacerbates pathology in a mouse model of NPC and its reversal by a beta-cyclodextrin. *Hum Mol Genet,* 21, 4857-4875.

19. Thinakaran, G., Teplow, D.B., Siman, R., Greenberg, B. and Sisodia, S.S. (1996) Metabolism of the "Swedish" amyloid precursor protein variant in neuro2a (N2a) cells. Evidence that cleavage at the "beta-secretase" site occurs in the golgi apparatus. *J Biol Chem,* 271, 9390-9397.

20. Kodam, A., Maulik, M., Peake, K., Amritraj, A., Vetrivel, K.S., Thinakaran, G., Vance, J.E. and Kar, S. (2010) Altered levels and distribution of amyloid precursor protein and its processing enzymes in Niemann-Pick type C1-deficient mouse brains. *Glia,* 58, 1267-1281.

21. Grimm, M.O., Grimm, H.S., Tomic, I., Beyreuther, K., Hartmann, T. and Bergmann, C. (2008) Independent inhibition of Alzheimer disease beta- and gamma-secretase cleavage by lowered cholesterol levels. *J Biol Chem,* 283, 11302-11311.

22. Song, M.S., Rauw, G., Baker, G.B. and Kar, S. (2008) Memantine protects rat cortical cultured neurons against beta-amyloid-induced toxicity by attenuating tau phosphorylation. *Eur J Neurosci*, 28, 1989-2002.

23. Mathur, B.N., Neely, M.D., Dyllick-Brenzinger, M., Tandon, A. and Deutch, A.Y. (2007) Systemic administration of a proteasome inhibitor does not cause nigrostriatal dopamine degeneration. *Brain Res*, 1168, 83-89.

24. Goldberg, A.L. (2003) Protein degradation and protection against misfolded or damaged proteins. *Nature*, 426, 895-899.

25. Oddo, S. (2008) The ubiquitin-proteasome system in Alzheimer's disease. *J Cell Mol Med*, 12, 363-373.

26. Hara, T., Nakamura, K., Matsui, M., Yamamoto, A., Nakahara, Y., Suzuki-Migishima, R., Yokoyama, M., Mishima, K., Saito, I., Okano, H. *et al.* (2006) Suppression of basal autophagy in neural cells causes neurodegenerative disease in mice. *Nature*, 441, 885-889.

27. Komatsu, M., Waguri, S., Chiba, T., Murata, S., Iwata, J., Tanida, I., Ueno, T., Koike, M., Uchiyama, Y., Kominami, E. *et al.* (2006) Loss of autophagy in the central nervous system causes neurodegeneration in mice. *Nature*, 441, 880-884.

28. Bjorkoy, G., Lamark, T. and Johansen, T. (2006) p62/SQSTM1: a missing link between protein aggregates and the autophagy machinery. *Autophagy*, 2, 138-139.

29. Nixon, R.A., Yang, D.S. and Lee, J.H. (2008) Neurodegenerative lysosomal disorders: a continuum from development to late age. *Autophagy*, 4, 590-599.

30. Poole, B. and Ohkuma, S. (1981) Effect of weak bases on the intralysosomal pH in mouse peritoneal macrophages. *J Cell Biol*, 90, 665-669.

31. Hui, L., Chen, X. and Geiger, J.D. (2012) Endolysosome involvement in LDL cholesterol-induced Alzheimer's disease-like pathology in primary cultured neurons. *Life Sci*.

32. Butterfield, D.A., Perluigi, M. and Sultana, R. (2006) Oxidative stress in Alzheimer's disease brain: new insights from redox proteomics. *Eur J Pharmacol*, 545, 39-50.

33. Vazquez, M.C., Balboa, E., Alvarez, A.R. and Zanlungo, S. (2012) Oxidative stress: a pathogenic mechanism for Niemann-Pick type C disease. *Oxid Med Cell Longev*, 2012, 205713.

34. Pratico, D. (2008) Oxidative stress hypothesis in Alzheimer's disease: a reappraisal. *Trends Pharmacol Sci*, 29, 609-615.

35. Wirths, O., Multhaup, G. and Bayer, T.A. (2004) A modified beta-amyloid hypothesis: intraneuronal accumulation of the beta-amyloid peptide--the first step of a fatal cascade. *J Neurochem*, 91, 513-520.

36. McPhie, D.L., Golde, T., Eckman, C.B., Yager, D., Brant, J.B. and Neve, R.L. (2001) beta-Secretase cleavage of the amyloid precursor protein mediates neuronal apoptosis caused by familial Alzheimer's disease mutations. *Brain Res Mol Brain Res*, 97, 103-113.

37. Berger-Sweeney, J., McPhie, D.L., Arters, J.A., Greenan, J., Oster-Granite, M.L. and Neve, R.L. (1999) Impairments in learning and memory accompanied by neurodegeneration in mice transgenic for the carboxyl-terminus of the amyloid precursor protein. *Brain Res Mol Brain Res*, 66, 150-162.

38. Frears, E.R., Stephens, D.J., Walters, C.E., Davies, H. and Austen, B.M. (1999) The role of cholesterol in the biosynthesis of beta-amyloid. *Neuroreport*, 10, 1699-1705.

39. Yamazaki, T., Chang, T.Y., Haass, C. and Ihara, Y. (2001) Accumulation and aggregation of amyloid beta-protein in late endosomes of Niemann-pick type C cells. *J Biol Chem*, 276, 4454-4460.

40. Puglielli, L., Tanzi, R.E. and Kovacs, D.M. (2003) Alzheimer's disease: the cholesterol connection. *Nat Neurosci*, 6, 345-351.

41. Tun, H., Marlow, L., Pinnix, I., Kinsey, R. and Sambamurti, K. (2002) Lipid rafts play an important role in Abeta biogenesis by regulating the beta-secretase pathway. *J Mol Neurosci*, 19, 31-35.

42. Vetrivel, K.S., Cheng, H., Lin, W., Sakurai, T., Li, T., Nukina, N., Wong, P.C., Xu, H. and Thinakaran, G. (2004) Association of gamma-secretase with lipid rafts in post-Golgi and endosome membranes. *J Biol Chem*, 279, 44945-44954.

43. Wahrle, S., Das, P., Nyborg, A.C., McLendon, C., Shoji, M., Kawarabayashi, T., Younkin, L.H., Younkin, S.G. and Golde, T.E. (2002) Cholesterol-dependent gamma-secretase activity in buoyant cholesterol-rich membrane microdomains. *Neurobiol Dis*, 9, 11-23.

44. Davis, W., Jr. (2008) The cholesterol transport inhibitor U18666a regulates amyloid precursor protein metabolism and trafficking in N2aAPP "Swedish" cells. *Curr Alzheimer Res*, 5, 448-456.

45. Runz, H., Rietdorf, J., Tomic, I., de Bernard, M., Beyreuther, K., Pepperkok, R. and Hartmann, T. (2002) Inhibition of intracellular cholesterol transport alters presenilin localization and amyloid precursor protein processing in neuronal cells. *J Neurosci*, 22, 1679-1689.

46. Jin, L.W., Shie, F.S., Maezawa, I., Vincent, I. and Bird, T. (2004) Intracellular accumulation of amyloidogenic fragments of amyloid-beta precursor protein in neurons with Niemann-Pick type C defects is associated with endosomal abnormalities. *Am J Pathol*, 164, 975-985.

47. Burgess, B.L., Parkinson, P.F., Racke, M.M., Hirsch-Reinshagen, V., Fan, J., Wong, C., Stukas, S., Theroux, L., Chan, J.Y., Donkin, J. *et al.* (2008) ABCG1

influences the brain cholesterol biosynthetic pathway but does not affect amyloid precursor protein or apolipoprotein E metabolism in vivo. *J Lipid Res*, 49, 1254-1267.

48. Halford, R.W. and Russell, D.W. (2009) Reduction of cholesterol synthesis in the mouse brain does not affect amyloid formation in Alzheimer's disease, but does extend lifespan. *Proc Natl Acad Sci U S A*, 106, 3502-3506.

49. Kojro, E., Gimpl, G., Lammich, S., Marz, W. and Fahrenholz, F. (2001) Low cholesterol stimulates the nonamyloidogenic pathway by its effect on the alpha -secretase ADAM 10. *Proc Natl Acad Sci U S A*, 98, 5815-5820.

50. Xiong, H., Callaghan, D., Jones, A., Walker, D.G., Lue, L.F., Beach, T.G., Sue, L.I., Woulfe, J., Xu, H., Stanimirovic, D.B. *et al.* (2008) Cholesterol retention in Alzheimer's brain is responsible for high beta- and gamma-secretase activities and Abeta production. *Neurobiol Dis*, 29, 422-437.

51. Burns, M., Gaynor, K., Olm, V., Mercken, M., LaFrancois, J., Wang, L., Mathews, P.M., Noble, W., Matsuoka, Y. and Duff, K. (2003) Presenilin redistribution associated with aberrant cholesterol transport enhances beta-amyloid production in vivo. *J Neurosci*, 23, 5645-5649.

52. Malnar, M., Kosicek, M., Mitterreiter, S., Omerbasic, D., Lichtenthaler, S.F., Goate, A. and Hecimovic, S. (2010) Niemann-Pick type C cells show cholesterol dependent decrease of APP expression at the cell surface and its increased processing through the beta-secretase pathway. *Biochim Biophys Acta*, 1802, 682-691.

53. Borbon, I.A. and Erickson, R.P. (2010) Interactions of Npc1 and amyloid accumulation/deposition in the APP/PS1 mouse model of Alzheimer's. *J Appl Genet*.

54. Amritraj, A., Peake, K., Kodam, A., Salio, C., Merighi, A., Vance, J.E. and Kar, S. (2009) Increased activity and altered subcellular distribution of lysosomal enzymes determine neuronal vulnerability in Niemann-Pick type C1-deficient mice. *Am J Pathol*, 175, 2540-2556.

55. Liao, G., Yao, Y., Liu, J., Yu, Z., Cheung, S., Xie, A., Liang, X. and Bi, X. (2007) Cholesterol accumulation is associated with lysosomal dysfunction and autophagic stress in Npc1 -/- mouse brain. *Am J Pathol*, 171, 962-975.

56. Nunan, J., Williamson, N.A., Hill, A.F., Sernee, M.F., Masters, C.L. and Small, D.H. (2003) Proteasome-mediated degradation of the C-terminus of the Alzheimer's disease beta-amyloid protein precursor: effect of C-terminal truncation on production of beta-amyloid protein. *J Neurosci Res*, 74, 378-385.

57. Qing, H., Zhou, W., Christensen, M.A., Sun, X., Tong, Y. and Song, W. (2004) Degradation of BACE by the ubiquitin-proteasome pathway. *FASEB J*, 18, 1571-1573.

58. Fraser, P.E., Levesque, G., Yu, G., Mills, L.R., Thirlwell, J., Frantseva, M., Gandy, S.E., Seeger, M., Carlen, P.L. and St George-Hyslop, P. (1998) Presenilin 1 is actively degraded by the 26S proteasome. *Neurobiol Aging,* 19, S19-21.

59. Bergman, A., Hansson, E.M., Pursglove, S.E., Farmery, M.R., Lannfelt, L., Lendahl, U., Lundkvist, J. and Naslund, J. (2004) Pen-2 is sequestered in the endoplasmic reticulum and subjected to ubiquitylation and proteasome-mediated degradation in the absence of presenilin. *J Biol Chem,* 279, 16744-16753.

60. He, G., Qing, H., Cai, F., Kwok, C., Xu, H., Yu, G., Bernstein, A. and Song, W. (2006) Ubiquitin-proteasome pathway mediates degradation of APH-1. *J Neurochem,* 99, 1403-1412.

61. He, G., Qing, H., Tong, Y., Cai, F., Ishiura, S. and Song, W. (2007) Degradation of nicastrin involves both proteasome and lysosome. *J Neurochem,* 101, 982-992.

62. Kumar, P., Ambasta, R.K., Veereshwarayya, V., Rosen, K.M., Kosik, K.S., Band, H., Mestril, R., Patterson, C. and Querfurth, H.W. (2007) CHIP and HSPs interact with beta-APP in a proteasome-dependent manner and influence Abeta metabolism. *Hum Mol Genet,* 16, 848-864.

63. Zhao, X. and Yang, J. (2010) Amyloid-beta peptide is a substrate of the human 20S proteasome. *ACS Chem Neurosci,* 1, 655-660.

64. Zheng, L., Terman, A., Hallbeck, M., Dehvari, N., Cowburn, R.F., Benedikz, E., Kagedal, K., Cedazo-Minguez, A. and Marcusson, J. (2011) Macroautophagy-generated increase of lysosomal amyloid beta-protein mediates oxidant-induced apoptosis of cultured neuroblastoma cells. *Autophagy,* 7, 1528-1545.

65. Yu, W.H., Cuervo, A.M., Kumar, A., Peterhoff, C.M., Schmidt, S.D., Lee, J.H., Mohan, P.S., Mercken, M., Farmery, M.R., Tjernberg, L.O. *et al.* (2005) Macroautophagy--a novel Beta-amyloid peptide-generating pathway activated in Alzheimer's disease. *J Cell Biol,* 171, 87-98.

66. Jaeger, P.A., Pickford, F., Sun, C.H., Lucin, K.M., Masliah, E. and Wyss-Coray, T. (2010) Regulation of amyloid precursor protein processing by the Beclin 1 complex. *PLoS One,* 5, e11102.

67. Tian, Y., Bustos, V., Flajolet, M. and Greengard, P. (2011) A small-molecule enhancer of autophagy decreases levels of Abeta and APP-CTF via Atg5-dependent autophagy pathway. *FASEB J,* 25, 1934-1942.

68. Hung, S.Y., Huang, W.P., Liou, H.C. and Fu, W.M. (2009) Autophagy protects neuron from Abeta-induced cytotoxicity. *Autophagy,* 5, 502-510.

69. Bove, J., Martinez-Vicente, M. and Vila, M. (2011) Fighting neurodegeneration with rapamycin: mechanistic insights. *Nat Rev Neurosci,* 12, 437-452.

70. Pacheco, C.D. and Lieberman, A.P. (2008) The pathogenesis of Niemann-Pick type C disease: a role for autophagy? *Expert Rev Mol Med,* 10, e26.

71. Koh, C.H., Whiteman, M., Li, Q.X., Halliwell, B., Jenner, A.M., Wong, B.S., Laughton, K.M., Wenk, M., Masters, C.L., Beart, P.M. *et al.* (2006) Chronic exposure to U18666A is associated with oxidative stress in cultured murine cortical neurons. *J Neurochem,* 98, 1278-1289.

72. Vazquez, M.C., del Pozo, T., Robledo, F.A., Carrasco, G., Pavez, L., Olivares, F., Gonzalez, M. and Zanlungo, S. (2011) Alteration of gene expression profile in Niemann-Pick type C mice correlates with tissue damage and oxidative stress. *PLoS One,* 6, e28777.

73. Schedin, S., Sindelar, P.J., Pentchev, P., Brunk, U. and Dallner, G. (1997) Peroxisomal impairment in Niemann-Pick type C disease. *J Biol Chem,* 272, 6245-6251.

74. Zampieri, S., Mellon, S.H., Butters, T.D., Nevyjel, M., Covey, D.F., Bembi, B. and Dardis, A. (2009) Oxidative stress in NPC1 deficient cells: protective effect of allopregnanolone. *J Cell Mol Med,* 13, 3786-3796.

75. Lloyd-Evans, E., Morgan, A.J., He, X., Smith, D.A., Elliot-Smith, E., Sillence, D.J., Churchill, G.C., Schuchman, E.H., Galione, A. and Platt, F.M. (2008) Niemann-Pick disease type C1 is a sphingosine storage disease that causes deregulation of lysosomal calcium. *Nat Med,* 14, 1247-1255.

Chapter 5: General Discussion and Conclusion

5.1 Summary of the findings

This thesis consists of studies which are designed to examine the role of altered intracellular cholesterol level/distribution in the brain on the development of AD-related pathology. The approach is based on the disruption of intracellular cholesterol trafficking leading to cholesterol accumulation in the EL system of mouse and cell culture models overexpressing mutant human APP. Using a wide variety of experimental paradigms in our newly developed mouse model and/or stable cell lines, we have shown that:

1. Intracellular cholesterol accumulation can alter expression profiles of a wide spectrum of genes in the cerebellum and hippocampal brain regions. These include the transcripts involved in brain cholesterol metabolism, Aβ clearance, intracellular vesicular trafficking and cell death/survival mechanisms thereby indicating an overall disturbance in the CNS cholesterol homeostasis and impairment of vital cellular functions (Chapter 2).
2. Intracellular cholesterol accumulation in an APP-Tg model of AD can reduce longeivity and exacerbate a wide variety of behavioral and neuropathological abnormalities including tau phosphorylation/cleavage, lysosomal dysfunction and neurodegeneration. Furthermore, we have shown that reversal of the accumulated cholesterol can be beneficial in attenuating the majority of these pathological changes, thereby establishing the significance of intracellular cholesterol levels/distribution in proper brain functioning (Chapter 3).
3. Cholesterol sequestration in the EL system can cause progressive intracellular accumulation of APP-CTFs and Aβ peptides by influencing both generation and clearance of the APP metabolites. While the increased levels of APP-CTFs are mainly due to impaired functioning of the lysosomal degradation machinery, elevated intracellular Aβ levels are possibly the consequence of different regulatory mechanisms including increased production by γ-secretase cleavage as well as reduced lysosomal degradation. Furthermore, our results show that intracellular accumulation of the APP-CTFs and Aβ peptides following altered cholesterol levels/distribution might be responsible for increasing oxidative damage and subsequent cell death, thereby suggesting that use of antioxidants might be beneficial in reversing the pathological changes (Chapter 4).

While in-depth analyses of the results have been included in the respective chapters, the purpose of this "General Discussion" is to evaluate our experimental findings in relation to what has been previously reported by others, the novelty of our work and to discuss the possible future directions - all of which will aid in further understanding the significance of cholesterol in proper brain functioning and development of future AD and NPC therapeutics.

5.2 ANPC mice: intracellular cholesterol accumulating APP-Tg models

To study the significance of cholesterol in the development of AD-related pathology, we have generated a new transgenic mouse line (ANPC) that overexpresses human APP harboring "Swedish" (KM670/671NL) and "Indiana" (V717F) mutations and lack functional Npc1 protein due to a spontaneous insertion mutation in the *Npc1* genomic sequence. The ANPC mice show massive accumulation of intracellular cholesterol in all major brain regions and produce high levels of human APP and $A\beta_{1\text{-}40/1\text{-}42}$ peptides thus recapitulating the respective characteristics of its two progenitor lines, the Npc1-null and the APP-Tg (TgCRND8) mouse models of NPC and AD, respectively (1, 2). Most of the APP-Tg models of AD including the one used in the current study recapitulate amyloid pathology and show spatial learning deficits but do not exhibit any overt loss of neurons as seen in AD brains. In TgCRND8 mice in particular, memory deficits are apparent at ~8 weeks (3), amyloid plaques first appear at about 3 months (1) and tau abnormalities develop only at later ages of 7 months or older (4). Here, we show that human APP overexpression when combined with altered intracellular level/distribution of cholesterol act in an additive manner to markedly exacerbate the pathology of the bigenic ANPC mice. Thus, the ANPC mice develop pathology starting at a very young age of 4-5 weeks and have a significantly reduced survival of no more than 9-11 weeks in our colony. The ANPC phenotype includes memory and motor deficits, gliosis, demyelination, degeneration of cerebellar Purkinje cells, abnormal tau phosphorylation/ cleavage and lysosomal dysfunction - all of which appear to be far more profound than either APP-Tg or Npc1-null littermates. In addition, ANPC mice have increased intracellular levels of human $A\beta_{1\text{-}40/1\text{-}42}$ and APP-CTFs that are significantly higher compared to the age-matched APP-Tg mice. A detailed comparison of the phenotypic, behavioral and

neuropathololological changes observed in the APP-Tg, Npc1-null and ANPC mice are provided in the Tables 5.1-5.3.

Research over the past two decades has generated ambiguity in establishing the the potential role for cholesterol in regulating APP processing leading to Aβ production. While the majority of the earlier *in vivo* studies have been done by modulating peripheral cholesterol levels by dietary intake or pharmacological treatments (Tables 1.3-1.5, Chapter 1), we have attempted to address the relationships between cholesterol and AD-related pathology by genetic manipulation of cellular cholesterol distribution which can have a more direct impact on the brain cholesterol metabolism. Importantly, ANPC mice accumulate cholesterol in the EL system which acts as a major site for APP/Aβ metabolism and exhibits striking alterations in "at risk" neurons of AD brains. Very clearly, our results suggest that intracellular cholesterol levels/distribution plays a crucial role in regulating the amyloidogenic processing of APP. Additionally, our results highlight the significance of a proper lysosomal clearance system that is required for the removal of the unwanted materials including the Aβ-containing fragments and maintaining cellular homeostasis. Taken together, our results show that altered cholesterol homeostasis in the ANPC mice leads to abnormal APP metabolism, increased Aβ generation and accumulation of toxic Aβ-containing fragments in the EL system, which as in NPC disease are also hallmarks of AD.

Although ANPC mice develop major features of AD-related pathology, caveats must be considered when interpreting ANPC phenotype and its relationship to human AD. First, ANPC mice display the majority of the pathological changes including abnormal tau phosphorylation/cleavage, increased $A\beta_{1\text{-}40/1\text{-}42}$ and APP-CTF levels and loss of neurons in the cerebellum, a region that is not affected until very late stages in AD brains (5, 6). The hippocampus of ANPC mice displays only reactive gliosis, demyelination and amyloid deposits but no loss of neurons or abnormal tau pathology in spite of having intracellular cholesterol accumulation. However, while the motor deficits in ANPC mice relate mostly to the loss of cerebellar neurons (7, 8), the observed deficits in novel object recognition tasks which use mostly cortical and hippocampal inputs (9)

Table 5.1: Behavioral and phenotypic characterization of mutant APP-Tg, Npc1-null and ANPC mice compared to the wild-type mice.

	APP-Tg			**Npc1-null**			**ANPC**		
Behavioral characterization	4wks	7wks	10wks	4wks	7wks	10wks	4wks	7wks	10wks
Novel object-recognition memory	-	-	↓	-	-	↓↓	-	↓↓	↓↓
Motor co-ordination (rotarod test)	-	-	-	-	-	↓	-	↓	↓↓
Gait asymmetry (footprint analysis)	-	-	-	-	-	↑↑	-	↑	↑↑↑
Open-field activity:									
(a) Walking	-	-	-	-	↓	↓	-	↓	↓
(b) Rearing	-	-	-	-	-	↓	-	↓	↓
(c) Pausing	-	-	-	-	-	↑	-	↑	↑
Phenotypic characterization									
Body weight	-	-	-	-	-	↓↓	↓	↓↓	↓↓↓
Survival	>90% mice survived past 90 days			~ 40% mice survived at 90 days (median survival: ~ 85 days)			All mice died by 77 days (median survival: 69 days)		

-, No change; ↑, significant increase; ↓, significant decrease; the number of arrows correspond to the degree of change observed.

Table 5.2: Neuropathological changes observed in the hippocampus of mutant APP-Tg, Npc1-null and ANPC mice compared to the wild-type mice.

	APP-Tg			**Npc1-null**			**ANPC**		
	4wks	7wks	10wks	4wks	7wks	10wks	4wks	7wks	10wks
Intracellular cholesterol accumulation	-	-	-	↑	↑	↑	↑	↑	↑
Astrocytic activation (GFAP)	-	-	↑	-	↑	↑↑	↑	↑	↑↑
Microglial activation (Iba1)	-	-	-	↑	↑	↑↑	↑	↑	↑↑
Demyelination (CNPase)	-	↑	↑	↑↑	↑↑↑	↑↑↑	↑↑↑	↑↑↑	↑↑↑
Neuronal loss	na	-	na	na	-	na	na	-	na
Presynptic loss (Synaptophysin)	-	-	-	-	-	-	-	-	-
Postsynaptic loss (PSD95)	-	-	-	-	-	↓	-	-	↓
Tau phosphorylation and cleavage	na	-	na	na	-	na	na	-	na
Lysosomal enzyme level/activity (CatB, CatD, GusB)	na	-	na	na	-	na	na	-	na
Lysosomal membrane destabilization	na	-	na	na	-	na	na	-	na
Aβ plaques	-	-	↑	-	-	-	-	-	↑

-, No change; ↑, significant increase; ↓, significant decrease; na, not analysed; the number of arrows correspond to the degree of change observed.

Table 5.3: Neuropathological changes observed in the cerebellum of mutant APP-Tg, Npc1-null and ANPC mice compared to the wild-type mice.

	APP-Tg			Npc1-null			ANPC		
	4wks	7wks	10wks	4wks	7wks	10wks	4wks	7wks	10wks
Intracellular cholesterol accumulation	-	-	-	↑	↑	↑	↑	↑	↑
Astrocytic activation (GFAP)	-	-	-	↑	↑↑	↑↑↑	↑↑	↑↑	↑↑↑
Microglial activation (Iba1)	-	-	-	↑	↑↑	↑↑	↑↑	↑↑	↑↑
Demyelination (CNPase)	-	-	-	↑	↑↑	↑↑	↑↑	↑↑	↑↑
Neuronal loss	na	-	na	na	↑	na	na	↑↑	na
Presynptic loss (Synaptophysin)	-	-	-	-	-	↓	-	-	↓
Post-synaptic loss (PSD95)	-	-	-	-	↓	↓	-	↓	↓
Tau phosphorylation and cleavage	na	-	na	na	↑	na	na	↑↑	na
Proteasomal activity	na	-	na	na	-	na	na	-	na
Lysosomal enzyme level/activity (CatB, CatD, GusB)	na	-	na	na	↑	na	na	↑↑	na
Lysosomal membrane destabilization	na	-	na	na	↑	na	na	↑↑	na
Aβ plaques	-	-	-	-	-	-	-	-	-
APP-CTF levels	↑	na	↑	na	na	na	↑↑	na	↑↑↑
Aβ levels	↑	↑	↑	na	na	na	↑	↑↑	↑↑↑
Oxidative stress level (Protein carbonylation)	-	na	-	na	na	na	-	na	↑

-, No change; ↑, significant increase; ↓, significant decrease; na, not analysed; the number of arrows correspond to the degree of change observed.

suggest that altered cellular cholesterol levels/distribution does affect the functioning of the hippocampal circuitry without any significant loss of neurons at the age groups studied. This is substantiated, in part, by our results showing that the ANPC mice, as the Npc1-null mice, do show significant loss of pre-synaptic and post-synaptic markers in the hippocampus but only at the terminal age of 10 weeks. Whether the hippocampal neurons would also be a target of neuronal death pathways at a later age, if the animals would have lived longer, remains a matter of open question. However, the mechanisms by which hippocampal neurons being spared from degeneration in ANPC as well as in Npc1-null animals still remain to be elucidated.

Second, AD brains do not show intracellular cholesterol accumulation as seen in NPC although disturbances in cholesterol metabolism have been reported in AD and also in APP-Tg mouse models (10-13). This together with the evidence that neurons bearing tangles as well as Aβ-containing plaques have higher levels of cholesterol in AD brains (14-16) makes it particularly important to evaluate the role of intracellular levels/distribution of cholesterol in the development of AD pathology.

Third, no patient has been described carrying both recessive mutations in NPC and a dominant mutation in APP and therefore unanticipated effects on APP processing and/or cholesterol metabolism could potentially occur as a consequence of combined mutations as seen in ANPC mice. Moreover, the high Aβ levels produced due to overexpression of mutant human APP raises the possibility of greater Aβ toxicity in ANPC brain than observed in NPC pathology. In general, most transgenic mouse models of human diseases face similar criticisms because of the overexpression of one or multiple disease-causing variants in genes that are required to recapitulate the human pathology, yet they have provided valuable insights into the pathogenesis and development of therapeutic strategies. The fact that ANPC mice display the majority of the pathological changes associated with AD including behavioral deficits, tau hyperphosphorylation/cleavage, intracellular accumulation of Aβ-related peptides, EL system dysfunction along with significant loss of neurons, which most APP-Tg models lack, suggests that the ANPC mice are potentially relevant and a valuable tool for

studying the importance of cellular cholesterol balance on the development of these pathological changes and the cross-talk between them.

5.3 Cholesterol in amyloidogenesis: possible implications in AD and NPC

Accumulating evidence points to a potential role for cholesterol in the development of AD. Repeated genetic studies have revealed a strong, dose-dependent association between the incidence of late-onset AD and the inheritance of the *APOE* ε4 genotype (17). Recent genome-wide association studies have also linked single nucleotide polymorphisms in several genes related to cholesterol metabolism such as *APOJ* (*CLU*), *LRP*, *CYP46A1*, *ABCA1* and *ACAT1* to AD, although the strength of some of these associations remain to be established (18-20). Several epidemiological studies have suggested that a high total plasma cholesterol level in mid-life is a risk factor for developing AD. Supporting this, previous retrospective studies reported that the prevalence of AD was lower in patients taking statins compared with those receiving other medications typically used in cardiovascular disease (21) or even compared to the total population (22). However, some of the recent prospective studies have brought the efficacy of statins in slowing the progression of AD into question (23-26).

In addition to the genetic and epidemiological studies, multiple lines of experimental data using *in vitro* and *in vivo* models have reported that cholesterol can influence APP processing, leading to Aβ generation which can subsequently influence AD pathology (Tables 1.3-1.6, Chapter 1). Considering the evidence that a subset of cellular APP, as well as β- and γ-secretases, are localized in cholesterol-rich lipid-raft domains (27-29), a number of *in vitro* studies have shown that the crucial factor influencing Aβ production and the risk of AD may depend not only on total cellular level of cholesterol but also on the subcellular distribution of the lipid (30-35). We have determined the effects of altered intracellular cholesterol distribution on APP metabolism including processing as well as clearance pathways, which work together in regulating the levels of APP metabolites, using *in vitro* and *in vivo* genetic models of human APP overexpression and Npc1 deficiency. We provide evidence that intracellular cholesterol distribution is intrinsically linked to APP proteolytic pathways and that disruption of

normal cholesterol trafficking enhances amyloidogenesis *via* increased Aβ generation and accumulation of Aβ and APP-CTFs without altering APP holoprotein expression. These findings agree with previous *in vitro* data that showed increased Aβ levels/production in cultured NPC model cells (34, 35) and also with results in Npc1-null mouse brain (35, 36).

Earlier studies have found a correlation between cholesterol levels and α-secretase (37, 38), β-secretase (39), or γ-secretase (29) activity. With regards to APP endoproteolysis, our results show that cholesterol accumulation within the EL system following Npc1 deficiency does not alter BACE1 levels, and the levels of sAPPβ fragments were unchanged both *in vivo* and *in vitro*. Although the levels of the α-secretase ADAM10, were found to be decreased in ANPC mouse brain compared with age-matched APP-Tg and Dhet mice, the corresponding sAPPα levels were unaltered, suggesting no change in α-secretase cleavage of APP. This was further substantiated by our *in vitro* studies showing no alteration in α-secretase levels and the corresponding sAPPα levels secreted into the culture media. However, the levels of the associated C-terminal APP cleaved products, α-CTF and β-CTF, were found to be significantly increased in our ANPC mouse model as well as in the Npc1-deficient N2aAPPsw cells (referred here as N2a-ANPC) compared with the respective controls, suggesting decreased catabolism of these fragments which are the substrates for γ-secretase. While similar activities of α- and β-secretase were previously reported in Npc1-deficient mouse brains compared to age-matched WT controls, γ-secretase activity was found to be increased in Npc1-null brain homogenates (36). Supporting this, our results in ANPC mouse brain homogenates also showed increased levels of γ-secretase components (nicastrin and PS1) and activity of this enzyme complex in an *in vitro* assay.

Interestingly, the increased γ-secretase activity generated enhanced levels of only the intracellular pool of the associated cleaved products, $A\beta_{1-40}$ and $A\beta_{1-42}$, without affecting the secretory pool of Aβ. These findings, though reported in earlier studies by Yamazaki and colleagues (35) and Jin and colleagues (40), do not explain fully how enhanced γ-secretase cleavage of β-CTFs leading to increased Aβ generation can also

lead to increased β-CTF levels without any alteration in β-secretase activity. Thus it appears that the observed increase in γ-secretase activity was not sufficient to cleave all of its available substrate, leading to a buildup of the APP-CTFs inside the cell. It is possible that the enzyme cannot cleave its available substrates due to their differential spatial distribution or even steric hindrance caused by the accumulated cholesterol or other lipids that occur in Npc1 deficiency. In this context, a further analysis of the different subcellular compartments in which the enzyme and its substrate APP-CTFs are localized in ANPC brain would probably help in understanding the contribution of the increased γ-secretase activity on the APP-CTFs leading to the generation of Aβ. Future experiments using γ-secretase inhibitor treatments in cultured cells would also help in determining whether EL cholesterol accumulation can in fact reduce the availability of the APP-CTF substrates to the γ-secretase complex, thereby promoting their accumulation inside the cells. Together, our results so far suggest that the accumulation of APP-CTFs is most likely due to a reduced clearance mechanism caused by lysosomal dysfunction, as reported in Npc1-null mice (41, 42), while the increased intracellular Aβ levels is probably due to increased generation by γ-secretase cleavage and/or reduced lysosomal degradation.

Although several studies have emphasized the pathological role of Aβ (especially $A\beta_{1-42}$) and β-CTF in AD, the pathological consequence of intraneuronal Aβ/APP-CTF accumulation in NPC is unknown. Aβ accumulates within vulnerable neurons of AD brains (43) and also in APP-Tg mice (44, 45). Accumulation of intraneuronal rather than extracellular Aβ has been shown to be an early step in Aβ aggregation and neurotoxicity (46-48). Within neurons, Aβ accumulates in various organelles including the endosomes/lysosomes and possibly exerts its neurotoxic effects by compromising organelle membrane integrity, causing organelle leakage and leading to eventual neuronal death (48-51). Intracellular accumulation of APP-CTFs has also been proposed to participate in the neurodegenerative process in AD by differential mechanisms. Accumulation of APP-β-CTFs is a characteristic feature of AD brains and has been reported to exhibit much higher toxicity than Aβ peptides in a variety of experimental conditions (52). Importantly, transgenic overexpression of APP-CTFs in mice and

cultured cells induces AD-like pathological features including impaired learning and memory (53, 54), strong inflammatory reactions involving astrocytosis (55, 56), abnormal calcium homeostasis (57) and eventually neuronal and synaptic degeneration (58-60). Furthermore, it has been recently reported that β-CTFs, independent of Aβ, can cause endosomal abnormalities characteristic of AD (61).

Our *in vivo* and *in vitro* results suggest that APP amyloidogenesis leading to neuronal degeneration in AD may also have a role in NPC pathology. We have demonstrated a substantial accumulation of Aβ and APP-CTFs, likely in aggregated state, in neurons and cultured cells following cholesterol accumulation due to Npc1 deficiency. The concordance of increased APP-CTFs and Aβ levels both in cultured cells and in ANPC brains suggest that they are the direct consequences of Npc1 deficiency. However in ANPC brains, a major portion of these deposits resided in the endosomal compartments that were distinct from those that sequestered the endogenous cholesterol, thereby suggesting absence of any direct or close interaction between the APP amyloidogenic fragments and the accumulated cholesterol. This probably suggests that EL system abnormalities rather than accumulated cholesterol *per se* are responsible for the accretion of Aβ and APP-CTFs in ANPC mouse brains. This is consistent with studies by Jin and colleagues in cultured cortical neurons treated with U18666a and NPC patient brains (40) and also with studies in AD brains where similar accumulation of Aβ/APP-CTFs is noted without any detectable accumulation of cholesterol in the EL system (62). In addition, we observed that levels of certain transcripts (including *A2m*, *Plat*, *Plau* and *Mme*) and some of the corresponding proteins (for example, neprilysin encoded by *Mme*) that are known to be involved in the degradation of Aβ-related peptides, were significantly upregulated in the cerebellum of ANPC and Npc1-null mice. Whether this upregulation merely reflects a compensatory response for the increased levels of amyloidogenic peptides or cholesterol accumulation can actually regulate the degradation of the Aβ peptides and other proteins in Npc1-null and ANPC brains remains to be elucidated. Furthermore, our results suggest that the accumulated Aβ/APP-CTFs in Npc1-deficient cells/neurons can cause increased generation of reactive oxygen species (ROS), contributing significantly to the neurodegeneration and pathology. This is

supported by results showing that the N2a-ANPC cells compared to the control N2a-APP cells are more susceptible to H_2O_2 induced toxicity, an effect that was reversible with prior treatment of these cells with β- or γ-secretase inhibitors. Furthermore, analyses of ANPC cerebellar tissue indicated the presence of age-dependent increased levels of oxidative stress markers in parallel with the accumulation of Aβ/APP-CTFs and the loss of Purkinje neurons. In summary, our studies support the growing consensus indicating a role for cholesterol in amyloidogenesis which by oxidative injury can accelerate neuronal degeneration and influence other pathological features, including the abnormal tau homeostasis, that are common to both AD and NPC pathology.

5.4 Cholesterol and Tau pathology: possible implications in AD and NPC

One of the most striking similarities that exists in the pathological features between AD and NPC includes the presence of intra-neuronal NFTs (63-65), raising the possibility of shared pathogenic mechanisms of neurodegeneration in both these diseases. In AD brains, the NFTs develop over many years or even decades before the onset of clinical signs of cognitive decline and their number and regional spread correlate strongly with the degree of cognitive impairment and neuronal death (66-68). However, only a small proportion of the various nerve cell types in the brain are prone to form NFTs, suggesting regional and cellular specificity in tangle formation. In AD, NFTs first appear in the trans-entorhinal region of the temporal lobe, lateral to the hippocampus, and then spread to the entorhinal cortex, hippocampus and association neocortex (68). In contrast to AD, NPC brains develop tangles in young adolescence (69) which are found predominantly in the hippocampus, medial temporal lobes, mid brain and brain stem, with only mild to moderate involvement of the cerebral cortex (63, 65). Notably, in both diseases the cerebellum does not form tangles probably because of a relatively low amount of tau itself (70, 71).

Despite differences in the distribution of NFTs in NPC and AD, the NFTs in both disorders are identical structurally and immunologically and consist of abundant paired helical filaments of hyperphosphorylated forms of the microtubule-associated tau protein (63-65). Tau hyperphosphorylation is an early event in the pathogenesis of AD and NPC

and appears before the development of NFTs. The phosphorylation and dephosphorylation of tau plays a physiological role in stabilizing the microtubules by the balance between activities of several kinases and phosphatases. The kinases that regulate tau phosphorylation include GSK-3, Cdk5, ERK1/2, calmodulin-dependent protein kinase II (CaMKII), protein kinase A (PKA), the stress-activated c-Jun N-terminal kinase (JNK) and p38 kinase, whereas the phosphatases that mediate dephosphorylation of tau are protein phosphatase 2A (PP2A), PP2B and PP1 (72). It is believed that hyperphosphorylation results in loss-of-function of the physiological tau *via* its diminished association with microtubules resulting in the destabilization of the cytoskeleton. This supposedly impacts the efficiency of numerous microtubule-based intracellular trafficking events that are essential for normal cellular function, subsequently leading to an overall neuronal dysfunction/death (73). Thus tau loss-of function is sufficient on its own to compromise the normal functioning of the neuron, leading to its death.

Of the many cellular trafficking processes, the two major protein quality control pathways, the ubiquitin-proteasomal pathway and the autophagic-lysosomal pathway, in particular require microtubule based trafficking for efficient protein degradation (74, 75). Dysfunction of each of these pathways has been implicated in neurodegeneration (76-79), and it is possible that loss of functional tau influences several of these pathways in AD and NPC. Indeed, a recent study by Pacheco and colleagues has demonstrated that tau deletion exacerbates the NPC phenotype in mice primarily by impairing protein degradation through autophagy, suggesting that diminishing functional tau might have dire consequences in certain neurodegenerative disorders (80). Our results reveal changes in tau phosphorylation in the cerebellum of ANPC and Npc1-null mice, including a reduction in total tau (both at mRNA and protein levels) and increase in phospho-tau levels at epitopes recognized by AT8, PHF1, AT100 and AT270 antibodies. These changes were accompanied by an increase in phospho-ERK1/2 and a decrease in p35 (a negative regulator of Cdk5 activity) levels which might be involved in regulating tau hyperphosphorylation in Npc1-null and ANPC brains. Although APP-Tg mice show tau abnormalities only at later ages of 7 months or older (4), we did not observe any changes

in total or phospho-tau levels or any of the tau kinases either in the hippocampus or cerebellum of the APP-Tg line at 7 weeks of age. Surprisingly, overexpression of APP in Npc1-null mice led to a substantial increase in tau abnormalities including a further reduction in total tau levels and an increase in tau phosphorylation in the cerebellum but not in the hippocampus of ANPC mice. This is particularly interesting in the context of a recent study showing that deletion of App in Npc1-null mice also causes similar tau abnormalities including a reduction in overall tau levels as well as an increase in AT8 and PHF1 immunoreactivity (81). While these findings, taken together, suggest that abnormal function/metabolism of APP disrupts normal tau homeostasis and sensitizes the mice to stresses of Npc1 deficiency, it would be challenging to define the pathways that regulate the cross talk between APP and tau function and their role in exacerbating the pathology.

Although tau hyperphosphorylation similar to those seen in early stages of AD and NPC has been noted in APP-Tg and Npc1-null mouse models, there is no evidence of its association with tangle formation or cell death in either model (4, 82). However, given the evidence that partial or complete loss of tau expression can reduce lifespan and aggravate pathology in Npc1-null mice (80), and Cdk5 inhibitors attenuating tau phosphorylation can ameliorate the phenotype in Npc1-null mice (83, 84), it is likely that alterations in tau levels and phosphorylation observed specifically in the cerebellum of ANPC and Npc1-null mice may be involved in the degeneration of Purkinje neurons. More recently, a growing number of studies indicate a potential role for tau proteolytic fragments in neuronal death pathways. Two proteases, caspase-3 and calpain, can mediate tau cleavage in the presence of Aβ peptides. Immunohistochemical studies have shown the presence of caspase-3-cleaved tau at Asp^{421} in neuronal lesions of several tauopathies including AD. Caspase-3-cleaved tau fragments exhibit a higher propensity to aggregate than full-length tau in the presence of Aβ peptides, and generation of these fragments has been shown to precede alterations in tau conformation, phosphorylation, and aggregation, suggesting cleavage is a relatively early event in NFT formation (85-87). Additionally, mutant forms of tau that are resistant to caspase-3 cleavage prevent caspase-induced cell death, indicating a direct relationship between the generation of tau fragments and neuronal demise (85, 86). Our findings show that caspase-cleaved tau

levels are specifically elevated in the affected cerebellar region of Npc1-null mice and more so in the ANPC mice in keeping with accelerated cell loss in this bigenic line. At the cellular level we observed cleaved tau immunoreactivity along with caspase-3 labeling in the degenerating Purkinje neurons of ANPC and Npc1-null mice, indicating a possible involvement of the cleaved tau fragments in a cell death mechanism. This is partly supported by our results showing that 2-HPC treatment, which rescued the Npc1 deficiency in mice, increases the number of surviving Purkinje cells along with a reduction in the phosphorylation and cleavage of tau protein. The generation of the other tau fragments, such as the calpain-cleaved tau, has also been linked to Aβ-induced neuronal death. Importantly, cholesterol levels have been shown to be a key parameter in regulating Aβ-induced tau proteolysis by calpain (88, 89). Other than caspase and calpain, cathepsin D has also been shown to cleave tau at neutral (cytosolic) pH, resulting in fragments corresponding in mass to those found in tangles in AD brains (90, 91). Given that the ANPC mice have severe disturbances in cholesterol homeostasis along with abnormally high intracellular Aβ and cytosolic cathepsin D levels, it is likely that tau can also be cleaved by calpain and cathepsin D in addition to caspase-3 in both ANPC and Npc1-null brains. A further examination of these different cleavage events would probably shed light on the initiating factors of tau pathology and their role in influencing AD and NPC pathogenesis.

5.5 Lysosomal system dysfunction and its role in neurodegeneration

The lysosomal system is an integral component of all nucleated cells. It consists of a dynamic network of organelles working to degrade and recycle cellular macromolecules, thereby controlling organelle and cell homeostasis. The importance of the lysosomal system for proper brain functioning is underscored by the fact that extensive neurodegeneration, mental retardation and often progressive cognitive decline are among the most prominent phenotypic features of more than 40 known primary lysosomal disorders involving defects in the synthesis, sorting or targeting of a ubiquitous lysosomal protein (92-95). The close connection between neurodegeneration and lysosomal system dysfunction is further highlighted by the growing number of studies reporting prominent

alterations in the lysosomal system in several neurodegenerative disorders including Huntington's disease, Parkinson’s disease, NPC disease and AD (96-100).

The lysosomal system comprises two major degradative pathways, the endocytic pathway and the autophagic pathway, each of which terminates in the lysosome which is often referred to as the “terminal degradation compartment” of the cell. The endocytic pathway internalizes extracellular materials (e.g., nutrients and trophic factors) as well as cellular proteins and lipids from the cell surface which it further modifies and recycles or degrades in the intracellular compartments involving a series of fission and fusion events. In neurons, endocytosis is especially critical, as it supports such specialized functions as synaptic transmission and retrograde trophic signaling (97). Endocytic pathways can be subdivided into two major pathways depending on their mode of internalization of the cargo: 1) clathrin-dependepent endocytosis where the cargo is recruited into developing clathrin-coated pits, and subsequently forms clathrin-coated vesicles (101) and 2) clathrin-independent endocytosis which does not require the formation of the clathrin coat and can be further classified into seemingly distinct pathways, based on their reliance on certain proteins and lipids, differential drug sensitivities and abilities to internalize particular cargoes (102). The endocytic pathway of mammalian cells comprises distinct membrane compartments. During endocytosis, internalized macromolecules are initially directed to the early endosomes which are the first major sorting station on the endocytic pathway. After internalization, many cell surface proteins and lipids are recycled back to the plasma membrane *via* the recycling endosomes. The other early endosomal cargos are directed to the late endosomal compartments either by budding off transport vesicles or by directly maturing to late endosomes. During this maturation process, an inward budding of the surface membrane often creates a collection of internal vesicles called as a multivesicular body (MVB) (103). Late endosomes/MVBs often contain proteins characteristic of lysosomes, including lysosomal membrane glycoproteins and acid hydrolases which are delivered when transport vesicles from the trans-Golgi network or lysosomes fuse with these compartments. Fusion of the late endosome with lysosome delivers the endocytosed macromolecules for final proteolytic degradation.

In contrast to endocytosis, autophagy involves the sequestration and degradation of cytoplasmic constituents of the cell. It is the principal degradative pathway for long-lived, stable proteins and is the only mechanism by which entire organelles such as mitochondria are recycled. Large membrane proteins and protein complexes (including oligomers and aggregates) that fail to pass through the narrow barrel of the proteasome can be degraded by autophagy (104-107). Autophagy is constitutively active in neurons and is essential for neuronal survival in part by clearing damaged, aggregated, or obsolete proteins in disease states and cellular aging. However, most of the recent studies propose a dual role of autophagy in cell survival and death pathways. While basal autophagy seems absolutely essential for neuronal survival, inappropriate or prolonged activation of autophagy can lead to complete degeneration of the cells involved (76, 77, 106, 108, 109). Knowledge of the autophagic pathway has advanced rapidly in the last few years and its dysfunction has emerged as a theme in neurodegenerative disorders. Three different autophagic pathways are known by which intracellular constituents enter lysosomes for degradation: (1) chaperone-mediated autophagy (CMA), (2) microautophagy, and (3) macroautophagy (110). In CMA, cytosolic proteins containing a KFERQ motif are selectively targeted by chaperone proteins to the lysosomal lumen for degradation. In microautophagy, small quantities of cytoplasm non-selectively enter lysosomes by invagination of the lysosomal membrane. The most common form of autophagy is however macroautophagy (usually referred to as autophagy), which mediates “in bulk” degradation of cytoplasmic constituents and has been the focus of recent research due to its potential roles in cell survival and degeneration. During macroautophagy, an elongated “isolation” membrane, created from a pre-autophagosomal structure (PAS) or “phagophore”, sequesters a region of cytoplasm to form a double-membrane-limited vesicle called autophagosome. Autophagosomes then fuse with late endosomes or lysosomes and become auto(phago)lysosomes, also called autolysososomes, where the cytosolic contents are degraded by lysosomal hydrolases (104, 106, 111).

Thus, both endocytosis and autophagy are multi-step processes, and deficiencies at any of the steps of the two pathways may consequently cause intracellular accumulation of aberrant proteins and glycoconjugate species, leading to neurodegeneration. Since both these pathways deliver their cargoes finally to lysosomes, an efficient functioning of either endocytic or autophagic machinery depends on the presence of functional lysosomes. Lysosomes are acidic (pH $\leq$ 5) membrane-bound organelles which contain more than 50 acid hydrolases, including proteases, lipases, nucleases, glucosidases, phospholipases and sulfatases that work together to contribute to the total catabolic function of the lysosomal system (112, 113). Most of the lysosomal hydrolytic enzymes are processed in the trans-Golgi network and subsequently trafficked to the late-endosomes and lysosomes under the regulation of two species (~ 46 kD cation-dependent and ~300 kD cation-independent) of mannose 6-phosphate (M6P) receptors. To prevent premature activation of the hydrolases outside of the lysosomes, the lysosomal hydrolytic enzymes are synthesized and transported in their precursor "proenzyme" forms which are cleaved into their "mature/active" forms in the late endosomes and lysosomes. The compartmentalized activity of the lysosomal enzymes is regulated by the lysosomal membrane which helps to maintain the acidic pH (4.6-5.0) within the lumen of the lysosome. The lysosomal membrane also plays a key role in importing the substances for degradation from the cytosol by contacting and fusing with other vesicles such as late-endosomes and autophagosomes, and exporting degradation products back to the cytosol for recycling (114, 115). Accordingly, defects in lysosomal enzymes and membranes can cause neurodegenerative diseases (92, 95, 97). Despite the universal cellular role of the lysosomal system, the neurons seem to be particularly vulnerable to lysosomal system dysfunction. The unique importance of the lysosomal system in maintaining neuronal homeostasis could be explained by the following three reasons: 1) neurons cannot reduce their concentration of aberrant unwanted proteins and damaged organelles by cell division, 2) endocytic and autophagic activities are particularly high at synapses and along the long neuritic processes, hence demanding an efficient clearing of the cargo-laden vesicular compartments for maintaining neuronal homeostasis and, 3) neurons are confronted with additional aging-related lysosomal degradative impairments. Thus, while impairments of the endosomal-autophagosomal-

lysosomal pathway can be tolerated to some extent by cells in peripheral tissues, these abnormalities can trigger selective neurodegenerative phenotypes in the CNS.

Among the various neurodegenerative diseases, both AD and NPC are particularly well-characterized by marked defects in the EL and autophagosomal–lysosomal pathways, all of which are intimately associated with APP processing and Aβ generation (116, 117). Furthermore, the endosomal system also plays a critical role in the intracellular processing and trafficking of cholesterol regulated by NPC1/2 proteins. Thus, the endocytic-autophagic-lysosomal degradative pathways possibly represent a convergence point for the pathogenetic mechanisms in AD and NPC pathologies, although the significance of this system in the development/progression of the either disease remains unclear.

In AD brains, the changes associated with the endocytic pathway include increased volume of Rab5-positive early endosomal compartments together with increased mobilization of proteins facilitating Rab5 function such as early endosome antigen 1 (EEA1) and rabaptin 5 and enhanced expression of Rab4, an index of endosome recycling in the hippocampal neurons that are preferentially vulnerable to degeneration (118, 119). These alterations, which possibly increase the rates of endocytosis and endosome recycling, appear prior to substantial Aβ deposition in the brain and are believed to be accelerated by inheritance of the ε4 allele of *APOE*, the major genetic risk factor for late-onset AD (61, 118, 120). Supporting this notion, a recent study suggests that the genes related to endocytosis, such as Rab5, Rab7 and Rab4, are among the first group to be upregulated in AD and are abnormally recruited to endosomes, which progressively enlarge during the disease progression (121). As seen in AD, enlarged early endosomal compartments are also noted in the vulnerable Purkinje cells of NPC brains (40, 122). In NPC as well as AD cases, the early endosomes are also found to accumulate APP-CTFs and Aβ peptides. In addition, the enlarged endosomal compartments in both the diseases contain abnormally high levels of the lysosomal hydrolase cathepsins B and D, suggesting that cathepsins are partially re-routed to early endosomes in the vulnerable neurons of AD and NPC brains (40, 118). This is, at least in

part, due to an increase in M6P receptor expression, which usually carries newly synthesized lysosomal enzymes from the trans-Golgi network to late-endosomes. Accordingly, overexpression of the cation-dependent M6P receptor in fibroblasts has been demonstrated to mistarget cathepsin D to early endosomes and to increase Aβ secretion, suggesting that activation of the early endosomes in AD brains could mechanistically relate to the increased production of Aβ peptides (123). Unlike AD, there are conflicting reports regarding M6P receptor expression in NPC, with the receptor level either being elevated (124) or unchanged (125). However, studies in Npc1-model cells have shown that cholesterol accumulation can cause redistribution of the cation-independent M6P receptors to endosomes and impair its retrograde transport from late endosomes to the trans-Golgi network (126, 127). In a recent study it has been shown that cholesterol enrichment not only disrupts trafficking of the cation-independent M6P receptor but also causes accumulation of Rab9 in late-endosomes, thus suggesting that targeting of a variety of proteins is likely to be impaired in NPC-deficient cells (124). In our studies, we did not observe any significant alteration in the expression of transcripts encoding the cation-independent M6P receptor (Igf2r) or the Rab GTPases including Rab5, Rab7 and Rab9 in Npc1-null and ANPC brains. However, certain other components of vesicular trafficking such as the levels of mRNAs encoding *Klc2*, *Kif1c*, *Anx6*, *Tubb4* and *Mapt* were found to be differentially altered in Npc1-null and ANPC brain regions. Taken together, these findings suggest that the overall intracellular vesicular movement including the EL pathway is possibly dysfunctional, which in turn might disrupt the sorting and recycling of various proteins and lipids and promote amyloidogenic APP processing within the endocytic pathway in both AD and NPC pathologies.

In addition to endocytic abnormalities, an increasing number of studies suggest an impairment of the autophagic-lysosomal pathway in AD and NPC disease, which could significantly contribute to amyloidogenesis. Abundance of autophagosomes and late autophagic vacuoles packed with Aβ and other potentially neurotoxic substances in dystrophic neurites is characteristic of AD as well as NPC brains (117, 128) and recent studies indicate that impaired clearance of autophagic vacuoles might contribute to this

pathology (129). Moreover, new studies are now revealing that the genetic factors that cause or the increase risk of AD also have significant effects on autophagic-lysosomal function (97). More specific to the mechanism of neurodegeneration in AD and NPC, Aβ generated in the endocytic and autophagic pathways can accumulate when degradation *via* the lysosomal pathway is impaired. The resultant accumulation of Aβ can cause free-radical generation, disruption of the lysosomal membrane impermeability and leakage of lysosomal hydrolases such as cathepsin D and β-hexosaminidase into the cytosol, prior to other morphological signs of cellular toxicity (49, 51, 130). This is further supported by the evidence that hydrolase leakage and cell death can be mitigated partly by the antioxidant n-propyl gallate, suggesting that the lysosomal membrane may be a target of lipid peroxidation induced by Aβ aggregates (51, 130). Moreover, recent studies employing experimental strategies to stimulate autophagy to restore lysosomal proteolysis to normal levels have yielded beneficial effects on neuronal function and cognitive performance in AD mouse models (131-133) – thus suggesting a crucial role for the autophagic-lysosomal pathway in the extensive neuritic dystrophy seen in AD, which can possibly be extended to NPC pathology as well.

In our studies, we found an age-dependent increase in the levels of the autophagic protein LC3-II in brains of ANPC mice. Similar increases in LC3-II levels have been previously reported in Npc1-null brains, suggesting that autophagic activity might be increased under conditions of cholesterol sequestration in late-endosomes/lysosomes (80, 125). Cholesterol depletion, either by inhibition of its synthesis or acute extraction, has been previously shown to induce autophagy under various experimental conditions (134, 135), suggesting that “lipid starvation” may also lead to autophagy (136). Whether the increased autophagic acitivity observed in the brains of ANPC and Npc1-null mice is because of “lipid starvation” in selected cellular organelles remains to be determined. Autophagic induction is generally regulated by the mTOR (mammalian target of rapamycin) kinase, with activated mTOR (Akt and MAPK signaling) suppressing autophagy, and negative regulation of mTOR (AMPK and p53 signaling) promoting it (137). Induction of mTOR-independent autophagy involving beclin-1 is also known to occur under conditions of starvation to preserve cell homeostasis (138). Earlier studies

have reported upregulation of beclin-1 dependent autophagy in models of NPC1 deficiency (139). In this regard, it would be interesting to evaluate whether beclin-1 and other molecules involved in early stages of autophagosome formation like Atg5/Atg12 are altered in ANPC brains in response to cholesterol accumulation. This would enable us to understand the potential contribution of the increased autophagic activity, if any, to the increasing LC3-II and amyloidogenic peptide levels in ANPC brains. However, it is also possible that reduced lysosomal clearance activity caused by the EL cholesterol sequestration in ANPC brains could decrease the turnover of autophagic vacuoles, leading to their progressive buildup in the cells/tissue. Our results clearly indicate an age-dependent increase in the most well-known autophagic substrate, p62, along with polyubiquitinated proteins in the brains of ANPC mice, thus suggesting that the increase in LC3-II levels in the brain could be a consequence of decreased lysosomal clearance. Interestingly, the elevated LC3-II levels in ANPC brains were also accompanied by parallel increases in APP-CTF and Aβ levels. Given that lysosomes and autophagic vacuoles could contribute to both generation and degradation of APP-CTFs (117, 140), it is possible that both processes, *i.e.* increased autophagic induction and inhibition of lysosomal clearance, might together contribute to the increased APP-CTF and Aβ levels in the ANPC brain. Although understanding the contribution of the former event towards increased Aβ/APP-CTF levels needs further experimentation, our results clearly suggest a crucial role for lysosomal degradation in regulating APP-CTF levels under conditions of cholesterol sequenstration. Thus, while treatment of the N2a-APP cells with chloroquine, a lysosomotropic agent neutralizing the lysosomal acidic pH and thereby decreasing the activity of the lysosomal hydrolases, produced an increase of LC3-II and APP-CTF levels, the N2a-ANPC cells showed only a minor increase, suggesting that lysosomal degradative activity is already impaired in these cells.

In keeping with these *in vitro* experiments, changes in the lysosomal function in the brain following cholesterol accumulation were also evident in the increased levels/expression of the lysosomal enzymes cathepsin B, cathepsin D and Gus B. Earlier studies have reported upregulation of lysosomal enzymes in at “risk neurons” in both diseases accompanied by autophagic vacuole accumulation (42, 125, 141). While the

upregulation of different lysosomal enzymes could be a consequence of defects in their own trafficking and degradation secondary to lysosomal cholesterol accumulation or a compensatory mechanism for the increasing accumulation of unwanted materials (142), our study clearly highlights a role for the increased levels of lysosomal enzymes, particularly cathepsin D, in neurodegeneration. Interestingly, increasing evidence suggests a dual role for cathepsin D in cell death and survival. Several studies have shown that increased cathepsin levels within the lysosomes can prevent sub-lethal damage (143), whereas, destabilization of lysosomal membrane integrity leading to sustained release of cathepsins into the cytosol can trigger cell death by activating a caspase-dependent intracellular signaling mechanism (125, 144, 145). In our study we clearly showed that levels/expression and activity of cathepsin D are increased in both ANPC and Npc1-null mice more prominently in the affected cerebellar region than in the relatively spared hippocampus. In addition, the cytosolic levels of cathepsin D and the pro-apoptotic molecules like cytochrome c and Bax are increased specifically in the cerebellum ANPC and Npc1-null mice. Furthermore, the increase in cathepsin D level, in keeping with the magnitude of Purkinje cell loss, is found to be higher in ANPC mice compared to the Npc1-null mice, suggesting a potential role for the enzyme in the degeneration of the cerebellar Purkinje neurons. These results raise the possibility that while increased cathepsin D levels mostly within the lysosomes of the hippocampus may counter the cellular abnormalities caused by increased levels of mutant human APP/APP-fragments and cholesterol sequestration, up-regulation of cathepsin D levels and activity together with its release into the cytosol might trigger cell death in the cerebellum of ANPC and Npc1-null mice. This is further supported by our observation of active caspase-3 labeled neurons in the degenerating Purkinje cell layer of the cerebellum but not in the hippocampus that is spared from cell death.

At present, however, the factors that might trigger breakdown of lysosomal membrane integrity, releasing its hydrolytic enzymes into the cytosol under conditions of NPC1 deficiency, remain unclear. Of the many known factors that can induce lysosomal membrane permeabilization (LMP), the best characterized mechanism is the reactive oxygen species (ROS)-mediated lysosomal destabilization. There is evidence that ROS

are produced as a normal by-product of cellular metabolism of oxygen and play important role in cell signaling and homeostasis. However, under conditions of stress, ROS levels might increase dramatically and cause significant damage of cell structures including oxidation of proteins, lipids and nucleic acids. Earlier studies have established that intracellular accumulation of Aβ peptides can cause rapid induction of ROS generation within lysosomes and disruption of lysosomal membrane proton gradients which precedes cell death (51, 130). Considering that inhibition of lysosomal proteolysis following cholesterol accumulation causes massive accumulation of amyloidogenic Aβ fragments, it is intriguing to speculate that increased intracellular Aβ levels in ANPC mouse brains might induce ROS-mediated LMP, leading to leakage of cathepsin D into the cytosol and subsequent cell death. Accordingly, we observed an age-dependent increase in oxidative stress markers, the protein carbonyls, in the affected cerebellum of ANPC mice. This is also substantiated, at least in part, by our H_2O_2 treatment experiments, which showed that the N2a-ANPC cells are more susceptible to H_2O_2-induced toxicity than the N2a-APP cells, suggesting pre-existing oxidative stress conditions in the former cell line. More interestingly, the observed increase in H_2O_2-toxicity was partially rescued by pre-treatment with β- or γ-secretase inhibitors reducing Aβ levels. Taken together, our studies suggest that the increased intracellular Aβ/APP-CTF accumulation caused by EL cholesterol sequestration might be involved in inducing ROS-mediated LMP which can subsequently trigger cell death *via* leakage of the lysosomal cathepsin D into the cytosol.

5.6. Conclusion

Our data provide the first *in vivo* evidence that human APP expression in a model of NPC disease exacerbates the disease phenotype by amplifying the changes caused by NPC1 deficiency alone, highlighting a crucial role for APP in the disease process. Consistent with the previous studies, our results suggest that intracellular cholesterol distribution is a major regulator of APP processing and Aβ generation. Additionally, our studies indicate that impaired lysosomal activity, as evident in NPC and AD pathogenesis, is a major contributor to increased generation and accumulation of toxic Aβ and/or tau species. Hence, from a broader perspective, our studies highlight that strategies aiming at

improving the lysosomal clearance might offer a promising therapeutic approach for treating both AD and NPC disease. In conclusion, our results are consistent with a mechanism of neurodegeneration in both AD and NPC brains in which altered cholesterol homeostasis is a key early event in the pathogenesis that could drive both amyloid and tau pathologies either in parallel or independent of each other.

5.7 References

1. Chishti, M.A., Yang, D.S., Janus, C., Phinney, A.L., Horne, P., Pearson, J., Strome, R., Zuker, N., Loukides, J., French, J. *et al.* (2001) Early-onset amyloid deposition and cognitive deficits in transgenic mice expressing a double mutant form of amyloid precursor protein 695. *J Biol Chem*, **276,** 21562-21570.

2. Loftus, S.K., Morris, J.A., Carstea, E.D., Gu, J.Z., Cummings, C., Brown, A., Ellison, J., Ohno, K., Rosenfeld, M.A., Tagle, D.A. *et al.* (1997) Murine model of Niemann-Pick C disease: mutation in a cholesterol homeostasis gene. *Science*, **277,** 232-235.

3. Francis, B.M., Kim, J., Barakat, M.E., Fraenkl, S., Yucel, Y.H., Peng, S., Michalski, B., Fahnestock, M., McLaurin, J. and Mount, H.T. (2012) Object recognition memory and BDNF expression are reduced in young TgCRND8 mice. *Neurobiol Aging*, **33,** 555-563.

4. Bellucci, A., Rosi, M.C., Grossi, C., Fiorentini, A., Luccarini, I. and Casamenti, F. (2007) Abnormal processing of tau in the brain of aged TgCRND8 mice. *Neurobiol Dis*, **27,** 328-338.

5. Larner, A.J. (1997) The cerebellum in Alzheimer's disease. *Dement Geriatr Cogn Disord*, **8,** 203-209.

6. Andersen, K., Andersen, B.B. and Pakkenberg, B. (2012) Stereological quantification of the cerebellum in patients with Alzheimer's disease. *Neurobiol Aging*, **33,** 197 e111-120.

7. Elrick, M.J., Pacheco, C.D., Yu, T., Dadgar, N., Shakkottai, V.G., Ware, C., Paulson, H.L. and Lieberman, A.P. (2010) Conditional Niemann-Pick C mice demonstrate cell autonomous Purkinje cell neurodegeneration. *Hum Mol Genet*, **19,** 837-847.

8. Middleton, F.A. and Strick, P.L. (1998) Cerebellar output: motor and cognitive channels. *Trends Cogn Sci*, **2,** 348-354.

9. Burwell, R.D., Saddoris, M.P., Bucci, D.J. and Wiig, K.A. (2004) Corticohippocampal contributions to spatial and contextual learning. *J Neurosci*, **24,** 3826-3836.

10. Martin, M., Dotti, C.G. and Ledesma, M.D. (2010) Brain cholesterol in normal and pathological aging. *Biochim Biophys Acta*, **1801,** 934-944.

11. Di Paolo, G. and Kim, T.W. (2011) Linking lipids to Alzheimer's disease: cholesterol and beyond. *Nat Rev Neurosci*, **12,** 284-296.

12. Matsuzaki, T., Sasaki, K., Hata, J., Hirakawa, Y., Fujimi, K., Ninomiya, T., Suzuki, S.O., Kanba, S., Kiyohara, Y. and Iwaki, T. (2011) Association of Alzheimer disease pathology with abnormal lipid metabolism: the Hisayama Study. *Neurology*, **77,** 1068-1075.

13. Pappolla, M.A., Bryant-Thomas, T.K., Herbert, D., Pacheco, J., Fabra Garcia, M., Manjon, M., Girones, X., Henry, T.L., Matsubara, E., Zambon, D. *et al.* (2003) Mild hypercholesterolemia is an early risk factor for the development of Alzheimer amyloid pathology. *Neurology,* **61,** 199-205.

14. Distl, R., Meske, V. and Ohm, T.G. (2001) Tangle-bearing neurons contain more free cholesterol than adjacent tangle-free neurons. *Acta Neuropathol,* **101,** 547-554.

15. Burns, M.P., Noble, W.J., Olm, V., Gaynor, K., Casey, E., LaFrancois, J., Wang, L. and Duff, K. (2003) Co-localization of cholesterol, apolipoprotein E and fibrillar Abeta in amyloid plaques. *Brain Res Mol Brain Res,* **110,** 119-125.

16. Panchal, M., Loeper, J., Cossec, J.C., Perruchini, C., Lazar, A., Pompon, D. and Duyckaerts, C. (2010) Enrichment of cholesterol in microdissected Alzheimer's disease senile plaques as assessed by mass spectrometry. *J Lipid Res,* **51,** 598-605.

17. Corder, E.H., Saunders, A.M., Strittmatter, W.J., Schmechel, D.E., Gaskell, P.C., Small, G.W., Roses, A.D., Haines, J.L. and Pericak-Vance, M.A. (1993) Gene dose of apolipoprotein E type 4 allele and the risk of Alzheimer's disease in late onset families. *Science,* **261,** 921-923.

18. Bertram, L., McQueen, M.B., Mullin, K., Blacker, D. and Tanzi, R.E. (2007) Systematic meta-analyses of Alzheimer disease genetic association studies: the AlzGene database. *Nat Genet,* **39,** 17-23.

19. Hollingworth, P., Harold, D., Jones, L., Owen, M.J. and Williams, J. (2011) Alzheimer's disease genetics: current knowledge and future challenges. *Int J Geriatr Psychiatry,* **26,** 793-802.

20. Lambert, J.C. and Amouyel, P. (2011) Genetics of Alzheimer's disease: new evidences for an old hypothesis? *Curr Opin Genet Dev,* **21,** 295-301.

21. Wolozin, B., Kellman, W., Ruosseau, P., Celesia, G.G. and Siegel, G. (2000) Decreased prevalence of Alzheimer disease associated with 3-hydroxy-3-methyglutaryl coenzyme A reductase inhibitors. *Arch Neurol,* **57,** 1439-1443.

22. Rockwood, K., Kirkland, S., Hogan, D.B., MacKnight, C., Merry, H., Verreault, R., Wolfson, C. and McDowell, I. (2002) Use of lipid-lowering agents, indication bias, and the risk of dementia in community-dwelling elderly people. *Arch Neurol,* **59,** 223-227.

23. Haag, M.D., Hofman, A., Koudstaal, P.J., Stricker, B.H. and Breteler, M.M. (2009) Statins are associated with a reduced risk of Alzheimer disease regardless of lipophilicity. The Rotterdam Study. *J Neurol Neurosurg Psychiatry,* **80,** 13-17.

24. Reiss, A.B. and Voloshyna, I. (2012) Regulation of cerebral cholesterol metabolism in Alzheimer disease. *J Investig Med,* **60,** 576-582.

25. Sparks, D.L., Kryscio, R.J., Sabbagh, M.N., Connor, D.J., Sparks, L.M. and Liebsack, C. (2008) Reduced risk of incident AD with elective statin use in a clinical trial cohort. *Curr Alzheimer Res,* **5,** 416-421.

26. Zandi, P.P., Sparks, D.L., Khachaturian, A.S., Tschanz, J., Norton, M., Steinberg, M., Welsh-Bohmer, K.A. and Breitner, J.C. (2005) Do statins reduce risk of incident dementia and Alzheimer disease? The Cache County Study. *Arch Gen Psychiatry,* **62,** 217-224.

27. Tun, H., Marlow, L., Pinnix, I., Kinsey, R. and Sambamurti, K. (2002) Lipid rafts play an important role in Abeta biogenesis by regulating the beta-secretase pathway. *J Mol Neurosci,* **19,** 31-35.

28. Vetrivel, K.S., Cheng, H., Kim, S.H., Chen, Y., Barnes, N.Y., Parent, A.T., Sisodia, S.S. and Thinakaran, G. (2005) Spatial segregation of gamma-secretase and substrates in distinct membrane domains. *J Biol Chem,* **280,** 25892-25900.

29. Wahrle, S., Das, P., Nyborg, A.C., McLendon, C., Shoji, M., Kawarabayashi, T., Younkin, L.H., Younkin, S.G. and Golde, T.E. (2002) Cholesterol-dependent gamma-secretase activity in buoyant cholesterol-rich membrane microdomains. *Neurobiol Dis,* **9,** 11-23.

30. Davis, W., Jr. (2008) The cholesterol transport inhibitor U18666a regulates amyloid precursor protein metabolism and trafficking in N2aAPP "Swedish" cells. *Curr Alzheimer Res,* **5,** 448-456.

31. Kosicek, M., Malnar, M., Goate, A. and Hecimovic, S. (2010) Cholesterol accumulation in Niemann Pick type C (NPC) model cells causes a shift in APP localization to lipid rafts. *Biochem Biophys Res Commun,* **393,** 404-409.

32. Malnar, M., Kosicek, M., Mitterreiter, S., Omerbasic, D., Lichtenthaler, S.F., Goate, A. and Hecimovic, S. (2010) Niemann-Pick type C cells show cholesterol dependent decrease of APP expression at the cell surface and its increased processing through the beta-secretase pathway. *Biochim Biophys Acta,* **1802,** 682-691.

33. Puglielli, L., Konopka, G., Pack-Chung, E., Ingano, L.A., Berezovska, O., Hyman, B.T., Chang, T.Y., Tanzi, R.E. and Kovacs, D.M. (2001) Acyl-coenzyme A: cholesterol acyltransferase modulates the generation of the amyloid beta-peptide. *Nat Cell Biol,* **3,** 905-912.

34. Runz, H., Rietdorf, J., Tomic, I., de Bernard, M., Beyreuther, K., Pepperkok, R. and Hartmann, T. (2002) Inhibition of intracellular cholesterol transport alters presenilin localization and amyloid precursor protein processing in neuronal cells. *J Neurosci,* **22,** 1679-1689.

35. Yamazaki, T., Chang, T.Y., Haass, C. and Ihara, Y. (2001) Accumulation and aggregation of amyloid beta-protein in late endosomes of Niemann-pick type C cells. *J Biol Chem,* **276,** 4454-4460.

36. Burns, M., Gaynor, K., Olm, V., Mercken, M., LaFrancois, J., Wang, L., Mathews, P.M., Noble, W., Matsuoka, Y. and Duff, K. (2003) Presenilin redistribution associated with aberrant cholesterol transport enhances beta-amyloid production in vivo. *J Neurosci,* **23,** 5645-5649.

37. Bodovitz, S. and Klein, W.L. (1996) Cholesterol modulates alpha-secretase cleavage of amyloid precursor protein. *J Biol Chem,* **271,** 4436-4440.

38. Kojro, E., Gimpl, G., Lammich, S., Marz, W. and Fahrenholz, F. (2001) Low cholesterol stimulates the nonamyloidogenic pathway by its effect on the alpha - secretase ADAM 10. *Proc Natl Acad Sci U S A,* **98,** 5815-5820.

39. Simons, M., Keller, P., De Strooper, B., Beyreuther, K., Dotti, C.G. and Simons, K. (1998) Cholesterol depletion inhibits the generation of beta-amyloid in hippocampal neurons. *Proc Natl Acad Sci U S A,* **95,** 6460-6464.

40. Jin, L.W., Shie, F.S., Maezawa, I., Vincent, I. and Bird, T. (2004) Intracellular accumulation of amyloidogenic fragments of amyloid-beta precursor protein in neurons with Niemann-Pick type C defects is associated with endosomal abnormalities. *Am J Pathol,* **164,** 975-985.

41. Boland, B., Smith, D.A., Mooney, D., Jung, S.S., Walsh, D.M. and Platt, F.M. (2010) Macroautophagy is not directly involved in the metabolism of amyloid precursor protein. *J Biol Chem,* **285,** 37415-37426.

42. Liao, G., Yao, Y., Liu, J., Yu, Z., Cheung, S., Xie, A., Liang, X. and Bi, X. (2007) Cholesterol accumulation is associated with lysosomal dysfunction and autophagic stress in Npc1 -/- mouse brain. *Am J Pathol,* **171,** 962-975.

43. Gouras, G.K., Tsai, J., Naslund, J., Vincent, B., Edgar, M., Checler, F., Greenfield, J.P., Haroutunian, V., Buxbaum, J.D., Xu, H. *et al.* (2000) Intraneuronal Abeta42 accumulation in human brain. *Am J Pathol,* **156,** 15-20.

44. Lord, A., Kalimo, H., Eckman, C., Zhang, X.Q., Lannfelt, L. and Nilsson, L.N. (2006) The Arctic Alzheimer mutation facilitates early intraneuronal Abeta aggregation and senile plaque formation in transgenic mice. *Neurobiol Aging,* **27,** 67-77.

45. Shie, F.S., LeBoeuf, R.C. and Jin, L.W. (2003) Early intraneuronal Abeta deposition in the hippocampus of APP transgenic mice. *Neuroreport,* **14,** 123-129.

46. D'Andrea, M.R., Nagele, R.G., Wang, H.Y., Peterson, P.A. and Lee, D.H. (2001) Evidence that neurones accumulating amyloid can undergo lysis to form amyloid plaques in Alzheimer's disease. *Histopathology,* **38,** 120-134.

47. Knauer, M.F., Soreghan, B., Burdick, D., Kosmoski, J. and Glabe, C.G. (1992) Intracellular accumulation and resistance to degradation of the Alzheimer amyloid A4/beta protein. *Proc Natl Acad Sci U S A,* **89,** 7437-7441.

48. Takahashi, R.H., Milner, T.A., Li, F., Nam, E.E., Edgar, M.A., Yamaguchi, H., Beal, M.F., Xu, H., Greengard, P. and Gouras, G.K. (2002) Intraneuronal Alzheimer abeta42 accumulates in multivesicular bodies and is associated with synaptic pathology. *Am J Pathol,* **161,** 1869-1879.

49. Glabe, C. (2001) Intracellular mechanisms of amyloid accumulation and pathogenesis in Alzheimer's disease. *J Mol Neurosci,* **17,** 137-145.

50. Ling, D., Song, H.J., Garza, D., Neufeld, T.P. and Salvaterra, P.M. (2009) Abeta42-induced neurodegeneration via an age-dependent autophagic-lysosomal injury in Drosophila. *PLoS One,* **4,** e4201.

51. Yang, A.J., Chandswangbhuvana, D., Margol, L. and Glabe, C.G. (1998) Loss of endosomal/lysosomal membrane impermeability is an early event in amyloid Abeta1-42 pathogenesis. *J Neurosci Res,* **52,** 691-698.

52. Chang, K.A. and Suh, Y.H. (2005) Pathophysiological roles of amyloidogenic carboxy-terminal fragments of the beta-amyloid precursor protein in Alzheimer's disease. *J Pharmacol Sci,* **97,** 461-471.

53. Berger-Sweeney, J., McPhie, D.L., Arters, J.A., Greenan, J., Oster-Granite, M.L. and Neve, R.L. (1999) Impairments in learning and memory accompanied by neurodegeneration in mice transgenic for the carboxyl-terminus of the amyloid precursor protein. *Brain Res Mol Brain Res,* **66,** 150-162.

54. Nalbantoglu, J., Tirado-Santiago, G., Lahsaini, A., Poirier, J., Goncalves, O., Verge, G., Momoli, F., Welner, S.A., Massicotte, G., Julien, J.P. *et al.* (1997) Impaired learning and LTP in mice expressing the carboxy terminus of the Alzheimer amyloid precursor protein. *Nature,* **387,** 500-505.

55. Bach, J.H., Chae, H.S., Rah, J.C., Lee, M.W., Park, C.H., Choi, S.H., Choi, J.K., Lee, S.H., Kim, Y.S., Kim, K.Y. *et al.* (2001) C-terminal fragment of amyloid precursor protein induces astrocytosis. *J Neurochem,* **78,** 109-120.

56. Chong, Y. (1997) Effect of a carboxy-terminal fragment of the Alzheimer's amyloid precursor protein on expression of proinflammatory cytokines in rat glial cells. *Life Sci,* **61,** 2323-2333.

57. Kim, H.S., Park, C.H., Cha, S.H., Lee, J.H., Lee, S., Kim, Y., Rah, J.C., Jeong, S.J. and Suh, Y.H. (2000) Carboxyl-terminal fragment of Alzheimer's APP destabilizes calcium homeostasis and renders neuronal cells vulnerable to excitotoxicity. *FASEB J,* **14,** 1508-1517.

58. Oster-Granite, M.L., McPhie, D.L., Greenan, J. and Neve, R.L. (1996) Age-dependent neuronal and synaptic degeneration in mice transgenic for the C terminus of the amyloid precursor protein. *J Neurosci,* **16,** 6732-6741.

59. Yankner, B.A., Dawes, L.R., Fisher, S., Villa-Komaroff, L., Oster-Granite, M.L. and Neve, R.L. (1989) Neurotoxicity of a fragment of the amyloid precursor associated with Alzheimer's disease. *Science,* **245,** 417-420.

60. McPhie, D.L., Golde, T., Eckman, C.B., Yager, D., Brant, J.B. and Neve, R.L. (2001) beta-Secretase cleavage of the amyloid precursor protein mediates neuronal apoptosis caused by familial Alzheimer's disease mutations. *Brain Res Mol Brain Res,* **97,** 103-113.

61. Jiang, Y., Mullaney, K.A., Peterhoff, C.M., Che, S., Schmidt, S.D., Boyer-Boiteau, A., Ginsberg, S.D., Cataldo, A.M., Mathews, P.M. and Nixon, R.A. (2010) Alzheimer's-related endosome dysfunction in Down syndrome is Abeta-independent but requires APP and is reversed by BACE-1 inhibition. *Proc Natl Acad Sci U S A,* **107,** 1630-1635.

62. Cataldo, A.M., Petanceska, S., Terio, N.B., Peterhoff, C.M., Durham, R., Mercken, M., Mehta, P.D., Buxbaum, J., Haroutunian, V. and Nixon, R.A. (2004) Abeta localization in abnormal endosomes: association with earliest Abeta elevations in AD and Down syndrome. *Neurobiol Aging,* **25,** 1263-1272.

63. Auer, I.A., Schmidt, M.L., Lee, V.M., Curry, B., Suzuki, K., Shin, R.W., Pentchev, P.G., Carstea, E.D. and Trojanowski, J.Q. (1995) Paired helical filament tau (PHFtau) in Niemann-Pick type C disease is similar to PHFtau in Alzheimer's disease. *Acta Neuropathol,* **90,** 547-551.

64. Ohm, T.G., Treiber-Held, S., Distl, R., Glockner, F., Schonheit, B., Tamanai, M. and Meske, V. (2003) Cholesterol and tau protein--findings in Alzheimer's and Niemann Pick C's disease. *Pharmacopsychiatry,* **36 Suppl 2,** S120-126.

65. Distl, R., Treiber-Held, S., Albert, F., Meske, V., Harzer, K. and Ohm, T.G. (2003) Cholesterol storage and tau pathology in Niemann-Pick type C disease in the brain. *J Pathol,* **200,** 104-111.

66. Gendron, T.F. and Petrucelli, L. (2009) The role of tau in neurodegeneration. *Mol Neurodegener,* **4,** 13.

67. Hanger, D.P., Anderton, B.H. and Noble, W. (2009) Tau phosphorylation: the therapeutic challenge for neurodegenerative disease. *Trends Mol Med,* **15,** 112-119.

68. Ohm, T.G., Glockner, F., Distl, R., Treiber-Held, S., Meske, V. and Schonheit, B. (2003) Plasticity and the spread of Alzheimer's disease-like changes. *Neurochem Res,* **28,** 1715-1723.

69. Love, S., Bridges, L.R. and Case, C.P. (1995) Neurofibrillary tangles in Niemann-Pick disease type C. *Brain,* **118 (Pt 1),** 119-129.

70. Braak, H., Braak, E., Bohl, J. and Lang, W. (1989) Alzheimer's disease: amyloid plaques in the cerebellum. *J Neurol Sci,* **93,** 277-287.

71. Bu, B., Klunemann, H., Suzuki, K., Li, J., Bird, T., Jin, L.W. and Vincent, I. (2002) Niemann-Pick disease type C yields possible clue for why cerebellar neurons do not form neurofibrillary tangles. *Neurobiol Dis,* **11,** 285-297.

72. Iqbal, K., Alonso Adel, C., Chen, S., Chohan, M.O., El-Akkad, E., Gong, C.X., Khatoon, S., Li, B., Liu, F., Rahman, A. *et al.* (2005) Tau pathology in Alzheimer disease and other tauopathies. *Biochim Biophys Acta,* **1739,** 198-210.

73. Ballatore, C., Lee, V.M. and Trojanowski, J.Q. (2007) Tau-mediated neurodegeneration in Alzheimer's disease and related disorders. *Nat Rev Neurosci,* **8,** 663-672.

74. Iwata, A., Riley, B.E., Johnston, J.A. and Kopito, R.R. (2005) HDAC6 and microtubules are required for autophagic degradation of aggregated huntingtin. *J Biol Chem,* **280,** 40282-40292.

75. Ravikumar, B., Acevedo-Arozena, A., Imarisio, S., Berger, Z., Vacher, C., O'Kane, C.J., Brown, S.D. and Rubinsztein, D.C. (2005) Dynein mutations impair autophagic clearance of aggregate-prone proteins. *Nat Genet,* **37,** 771-776.

76. Martinez-Vicente, M. and Cuervo, A.M. (2007) Autophagy and neurodegeneration: when the cleaning crew goes on strike. *Lancet Neurol,* **6,** 352-361.

77. Komatsu, M., Waguri, S., Chiba, T., Murata, S., Iwata, J., Tanida, I., Ueno, T., Koike, M., Uchiyama, Y., Kominami, E. *et al.* (2006) Loss of autophagy in the central nervous system causes neurodegeneration in mice. *Nature,* **441,** 880-884.

78. Rubinsztein, D.C. (2006) The roles of intracellular protein-degradation pathways in neurodegeneration. *Nature,* **443,** 780-786.

79. Hara, T., Nakamura, K., Matsui, M., Yamamoto, A., Nakahara, Y., Suzuki-Migishima, R., Yokoyama, M., Mishima, K., Saito, I., Okano, H. *et al.* (2006) Suppression of basal autophagy in neural cells causes neurodegenerative disease in mice. *Nature,* **441,** 885-889.

80. Pacheco, C.D., Elrick, M.J. and Lieberman, A.P. (2009) Tau deletion exacerbates the phenotype of Niemann-Pick type C mice and implicates autophagy in pathogenesis. *Hum Mol Genet,* **18,** 956-965.

81. Nunes, A., Pressey, S.N., Cooper, J.D. and Soriano, S. (2011) Loss of amyloid precursor protein in a mouse model of Niemann-Pick type C disease exacerbates its phenotype and disrupts tau homeostasis. *Neurobiol Dis,* **42,** 349-359.

82. German, D.C., Quintero, E.M., Liang, C.L., Ng, B., Punia, S., Xie, C. and Dietschy, J.M. (2001) Selective neurodegeneration, without neurofibrillary tangles, in a mouse model of Niemann-Pick C disease. *J Comp Neurol,* **433,** 415-425.

83. Hao, Y., Pan, D., Zhang, M., Xu, J., Li, L., Wei, J. and Wang, X. (2009) The neuroprotective effects of cyclin-dependent kinase-5 inhibition in mice with

Niemann-Pick disease type C. *J Huazhong Univ Sci Technolog Med Sci,* **29,** 324-329.

84. Zhang, M., Li, J., Chakrabarty, P., Bu, B. and Vincent, I. (2004) Cyclin-dependent kinase inhibitors attenuate protein hyperphosphorylation, cytoskeletal lesion formation, and motor defects in Niemann-Pick Type C mice. *Am J Pathol,* **165,** 843-853.

85. Chung, C.W., Song, Y.H., Kim, I.K., Yoon, W.J., Ryu, B.R., Jo, D.G., Woo, H.N., Kwon, Y.K., Kim, H.H., Gwag, B.J. *et al.* (2001) Proapoptotic effects of tau cleavage product generated by caspase-3. *Neurobiol Dis,* **8,** 162-172.

86. Cotman, C.W., Poon, W.W., Rissman, R.A. and Blurton-Jones, M. (2005) The role of caspase cleavage of tau in Alzheimer disease neuropathology. *J Neuropathol Exp Neurol,* **64,** 104-112.

87. Gamblin, T.C., Chen, F., Zambrano, A., Abraha, A., Lagalwar, S., Guillozet, A.L., Lu, M., Fu, Y., Garcia-Sierra, F., LaPointe, N. *et al.* (2003) Caspase cleavage of tau: linking amyloid and neurofibrillary tangles in Alzheimer's disease. *Proc Natl Acad Sci U S A,* **100,** 10032-10037.

88. Nicholson, A.M. and Ferreira, A. (2009) Increased membrane cholesterol might render mature hippocampal neurons more susceptible to beta-amyloid-induced calpain activation and tau toxicity. *J Neurosci,* **29,** 4640-4651.

89. Park, S.Y. and Ferreira, A. (2005) The generation of a 17 kDa neurotoxic fragment: an alternative mechanism by which tau mediates beta-amyloid-induced neurodegeneration. *J Neurosci,* **25,** 5365-5375.

90. Bednarski, E. and Lynch, G. (1996) Cytosolic proteolysis of tau by cathepsin D in hippocampus following suppression of cathepsins B and L. *J Neurochem,* **67,** 1846-1855.

91. Kenessey, A., Nacharaju, P., Ko, L.W. and Yen, S.H. (1997) Degradation of tau by lysosomal enzyme cathepsin D: implication for Alzheimer neurofibrillary degeneration. *J Neurochem,* **69,** 2026-2038.

92. Bellettato, C.M. and Scarpa, M. (2010) Pathophysiology of neuropathic lysosomal storage disorders. *J Inherit Metab Dis,* **33,** 347-362.

93. Ohmi, K., Kudo, L.C., Ryazantsev, S., Zhao, H.Z., Karsten, S.L. and Neufeld, E.F. (2009) Sanfilippo syndrome type B, a lysosomal storage disease, is also a tauopathy. *Proc Natl Acad Sci U S A,* **106,** 8332-8337.

94. Wraith, J.E. (2002) Lysosomal disorders. *Semin Neonatol,* **7,** 75-83.

95. Bahr, B.A. and Bendiske, J. (2002) The neuropathogenic contributions of lysosomal dysfunction. *J Neurochem,* **83,** 481-489.

96. Nixon, R.A., Mathews, P.M. and Cataldo, A.M. (2001) The neuronal endosomal-lysosomal system in Alzheimer's disease. *J Alzheimers Dis,* **3,** 97-107.

97. Nixon, R.A., Yang, D.S. and Lee, J.H. (2008) Neurodegenerative lysosomal disorders: a continuum from development to late age. *Autophagy,* **4,** 590-599.

98. Cherra, S.J., 3rd, Dagda, R.K. and Chu, C.T. (2010) Review: autophagy and neurodegeneration: survival at a cost? *Neuropathol Appl Neurobiol,* **36,** 125-132.

99. Jaeger, P.A. and Wyss-Coray, T. (2009) All-you-can-eat: autophagy in neurodegeneration and neuroprotection. *Mol Neurodegener,* **4,** 16.

100. Dehay, B., Ramirez, A., Martinez-Vicente, M., Perier, C., Canron, M.H., Doudnikoff, E., Vital, A., Vila, M., Klein, C. and Bezard, E. (2012) Loss of P-type ATPase ATP13A2/PARK9 function induces general lysosomal deficiency and leads to Parkinson disease neurodegeneration. *Proc Natl Acad Sci U S A,* **109,** 9611-9616.

101. Mukherjee, S., Ghosh, R.N. and Maxfield, F.R. (1997) Endocytosis. *Physiol Rev,* **77,** 759-803.

102. Mayor, S. and Pagano, R.E. (2007) Pathways of clathrin-independent endocytosis. *Nat Rev Mol Cell Biol,* **8,** 603-612.

103. Piper, R.C. and Luzio, J.P. (2001) Late endosomes: sorting and partitioning in multivesicular bodies. *Traffic,* **2,** 612-621.

104. Mizushima, N. (2007) Autophagy: process and function. *Genes Dev,* **21,** 2861-2873.

105. Klionsky, D.J. (2007) Autophagy: from phenomenology to molecular understanding in less than a decade. *Nat Rev Mol Cell Biol,* **8,** 931-937.

106. Garcia-Arencibia, M., Hochfeld, W.E., Toh, P.P. and Rubinsztein, D.C. (2010) Autophagy, a guardian against neurodegeneration. *Semin Cell Dev Biol,* **21,** 691-698.

107. Cuervo, A.M., Bergamini, E., Brunk, U.T., Droge, W., Ffrench, M. and Terman, A. (2005) Autophagy and aging: the importance of maintaining "clean" cells. *Autophagy,* **1,** 131-140.

108. Levine, B. and Kroemer, G. (2008) Autophagy in the pathogenesis of disease. *Cell,* **132,** 27-42.

109. Wong, E. and Cuervo, A.M. (2010) Autophagy gone awry in neurodegenerative diseases. *Nat Neurosci,* **13,** 805-811.

110. Cuervo, A.M. (2004) Autophagy: many paths to the same end. *Mol Cell Biochem,* **263,** 55-72.

111. Ohsumi, Y. (2001) Molecular dissection of autophagy: two ubiquitin-like systems. *Nat Rev Mol Cell Biol,* **2,** 211-216.

112. de Duve, C. (2005) The lysosome turns fifty. *Nat Cell Biol,* **7,** 847-849.

113. Luzio, J.P., Pryor, P.R. and Bright, N.A. (2007) Lysosomes: fusion and function. *Nat Rev Mol Cell Biol,* **8,** 622-632.

114. Saftig, P. and Klumperman, J. (2009) Lysosome biogenesis and lysosomal membrane proteins: trafficking meets function. *Nat Rev Mol Cell Biol,* **10,** 623-635.

115. Callahan, J.W., Bagshaw, R.D. and Mahuran, D.J. (2009) The integral membrane of lysosomes: its proteins and their roles in disease. *J Proteomics,* **72,** 23-33.

116. Nixon, R.A. (2005) Endosome function and dysfunction in Alzheimer's disease and other neurodegenerative diseases. *Neurobiol Aging,* **26,** 373-382.

117. Nixon, R.A. (2007) Autophagy, amyloidogenesis and Alzheimer disease. *J Cell Sci,* **120,** 4081-4091.

118. Cataldo, A.M., Barnett, J.L., Pieroni, C. and Nixon, R.A. (1997) Increased neuronal endocytosis and protease delivery to early endosomes in sporadic Alzheimer's disease: neuropathologic evidence for a mechanism of increased beta-amyloidogenesis. *J Neurosci,* **17,** 6142-6151.

119. Cataldo, A.M., Hamilton, D.J., Barnett, J.L., Paskevich, P.A. and Nixon, R.A. (1996) Properties of the endosomal-lysosomal system in the human central nervous system: disturbances mark most neurons in populations at risk to degenerate in Alzheimer's disease. *J Neurosci,* **16,** 186-199.

120. Cataldo, A.M., Peterhoff, C.M., Troncoso, J.C., Gomez-Isla, T., Hyman, B.T. and Nixon, R.A. (2000) Endocytic pathway abnormalities precede amyloid beta deposition in sporadic Alzheimer's disease and Down syndrome: differential effects of APOE genotype and presenilin mutations. *Am J Pathol,* **157,** 277-286.

121. Ginsberg, S.D., Alldred, M.J., Counts, S.E., Cataldo, A.M., Neve, R.L., Jiang, Y., Wuu, J., Chao, M.V., Mufson, E.J., Nixon, R.A. *et al.* (2010) Microarray analysis of hippocampal CA1 neurons implicates early endosomal dysfunction during Alzheimer's disease progression. *Biol Psychiatry,* **68,** 885-893.

122. Nixon, R.A. (2004) Niemann-Pick Type C disease and Alzheimer's disease: the APP-endosome connection fattens up. *Am J Pathol,* **164,** 757-761.

123. Mathews, P.M., Guerra, C.B., Jiang, Y., Grbovic, O.M., Kao, B.H., Schmidt, S.D., Dinakar, R., Mercken, M., Hille-Rehfeld, A., Rohrer, J. *et al.* (2002) Alzheimer's disease-related overexpression of the cation-dependent mannose 6-phosphate receptor increases Abeta secretion: role for altered lysosomal hydrolase distribution in beta-amyloidogenesis. *J Biol Chem,* **277,** 5299-5307.

124. Ganley, I.G. and Pfeffer, S.R. (2006) Cholesterol accumulation sequesters Rab9 and disrupts late endosome function in NPC1-deficient cells. *J Biol Chem,* **281,** 17890-17899.

125. Amritraj, A., Peake, K., Kodam, A., Salio, C., Merighi, A., Vance, J.E. and Kar, S. (2009) Increased activity and altered subcellular distribution of lysosomal enzymes determine neuronal vulnerability in Niemann-Pick type C1-deficient mice. *Am J Pathol,* **175,** 2540-2556.

126. Kobayashi, T., Beuchat, M.H., Lindsay, M., Frias, S., Palmiter, R.D., Sakuraba, H., Parton, R.G. and Gruenberg, J. (1999) Late endosomal membranes rich in lysobisphosphatidic acid regulate cholesterol transport. *Nat Cell Biol,* **1,** 113-118.

127. Ikeda, K., Hirayama, M., Hirota, Y., Asa, E., Seki, J. and Tanaka, Y. (2008) Drug-induced phospholipidosis is caused by blockade of mannose 6-phosphate receptor-mediated targeting of lysosomal enzymes. *Biochem Biophys Res Commun,* **377,** 268-274.

128. Pacheco, C.D. and Lieberman, A.P. (2008) The pathogenesis of Niemann-Pick type C disease: a role for autophagy? *Expert Rev Mol Med,* **10,** e26.

129. Boland, B., Kumar, A., Lee, S., Platt, F.M., Wegiel, J., Yu, W.H. and Nixon, R.A. (2008) Autophagy induction and autophagosome clearance in neurons: relationship to autophagic pathology in Alzheimer's disease. *J Neurosci,* **28,** 6926-6937.

130. Ditaranto, K., Tekirian, T.L. and Yang, A.J. (2001) Lysosomal membrane damage in soluble Abeta-mediated cell death in Alzheimer's disease. *Neurobiol Dis,* **8,** 19-31.

131. Spilman, P., Podlutskaya, N., Hart, M.J., Debnath, J., Gorostiza, O., Bredesen, D., Richardson, A., Strong, R. and Galvan, V. (2010) Inhibition of mTOR by rapamycin abolishes cognitive deficits and reduces amyloid-beta levels in a mouse model of Alzheimer's disease. *PLoS One,* **5,** e9979.

132. Sun, B., Zhou, Y., Halabisky, B., Lo, I., Cho, S.H., Mueller-Steiner, S., Devidze, N., Wang, X., Grubb, A. and Gan, L. (2008) Cystatin C-cathepsin B axis regulates amyloid beta levels and associated neuronal deficits in an animal model of Alzheimer's disease. *Neuron,* **60,** 247-257.

133. Yang, D.S., Kumar, A., Stavrides, P., Peterson, J., Peterhoff, C.M., Pawlik, M., Levy, E., Cataldo, A.M. and Nixon, R.A. (2008) Neuronal apoptosis and autophagy cross talk in aging PS/APP mice, a model of Alzheimer's disease. *Am J Pathol,* **173,** 665-681.

134. Cheng, J., Ohsaki, Y., Tauchi-Sato, K., Fujita, A. and Fujimoto, T. (2006) Cholesterol depletion induces autophagy. *Biochem Biophys Res Commun,* **351,** 246-252.

135. Lajoie, P., Guay, G., Dennis, J.W. and Nabi, I.R. (2005) The lipid composition of autophagic vacuoles regulates expression of multilamellar bodies. *J Cell Sci,* **118,** 1991-2003.

136. Bi, X. and Liao, G. (2007) Autophagic-lysosomal dysfunction and neurodegeneration in Niemann-Pick Type C mice: lipid starvation or indigestion? *Autophagy,* **3,** 646-648.

137. Laplante, M. and Sabatini, D.M. (2009) mTOR signaling at a glance. *J Cell Sci,* **122,** 3589-3594.

138. Wei, Y., Pattingre, S., Sinha, S., Bassik, M. and Levine, B. (2008) JNK1-mediated phosphorylation of Bcl-2 regulates starvation-induced autophagy. *Mol Cell,* **30,** 678-688.

139. Pacheco, C.D., Kunkel, R. and Lieberman, A.P. (2007) Autophagy in Niemann-Pick C disease is dependent upon Beclin-1 and responsive to lipid trafficking defects. *Hum Mol Genet,* **16,** 1495-1503.

140. Haass, C., Koo, E.H., Mellon, A., Hung, A.Y. and Selkoe, D.J. (1992) Targeting of cell-surface beta-amyloid precursor protein to lysosomes: alternative processing into amyloid-bearing fragments. *Nature,* **357,** 500-503.

141. Yu, W.H., Cuervo, A.M., Kumar, A., Peterhoff, C.M., Schmidt, S.D., Lee, J.H., Mohan, P.S., Mercken, M., Farmery, M.R., Tjernberg, L.O. *et al.* (2005) Macroautophagy--a novel Beta-amyloid peptide-generating pathway activated in Alzheimer's disease. *J Cell Biol,* **171,** 87-98.

142. Butler, D., Nixon, R.A. and Bahr, B.A. (2006) Potential compensatory responses through autophagic/lysosomal pathways in neurodegenerative diseases. *Autophagy,* **2,** 234-237.

143. Bendiske, J. and Bahr, B.A. (2003) Lysosomal activation is a compensatory response against protein accumulation and associated synaptopathogenesis--an approach for slowing Alzheimer disease? *J Neuropathol Exp Neurol,* **62,** 451-463.

144. Chwieralski, C.E., Welte, T. and Buhling, F. (2006) Cathepsin-regulated apoptosis. *Apoptosis,* **11,** 143-149.

145. Turk, B., Stoka, V., Rozman-Pungercar, J., Cirman, T., Droga-Mazovec, G., Oresic, K. and Turk, V. (2002) Apoptotic pathways: involvement of lysosomal proteases. *Biol Chem,* **383,** 1035-1044.